



**THE STRUCTURE AND METAMORPHISM  
OF THE PEWSEY VALE AREA  
NORTH-EAST OF WILLIAMSTOWN, S. A.**

**BY**

**ROBIN OFFLER**

**B.Sc.(Hons.) Adelaide.**

**Department of Geology,**

**The University of Adelaide.**

**JULY, 1966.**

TABLE OF CONTENTS.

Page.

SUMMARY

ACKNOWLEDGEMENTS

INTRODUCTION

	1.
"Archean".	1.
Adelaide Supergroup.	2.
Kanmantoo Group.	3.
Early Palaeozoic Orogeny	5.
Purpose of the present investigation.	6.
Physiography.	7.
Previous investigations	7.
<u>CHAPTER 1. STRATIGRAPHY.</u>	9.
Adelaide Supergroup.	9.
Kanmantoo Group.	10.
Tertiary.	12.
<u>PETROLOGY AND PETROGRAPHY OF THE KANMANTOO GROUP. ROCKS.</u>	13.
<u>CHAPTER 2. QUARTZO-FELDSPATHIC SCHISTS AND MIGMATITES.</u>	14.
Introduction.	14.
Quartzo-feldspathic Schists outside the Migmatite Zone.	14.
Quartzo-feldspathic Schists within the Migmatite Zone.	17.
Veins.	19.
Origin of the Migmatites	22.
Relative Age of the Migmatites	24.

25329B

<u>CHAPTER 3. THE TANUNDA CREEK GNEISS.</u>	26.
Introduction.	26.
Transitional Zone.	26.
Petrography of the Transitional Zone.	27.
Petrography of the Tanunda Creek Gneiss.	29.
Mineralogical variation.	30.
Relation to Structure.	31.
Origin of the Tanunda Creek Gneiss.	32.
<u>CHAPTER 4. CALC-SILICATE ROCKS AND CALC-SCHISTS.</u>	34.
Introduction.	34.
Petrography.	34.
Amphibole - clinopyroxene relationships.	40.
Origin of the Calc-silicate rocks.	40.
<u>CHAPTER 5. THE PELITIC SCHISTS AND GRAPHITIC SCHISTS.</u>	42.
PELITIC SCHISTS.	42.
Introduction.	42.
Petrography and paragenesis.	42.
GRAPHITIC SCHISTS.	48.
<u>PETROLOGY AND PETROGRAPHY OF THE ADELAIDE SUPERGROUP</u>	
ROCKS.	50.
<u>CHAPTER 6. THE NON CALCAREOUS ROCKS.</u>	51.
THE PELITIC AND SEMI-PELITIC SCHISTS.	51.
Mineral assemblages.	51.
Bimica Schists.	51.
Garnet Schists.	55.
QUARTZITES.	57.
PEBBLE BEDS.	59.

<u>CHAPTER 7. CALC-SCHISTS AND CALC-SILICATE ROCKS.</u>	60.
Petrography.	61.
Metamorphic segregations.	65.
Conclusions.	66.
<u>CHAPTER 8. METAMORPHISM.</u>	67.
Metamorphic zoning, facies and grade.	67.
Metamorphic Zoning.	67.
Metamorphic facies and grade.	69.
Type of metamorphism.	70.
Physical conditions during metamorphism.	71.
Oxide assemblages in the rocks of the Kanmantoo Group and their significance.	74.
<u>CHAPTER 9. INTRUSIVE ROCKS.</u>	75.
Introduction.	75.
MT. KITCHENER INTRUSION.	
Petrography.	76.
Unaltered rocks.	76.
Albitites.	78.
Origin of the Mt.Kitchener Intrusion.	80.
Regional setting.	81.
Conclusions.	81.
PEGMATITES.	82.
Petrography.	83.
Country rock alteration.	86.
Discussion.	86.

<b>DOLERITES, META-DOLERITES AND AMPHIBOLITES.</b>	<b>37.</b>
<b>Petrography.</b>	<b>37.</b>
<b>Dolerites.</b>	<b>38.</b>
<b>Meta-dolerites and amphibolites.</b>	<b>39.</b>
<b>Factors affecting the recrystallization of the dolerites.</b>	<b>90.</b>
<b>Absence of garnet in the meta-dolerites.</b>	<b>91.</b>
<b><u>CHAPTER 10. ALBITITES AND ASSOCIATED ROCKS.</u></b>	<b>93.</b>
<b>Field occurrence of the Pawsey Vale Albitites.</b>	<b>93.</b>
<b>Petrography.</b>	<b>94.</b>
<b>Transitional rocks.</b>	<b>96.</b>
<b>Talc ore bodies.</b>	<b>98.</b>
<b>Discussion.</b>	<b>99.</b>
<b>Chemical and mineralogical changes involved in the albitization.</b>	<b>99.</b>
<b><u>CHAPTER 11. STRUCTURE.</u></b>	<b>103.</b>
<b>FOLDING.</b>	<b>103.</b>
<b>First Deformation B<sub>1</sub>.</b>	<b>104.</b>
<b>Minor B<sub>1</sub> structures.</b>	<b>104.</b>
<b>Major B<sub>1</sub> structures.</b>	<b>107.</b>
<b>Second Deformation B<sub>2</sub>.</b>	<b>108.</b>
<b>Minor B<sub>2</sub> structures.</b>	<b>108.</b>
<b>Major B<sub>2</sub> structures.</b>	<b>109.</b>
<b>Third Deformation B<sub>3</sub>.</b>	<b>109.</b>
<b>Minor B<sub>3</sub> structures.</b>	<b>109.</b>
<b>Major B<sub>3</sub> structures.</b>	<b>111.</b>
<b>Macroscopic Geometry.</b>	<b>113.</b>

Discussion.	113.
CHRONOLOGICAL ANALYSIS OF CRYSTALLIZATION AND DEFORMATION IN THE ADELAIDE SUPERGROUP AND KANMANTOO GROUP ROCKS.	115.
Introduction.	115.
Crystal growth pre-tectonic to B <sub>1</sub> .	115.
Crystal growth syntectonic to B <sub>1</sub> .	116.
Crystal growth post tectonic to B <sub>1</sub> .	116.
Crystal growth syntectonic to B <sub>2</sub> .	117.
Crystal growth post tectonic to B <sub>2</sub> .	117.
Crystal growth syntectonic to B <sub>3</sub> .	118.
Crystal growth post tectonic to B <sub>3</sub> .	118.
Conclusions.	119.
PETROFABRICS.	119.
Introduction.	119.
Quartz Petrofabrics - Adelaide Supergroup Quartzites.	120.
Discussion.	122.
Quartz and Biotite Petrofabrics. - Kanmantoo Group.	123.
Discussion.	124.
FAULTING.	125.
The Nairne Fault.	125.
Faults in the Kanmantoo Group rocks.	126.
<u>BIBLIOGRAPHY.</u>	
APPENDIX 1	CHEMICAL ANALYSES OF CO-EXISTING FELDSPARS. (1)
APPENDIX 2	MUSCOVITE GEOTHERMOMETRY AND COMPARISON OF (111) MUSCOVITE COMPOSITIONS DETERMINED BY X-RAY DIFFRACTOMETRY AND WET CHEMICAL ANALYSIS

APPENDIX 3	COMPARISON OF PLAGIOCLASE COMPOSITIONS DETERMINED BY OPTICAL, X-RAY AND CHEMICAL TECHNIQUES.	(viii)
APPENDIX 4	SCAPOLITE PETROFABRICS QUARTZ PETROFABRICS - BIMICA SCHISTS, ADELAIDE SUPERGROUP.	(xiv)
APPENDIX 5	DESCRIPTION OF PETROFABRIC SPECIMENS	(xvi)
APPENDIX 6	OPTIC AXIAL ANGLE AND REFRACTIVE INDEX DETERMINATIONS. DETERMINATION OF SCAPOLITE COMPOSITIONS.	(xix)



## SUMMARY.

The structure and petrology of Upper Precambrian and Cambrian rocks have been studied in detail, in an area 28 miles north-east of Adelaide, South Australia. The rocks occur within a broad zone of high grade metamorphism on the eastern side of the Mt. Lofty Ranges.

The Upper Precambrian succession consists predominantly of pelitic and semi-pelitic schists, quartzites, calc-silicate rocks and calc-schists, and the Cambrian sequence of quartzo-feldspathic schists, migmatites, granite gneiss, calc-silicate rocks and minor pelitic schists and quartzites.

The rocks have reached the sillimanite grade of metamorphism and the metamorphism is of the low pressure-intermediate type.

Dolerites, pegmatites, minor granodiorites and granites intrude the meta-sediments.

Mineralogical and structural relationships of the granite gneiss, indicate that it has been formed by recrystallization of the quartzo-feldspathic schists. Small scale metamorphic differentiation, appears to have accompanied the recrystallization. The migmatites are believed to have been formed by metamorphic differentiation rather than by anatexis.



Three phases of deformation are recognised in the Upper Precambrian rocks and two in the Cambrian. The second deformation recorded in the Upper Precambrian rocks does not appear in the Cambrian rocks. Each deformation has been accompanied by the formation of foliation. In the Proterozoic rocks deformed by the second and third phases of folding, the foliation is a crenulation cleavage. The deformations in both the Upper Proterozoic and Cambrian sequences are considered to be related. Petrofabric studies of quartz, scapolite and biotite are related to the respective macroscopic structures. An analysis of the chronology of crystallization and deformation of these rocks indicates that crystallization continued during and after each phase of deformation.

Faulting commenced either prior to or during metamorphism. Intense metasomatic activity followed a later phase of faulting resulting in the widespread development of albitites and in some cases talc ore bodies. The albitites formed in the fault zone were subsequently brecciated by further movement and later healed by the introduction of more metasomatic fluid.

## ACKNOWLEDGEMENTS.

This project was initially suggested to the author by Dr.A.W. Kleeman. The author has discussed various aspects of the field work with Dr.J.L. Talbot and Dr.K.J. Mills of the University of Adelaide, and Dr.B. Hobbs of the University of Sydney. Certain sections of the petrology have been discussed with Dr.R.L. Oliver, Dr.A.W. Kleeman, Mr.D. Virgo of the University of Adelaide and Dr.A.J.R. White of the Australian National University. Mr.A. Whittle, D. Ayres and W. Lindquist, Economic Geology Dept., University of Adelaide, assisted the author with the microragraphy.

Dr.A.W. Kleeman read part of the initial draft and Dr.B. Daily read the Introduction and Stratigraphy sections. The author is particularly indebted to Dr.J.L. Talbot for his reading and critical examination of the whole manuscript.

Mr.J. Lorenzin prepared the thin sections and Miss A.M.C. Swan assisted with the layout of some maps. Mrs.R. Shertland typed the draft copies and the final manuscript, and Miss S. Sumner the text figure descriptions. The author also wishes to express his gratitude to his wife for the preparation of the photographic figures and for the help and encouragement she gave during the writing of the thesis.

The expenses incurred during the field work and the reproduction of the line drawings were defrayed by the University of Adelaide Research Grant Fund.

This thesis contains no material which has been  
accepted for the award of any other degree or  
diploma in any University and that, to the best  
of my knowledge and belief, contains no material  
previously published or written by another person,  
except where due reference is made in the text of  
the thesis.

All specimens referred to in this thesis are catalogued in the museum of the Geology Department of the University of Adelaide. Specimens with the prefix A200- have been collected by the author; those with the prefix A126- , or GAC- and A9- are specimens lent to the author by Dr.A.W. Kleeman (University of Adelaide) and Dr.G.A. Chinner (University of Cambridge). The catalogued information includes the name of the rock, the catalogue number and the approximate location. The location of each specimen is given as a national grid reference as shown on the Gawler 1 inch to 1 mile Military Sheet (Fig.2) and reproduced on Plate 1.

## INTRODUCTION.

The area investigated and discussed in this thesis covers 35 square miles of pastoral country in the Pewsey Vale area, approximately 28 miles north-east of Adelaide (Figs.1 and 2). It contains folded and metamorphosed Upper Precambrian and Cambrian rocks in faulted contact. Intruding them are small bodies of dolerite, granite and pegmatite (Plate 1). Extensive metasomatism has altered some of the metamorphic and igneous rocks to albitites.

This region forms part of the Mt. Lofty Ranges, an arcuate belt made up of "Archean", Precambrian and Cambrian rocks (Figs.1 and 3). Unconsolidated Permian and Tertiary sediments also occur within the ranges (Fig.3). The relationship between the older rocks is shown in Table 1.

### "Archean".

The "Archean" rocks occur as isolated inliers overlain unconformably by rocks of the Adelaide Supergroup (Fig.1). They consist of high grade meta-sediments, metasomatic and igneous rocks, which have undergone retrograde metamorphism before the deposition of the Adelaide Supergroup (Talbot, 1963).

The terms "Houghtonian Complex" (Howchin, 1926), "Barossa Series" (Woolnough, 1908; Hossfeld, 1935) and "Houghton Complex" (Talbot, op.cit.), have been used to describe the

FIG.1.

General relationships between the  
Lower Precambrian, Upper Precambrian  
and Cambrian. The area studied is  
outlined.

# LOCALITY MAP

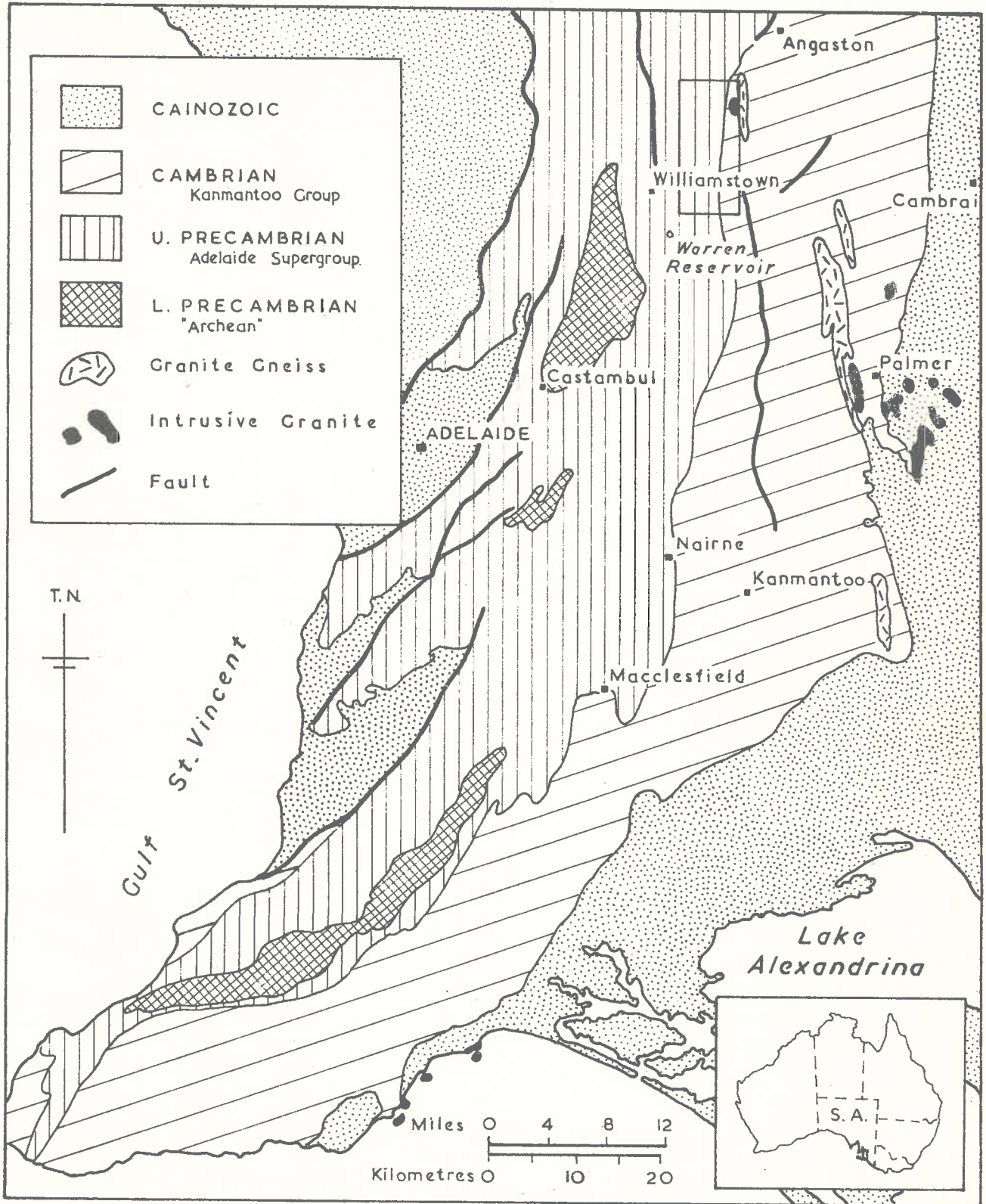


FIG. 1

FIG.2.

Part of the Gawler Military Sheet.

Scale 1 inch = 1 mile. The area  
studied is outlined.



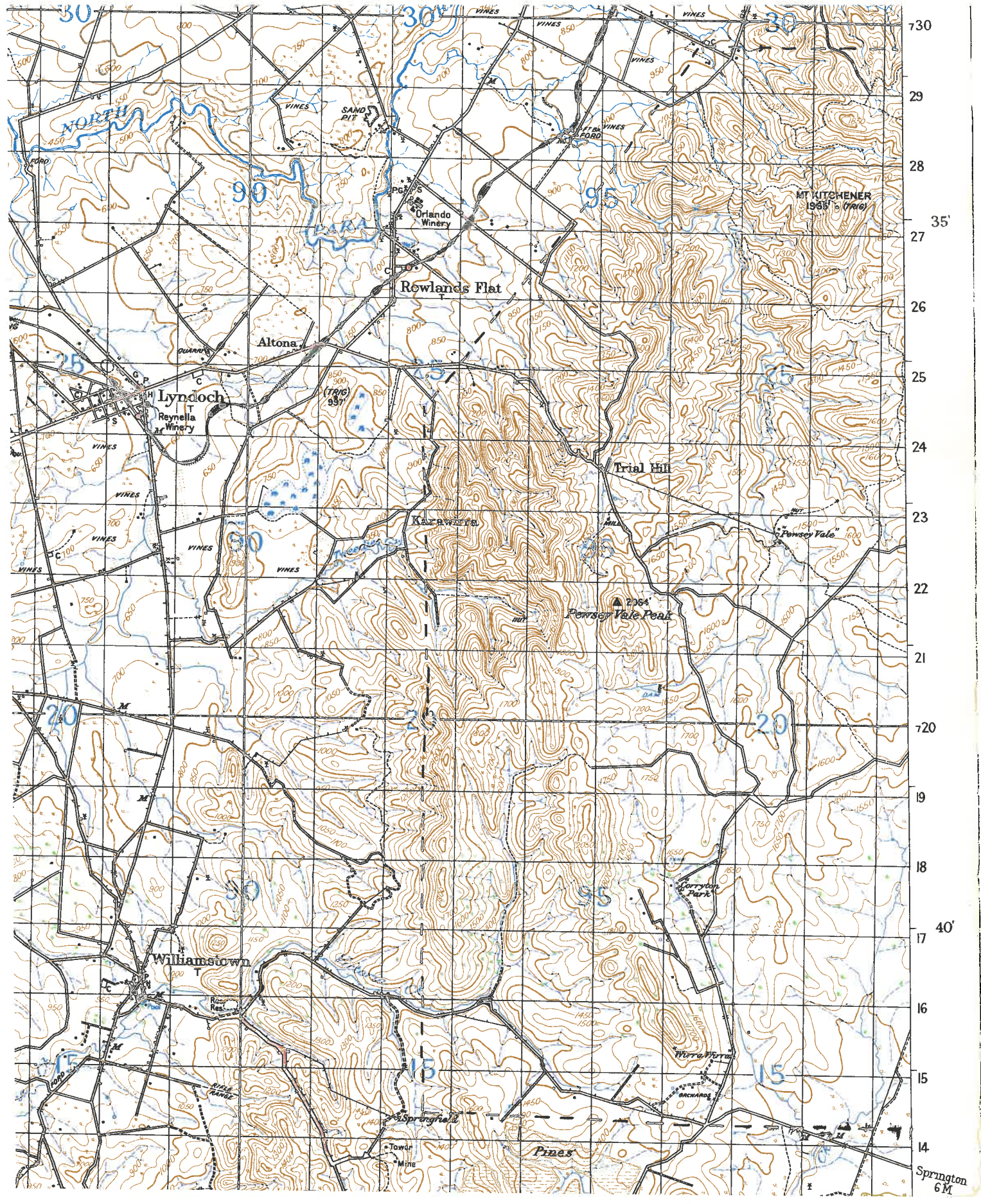


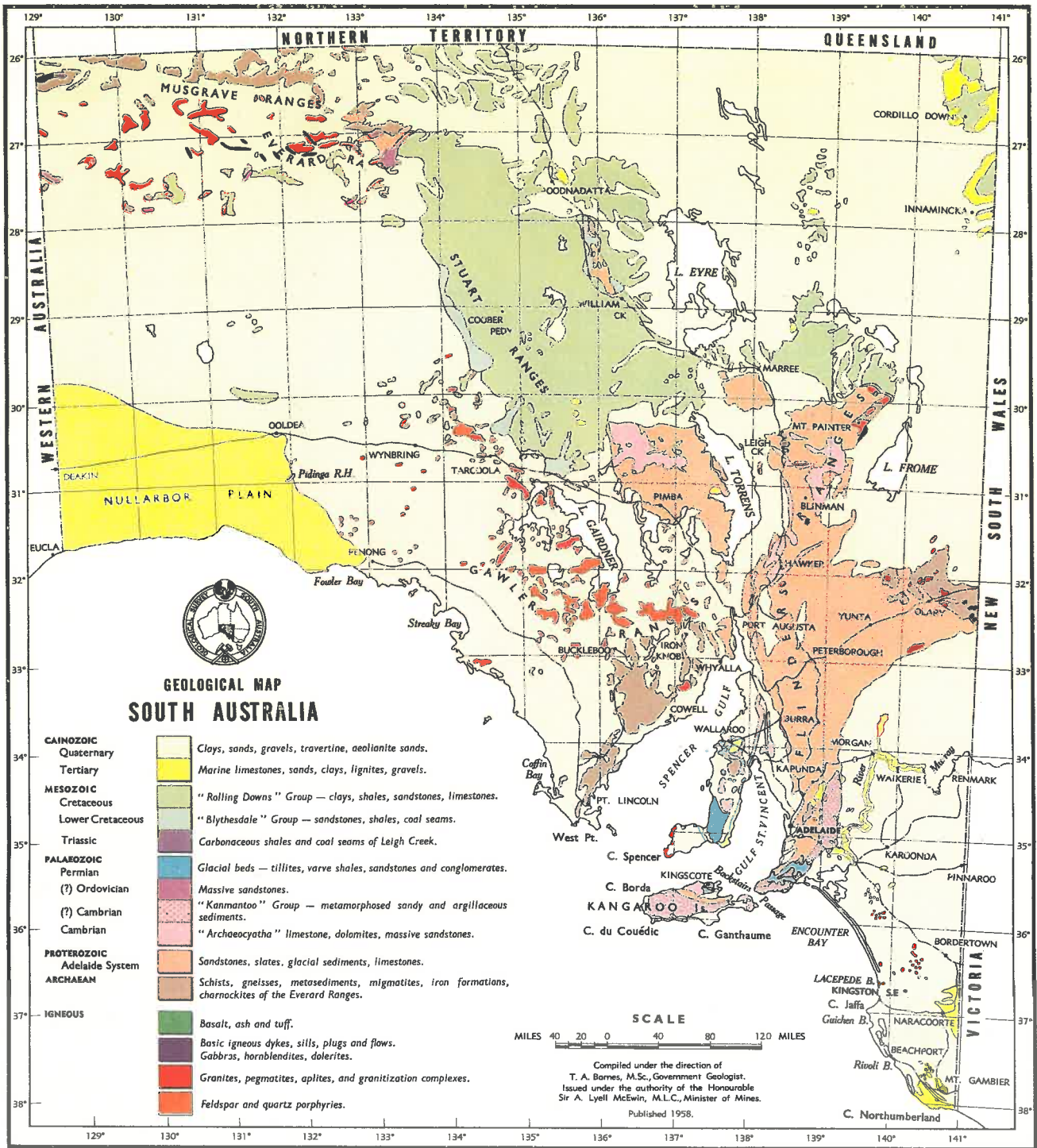
TABLE 1.

Age	Eastern Mt. Lofty Ranges.	Western Mt. Lofty Ranges
Cambrian	Kannantoo Group Lower Cambrian 1	Kannantoo Group <sup>2</sup> Lower Cambrian
Contact	Conformable, unconformable or faulted.	Conformable or unconformable.
Proterozoic	Adelaide Supergroup.	Adelaide Supergroup.
Contact	Violent unconformity.	
"Archean"		

1. Age documented by fossils only in the Delamere region, in the Southern Mt. Lofty Ranges.
2. Only 450 feet exposed compared with 30,000 feet in the Cape Jervis region - see text.

FIG. 3.

Geological map of South Australia.



rocks of the Houghton-Baressa inlier (Plate 2<sup>1</sup>). An "Archean" age was first proposed by Howchin (1908) for these basement rocks. Their true age is however, unknown. Radiometric determinations indicate that they are at least of Middle Proterozoic age (U/Pb, 1,510m.y.±100, Collins et al., 1953; 1,660 m.y.±25, Greenhaigh and Jeffery, 1959), but<sup>as</sup> these ages refer only to the age of metamorphism, the rocks can be expected to be much older.

#### Adelaide Supergroup.

Unconformably overlying the "Archean" basement is a thick sequence, (28,000 feet, Mawson and Sprigg, 1950) of limestones, quartzites, shales and glaciogenic sediments, which were deposited in an elongated zone extending from Kangaroo Island to the northern border of the state. This site of extensive sedimentation, referred to as the "Adelaide Geosyncline" (Sprigg, 1932), was active during the late Precambrian and early Palaeozoic times.

The Adelaide Supergroup rocks have previously been referred to as the "Adelaide Series" (David, 1923), the "Adelaide System" (Clarke, 1938; Mawson, 1948) and the "Adelaide Supergroup" (Daily, 1963). Mawson and Sprigg (1950) formally defined the Adelaide System and subdivided the sequence found in the Adelaide region into three series, the Torrensian, Sturtian and Marinoan. Subsequently,

---

1. All locality names mentioned subsequently in the text are given in Plate 2.

Sprigg (1952) added a fourth division, the Willouran Series,<sup>1</sup> which is considered to be older than the Torrensian. Daily (op.cit.) proposed that the terms Supergroup and Group replace the time-rock terms System and Series, a proposal which has been adopted in this thesis.

The Adelaide Supergroup rocks pass conformably<sup>2</sup> into fossiliferous Lower Cambrian on the western and lower south-eastern sides of the Mt. Lofty Ranges, and are therefore considered to be Upper Proterozoic in age. Rb/Sr determinations indicate that the base of the Adelaide Supergroup rocks is either Middle or Upper Proterozoic (Compston et al., in press).

### Kanmantoo Group.<sup>3</sup>

The Kanmantoo Group sediments occupy an arcuate belt on the eastern side of the Mt. Lofty Ranges from beyond Angaston in the north, to Kangaroo Island in the south, a distance exceeding 200 miles (Sprigg and Campana, 1953; Figs. 1 and 3). They consist of a thick (more than 30,000 feet), unfossiliferous and monotonous sequence of greywackes, silty phyllites, siltstones, and micaceous quartzites, with minor orthoquartzites, conglomerates and limestones (Sprigg

- 
1. Type area about 350 miles north of Adelaide.
  2. An unconformity between the Cambrian and Precambrian in the Normanville-Sellick Hill region was originally proposed by Thomson and Horwitz (1961), but in 1962 they apparently rejected this hypothesis (Thomson and Horwitz, 1962).
  3. Type section occurs between Campbell Creek and Rosetta Head, Victor Harbour, in the Cape Jervis region (Sprigg and Campana, 1953).

and Campana, op.cit.) The deposition of these "flysch like" sediments is believed to have been initiated by a Lower Cambrian orogeny (Daily, 1956).

In the southern Mt. Lofty Ranges, the Kanmantoo Group conformably overlies fossiliferous Lower Cambrian, but in other areas the stratigraphic and structural relationships are not clear, since outcrops are poor and fossiliferous or distinctive lithological marker horizons are absent. However, despite these difficulties many interpretations have been put forward.

Originally, the Adelaide Supergroup and Kanmantoo Group rocks were considered to be in faulted contact (the Nairne Fault, Sprigg et al., 1951). Subsequently, Campana and Horwitz (1955) suggested that the Kanmantoo Group was transgressive over folded "Adelaide System" sediments, but this was later rejected by Kleeman and Skinner (1959) on the grounds that there was no evidence for an earlier period of folding involving the "Adelaide System". In the same year Horwitz et al. (1959) proposed that both the Lower Cambrian and Kanmantoo Group sediments were transgressive over eroded and folded "Adelaide System" rocks. The author has found that the Kanmantoo Group and Adelaide Supergroup rocks are in faulted contact in the Pewsey Vale region (see Chapter 11).

Because of the widespread metamorphism affecting the Kanmantoo Group, its age was regarded as "Archean" (Woolnough, 1908; Hossfeld, 1935), or Precambrian (Howchin, 1929). Madigan (1925) was the first to assign a Cambrian age to these rocks. Later, on structural and stratigraphic evidence, Sprigg and Campana (1953) suggested a Cambrian to Ordovician age. It is now generally accepted that the Kanmantoo Group is Cambrian in age, and this has been supported by recent radiometric datings (White et al., in press).

#### Early Palaeozoic Orogeny.

The Adelaide Supergroup and Kanmantoo Group sediments were deformed and metamorphosed during an early Palaeozoic orogeny. Deformation "was achieved by jostling and warping of the Archean basement of the geosyncline" (Webb, 1958).

The metamorphism (Rb/Sr, approx. 465m.y., Compston et al., in press) produced at its peak, a north-south elongate belt of amphibolite facies rocks, extending from Tanunda to below Strathalbyn, on the eastern side of the Mt. Lofty Ranges (Fig. 4). Within this belt there are granite gneisses, migmatites and pelitic schists containing andalusite, kyanite,


- 
1. In this category Madigan included rocks which are now known to belong to the Adelaide Supergroup.



FIG.4.

General relationships of the meta-  
morphic zones in the Mt. Lofty Ranges.

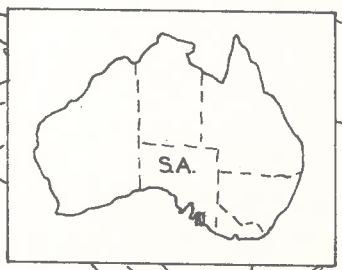
FIG. 4.

-  NON METAMORPHOSED TO L. GREENSCHIST FACIES.
-  M-U. GREENSCHIST FACIES.
-  ALMAND. AMPHIBOLITE FACIES.
-  MIGMATITE ZONE.
-  GRANITE GNEISS
-  GRANITE

T.N.



Gulf St. Vincent.



R.A. 66

and sillimanite, as well as synkinematic dolerite and granite intrusions (e.g. Palmer Granite, Rb/Sr, 480m.y.+15, White et al., in press).

Igneous activity culminated in the intrusion of post kinematic granites of batholithic dimensions into the Kannantoo meta-sediments (Victor Harbour Granite, K/A, 457 m.y. Everden<sup>n</sup> and Richards, 1962). A revival of tectonic activity occurred during the Tertiary Period, particularly in the late Pliocene to Early Pleistocene times. The area now occupied by the Mt. Lofty Ranges was strongly uplifted by doming and faulting, and the landscape rejuvenated.

#### Purpose of the Present Investigation.

Since the publication of the first 1" to 1 mile sheet by the S.A. Geological Survey in 1951, major advances have been made in the understanding of the stratigraphy and structure of the Precambrian and Cambrian rocks of the Mt. Lofty Ranges. However, more detailed structural, stratigraphic, metamorphic and igneous studies still remain to be done, particularly on the eastern side of the ranges, where deformation and metamorphism are dominant aspects of the geology. Here our knowledge of the position of mineral isograds and their significance, and the relationship of deformation to metamorphism, is extremely limited. In addition, the number of phases of folding recorded in these rocks is known only in a few, small isolated areas. Furthermore, many stratigraphical

problems are as yet unsolved, particularly the relationship between the Kanmantoo Group and the Adelaide Supergroup meta-sediments.

It is the purpose of the present investigation to try and elucidate some of the problems outlined above by the mapping and study of a small representative area (Fig.1).

#### Physiography.

The physiographic features in the present area have resulted from Tertiary to Recent uplift of an old eroded (Pre-Tertiary) land surface (Campana, 1955; Dalgarno, 1961). Remnants of this surface are now found at elevations of 1,500 to 1,600 feet, 500 feet above the floor of the adjacent Barossa Valley. Mt. Kitchener (elevation 1,965 feet), Pewsey Vale Peak (elevation 2,064 feet), are former monadnocks (Specht et al., 1961). Dissection of this plateau has been most active along the fault scarp east of Rowlands Flat (Fig.2, 5a). Away from the fault scarp, the topography is mature, outcrops are more scattered, and alluvial flats cover much of the area (Fig.5b). The main watercourse is Jacobs Creek, an antecedent stream, which cut down through the Palaeozoic rocks during the Tertiary uplift.

#### Previous Investigations.

The earliest geological investigations in this area were entirely petrological (Moulden, 1895; Woolnough, 1904). Hossfeld (1935) produced the first geological map of the area in his study of the "Geology of part of the North Mt. Lofty

FIG.5A.

General view of the fault scarp topography adjacent to Tweedies Gully, looking north-west from location 940 200. Barossa Valley appears in the background.

FIG.5B.

General view of the more mature topography beyond the fault scarp, looking east from Pewsey Vale Peak.



FIG.5A.



FIG.5B.

Ranges". Subsequently, Whittle (1951) mapped and assessed the talc deposits on the western side of the area and later, Campana (1953) included this area in his regional mapping of the Gawler Sheet. Chinner (1955) mapped a portion of the area during his investigation of the granite gneisses of the Barossa Ranges.

CHAPTER 1.STRATIGRAPHY.Adelaide Supergroup.

In the area studied the Adelaide Supergroup sediments are represented principally by mica schists with less common quartzites, calc-silicate rocks, calc-schists and garnet schists (Plate 1). Many of the quartzite and garnet schist bands can be traced over distances of 2 to 3 miles. A few of the thinly bedded quartzites in the upper part of the sequence grade laterally to quartz rich calc-silicate rocks. Sedimentary structures, such as cross-bedding and heavy mineral layering, are rare, and are generally confined to the quartzites. On a regional scale, extensive thinning of the less competent beds has occurred on the limbs of the major folds, while others (e.g. the beds overlying the garnet schists in unit 1) are markedly thickened.

The sequence can be broadly subdivided into three main lithological units, a lower unit of (1) mica schists and calc-schists, a middle unit (2) of muscovite rich schists and (3), an upper unit of quartzites, calc-silicates and mica schists<sup>1</sup> (Table 2). The sequence is approximately 5,000 feet thick.

In his report on the Geology of the Gawler Military Sheet,

---

1. The thickness was measured parallel to the axial plane of the major folds.



Campana (1955) correlates the rocks in this area with the "Torrensian Series",<sup>1</sup> and equates the quartzites of unit (3) with the "Stonyfell Quartzite" in the type section near Adelaide (Table 2). The author agrees with Campana's first correlation because the meta-sediments in the present area are structurally continuous with Torrens Group meta-sediments near Williamstown. However, his second correlation must be treated with caution as the Powsey Vale Quartzites cannot be traced continuously to the "Stonyfell Quartzite" in the type section.

During the present investigation two small pebble beds, which resemble tillite, were found in the upper part of the sequence. They could be equated with the Sturt Tillite in the type section, but in the absence of any evidence for a glacial origin, it is considered unwise to make this correlation.

#### Kanmantoo Group.

The meta-sediments of the Kanmantoo Group are separated from the Adelaide Supergroup rocks by the Nairne Fault (see page 4). These meta-sediments consist principally of cross-bedded quartz-feldspathic schists, migmatites and granite gneisses, with intercalations of calc-silicate rocks, pelitic schists, minor quartzites and graphitic schists. The only

---

1. Now called the Torrens Group-see page 3.

TABLE 2.

ADELAIDE SUPERGROUP SUCCESSION.

<u>Pewsey Vale Area.</u>	<u>Type Area.</u> (Mawson and Sprigg 1950).
<p>3. Interbedded calc-silicate rocks, calc-schists, mica schists, minor garnet schists. Quartzites, quartz rich calc-silicate rocks, mica schists. Pebble bed. Quartz rich calc-silicate rocks, quartzites, mica schists. Pebble bed. Quartzites. Minor mica schists, quartz rich calc-silicate rocks.</p> <p>2. Muscovite rich schists, minor quartzites, mica schists, sillimanite-muscovite schists.</p> <p>1. Calc-silicate rocks, calc-schists, mica schists, garnet schists.</p>	<p>Glen Osmond slates with occasional thin dolomite bands. Beaumont Dolomites and interbedded slates.</p> <p>Upper slates (and phyllitic phases) with minor quartzites.</p> <p>+Stonyfell quartzite, in part arkosic and argillaceous.</p> <p>Lower slates (and phyllites) with included minor quartzites.</p> <p>Montacute Dolomite -- blue and grey dolomites, limestones and sedimentary magnesites with chert bands and minor quartzites. Slates and phyllites with minor quartzites.</p> <hr/> <p>Violent unconformity with "Archean".</p>

+ Correlation after Campana (1955).

persistent marker beds occur in the lower part of the sequence west of Mt. Kitchener (Plate 1). The sequence is presented in Table 3. The minimum thickness of units 1 to 6 is approximately 1,500 feet. However, the thickness of the quartzofeldspathic schists, migmatites etc. of unit 7 cannot be determined, as they have been tightly folded and strongly transposed.

Chinner (1955) proposed the name "Kitchener Sequence" for the schists, calc-silicates and quartzite in the Mt. Kitchener region and equated the quartzofeldspathic schists, granite gneisses and migmatites, which conformably overlie them, with the Kannantoo Group. However, this present study supports Campana (1955), who correlated the whole of the succession in this area with the Kannantoo Group. Furthermore, the units underlying the quartzofeldspathic schists can be tentatively correlated with those above the impure marbles recorded by Mills (1964) in the Cambrai region. Mills (op.cit.) considers that the impure marbles are equivalent to the Macclesfield Marble, a formation earlier placed in the Lower Cambrian by Sprigg and Wilson (1954), and later in the basal portion of the Kannantoo Group (Horwitz et al., 1959). If the more recent investigations of Horwitz et al. (op.cit.) are correct, the lowest unit of the Pewsey Vale succession is above the base of the Kannantoo Group.

The thick sequence of cross-bedded quartzofeldspathic

TABLE 3.

KANMANTOO GROUP SUCCESSION.

YOUNGEST	7	+Cross-bedded quartzo-feldspathic schists, migmatites, granite gneisses, minor sillimanite schists, calc-silicate rocks.
	6	Calc-silicate rocks, minor calc-schists, quartzo-feldspathic schists.
		Fault.
	5	Quartzite.
	4	Sillimanite schists, garnet schists, fine grained quartz-biotite schists. Migmatites, quartzo-feldspathic schists. Fine grained, cross-bedded, quartz-biotite schists with minor pelitic schist intercalations. Porphyroblastic muscovite schists and minor quartzo-feldspathic schists.
	3	Calc-silicate rock, often garnet bearing.
	2	Quartzite.
	1	Graphite schist, minor calc-silicate rock. Quartzo-feldspathic schists.

OLDEST

+ Inman Hill Formation equivalent.

schists at the top of the succession (Table 3) are lithologically similar to the meta-arkoses of the Inman Hill Formation (Forbes, 1957), one of the most persistent units in the Kanmantoo Group. On the basis of mapping on the adjacent Cambrai sheet, Thomson (pers. comm.) correlates the Pewsey Vale quartzo-feldspathic schists with the Inman Hill Formation to the south. In other parts of the Mt. Lofty Ranges, the Inman Hill Formation is overlain conformably by the Brukunga Formation (Thomson and Horwitz, 1962), but this has not been observed in the present area. Thus, the succession in the Pewsey Vale region appears to occur above the base of the Kanmantoo Group and below the Brukunga Formation.

#### Tertiary.

Ferruginous quartz gravels of possible Tertiary age (Campana, 1955) form small knolls at an elevation of 1,600 to 1,700 feet on the slopes of the quartzite ridges in the southeast corner of the area (Plate 1). The gravels consist of angular fragments of quartz and quartzite of varying size, some boulders reaching a maximum diameter of 18 inches. In the better exposed outcrops the grain size grades from coarse at the base to fine at the top. The angularity of the fragments, and the proximity of the quartzite ridges suggest that the gravels are scree deposits.

At an elevation of 1,550 feet lateritic profiles are developed, which are believed to have been formed during the Tertiary. At a lower elevation, grey sands are exposed.

PETROLOGY AND PETROGRAPHY OF THE KANMANTOOGROUP ROCKS.

The purpose of the next four chapters is to summarise the petrology and petrography of the various rock types in the Kanmantoo Group. The genesis of the Tanunda Creek Gneiss and the migmatites will be discussed, and the paragenesis of certain minerals in the pelitic schists will also be given. From the data provided in these discussions, conclusions will be made in a later chapter concerning the possible metamorphic temperatures and pressures to which the Kanmantoo Group rocks have been subjected. Reference will also be made to the significance of the sillimanite-potash feldspar assemblage in the pelitic schists.

The symbols  $S_1$  and  $S_3$  will be referred to in the text, where  $S_1$  is a foliation formed during the first deformation ( $B_1$ ) and  $S_3$  a foliation related to the second deformation ( $B_3$ ).

CHAPTER 2.QUARTZO-FELDSPATHIC SCHISTS AND MIGMATITES.Introduction.

Almost two thirds of the rocks of the Kanmantoo Group in the area mapped are quartzo-feldspathic schists (Plate 1). In different parts of the area they grade into migmatites or into the Tanunda Creek Gneiss (Chapter 3).

Quartzo-feldspathic Schists outside the Migmatite Zone.

The quartzo-feldspathic schists are generally well bedded, fine grained, pink to grey coloured rocks which closely resemble arkoses. The bedding is defined by the concentration of mica in layers and more rarely by heavy mineral layers. The schists part readily along these mica layers to form tabular outcrops. Associated with the "arkosic" schists are the "greywacks" variants which are strongly foliated and occur as sub-rounded outcrops. Cross-bedding is well developed and some fore-set units are up to 12 inches thick.

Petrography.

In thin section the quartzo-feldspathic schists are granoblastic (0.15 to 0.2mm.) and exhibit a poor to strong foliation. Some specimens show both bedding S and schistosity  $S_1$  or  $S_3$ . Many show a well defined girdle fabric in sections perpendicular to either  $B_1$  or  $B_3$ .

They consist of quartz, plagioclase, potash feldspar biotite and muscovite with zircon, magnetite, hematite,

tourmaline, apatite and monazite as accessories. Fourteen micrometric analyses given by Chinner (1955) and six determined by the author (Table 4) are plotted in Fig.6. It can be seen that they occupy the arkose and greywacke fields. The quartzo-feldspathic schists in this area are equivalent to the Inman Hill Formation, <sup>a formation</sup> consisting of meta-arkoses and meta-greywackes in the lower grade regions of the Mt. Lofty Ranges (Forbes, 1957; George, 1963). Stratigraphic and micrometric evidence therefore suggest that the quartzo-feldspathic schists are metamorphosed greywackes and arkoses.

The common mineral assemblages in the schists are:

- (1) Quartz-plagioclase-biotite-muscovite.
- (2) Quartz-plagioclase-biotite-muscovite-potash feldspar.
- (3) Quartz-plagioclase-muscovite.

Plagioclase ranges in composition from An<sub>11</sub> to An<sub>16</sub>.<sup>1</sup> Albite twinning is common and the lamellae are broad and continuous. Microfaulting of the twin boundaries is rare. Most plagioclases are fresh, but some are partially altered to sericite. Potash feldspar is commonly perthitic and exhibits cross-hatched twinning, which in some specimens is faint or shadowy. Monoclinic and triclinic forms have been identified by X-ray diffraction (Table 5). The biotite in these rocks is characteristically deep

---

1. See Appendix 1 for the chemical analyses of the plagioclases and potash feldspars.



**TABLE 4.**

**Modal Analyses of the Quartzo-feldspathic Schists.**

<u>Spec.No.</u>	40	39B	2	48	366-7C	866
Quartz	43.8	37.3	46.2	44.4	54.5	43.2
Plagioclase	22.4	24.4	31.4	45.8	26.2	24.8
K.Feldspar	5.7	-	4.3	2.5	3.0	15.8
Biotite )		29.2	15.0	6.3	15.1	10.6
)	26.9					
Muscovite )		6.9	3.1	1.0	-	-
Accessories	1.2	2.2	-	-	1.2	0.6
	<u>100.0</u>	<u>100.0</u>	<u>100.0</u>	<u>100.0</u>	<u>100.0</u>	<u>100.0</u>
<b>Total number counts</b>	<b>2,570</b>	<b>2,740</b>	<b>2,749</b>	<b>3,021</b>	<b>1,387</b>	<b>2,227</b>

FIG.6.

Composition of quartzo-feldspathic schists in terms of quartz, feldspar and micas (diagram after Pettijohn, 1949, p.227). Analyses by Chinner (1955) are designated by the full circle symbol; those by the author as a circle.

FIG 6

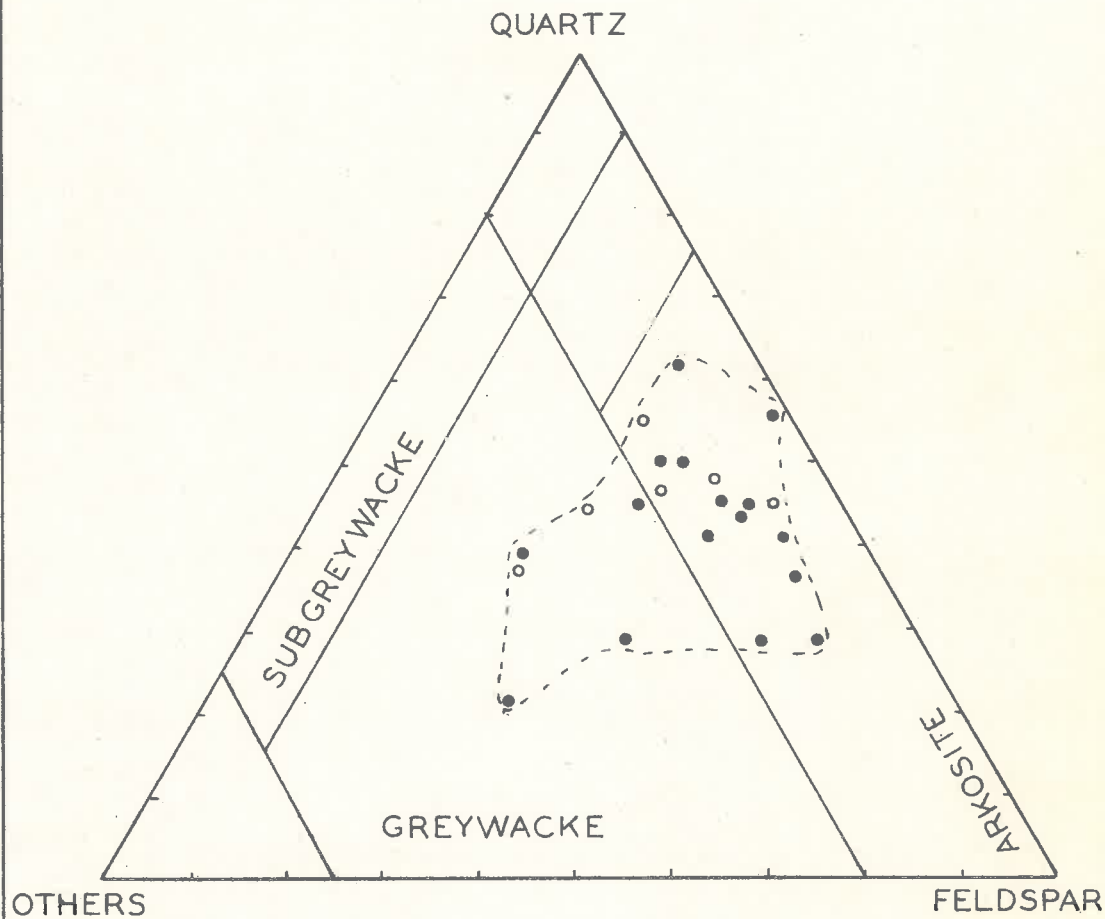


TABLE 5.

Obliquity<sup>1</sup> =  $\Delta$  values of the Alkali Feldspars.

<u>Spec. No.</u>	<u>Rock Type.</u>	$\Delta$	<u>Comments.</u>		
423 <sup>2</sup>	Quartzo-feldspathic schist	0.870-0.925	Sharp microcline twinning		
561 <sup>2</sup>	"	Near monoclinic <sup>3</sup>	Wavy	"	"
442 <sup>2</sup>	"	0.800-0.888	Sharp	"	"
670B	"	Near monoclinic <sup>3</sup>	Wavy	"	"
27	"	Monoclinic	No	"	"
871A <sup>2</sup>	"	0.875	Sharp	"	"
17	Pegmatitic segregation	0.888	"	"	"
39A	" "	0.925	"	"	"
869-1	" "	0.891	"	"	"

1. Obliquity (triclinicity) values have been measured according to the method of Goldsmith and Laves, (1954).
2. Quartzo-feldspathic schists within the migmatite zone.
3. Feldspars whose 131 and 131 peaks have coalesced to form a broad single peak, are considered to be "near monoclinic".

brown in colour (X = very pale brown to straw yellow, Y = Z = deep brown) and contains abundant pleochroic haloes. A chemical analysis of a typical biotite is given in Table 25 Chapter 10. Its composition is similar to that obtained by White (in prep.) for biotites from quartzo-feldspathic schists adjacent to the migmatite zone in the Palmer region. Muscovite appears either as thin bladed flakes parallel to the biotite foliation ( $S_1$  or  $S_3$ ) or as squat porphyroblasts cutting the foliation. Quartz occurs as equidimensional grains 0.1-0.2mm. in diameter, showing curved or slightly sutured borders. Undulose extinction is ubiquitous. Quartz-quartz contacts are normally curved except in the quartzo-feldspathic schists adjacent to the Tanunda Creek Gneiss, where they are straight and triple point junctions are at  $120^\circ$ .

#### Accessory Minerals.

Hematite, hematite-rutile and hematite-magnetite assemblages have been recognized in the quartzo-feldspathic schists. The hematite in all assemblages contains irregular or lamellar bodies of ilmenite and commonly occurs as rhombohedral plates. Rutile is intimately associated with the hematite and magnetite forms small octahedra. Tourmaline has a pleochroism (E = very pale green, O = deep green) which is common to all rock types of the Kannantoo Group. This contrasts with the colourless to golden brown pleochroism shown by most tourmalines in the Adelaide

Supergroup rocks. Zircon grains are characteristically well rounded (Fig.16, Chapter 3). Minor xenoblastic hornblende (X = pale olive green, Y = olive green, Z = deep green) and pale yellow secondary epidote occurs in the schists adjacent to the Tanunda Creek Gneiss.

Quartzo-feldspathic Schists within the Migmatite Zone.

West and south of Mt. Kitchener, strongly folded quartzo-feldspathic schists contain abundant quartz-feldspar veins and pods of variable grain size. Most veins are parallel to bedding (S), axial plane foliation (S<sub>1</sub> or S<sub>3</sub>) or the transposed limbs of small folds (Fig.7a; see also Ramsay, 1958, 1963), but some are parallel to joint planes. Many are discordant to foliation and others are tightly folded; the folds exhibit ptygmatic or similar profiles (Fig.7b). Pegmatitic pods occur in the hinges of small folds. Perthitic potash feldspar crystals up to 2 cm. in diameter have been observed in rare coarse grained veins. Biotite selvages and schlieren can be seen around and within most veins. Within the migmatite zone, the quartzo-feldspathic schists are more strongly foliated and coarser grained. Many have recrystallized to augen schists, the augen consisting of coarse quartz-feldspar aggregates or feldspar porphyroblasts. In a single hand specimen all variations between veins, augen schists and finer grained quartzo-feldspathic schists may be present (Fig.8).

The features shown by the rocks in this zone, namely the development of planar or folded veins surrounded by biotite

FIG.7A.

Leucocratic veins and pods parallel  
to foliation in migmatite. Location  
984 253. Scale in inches.

FIG.7B.

Folded, steeply plunging leucocratic  
veins in migmatite. Location 973 186.  
Pencil 6 inches long (15 cms).

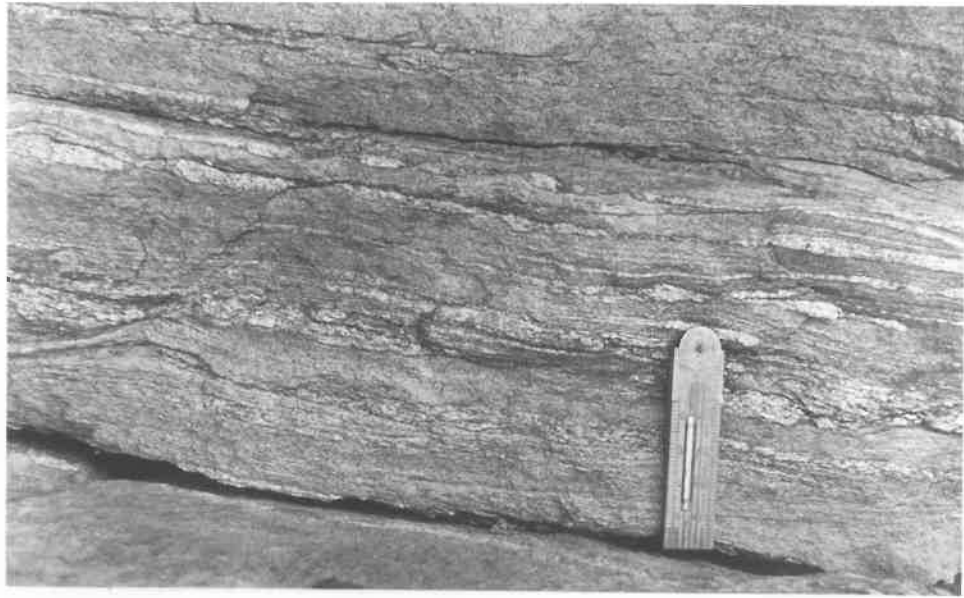


FIG. 7A.



FIG. 7B.



FIG.8.

A migmatite showing pegmatite (top),  
augen of feldspar (centre and bottom)  
and fine grained quartzo-feldspathic  
schist. Location 978 283. Spec.  
No. A200-814A.

FIG.9.

Photomicrograph showing corroded  
skeletal relics of muscovite (M)  
in microcline perthite (Mi).  
Location 971 160. Spec. No.A200-2B.

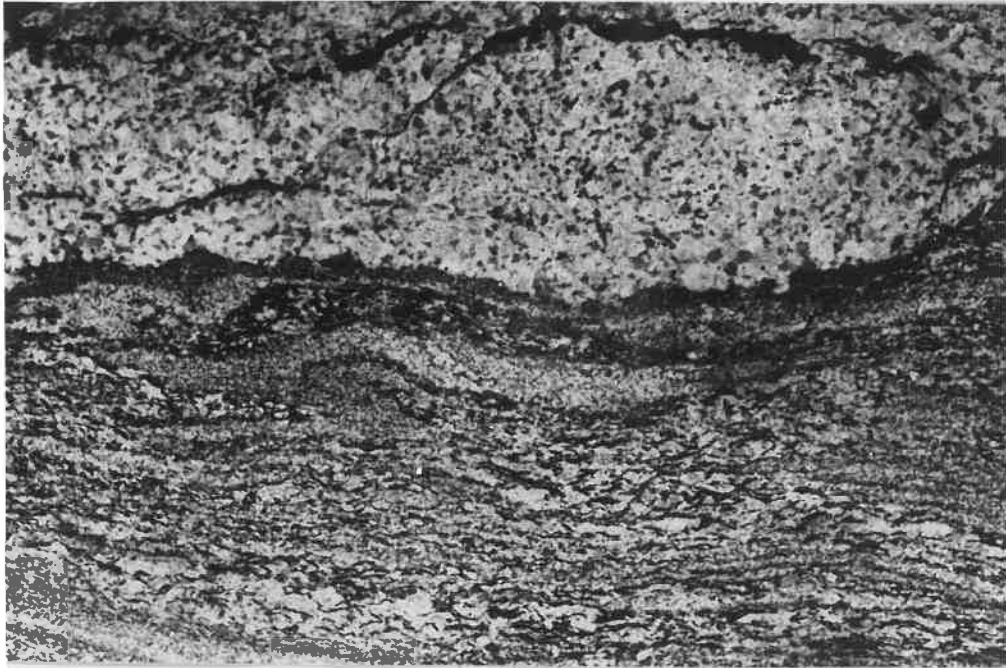


FIG. 8.

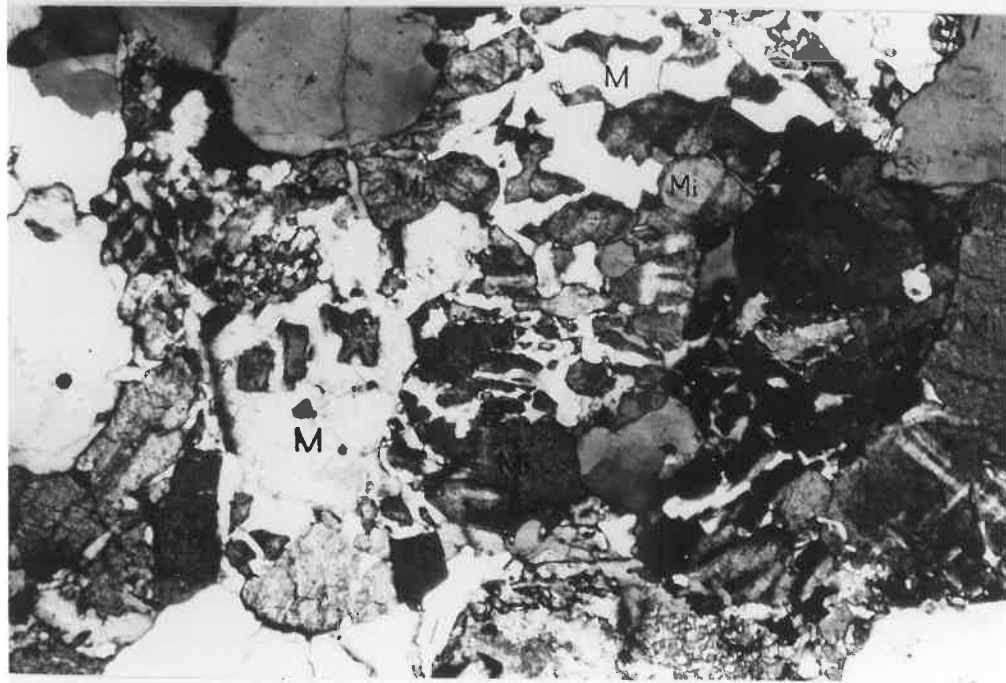


FIG. 9.

selvedges, and feldspar augen in schists, are similar to those described for other migmatite zones. (Read, 1931; Harry, 1952, 1954; Gindy, 1953; Mehnert, 1953, 1957, 1962).

### Petrography.

#### Quartzo-feldspathic Schists.

These rocks are coarser grained (0.2 to 0.5mm.) than the non-migmatized quartzo-feldspathic schists, and texturally show features <sup>typical</sup> of high grade metamorphic rocks. For example, quartz-feldspar boundaries are highly sutured, quartz - quartz interfaces are curved or amoeboid and potash feldspar-plagioclase boundaries are lobate. Plagioclase-plagioclase boundaries however, are straight and 120° triple points are present. Myrmekite has been observed in a few samples.

Suturing of feldspars by quartz has been ascribed to the replacement origin of quartz (Read, 1931; Cheng, 1944; Harry, 1954). However, there is no indication of a metasomatic introduction of SiO<sub>2</sub> in the quartzo-feldspathic schists. Small scale movement of SiO<sub>2</sub> activated by pressure or concentration gradients could also explain the sutured feldspar contacts.

Sillimanite and garnet are the only additional minerals to appear in the quartzo-feldspathic schists of the migmatite zone. The sillimanite occurs as fibrolitic tufts in biotite (c.f. Chapman, 1952; Chinner, 1961) or as isolated needle-like prisms associated with quartz.

Garnet appears sporadically as small crystals in a few specimens. Biotite is normally deep brown, but in the sillimanite bearing schists it is a characteristic reddish brown. Muscovite is less common in the migmatite zone and plagioclase compositions range from  $An_{10}$  to  $An_{21}$ . X-ray diffraction studies show that both monoclinic and triclinic forms of potash feldspar are present and that obliquity values vary in single specimens (e.g. 423, Table 5). Such variations in structural state seem to be common in rocks metamorphosed under the P-T conditions of the amphibolite facies (Heier, 1957, 1960; Shidô, 1958; Guitard et al., 1960; Dietrich, 1962; Smithson, 1962).

#### Veins.

The veins have the same texture as the quartz-feldspathic schists in the migmatite zone, but are coarser grained (0.4 to 4.5mm.). Most consist of quartz, potash feldspar and plagioclase (Table 6) and in some the potash feldspar content is higher than in the country rock (e.g. 48, Table 6).

The mineral assemblages present are:

- (1) Quartz-plagioclase-biotite-muscovite.
- (2) Quartz-plagioclase-potash feldspar-muscovite.
- (3) Quartz-plagioclase-muscovite-(sillimanite).
- (4) Quartz-plagioclase-potash feldspar-biotite-muscovite-(sillimanite).

Apatite, tourmaline, magnetite, zircon and rutile are accessories.

TABLE 6.

Diag.No.	<u>Modal Analyses of Veins.</u>							<u>Modal Analyses of Parent Rocks.</u>	
	6	3	2	5	1	7	4		
Rock No.	2B	48	2	17	814D	873	874A	2	48
Quartz	32.5	40.8	41.9	56.0	30.2	36.6	24.3	46.2	44.4
Plagioclase	19.5	31.5	34.7	20.6	61.3	16.9	38.8	31.4	45.8
K.Feldspar	39.7	20.6	11.5	21.0	2.0	29.8	31.9	4.3	2.5
Biotite	)	6.3	7.9	0.7	6.0	1.0	2.5	15.0	6.2
Muscovite	) 8.3	0.8	4.0	1.7	0.3	15.4	2.5	3.0	0.8
Magnetite	-	-	-	-	0.1	0.3	-	)	
Tourmaline	-	-	-	-	0.1	-	-	) 0.1	0.3
	-----	-----	-----	-----	-----	-----	-----	-----	-----
	100.0	100.0	100.0	100.0	100.0	100.0	100.0	100.0	100.0
	-----	-----	-----	-----	-----	-----	-----	-----	-----
Total No. Counts	1,920	1,783	2,573	6,003	2,560	2,257	1,422	2,749	2,251

Plagioclase ( $An_{10}$  to  $An_{23}$ ) shows a marked increase in grain size within the veins, ranging from 0.9mm. in the small pods to 4.5mm. in the pegmatitic veins. It has the same composition as the plagioclase in the parent rock, a characteristic of migmatites in other metamorphic terrains (Ramberg, 1956; Mehnert, Pt. III, 1962). Albite rims ( $An_2$ ) appear where plagioclase is in contact with potassium feldspar. Inclusions of relic quartz and plagioclase from the parent rock are present in the vein plagioclases.

Potash feldspar is structurally triclinic, the obliquities varying from 0.888 to 0.925 (Table 5). Both vein and shadow perthite are well developed, the vein perthite "healing" the fractures in deformed crystals. The zones around these fractures are totally barren of shadow perthite and it would appear that the albite has migrated into the fractures under the influence of a pressure gradient (Gates, 1953). Inclusions of relic biotite, magnetite and quartz from the host rock are commonly trapped in the potash feldspar and a peripheral zoning similar to that figured by Shido (1958, p. 168) occurs in some grains.

Quartz occurs as amoeboid, strongly sutured grains. The presence of curved quartz-quartz interfaces and variable triple junction angles indicates that the quartz has not reached textural equilibrium (Rast, 1965). Many quartz grains show undulose extinction, healed fractures and more rarely deformation lamellae.

Biotite (X = pale brown, Y = Z = deep chocolate brown) forms selvages at the country rock-vein border. Within the selvages

it shows a marked increase in grain size (e.g. in 814D 0.25mm. width compared with 0.05mm. in the schists). Rarely, reaction rims of albite and rutile occur between biotite and plagioclase. Muscovite is a common constituent of most veins, appearing as porphyroblasts or as skeletal corroded flakes in potash feldspar or plagioclase (Fig.9). Some grains contain altered, limonite stained biotite. Tourmaline forms poikiloblastic crystals enclosing microcline, plagioclase and quartz. Its size (up to 7.5mm.) is usually greater than that of other minerals and the pleochroic scheme (E = pale green, O = deep green) is similar to that of the tourmaline in the parent rock. Sillimanite is comparatively rare in these veins and occurs as very fine needle like crystals in quartz or microcline. The zircon in the migmatites are generally well rounded, but some are angular.

#### Quartz Veins.

Milky white quartz veins of varying dimensions occur in the quartzo-feldspathic schists and migmatites (Plate 1). The larger veins are approximately 100-300 feet long and 5-10 feet wide. They are generally parallel to bedding or foliation. ( $S_1$  or  $S_3$ ), but rare discordant veins have been observed. Many of the smaller veins fill tension gashes or joint planes and some have been boudined or folded during the second deformation ( $B_3$ ). All veins are devoid of silicate and

sulfide mineralization and there is no suggestion of wall rock alteration in the adjacent country rock. It is therefore considered that they have formed by the process of metamorphic segregation.

#### Origin of the Migmatites.

The origin of migmatites has been the subject of much research in the last 100 years. Ideas concerning their origin can be grouped into four categories:

- (1) Lit-par-lit magmatic injection (Sederholm, 1923; Read, 1931).
- (2) Anatectic melting (Eskola, 1933; Harne, 1962; Mehnert, 1962; Mills, <sup>1</sup>1964).
- (3) Metamorphic differentiation (Stillwell, 1922; Ramberg, 1952, 1956; White, <sup>1</sup>1956).
- (4) Metasomatism (Wagnann, 1935; Engel and Engel, 1958).

The corollaries of these hypotheses are discussed briefly in relation to the Pewsey Vale migmatites.

If the granitic portions of a migmatite are the result of lit-par-lit injection or anatexis they should have compositions which group around the low temperature trough of the Or-Ab-An-SiO-H<sub>2</sub>O system (Kleeman, 1965).

Where metasomatism is the cause of migmatization, distinct changes in mineralogy and composition should occur in the parent rock within the migmatite zone. For example, Engel and

---

1. Two hypotheses have been postulated by these authors for migmatites on the eastern side of the Mt. Lofty Ranges.



Engel (1958) noted with increasing migmatisation an increase in potash feldspar, a decrease in plagioclase, biotite and quartz, and an increase of the soda content of the plagioclase.

Migmatites formed by metamorphic differentiation should show:

- (a) a mineralogical compositional interdependence between host rock and pegmatite (Ramberg, 1956),
- (b) a zone surrounding the differentiation products (porphyroblasts, veinlets etc.) impoverished in constituents required for these products (Eskola, 1932; Ramberg, 1952; Reitan, 1960),
- (c) the same grade of metamorphism in the parent rock and migmatite (Ramberg, 1956).

To investigate these inferences, a close examination of the mineralogy of the veins and the parent rocks have been made. Six veins and two parent rocks have been micrometrically analysed (Table 6). The veins have been recalculated in terms of Or-Ab-An and are plotted in Fig. 10. The veins have a wide variation in composition and are not grouped about the low temperature trough, suggesting that they are neither magmatic nor anatectic in origin.

It is also unlikely that metasomatism has contributed to the formation of the migmatites, as the mineral assemblages of the migmatized and non-migmatized quartzo-feldspathic schists are the same. In addition, no major increase or decrease in either potash feldspar, plagioclase or quartz is observable in highly migmatized zones.

FIG.10.

Modal analyses of veins recalculated in terms of Or-Ab-An, plotted on the  $\text{SiO}_2$ -saturated surface of the Or-Ab-An- $\text{SiO}_2$  system at 5000 bars  $P_{\text{H}_2\text{O}}$ , projected onto the Or-Ab-An face of the tetrahedron (after Kleeman, 1965).

FIG.11.

Orientation of planar veins and axes of folded veins in migmatites. Fold axes are represented as x, axial plane of folded veins as o, veins parallel to the axial surface of  $B_1$  folds as +, veins parallel to the axial surface of  $B_3$  folds as ●, and veins parallel to foliation as ..

FIG. 10

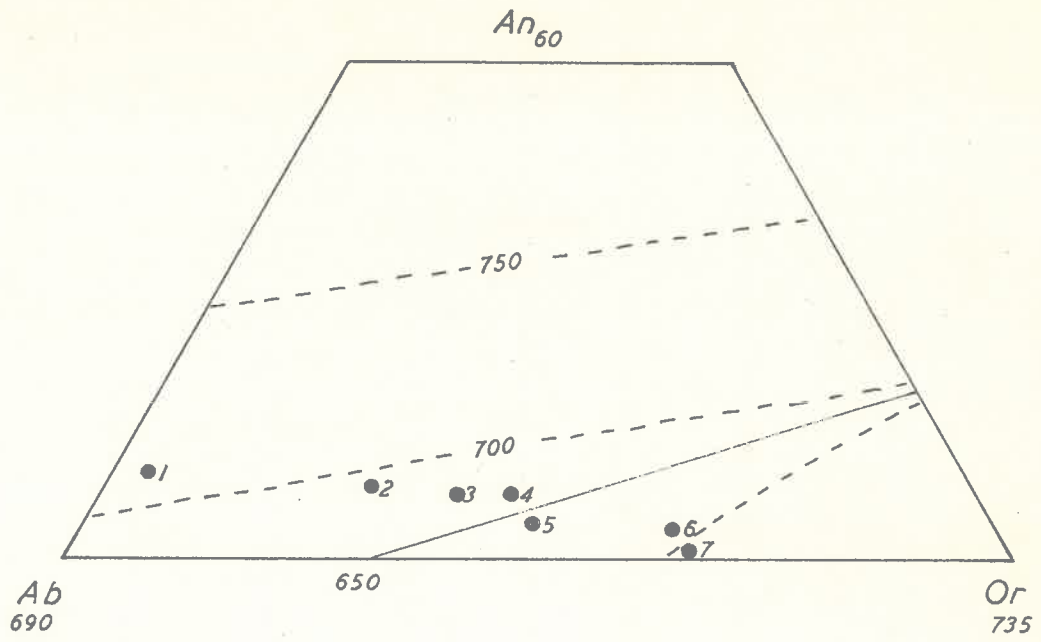
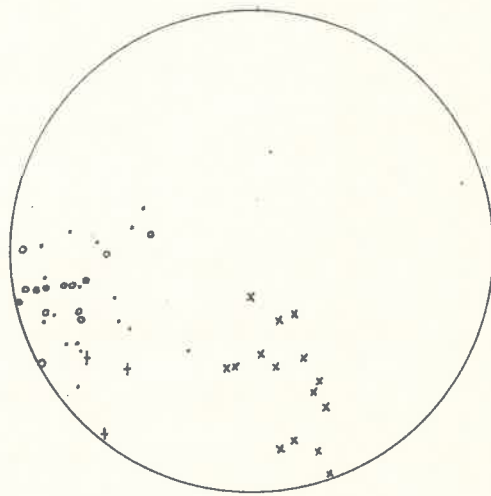


FIG. 11



The author considers that metamorphic differentiation satisfactorily explains the strong mineralogical and compositional interdependence shown by these rocks namely:

- (1) The plagioclase compositions in the host rock and vein are the same.
- (2) The accessory mineral suites in the parent rock and pegmatites are the same.
- (3) The mineralogy in the veins and host rocks are similar.

These relationships are consistent with recrystallization in situ but in some cases the potash feldspar content in the veins is higher than in the country rock (Table 6), suggesting that material has been added to the veins during the differentiation.

Presumably the processes of concretion, secretion and solution (Eskola, 1932; Ramberg, 1952) have contributed to the formation of the veins, pods, augen and pegmatites. The localisation of many veins in planes parallel to the sheared off limbs of small folds or to axial plane foliation, suggests that deformation has been important in initiating and creating sites for metamorphic differentiation (c.f. Ramberg, 1952, 1956).

#### Relative Age of the Migmatites.

As previously mentioned, the veins in the quartzofeldspathic schists of the migmatite zone, occur as planar or folded sheets. The orientation of these veins has been measured and plotted in Fig. 11. The folded veins plunge 5° to

75° in a direction 165°, and their axial planes strike 165° and dip 30° east to vertical. Their orientation suggests that they have been folded during the B<sub>3</sub> deformation. The orientation of the undeformed veins is consistent with the geometry of S<sub>1</sub> and S<sub>3</sub> (see Chapter 11). It appears then that these veins have formed during both periods of deformation.

### CHAPTER 3.

## THE TANUNDA CREEK GNEISS.<sup>1</sup>

### Introduction.

The Tanunda Creek Gneiss occurs within a zone of granite gneisses and migmatites on the eastern side of the Mt. Lofty Ranges (Fig.4). A portion of this gneiss outcrops on the eastern side of the area. It forms tor-like, tabular or stumpy outcrops, depending upon the composition and the fabric of the gneiss. Inclusions of quartzo-feldspathic schists and quartz reefs occur in the gneiss.

In hand specimen most of the gneiss is medium grained, strongly lineated and poorly foliated. Augen like aggregates of feldspar occur in some gneisses, and in biotite rich variants, foliation is well defined.

### Transitional Zone.

A zone containing unaltered country rock, schists with feldspar porphyroblasts and lenses or pods of gneiss, separates the quartzo-feldspathic schists from the main body of the gneiss. In this zone many gneissic pods are bordered by quartz lenses (Fig.12a) and others are surrounded by fine grained "aplitic" coronae (Fig.12b). The "aplitic" rocks also develop as isolated, irregular, bodies in the country rock or as cross-cutting "dykes" (Fig.13). Some gneiss lenses distort the

---

1. The name "Tanunda Creek" is taken from a stream which cuts the gneiss, north-east of Mt. Kitchener. This new name is used informally in this thesis to include both "Tanunda Creek Granite" and "Moorooroo Gneiss" erected by Hossfeld (1925, 1935) to describe different portions of the gneiss.

FIG.12A.

Lenticular pods of quartz (Q) at the border between granite gneiss (G) and fine grained quartzo-feldspathic schist (S). Location 983 315.

FIG.12B.

Granite gneiss pods (G) in well bedded fine grained quartzo-feldspathic schists (S). Note "aplitic" coronae (arrow) and discordant contact of the gneiss with the quartzo-feldspathic schists (barbed arrow). Location 983 315. Pen 5.5 inches (13.5 cms).



FIG. 12A.



FIG. 12B.



bedding, while others are clearly discordant to this layering. All the "aplitic" and gneissic bodies appear to be oriented parallel to structural surfaces such as bedding, foliation or fracture zones.

Petrography of the Transitional Zone.

Schists with feldspar porphyroblasts.

In many of the quartzo-feldspathic schists bordering the Tanunda Creek Gneiss, plagioclase and microcline perthite occur as porphyroblasts (0.45 to 1.0mm. in diam.) or as aggregates of smaller randomly oriented individuals. The foliation curves around many porphyroblasts. In the hornblende bearing schists the plagioclases are irregularly zoned (Fig.14) and different grains show a wide variation in composition (e.g. 564, Table 7). Such textural and compositional variations suggest that equilibrium textures have not been achieved during the crystallization of the porphyroblasts. Most porphyroblasts show a patchy alteration to either muscovite, epidote or both, and in some, potash feldspar inclusions are arranged in zones parallel to the crystal faces of the plagioclase. Myrmekite occurs at the contacts between the plagioclase in the ground mass and potash feldspar porphyroblasts.

"Aplitic" bodies and corause.

These rocks occur in bands of quartzo-feldspathic schists

FIG.13.

Irregular and dyke-like bodies of  
"aplite" in well bedded quartzo-  
feldspathic schists. Location 983 315.

FIG.14.

Irregular zoning in plagioclase from  
a hornblende bearing porphyroblastic  
schist collected from the transitional  
zone. Location 997 237. Spec. No.  
A200-584. X 50.

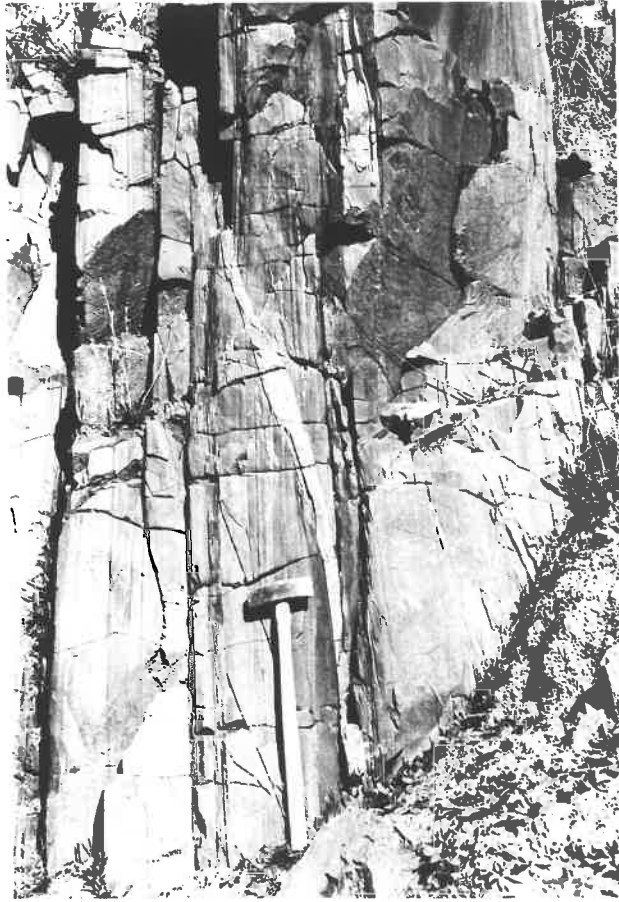


FIG. 13.

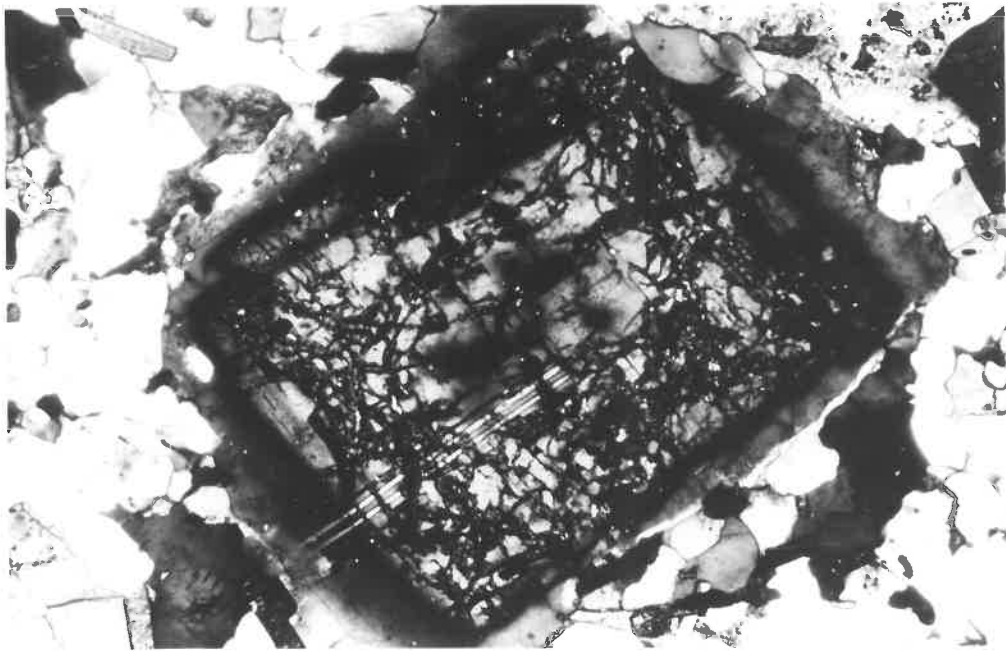


FIG. 14.

TABLE 7.

Composition of Plagioclases.

(U-stage determinations)

<u>Spec. No.</u>	<u>Composition</u>	<u>Twin Laws</u>
<b>Tanunda Creek Gneiss</b>		
878	An12.5-13	Albite
845	An23-27	"
72	An4-7	"
22	An10-12	"
798	An20	"
<b>Transitional Zone Specimens</b>		
866-7C	An16	"
" 7F	An17	"
" 7B	An8-10	"
" 7G	An20	"
584 (grain 1)	An40 (intermediate zone)	Albite
( " " )	An12 (core, rim)	"
(grain 2)	An29 (core)	"
( " " )	An13 (rim)	"
(overall variation)	An20-28	Albite, Carlsbad Pericline

rich in potash feldspar<sup>1</sup> and consist of microcline perthite, quartz, and slightly turbid plagioclase rimmed by albite. They differ from the gneiss and the parent rock in having more potash feldspar and little or no biotite (Table 8). Their grain size is generally similar to the country rock (0.15mm.), although porphyroblasts occur in some specimens. The microcline shows a preferred orientation, "tartan" twinning appearing in the majority of grains in sections cut perpendicular to the lineation (B<sub>3</sub>). Minor biotite appears as digested relics replaced by rutile and limonite. Rarely, remnants of heavy mineral bands (e.g. magnetite) cut through these rocks.

#### Country rock - gneiss contacts.

The contact between the gneiss and country rock is extremely sharp on the microscopic scale (Fig.15a). The most noticeable change is an approximately four fold increase in grain size in the gneiss. Relics of the country rock occur around and within porphyroblastic quartz, plagioclase and microcline perthite. The porphyroblasts show concave boundaries towards the small grains. Similar textures are observed in metals where growing grains consume the surrounding matrix (Burgers, 1963, Fig.18). The biotite is also coarser grained and

- 
1. Several large slabs were collected from various bands including those with the "aplitic" coronae. Staining with sodium cobaltinitrite showed that the "aplite" bearing bands were higher in potash feldspar content.

FIG.15A.

Photomicrograph of granite gneiss-  
quartzo feldspathic schist contact.  
Note change in grain size. Location  
983 315. Spec. No.A200-866. X 40.

FIG.15B.

Photomicrograph of a typical granite  
gneiss. Location 992 266. Spec. No.  
A200-798. X 40.



FIG.15A.

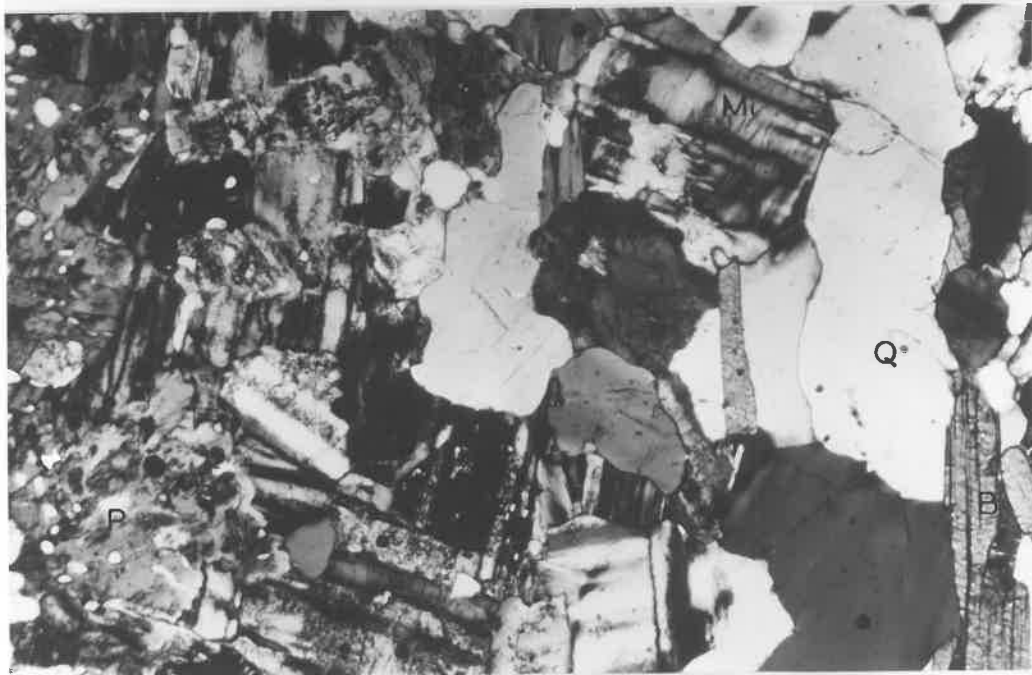


FIG.15B.

shows a poorer preferred orientation.

Petrography of the Tanunda Creek Gneiss.

In thin section most gneisses consist of medium grained (0.5 to 0.9mm.) aggregates of plagioclase, potash feldspar and quartz. The grains bear a characteristic curvilinear relationship to one another (Fig. 15b). Biotite forms a poorly defined foliation between these aggregates. The grains in these aggregates are commonly equidimensional, but in some specimens they are elongate in the plane of the foliation or parallel to the lineation ( $B_3$ ). Augen of potash feldspar are characteristic of many gneisses.

The plagioclases in the gneisses are generally smaller in grain size (0.6mm.) than plagioclase porphyroblasts in the transitional zone and show a greater range in composition ( $An_4$  to  $An_{27}$ ; Table 7) than the plagioclases in the quartzofeldspathic schists. Quartz and biotite relics occur in the plagioclases, indicating that a primary recrystallization texture was present before the formation of the gneisses. Albite rims are generally present at plagioclase-potash feldspar contacts and are probably the result of the unmixing of albite from the potash feldspar (Ramberg, 1962). Myrmekite tends to be more common in gneisses containing more calcic plagioclases (c.f. Phillips, 1964). Microcline perthite ( $2V_x = 66-77$ ;  $\Delta = 0.806$ ; Table 9) exhibits an irregular zoning and rare Carlsbad twinning. Quartz is found as irregular aggregates or as highly sutured, deformed grains showing undulose extinction, deformation lamellae and



TABLE 8.

Modal Analyses of Tanunda Creek Gneiss, Aplitic  
Corona and Country Rock.

<u>Spec. No.</u>	<u>866-7C</u>	<u>866-7C</u>	<u>866</u>	<u>866</u>
	<u>Gneiss</u>	<u>"Aplitic" Corona</u>	<u>Gneiss</u>	<u>Country Rock</u>
Quartz	39.7	51.6	31.7	48.2
Plagioclase	27.4	15.5	38.8	24.8
K. Feldspar	23.4	31.8	17.5	15.8
Biotite	0.0	0.5	10.2	10.6
Magnetite	0.6	0.6 <sup>+</sup>	0.5	-
Accessories (sphene, mus- covite)	0.9	-	1.5	0.6
	<u>100.0</u>	<u>100.0</u>	<u>100.0</u>	<u>100.0</u>

+ Limonite

<u>Total No. of counts</u>	<u>3,392</u>	<u>3,594</u>	<u>3,842</u>	<u>2,227</u>
--------------------------------	--------------	--------------	--------------	--------------

TABLE 9.

2Vx and Obliquity Values of the Alkali Feldspars  
in the Tanunda Creek Gneiss.

<u>Spec. No.</u>	Obliquity = $\Delta$	<u>2Vx</u>	<u>Comments</u>
845A	-	76-77	Microcline Twinning
878	-	66-68	" "
798	-	72-77	" "
866-1 <sup>+</sup>	0.913	-	" "
866-7 <sup>+</sup>	0.919	-	" "
878-1	0.806	-	" "

---

+ "Aplitic" vein.

curved interfaces at quartz-quartz contacts. Biotite (X = straw yellow to pale brown, Y = Z = deep brown) is the main ferromagnesian mineral and with hornblende (X = pale olive green, Y = olive green, Z = deep green) is associated with sphene, apatite and epidote in more lime rich gneisses. Muscovite occurs in accessory amounts and is commonly corroded by plagioclase and potash feldspar. Small growths of muscovite have been observed at the tip of some biotites. Magnetite and magnetite-hematite are the two primary oxide assemblages in the Tanunda Creek Gneiss. Magnetite forms skeletal aggregates distributed unevenly throughout the ground mass, and shows varying degrees of oxidation to martitic hematite. The primary hematite contains fine to coarse exsolution lamellae of ilmenite. The zircon in the gneisses are generally less rounded than the zircons in the schists (Fig.16) and show overgrowths, rare outgrowths and zoning (c.f. Poldervaart and Eckelmann, 1955, Plate 1).

#### Mineralogical Variation.

Micrometric analyses of the gneiss<sup>1</sup> and the quartzofeldspathic schists<sup>1</sup> are plotted in Figs.17a and b. The fields occupied by these two groups overlap, but the gneiss shows less variation in composition than the schists. Furthermore, the gneiss generally contains more potash feldspar and less quartz than the schists.

---

1. The majority of these analyses were determined by Chinner (1955). See Tables 4 and 8 for those determined by the author.

FIG.16.

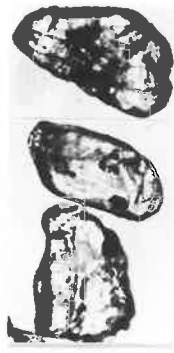
Zircons separated from the Tanunda Creek  
Gneiss. Note overgrowths (b1, f, g),  
outgrowths (b1), and zoning(d). Spec. Nos.  
A200-798, 796. Locations 992 266, 992 271.

Zircons from a quartzo-feldspathic schist  
(Spec. No. A200-40, Location 983 164) at  
the bottom of the figure. Note higher  
proportion of rounded grains.

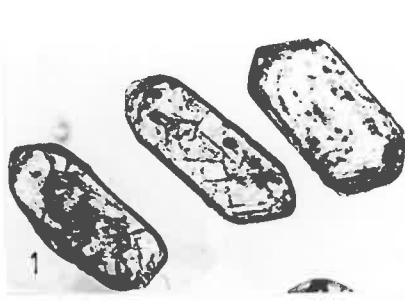
h, j X100.

a, b, i, k X250.

c-g X500.



a



b



c



d



e



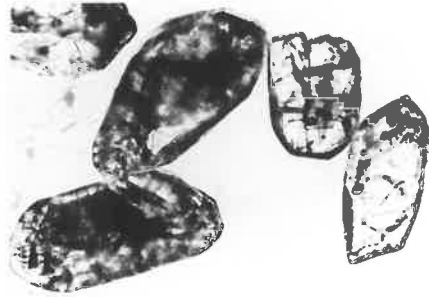
f



g



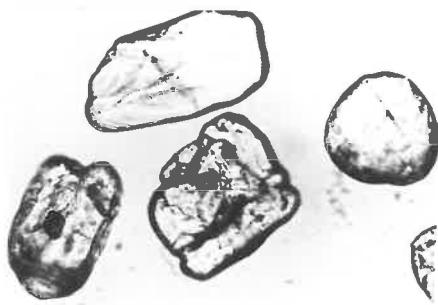
h



i



j



k

FIG. 16

FIG.17A.

Composition of the quartzo-feldspathic schists and the Tanunda Creek Gneiss expressed in terms of quartz-feldspar-others (mica, accessories etc.).

FIG.17B.

Composition of the quartzo-feldspathic schists and the Tanunda Creek Gneiss expressed in terms of quartz-potash-feldspar-plagioclase.

FIG. 17a.

Q-F Schists.  
○ Chinner, 1955.  
● Offler.

Tanunda Creek Gneiss.  
• Chinner, 1955.  
◊ Offler.

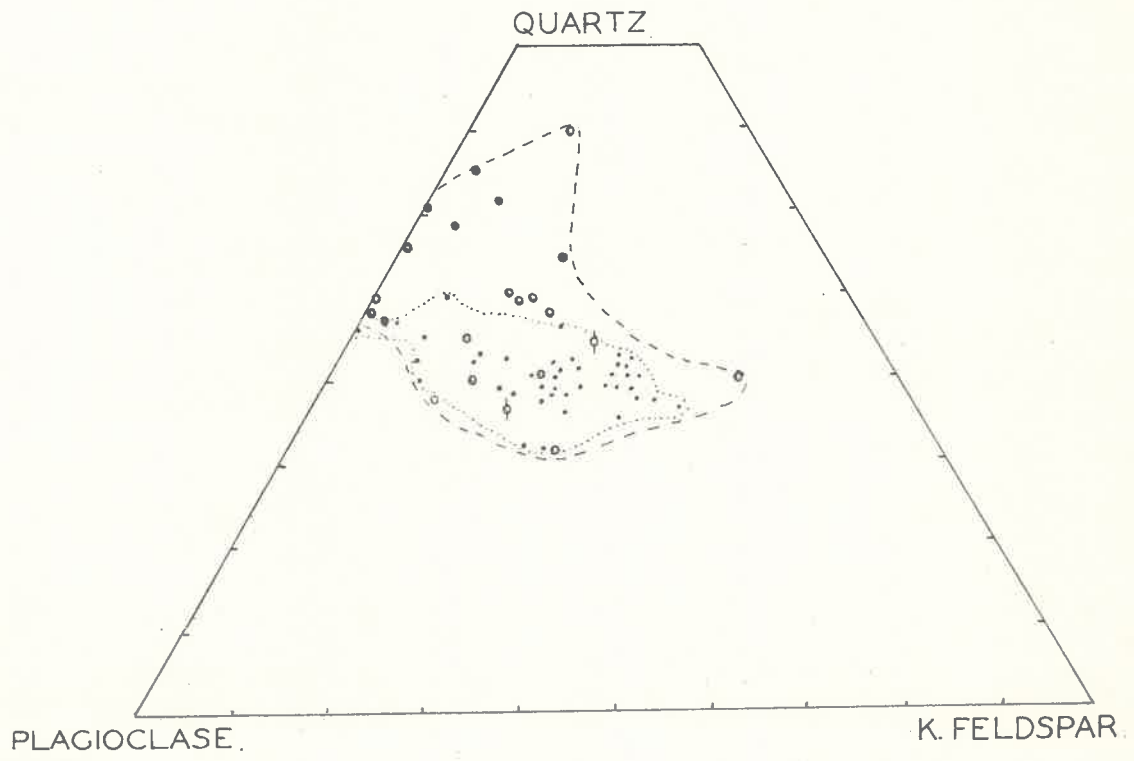
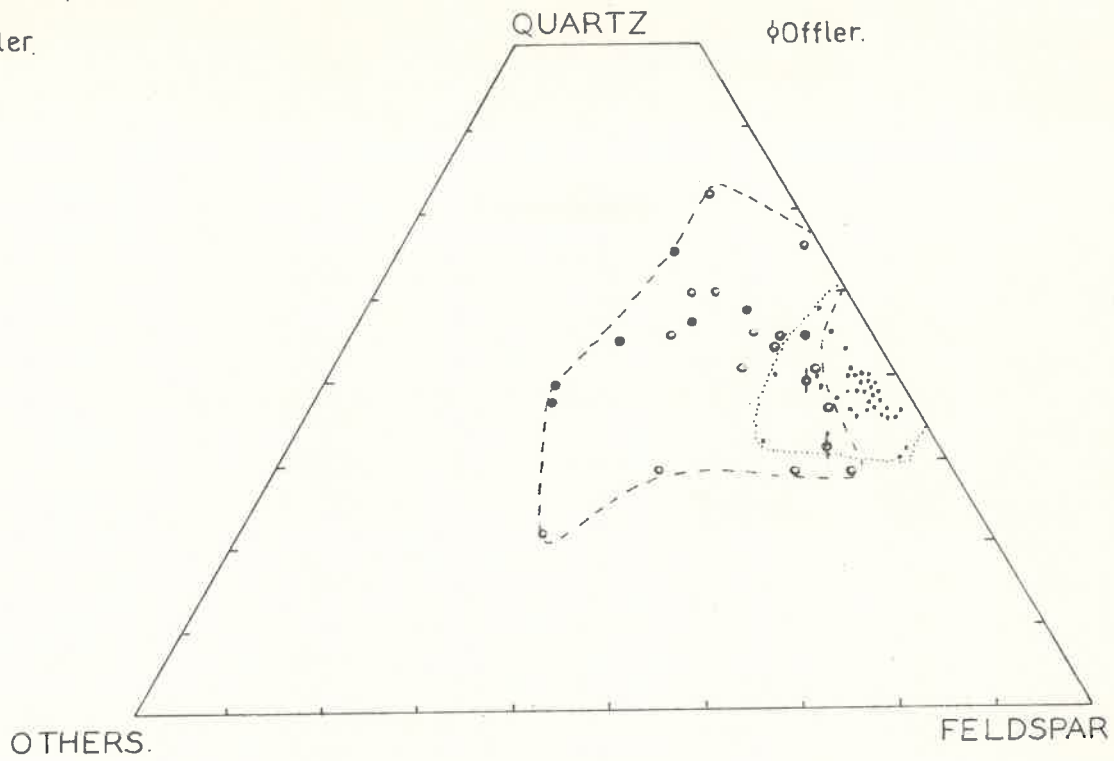


FIG. 17b.

Ra'66

Modal analyses of a gneiss<sup>1</sup> and adjacent country rock<sup>1</sup>, and of a gneiss and its "aplitic" corona, collected from the transitional zone are shown in Table 8. These analyses show a lower quartz content in the gneiss compared with the schist and a high potashfeldspar content in the "aplitic" corona, confirming the generalisation deduced from Chinner's data that the gneiss is formed from the country rock by modification of the mineralogy.

#### Relation to Structure.

The prominent structure in the Tanunda Creek Gneiss is a lineation due to elongate biotite, feldspar or quartz. The plunge of this lineation steepens from 20° in the south to 80°, east of Mt. Kitchener. It then shallows to 55°, north of the area mapped (Chinner, 1955). A weak foliation marked by sparse layers of biotite varies about an axis  $\beta$  which falls within the field of the lineations (Fig. 18). The orientation of this axis and the lineations is consistent with the geometry of the first phase of folding  $B_1$  (Chapter 11). However, the lineations (circled) to the left of  $\beta$  have<sup>an</sup> orientation which is consistent with the geometry of the second phase of folding  $B_3$ . In the Tanunda Creek/<sup>Gneiss</sup> and the quartz-feldspathic schists north-east of the area mapped, Fleming (pers. comm.) has noted lineations

---

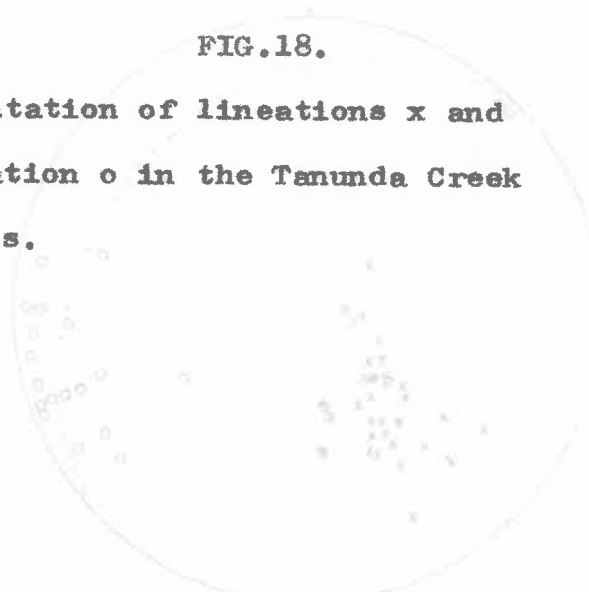
1. The gneiss and parent rock are in contact.



FIG 18

FIG.18.

Orientation of lineations x and  
foliation o in the Tanunda Creek  
Gneiss.



with two distinct orientations, which the present author equates with the  $B_1$  and  $B_3$  phases of deformation. These observations therefore suggest that the Tanunda Creek Gneiss has been involved in two periods of deformation.

#### Origin of the Tanunda Creek Gneiss.

The Tanunda Creek Gneiss may represent:

- (1) a magmatic intrusion which has been deformed and recrystallized (e.g. the Older Orthogneisses of Carn Chiunneag and Inchbae, Harker, 1962);
- (2) a granite gneiss which has been formed by the metasomatic alteration of the country rock (e.g. the composite granitic gneiss of Western Ardour, Harry, 1954);
- (3) a granite gneiss formed by the recrystallization of the parent rock without the addition of alkalis or the removal of basic material (e.g. the Rathjen Granitic Gneiss, White, 1956).

Since the zircons in the Tanunda Creek Gneiss do not show the euhedral morphology typical of magmatic granites (Poldervaart, 1956), but the shape and outgrowths of autochthonous granites (Poldervaart and Eckelmann, 1955), the first hypothesis can be rejected.

Hypotheses two and three cannot be differentiated on chemical grounds since the fields of the schists and the gneiss overlap (Figs. 17a and b). However, there are certain features in the transitional zone which suggest a strong sedimentary control for the composition of the gneiss.

- (1) Potash feldspar rich "aplitic" coronae and gneisses occur only in certain bands which are themselves rich in potash feldspar.

(2) The mineral assemblages of the parent rock and the gneiss are the same.<sup>1</sup>

The features described above are consistent with metamorphic crystallization and minor differentiation. It is considered that the "aplitic" coronae around the gneissic pods and the quartz at gneiss-country rock contacts are the products of this differentiation, and that they have been formed by the migration of "excess" quartz and potash feldspar away from the sites of recrystallization. The processes controlling the formation of the gneiss in the transitional zone are likely to have been operative in the zone of the Tanunda Creek Gneiss. This is suggested by the abundance of quartz reefs in the gneiss zone and by the similarity in the compositions of the gneisses in both zones.

The location of the Tanunda Creek Gneiss in a high grade metamorphic belt and within the hinge zone of an isoclinal fold, suggests that high metamorphic temperatures and deformation have been instrumental in its formation.

---

1. Compare this with the composite granitic gneiss of Western Ardgour which differs from the parent rock (oligoclase-biotite-quartz gneiss) "in containing more quartz and less biotite, and in the presence of microcline with myrmekite and other metasomatic products". (Harry, 1954).

CHAPTER 4.CALC-SILICATE ROCKS AND CALC-SCHISTS.Introduction.

Calc-silicate rocks of the Kanmantoo Group are relatively restricted in occurrence. They form prominent ridges west of Mt. Kitchener and small, lenticular bodies in the migmatite zone (Plate 1). Most rocks are fine grained and banded, the banding ranging in thickness from 1mm. to 3cm. (Figs. 19a and b). Weathering of these rocks, produces a flaggy skeletal-like outcrop. Calc-schists and unbanded calc-silicate rocks are less common. Many of the calc-silicate rocks are lineated (e.g. hornblende prisms parallel to  $B_1$ ) and small  $B_1$  and  $B_3$  folds are prevalent in certain areas (see Chapter 11).

Petrography.

The deep green and white layering characteristic of most calc-silicate rocks is due to the relative proportions of hastingsite, diopside and potash feldspar or scapolite. Texturally, individual layers are fine grained (0.06 to 0.16mm.) granoblastic aggregates of calc-silicate minerals (Fig. 21). Clinopyroxenes and amphiboles are disseminated throughout the matrix as single grains or clusters, and in some rocks they form small (1.0 to 2.0mm. in diam.) porphyroblasts. In the unbanded calc-silicate rocks, the light and dark minerals are intimately intermingled and layering cannot be recognised. Rare sinuous veins of scapolite,

FIG.19A.

B<sub>3</sub> fold showing characteristic banding  
in calc-silicate rock. Location 975 289.  
Spec. No.A200-411.

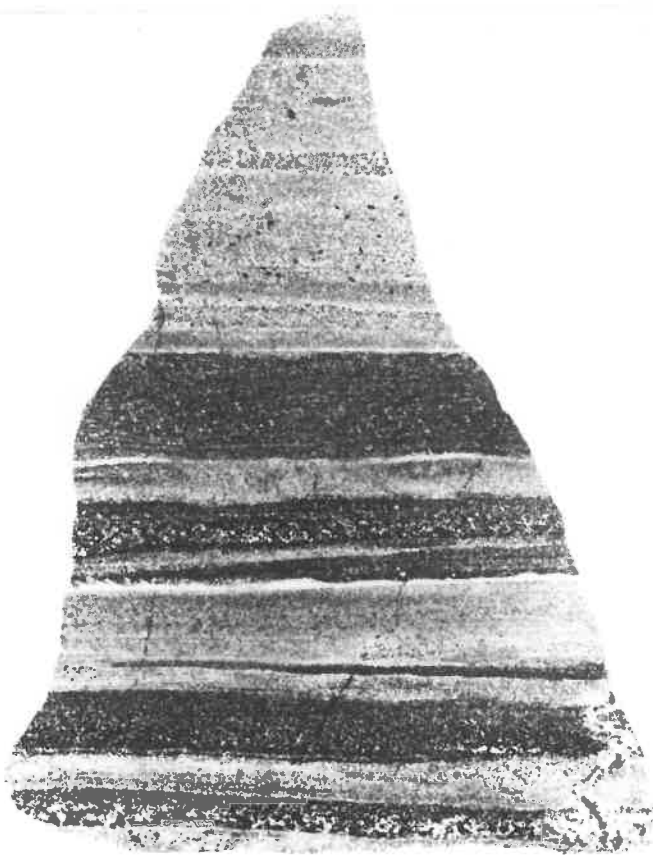
FIG.19B.

Large thin section of a banded calc-  
silicate rock. Note sinuous metamorphic  
segregation vein at the bottom right  
hand corner of diagram. Location 981 290.  
Spec. No.GAC 605.



0 3cm

FIG.19A.



0 3cm

FIG.19B.

potash feldspar and diopside traverse some calc-silicate rocks. In some specimens (e.g.411) diopside aggregates outline  $B_3$  folds, suggesting that crystallization continued after the  $B_3$  phase of folding.

The calc-silicate rocks vary greatly in mineralogy. The type of variation is illustrated in Table 10. The assemblages present are listed below and are also represented on an ACFK diagram (Fig.20).

1. Diopside-scapolite-(plagioclase)-amphibole<sup>1</sup>-potash feldspar.
  - a. Diopside-scapolite-amphibole.
  - b. Amphibole-scapolite-potash feldspar.
  - c. Diopside-scapolite-potash feldspar.
  - d. Diopside-amphibole-potash feldspar.
  - e. Diopside-scapolite-plagioclase.
  - f. Diopside-potash feldspar.
  - g. Diopside-scapolite.
  - h. Scapolite-potash feldspar.
  - i. Diopside-potash feldspar.
2. Diopside-scapolite-(plagioclase)-calcite.
3. a. Diopside-biotite-scapolite-(plagioclase).
  - b. Amphibole-potash feldspar-biotite.

Quartz is absent from assemblages 1 and 1b and scapolite is more common than plagioclase. Sphene is an important constituent in some rocks (e.g.414, Table 10), and apatite, pyrite and magnetite are minor accessories.

1. Common hornblende or a member of the pargasite-ferrohastingsite series.

TABLE 10.

Estimated volume percentages of constituents  
in Calc-silicate rocks and Calc-schists.

<u>Spec.No.</u>	414			277		
	Band No.			Band No.		
	1	2	3	1	2	3
Diopside	10	45	5	20	-	40
Scapolite	35	5	45	10	40	55
Quartz	10	+	-	-	-	-
K.Feldspar	45	50	45	40	55	5
Hastingsite	-	-	-	25	5	-
Sphene	-	-	5	-	-	-



FIG.20.

A.C.F.K. diagram showing the mineral assemblages present in the calc-silicate rocks.

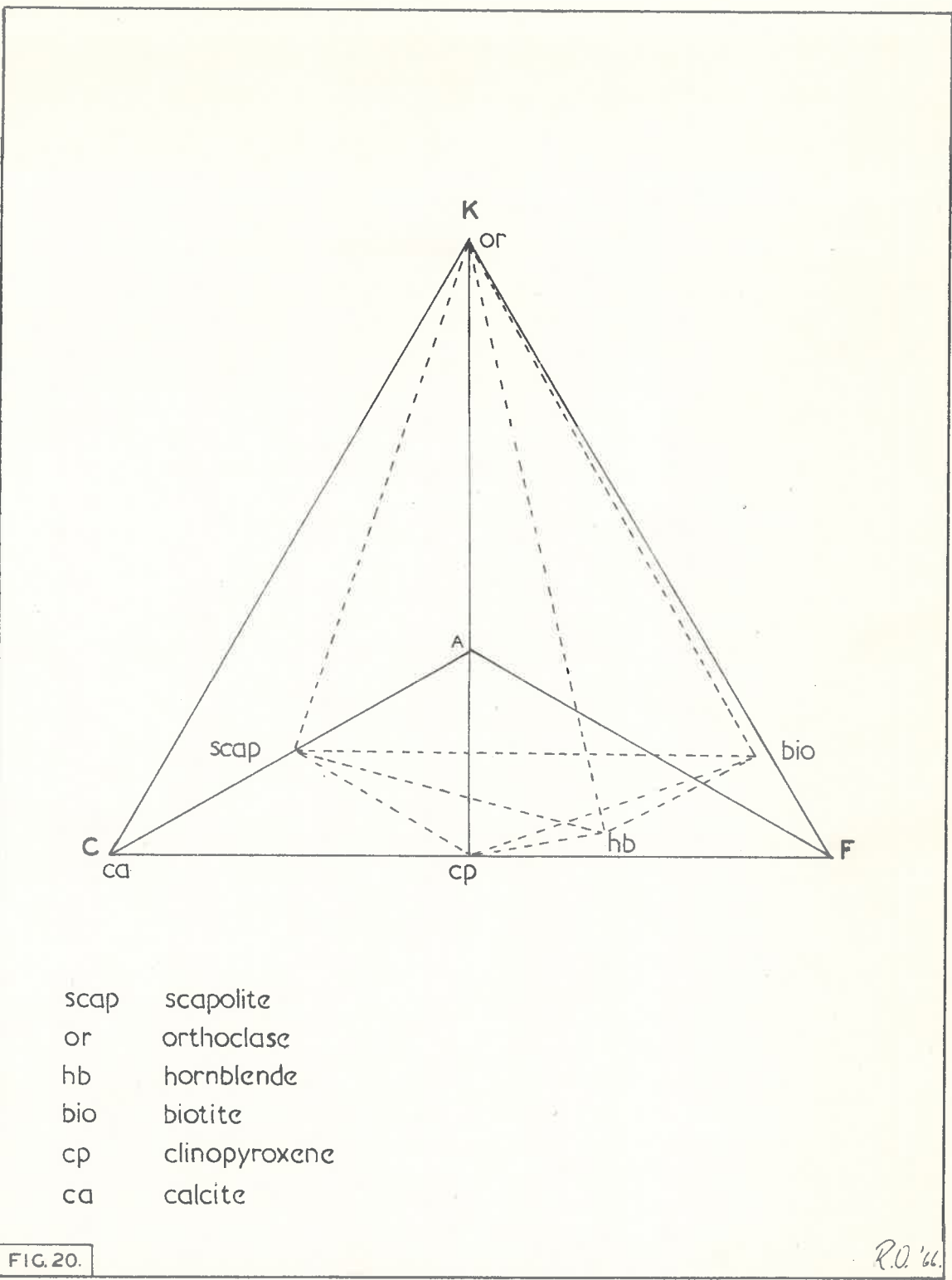


FIG.21.

Photomicrograph of banded, fine grained  
calc-silicate<sup>rock</sup>, showing layers of diopside-  
orthoclase- (scapolite) and orthoclase-  
scapolite- (diopside). Location 975 289.  
Spec. No. A200-411. X 40.

FIG.22.

Photomicrograph showing secondary  
hornblende enclosing diopside. Scapo-  
lite is the colourless mineral in the  
matrix. Location 983 293. Spec. No.  
A200-768. X 80.

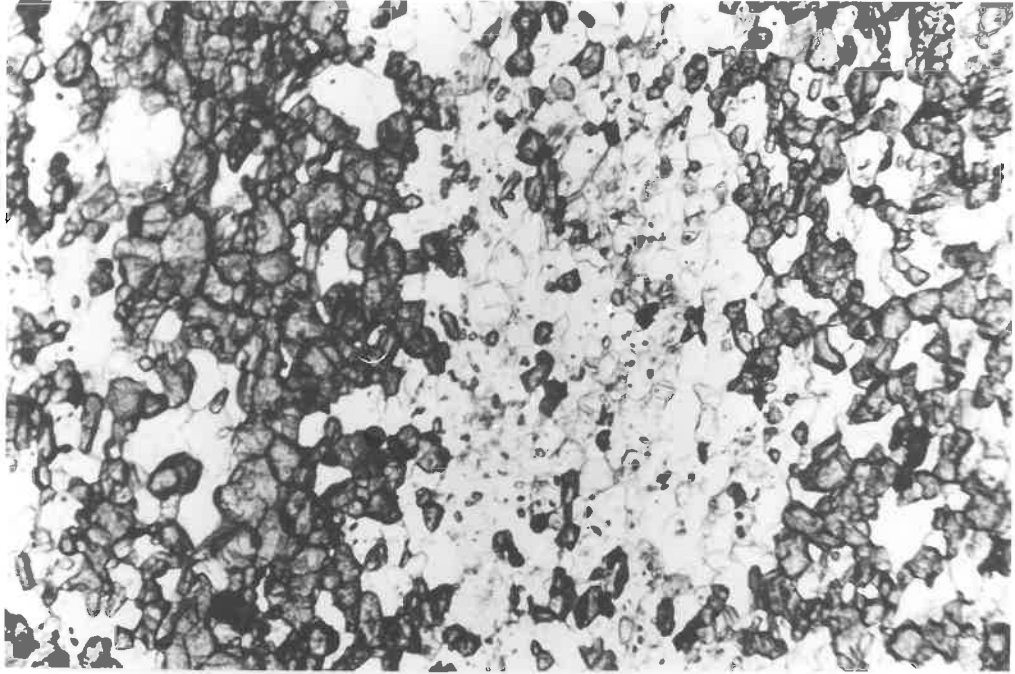


FIG. 21.

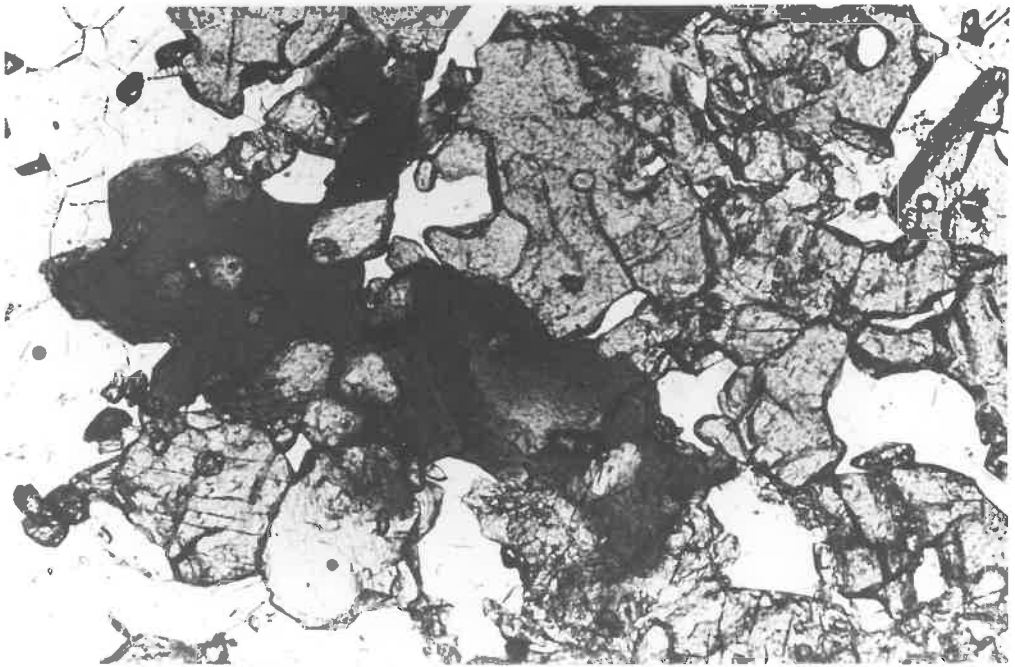


FIG. 22.

Pale green to bright green clinopyroxene (diopside-hedenbergite) is a major constituent (up to 40 p.c.) of most calc-silicate rocks. Its range of composition as determined optically (Hess, 1949), varies from 20 to 60 percent hedenbergite (Table 11). In the Milendeila and Tungkillo calc-silicate rocks, the clinopyroxenes vary from 15 to 30 percent hedenbergite (White, 1959) and in the Caabrai region, Mills (1964) records a compositional range of 37 to 70 percent hedenbergite.

The amphiboles in the calc-silicate rocks are considered to be members of the hastingsite - ferrohastingsite and common hornblende series. The two groups are distinguished on the basis of pleochroism, 2V and refractive index (see Table 11 for 2V and R.I. measurements). The following pleochroic schemes are found to be typical of the two groups of amphiboles.

Hastingsite -  
Ferrohastingsite.

X = pale olive green -  
bright yellow green.

Y = green - deep green.

Z = blue green - intense  
deep green

Hornblende.

X = pale green -  
olive green.

Y = olive green.

Z = green -  
deep green.

Most amphiboles appear to be in equilibrium with diopside, but secondary grains of hastingsite enclose grains of diopside and scapolite (Fig. 22; c.f. White, op.cit., Plate 6). In some sections cut perpendicular to the B<sub>1</sub>

TABLE 11.

Optical Properties of minerals in the  
Calc-silicate Rocks.

<u>Spec. No.</u>	<u>Clinopyroxene</u>				<u>Amphibole</u>			
	<u>2Vx</u>	<u>n<sub>β</sub></u>	<u>Z C</u>	<u>% hed†</u>	<u>2Vx</u>	<u>n<sub>α</sub></u>	<u>Z C</u>	<u>M 2</u>
277a		1.696		46	low	1.679	18	39
277b		1.695		45				
609a	30	1.695		45	65	1.675	20	44
609b	40	1.696		46				
605		1.693		41		1.666		46
587		1.713		60	low	1.684		30
623	59	1.687	44	20	60	1.669	15	44
587		1.700		40	56	1.684	21	30
212		1.697	35	35	50	1.683	24	60
408	60	1.694	44	30				
768	58	1.712	47	59	44			

<u>Spec. No.</u>	<u>Scapolite</u>		<u>Plagioclase</u>	
	<u>n<sub>o</sub></u>	<u>% Me</u>	<u>% An</u>	
277a	1.572	53.0		
277b	"	"		
609b	1.575	57.0		
623	1.576	58.5		
408	1.560	36.5		
768	1.577	59.5		
51	1.566	45		
411	1.555	30		
404	1.577	60	38	
580	1.560	36.5	8-10	
149	1.556	31		
820			48	
406			49-55 (zoned)	
586			44-57 ( " )	

1. hed = hedenbergite  
2. M = Mg/Mg+Fe<sup>2+</sup>+Fe<sup>3+</sup>+Mn.

lineation, idioblastic basal sections of hornblende become obvious.

The hastingsites range in composition from 30 to 60 percent  $Mg^{2+}/Mg^{2+} + Fe^{2+} + Fe^{3+} + Mn$  (based on the curves of Deer et al., 1963). Mills (op.cit.), notes that hastingsites with less than 20 percent  $Mg^{2+}/Mg^{2+} + Fe^{2+} + Fe^{3+} + Mn$  are limited to higher grade calc-silicate rocks. The optical properties of the common hornblendes indicate that they are reasonably rich in iron (44 to 45 p.c.  $Mg^{2+}/Mg^{2+} + Fe^{2+} + Fe^{3+} + Mn$ ). (Table 11). Another feature is the extreme variation in the amphibole content of the bands within a single specimen (e.g. 277; Table 10). Such variations suggest that conditions controlling the stability of the amphiboles have fluctuated considerably over short distances. It has been pointed out that the stability of amphiboles is dependent upon oxygen pressure (Ernst, 1962, 1963, 1965; Gilbert, 1964) and water vapour pressure (Ernst, 1962). In addition, calcic aluminous amphiboles are considered to be stable in rocks containing low  $SiO_2/Al_2O_3$  and Ca-Mg/Al-K ratios (Layton, 1963; Misch, 1964).

The variability of the amphibole content in the calc-silicate rocks is most simply explained by variations in bulk composition, particularly variations in the Ca-Mg/Al-K and  $SiO_2/Al_2O_3$  ratios.

Scapolite normally appears as small equidimensional grains associated with other calc-silicate minerals and more rarely as porphyroblasts studded with inclusions of diopside. The composition of the scapolite varies from 30 to 60 percent

meionite<sup>1</sup> (Table 11), and may vary from band to band within the same specimen. Sodium rich scapolites<sup>2</sup> are associated with diopside, albite and calcite (e.g. 590, 408) or more rarely with potassium feldspar and diopside (402B). The scapolites in the Milendella-Tungkillo region (White, 1959) and Cambrai region (Mills, 1964) show a more limited range of composition ( $Me_{45-60}$  and  $Me_{55-60}$ , respectively).

Twinning in the potash feldspars is poorly developed or absent and perthitic textures are rare. Intermediate to fully monoclinic structural forms are confirmed by X-ray and optical studies (Table 12). Plagioclase is poorly zoned and varies in composition from  $An_8$  to  $An_{65}$  (Table 11). Biotite (X = very pale brown, Y = Z = brown to rust brown) is common in the calc-schists where it may occur axial plane ( $S_1$ ) to small folds. Quartz is ubiquitous in most rocks, but is generally not a major constituent (maximum content, 35 p.c., 404.) Epidote ( $2V_x = 71$ , 35 p.c.  $Fe^{III}$  molecule, Troger, 1959) occurs as a secondary mineral replacing diopside, hastingsite or hornblende, and scapolite.

#### Garnet bearing calc-silicates.

In some rocks garnet forms as skeletal, pale brown aggregates enclosing calcite, quartz and diopside (Fig. 23), and as reaction rims between diopside and scapolite.

- 
1. See Appendix 6 for the method of determination of scapolite compositions.
  2. Observations based on refractive index or birefringence determinations.



TABLE 12.

2Vx and Obliquity Values of the Alkali Feldspars  
in the Calc-silicate rocks of the Kanmantoo

GROUP.

<u>Spec.No.</u>	<u>Obliquity = <math>\Delta</math></u>	<u>2Vx</u>	<u>Comments</u>
623	Near monoclinic	66-73	Poor microcline twinning
277 <sup>1</sup>	Monoclinic	54-55	Very faint wavy twinning
277 <sup>2</sup>	"	-	" " "
404	0.614	-	Wavy twinning
590	Monoclinic	-	No twinning

---

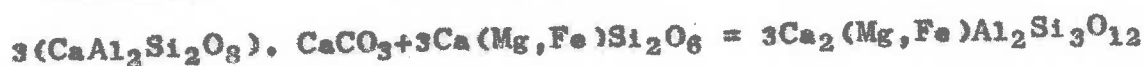
1. Diopside bearing band.
2. Ferrohastingsite bearing band.

It has an R.I. of  $1.848 \pm 0.01$  and a cell size of  $12.016 \pm 0.005$ , indicating a garnet rich in andradite (Skinner, 1956). Minor pale yellow epidote and deep yellowish green hastingsite are locally associated with the garnet.

The reactions leading to the formation of garnet are probably quite complex. White (1959) suggested the following equations for the formation of garnet from scapolite and diopside.



meionite                      calcite quartz                      grossularite.



meionite                      diopside                      grossularite with  
some almandine  
and pyrope



calcite quartz

It is necessary, however, to obtain  $\text{Fe}^{3+}$  for the andradite molecule and unless Fe metasomatism is postulated, (as suggested by White, op.cit. for the Milendella garnet skarns) there must be considerable oxidation of the  $\text{Fe}^{2+}$  from the diopside. However, andradite can replace diopside at high oxygen pressures or lower temperatures according to the experimental work of Ernst, (1965) (Fig.24, paths AB and AC). As the garnet appears to be secondary in origin, it is possible that the andradite molecule in the garnet has formed as a result of a fall in temperature during a period of retrogressive metamorphism.

FIG. 23.

Garnet (G) enclosing diopside (D),  
scapolite (S), calcite (C) and  
quartz (Q). Location 981288.  
Spec. No. A200-923. X 40.

FIG. 24.

Diagram taken from Ernst (1965).  
Paths AB and AC show that andradite  
can be produced either by increase  
in oxygen fugacity or decrease in  
temperature.

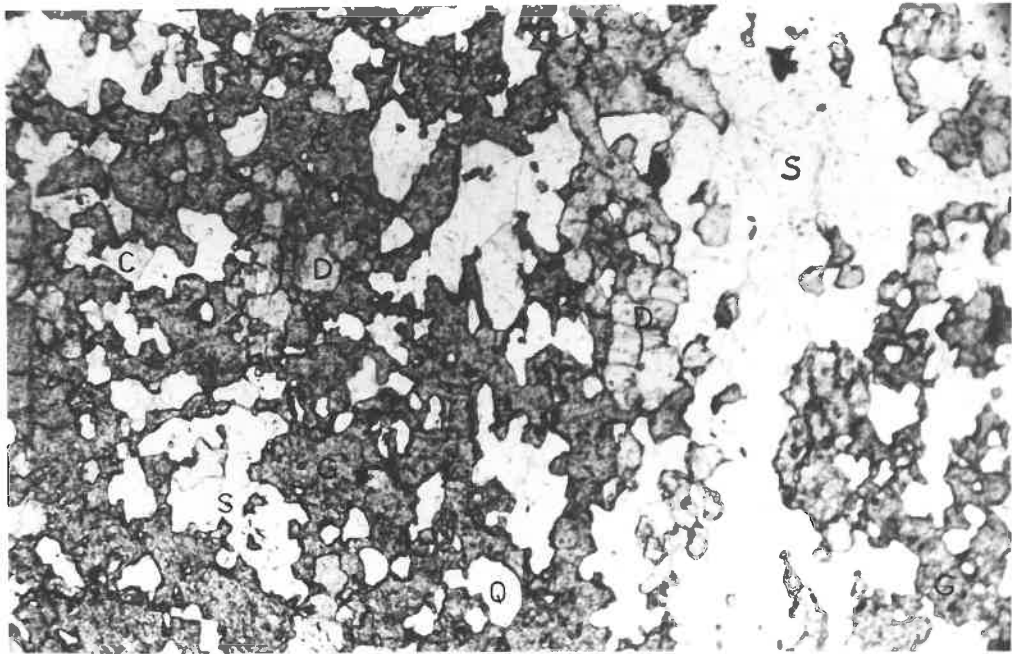


FIG. 23.

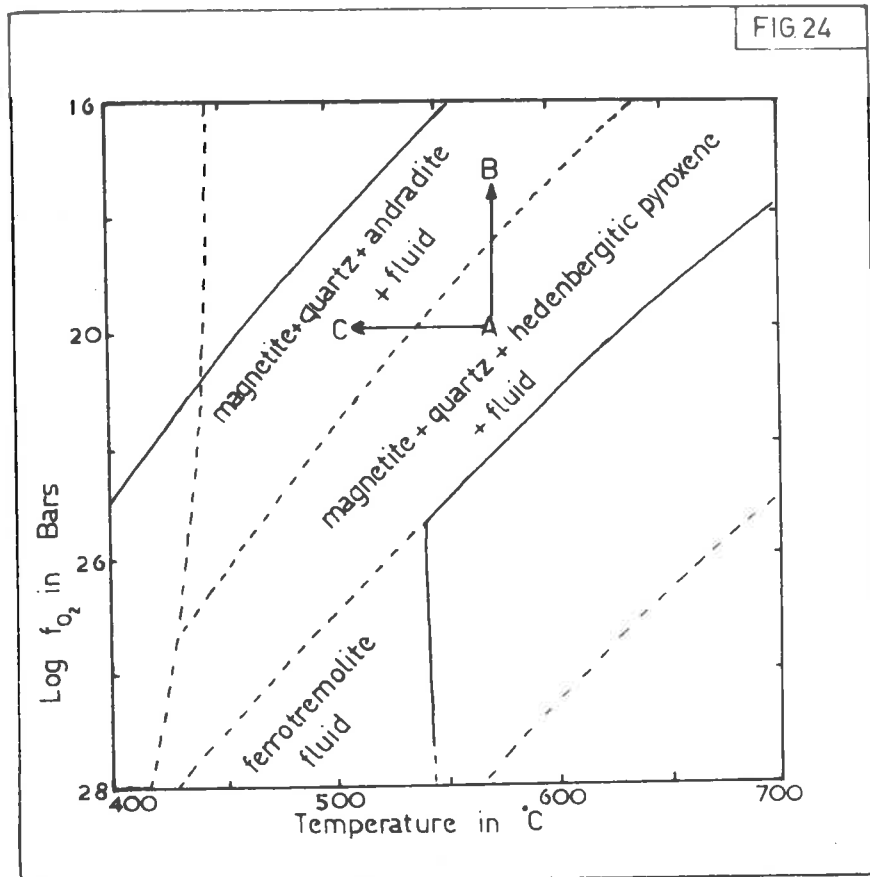


FIG. 24.

### Amphibole - clinopyroxene relationships.

To study the distribution of Fe between co-existing amphibole and clinopyroxene in the calc-silicate rocks, the refractive indices of the amphiboles ( $n_{\alpha}$ ) and clinopyroxenes ( $n_{\beta}$ ) from 8 specimens have been measured. They are listed in Table 11 and are plotted in Fig.25a, together with values obtained by Mills (1964) for co-existing clinopyroxenes and hastingsites from calc-silicate rocks of the same grade and mineralogy as those in the present area.

It can be seen that the amphiboles in the Pewsey Vale rocks contain more Fe<sup>1</sup> with respect to diopside than those in Mills's area. Kretz (1960) has studied the distribution of elements between biotite, amphibole and clinopyroxene in skarn rocks, metamorphosed in the P-T region of the upper amphibolite facies, and noted that "an increase in Al concentration of amphibole causes this mineral to acquire a higher concentration of Fe relative to that of the co-existing pyroxene" (Fig.25b). It is possible then that the relative separation of the distribution curves in Fig.25a is due to the difference in Al content of the amphiboles in the two areas.

### Origin of the Calc-silicate rocks.

The original sediments from which the calc-silicate rocks were formed were probably calcareous shales and "sandy" dolomites.

- 
1. It is assumed that the refractive indices are an approximate measure of the iron content in these minerals. Mills (op.cit.) found a good correlation between magnetic susceptibility and refractive index for hastingsite amphiboles.

FIG.25A.

Refractive index diagram of co-existing amphiboles and clinopyroxenes in calc-silicate rocks from Pewsey Vale (full circle) and Cambrai (circle; Mills, 1964).

FIG.25B.

Diagram after Kretz (1960) showing distribution of  $Fe/Fe+Mg+Mn+Ti$  between coexisting amphiboles and clinopyroxenes. The range in  $Al_2O_3$  content of the amphiboles is given at the top of each curve.

FIG. 25a

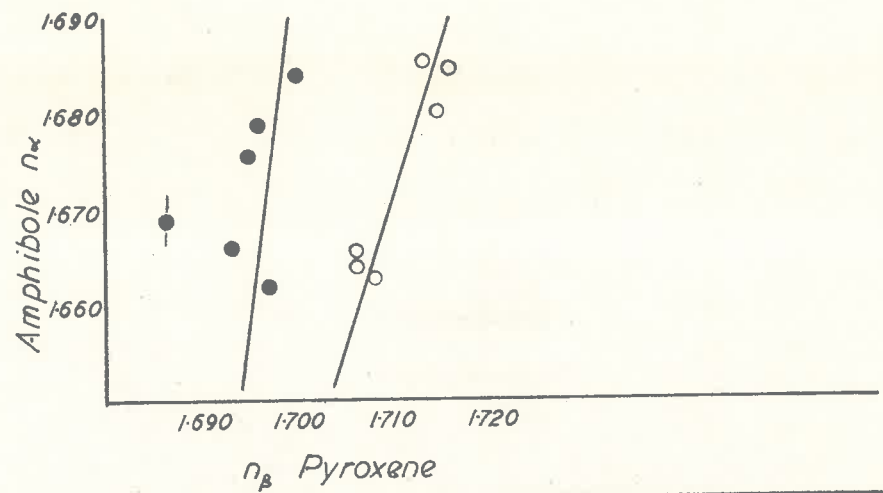
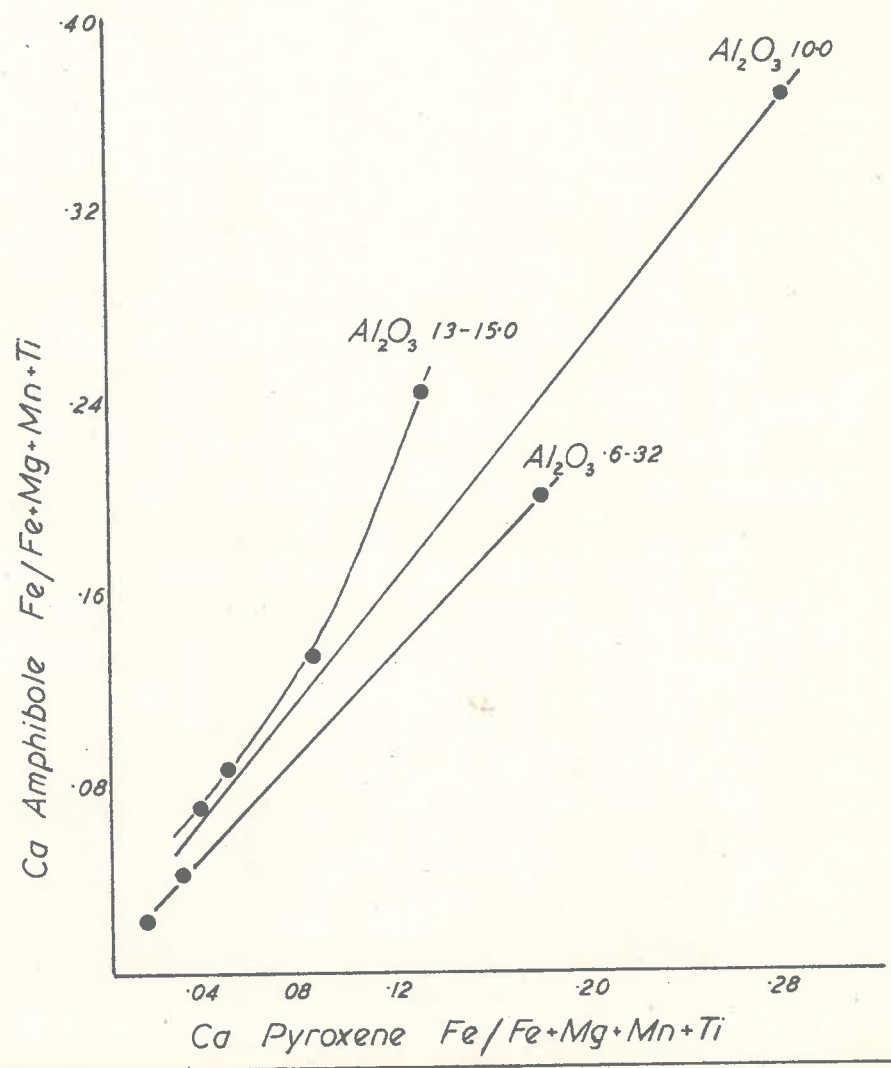


FIG. 25b



Ro'61

The layering in most rocks<sup>1</sup> is best interpreted as sedimentary banding, accentuated to some degree by metamorphism. Variations in bulk composition of these bands have most likely been the main cause of the variation in mineral assemblages. The abundance of potash feldspar in many bands suggests that the  $K_2O$  content of the original sediment was unusually high. However, this does not necessarily indicate that potash metasomatism has occurred, as calcareous shales with as much as 10 percent  $K_2O$  are recorded in the literature (Pettijohn, 1957, p.370). The predominance of scapolite over plagioclase in the calc-silicate rocks is probably the result of high  $U_{Cl_2}$  and  $U_{CO_2}$  (Shaw et al., 1963; Shaw et al., 1965). Presumably, the volatiles required for the crystallization of scapolite, were derived from the sediments, an hypothesis proposed by White (1959) for the origin of scapolite in the marbles and calc-silicates of the Milendella and Tungkillo regions.

In conclusion, the calc-silicate rocks in the Pewsey Vale area are considered to be regionally metamorphosed calcareous shales and "sandy" dolomites.

---

1. In some rocks the layering is the result of transposition of the original bedding by folding on  $S_3$  - see Chapter 11.



CHAPTER 5.THE PELITIC AND GRAPHITIC SCHISTS.PELITIC SCHISTS.Introduction.

Pelitic schists constitute a minor proportion of the Kanmantoo Group Rocks in the Pewsey Vale area. They occur as small lenses in the migmatite zone and overly the calc-silicate rocks west of Mt. Kitchener (Plate 1). Sillimanite, garnet, potash feldspar and muscovite are found as porphyroblasts in many of the schists; the sillimanite commonly exhibits a preferred orientation parallel to the  $B_1$  fold axis. Large muscovite porphyroblasts are particularly abundant in some schist units (Plate 1). Small veins and pods of quartz, plagioclase and muscovite also occur in the pelites of the migmatite horizon, west of Mt. Kitchener.

Petrography and paragenesis.

The pelitic schists are generally fine grained (0.16 to 0.03mm.), equigranular, foliated rocks in which  $S_1$  is marked by alternating layers of biotite and/or muscovite and quartz. The schists within the migmatite horizon are coarser grained (av. = 0.45mm.) less foliated and are texturally similar to the quartzo-feldspathic schists in the migmatite zone. The foliation in some schists is crenulated about  $B_3$ .

The following mineral assemblages are present;

- (1) Potash feldspar-biotite-sillimanite-plagioclase-(garnet).
- (2) Potash feldspar-biotite-sillimanite-plagioclase-muscovite-(andalusite).
- (3) Biotite-sillimanite-plagioclase-muscovite.
- (4) Biotite-sillimanite-garnet-(andalusite).
- (5) Biotite-sillimanite-plagioclase.

Quartz occurs in all assemblages and apatite, zircon, tourmaline (E = very pale green, O = deep green), magnetite, hematite and graphite are accessories. The hematite contains exsolution bodies of ilmenite. More than 90 percent of the rocks examined contain either assemblage (2) or (5).

Potash feldspar normally appears as xenoblastic grains in the matrix of the schists, but less commonly as pre-tectonic(?) porphyroblasts (up to 1.3mm. in diam.) containing inclusions of biotite, quartz, plagioclase, tourmaline and rare epidote. X-ray and optical studies show that either microcline or orthoclase are present in the schists (Table 13). Shadow perthite is common in most potash feldspars. Plagioclase (An<sub>10</sub> to An<sub>41</sub>, Table 14) is a common constituent of most schists (maximum, 30 p.c., 904,628). Deformation and composition (or primary) twins (Vance, 1961; Vernon, 1965) co-exist in many specimens (e.g. 124A, 100B); albite and pericline are the common twin laws. Some grains show poor zoning. Sillimanite is commonly present as matted

TABLE 13.

2Vx and Obliquity Values of the Alkali Feldspars  
in the Pelitic Schists of the Kanmantoo Group.

<u>Spec.No.</u>	<u>Obliquity = <math>\Delta</math></u>	<u>2Vx</u>	<u>Comments</u>
124A	Monoclinic	46.5-55	No twinning
124B	Near Monoclinic	( 52-56	Faint twinning
		(	in some grains
		( 64-65	Twinning better
		(	developed
814B	-	78-80	Microcline twinning
100B	0.888	78-80	" "
887	0.875	-	" "

TABLE 14.

Composition of Plagioclases in the Pelitic Schists.

(U-stage determinations)

<u>Spec.No.</u>	<u>Composition</u>	<u>Twin Laws</u>
124B	An37-41	Albite, Pericline
628	An30-38	Albite
100B	An31-34	"
442	An10	"
270	An11-12	"
271	An18-20	"
823B	An15-16	"
"	An12.5(rim) An14(core)	"
124A	An35-38	Albite, Pericline
824	An15-16	"

fibrous aggregates (fibrolite) in biotite or more rarely in muscovite, as needle like inclusions in plagioclase and quartz, and as stout prisms up to 5mm. in length associated with quartz in the matrix. It also replaces andalusite porphyroblasts (Fig.26a) and occurs with microcline in muscovite porphyroblasts (Fig.26b). Both fibrolite and sillimanite are present in some specimens (e.g. 100B c.f. Chinner, 1961). The replacement of biotite by fibrolite is not accompanied by the formation of iron ore "dust" or potash feldspar granules (contrast with Woodland, 1963; De Keyser, 1965). In a few specimens the sillimanite exhibits a preferred orientation, the c-axes lying parallel to the lineation  $B_1$ ; in others, fibrolitic mats are folded about the  $B_3$  axis and therefore predate the  $B_3$  phase of folding. Most sillimanite appears to have grown statically, prior to the second deformation.

As already noted petrographic evidence suggests that sillimanite has formed from andalusite and from the breakdown of muscovite according to the following reaction (Heald, 1950):



This reaction appears to have gone to completion in only a few rocks. There is no indication that plagioclase has participated in the development of sillimanite as suggested by Guidotti (1963) (contrast with Guidotti and Evans, 1964).

FIG.26A.

Photomicrograph of pelitic schist showing sillimanite (S) surrounded by a fine mat of sericite. Andalusite (A) and microcline (K) occur to the right of sillimanite. Location 977 286. Spec. No.A200-814A. X100.

FIG. 26B.

Photomicrograph of pelitic schist showing sillimanite (S), microcline (Mi) and relic muscovite (M). Location 976 288. Spec. No.GAC 270. X 100.

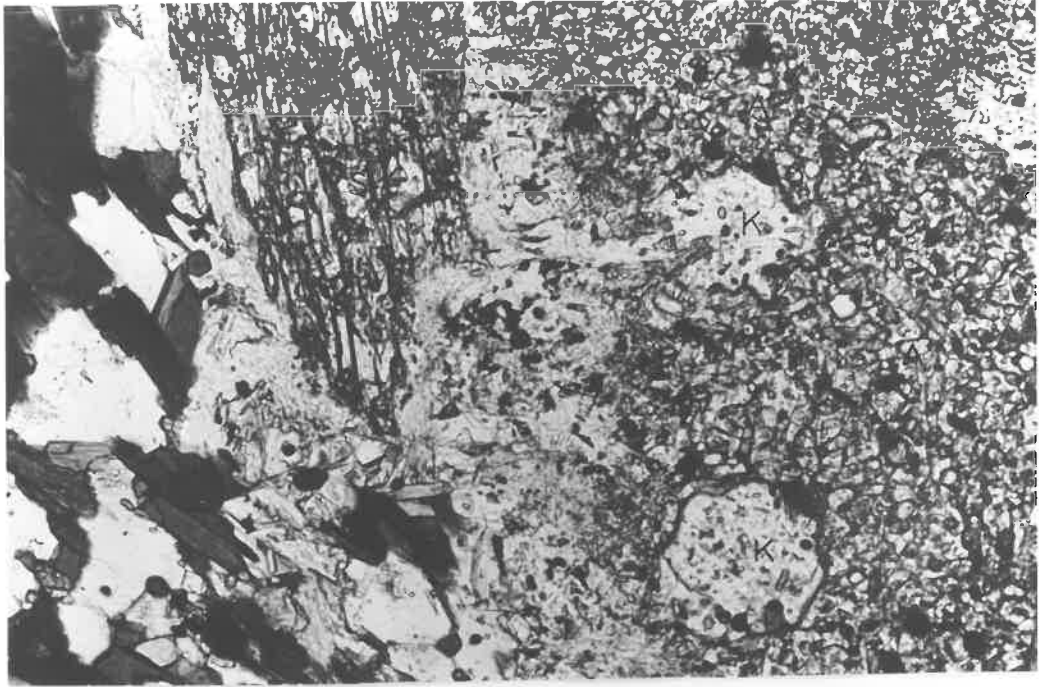


FIG 26A.

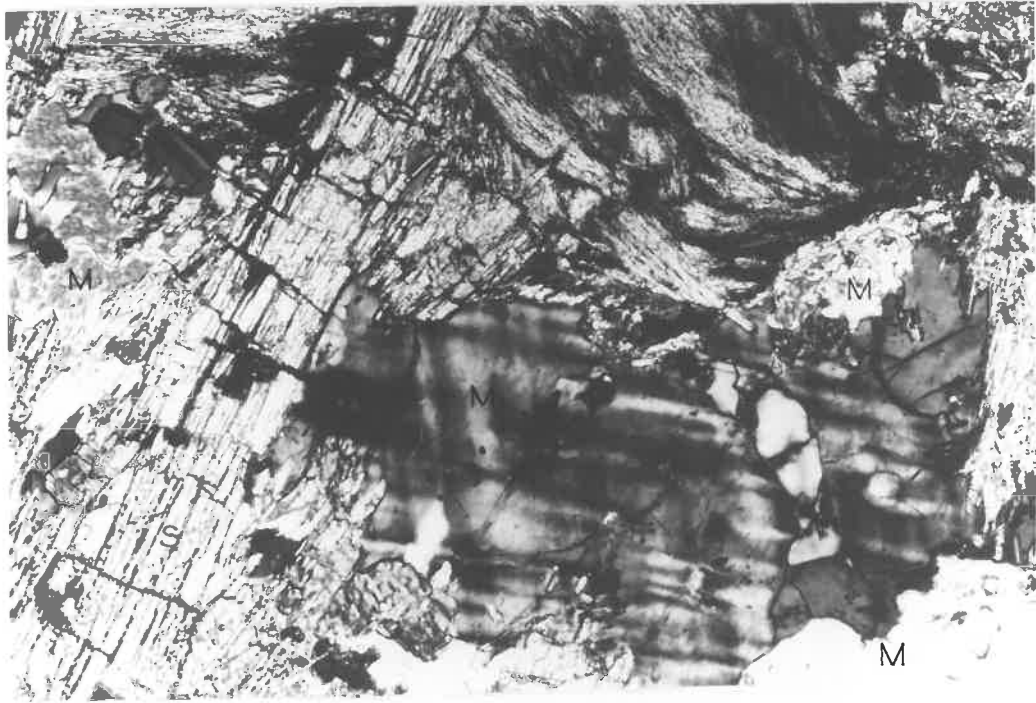
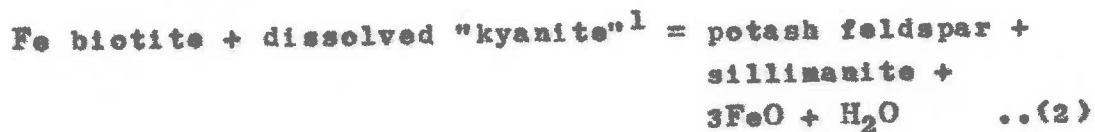


FIG. 26B.

Sillimanite may also have originated from the breakdown of biotite (Francis, 1956), since biotite and fibrolite are closely associated.



However, the fibrolite and biotite are associated in both the sillimanite-potash feldspar and sillimanite-muscovite schists. If the above reaction has taken place, then the biotite has decomposed in some cases within the muscovite stability field. However, biotites characteristic of pelitic schists (45 to 55 p.c. annite<sup>2</sup>) decompose only within the muscovite stability field under high oxygen pressures ( $\text{PO}_2 \approx$  hematite-magnetite buffer; Fig. 27). Since graphite and magnetite are the most common accessories in these rocks, it seems reasonable to assume that the  $\text{PO}_2$  was probably close to that of the quartz-magnetite-fayalite buffer. At the  $\text{PO}_2$  of this buffer no biotite will decompose within the muscovite stability field (Fig. 27). In those rocks with titaniferous hematite as an accessory, the  $\text{PO}_2$  will be much higher than the Q-M-F buffer, but still less than the magnetite-hematite buffer (see Fig. 5, p. 316, Buddington and Lindsley, 1964). Even under these conditions it is most

- 
1. In the Pevsey Vale rocks the unstable aluminosilicate is andalusite. Note also that a Mg rich biotite results from this reaction.
  2. See analyses of biotites in Vallance (1960) and Hayama (1964).



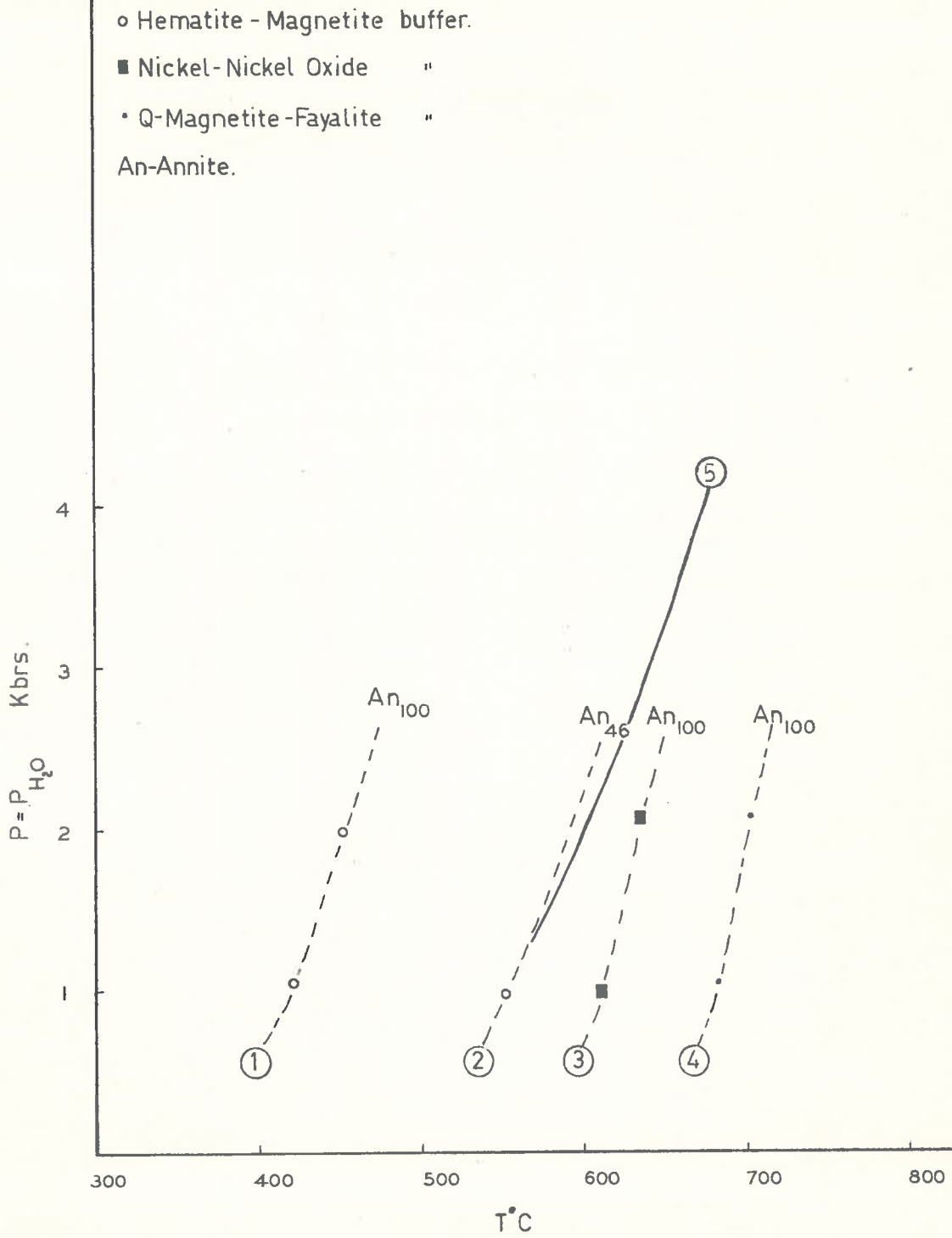
FIG.27.

Stability relationships of biotite and muscovite.

Curves 1 to 4: Stability curves of biotite of varying annite content at different oxygen buffers. Data obtained from Wones and Eugster, (1965).

Curve 5: Stability curve for muscovite in the presence of quartz at  $P_{H_2O} = P_{Load}$  (Evans, 1965).

FIG. 27.



Row

unlikely that the biotites were of the appropriate composition to break down. It is therefore, concluded that sillimanite has not originated from the decomposition of biotite. This is further substantiated by the lack of potash feldspar and iron ore in association with the fibrolite and biotite. The author considers that the sillimanite has nucleated on the surface of the biotite (Chinner, 1961), and that the Al and Si required for the growth of the sillimanite has<sup>been</sup> derived from the solution of unstable andalusite.

Andalusite is a rare constituent in the pelitic schists. It occurs as post tectonic (i.e. post  $S_1$ ) anhedral polikloblasts, studded with inclusions of biotite, quartz and more rarely microcline (e.g. 814A). Its presence in rocks in which sillimanite appears to be the stable phase testifies to the sluggish nature of the polymorphic inversion (Clark et al., 1957; Clark 1961; Khitarov et al., 1963; Bell, 1963).

The association of andalusite and microcline is of particular interest. This mineral pair is commonly found in pelitic rocks in contact metamorphic aureoles (e.g. Best and Weiss, 1964) and in the more widespread low pressure - high temperature metamorphic terrains (e.g. Shidô, 1958). It is normally assumed that they form from the decomposition of muscovite in the presence of quartz (Turner and Verhoogen, 1960). Their appearance in the Kanmantoo Group schists

suggests that metamorphic temperatures were unusually high or pressures were low or the decomposition of muscovite took place under locally dry (i.e.  $P_{H_2O} < P_{Lead}$ ) metamorphic conditions. In view of the extreme stability of muscovite in most of the Kannantoo Group rocks, it is more likely that the latter condition prevailed.

Biotite (X = pale brown to straw yellow, Y = Z = rust brown to deep olive brown) is ubiquitous (20 to 25 p.c.) and normally exhibits a strong preferred orientation parallel to  $S_1$ . In some specimens this foliation is intensely plicated about  $B_3$ . Muscovite is an abundant constituent of many pelitic schists. It forms both large (1.8 to 4.5mm. in diam.) and small (1.0 to 1.6mm. in diam.) porphyroblasts discordant to  $S_1$  and appears to replace fibrolite swarms. At several of the biotite-muscovite contacts, rutile occurs as a breakdown product. In some rocks, the muscovite porphyroblasts have subsequently broken down to sillimanite and microcline (Fig.26b), whereas in others they have been refolded about  $B_3$ , resulting in curved crystals with variable extinction. The growth of these large muscovites is probably related to a high activity of water and potassium in the fluid phase (Chinner, 1961) after the cessation of  $B_1$  movements (see Chapter 11). Quartz (0.03 to 0.45mm. in diam.) is found as mosaic-like aggregates between mica rich foliae. In the coarse "migmatitic" variants the grain boundaries of the

quartz are highly sutured. Garnet forms post tectonic skeletal porphyroblasts (0.45 to 1.3mm.) which are pre-tectonic to S<sub>3</sub>. The rotational features common to the garnets in the Adelaide Supergroup schists, are lacking in these porphyroblasts. In some specimens garnet appears to replace biotite and sillimanite, and in others the zone around the garnet porphyroblasts is depleted in sillimanite. Furthermore, biotite within this zone is altered to a yellow brown mica (more Mg rich biotite (?)) containing nests of rutile. It would appear then, that the following reaction (Winkler, 1965) has been operative in the formation of the garnet.



#### GRAPHITIC SCHISTS.

In the valley between the Mt. Kitchener intrusion and the Tanunda Creek Gneiss, banded, grey to buff coloured rocks, form low, discontinuous outcrops. Small gold diggings follow the line of outcrop (Plats 1). Most rocks have weathered to a white kaolinitic clayrock which extends to over a depth of 70 feet below the valley floor at Falkenburg's Hut (Chinner, 1955). Albite veins, limonite veins and pseudomorphs after pyrite, are a feature of some outcrops. B<sub>1</sub> folds and lineations (a white mineral streaking) are prevalent in the less kaolinised outcrops.

### Petrography.

In thin section the least altered specimens appear to consist of a fine grained (0.03mm.) mixture of quartz (25 to 35 p.c.), microcline (30 to 35 p.c.) and graphite (15 p.c.) with accessory zircon and ilmenite. The graphite is either evenly distributed throughout the rock or concentrated in bands. A colourless to pale brown micaceous mineral, which possibly represents kaolinite forming from biotite is also present. In other specimens, albite and albite-quartz pods, veins and bands are ubiquitous; graphite is absent and microcline is extremely turbid. A yellow brown subrounded or rectangular unidentifiable mineral, containing droplets of rutile (?) also occurs. The strongly kaolinised samples contain relics of graphite, turbid microcline or albite.

The alteration of the graphite schists may be due to the introduction of hydrothermal or pneumatolytic fluids, as suggested by Gaskin and Sampson (1951) for the kaolinite deposits east of Mt. Crawford. However, the occurrence of the kaolinised schists at the same elevation as presumed Tertiary sediments east of the Tanunda Creek Gneiss (Chinner, 1955) suggests that the kaolinisation could be due to deep weathering during the period of peneplanation which took place before the uplift of the Tertiary.

PETROLOGY AND PETROGRAPHY OF  
THE ADELAIDE SUPERGROUP ROCKS.

The next three chapters summarize the petrography and petrology of the Adelaide Supergroup rocks. To avoid unnecessary repetition the petrology and petrography of these rocks are discussed on a lithological rather than a stratigraphical basis. Reference will be made to the symbols  $S_1$ ,  $S_2$ , and  $S_3$  in the text.  $S_1$  is a foliation produced during the first phase of folding ( $B_1$ ), while  $S_2$  and  $S_3$  are crenulation cleavages related to the  $B_2$  and  $B_3$  deformations.

CHAPTER 6.THE NON CALCAREOUS ROCKS.THE PELITIC AND SEMI-PELITIC SCHISTS.

The pelitic and semi-pelitic schists of the Adelaide Supergroup in the Pewsey Vale area can be subdivided in the field into two main groups, the garnet schists and the bimica schists. The muscovite rich schists of unit 2 (Chapter 1) have been included in the bimica schists.

Mineral assemblages.

The mineral assemblages present in these rock types are:

1. Biotite-garnet-plagioclase-muscovite-sillimanite.
  - a) Biotite-garnet-plagioclase-sillimanite.
  - b) Biotite-garnet-plagioclase.
2. Biotite-muscovite-sillimanite-plagioclase.
  - a) Muscovite-sillimanite-plagioclase.
  - b) Muscovite-sillimanite-biotite.
  - c) Muscovite-biotite-plagioclase.
  - d) Biotite-plagioclase-sillimanite.
  - e) Muscovite-biotite.
  - f) Biotite-sillimanite.
  - g) Biotite-plagioclase.

Bimica Schists.

Bimica schists are ubiquitous in all parts of the sequence. A high proportion of muscovite to biotite gives rise to the silvery blue muscovite rich schists of unit 2 (Chapter 1). These schists change to a silvery brown colour on the western side of the area, due to a slight increase in the biotite content. A lineation ( $B_1$ ) defined by elongate knots of muscovite,



biotite or sillimanite is common and in most schists one or two crenulations ( $B_2$  and  $B_3$ ) are present. The strong foliation ( $S_1$  or  $S_2$ ) in these rocks results in platy or slabby outcrops. Many of the schists contain coarse quartz segregations, some of which have been folded about the  $B_1$  and  $B_3$  axes; rare sillimanite-quartz segregations also occur.

Petrography. Most schists are fine grained (0.05 to 0.08mm.), well foliated ( $S_1$ ) and exhibit crenulations parallel to  $B_2$  or  $B_3$ . Complete transposition of  $S_1$  into  $S_2$  or  $S_3$  is uncommon. Many schists are strongly lineated ( $B_1$ ), the lineation being defined by elongate augen of quartz, muscovite and/or sillimanite and biotite, or by biotite, sillimanite and muscovite. The augen are commonly refolded about  $B_2$  and  $B_3$  axes.

The schists consist of quartz (30 to 60 p.c.), muscovite (10 to 20 p.c.), biotite (15 to 30 p.c.) and plagioclase (5 to 20 p.c.). Muscovite (15 to 30 p.c.) rich and biotite poor (0 to 15 p.c.) variants are characteristic of the middle part of the sequence (Chapter 1). Graphite and tourmaline are accessories.

Quartz is generally found as strain free, equigranular mosaics between biotite folias, but is elongate in schists very rich in mica. This suggests that the micas have exerted an "influence on the grain shape of the growing quartz crystals" (Talbot, 1964). The grain size of quartz is commonly greater in schists showing well developed  $S_2$ . Quartz deformed

by  $B_3$  movements commonly undergoes a subsequent static recrystallization, but in some specimens it partially recrystallizes to small polygonal mosaics and in others it remains as strongly deformed grains with serrated intergranular boundaries. Most muscovite parallels  $S_1$  either as single foliae or as skeletal porphyroblasts in lenses associated with quartz; some is post tectonic to  $S_1$  or elongate along  $S_2$ . These muscovites affected by the  $B_3$  deformation are commonly kinked, bent or broken. X-ray diffraction patterns suggest that the muscovites have a 2M1 structure (Smith and Yoder, 1956) and contain approximately 15 percent paragonite (Zen and Albee, 1964). Biotite (X = very pale brown to straw yellow brown, Y = Z = red brown to light yellow brown) delineates  $S_1$  and  $S_2$  and develops similar  $B_3$  deformation features to muscovite. Sillimanite is frequently found as fibrolitic mats or stout prisms in muscovite. Rare outgrowths of sillimanite also occur at high angles to quartz-muscovite grain boundaries, suggesting that the sillimanite has nucleated on the muscovite. In addition, it is found as lineated prisms parallel to  $B_1$ , or in augen with biotite, quartz and muscovite. The sillimanite within individual augen is strongly oriented, but its orientation varies from augen to augen. Perhaps the sillimanite has epitaxially replaced an earlier formed, randomly oriented aluminosilicate.

The association of fibrolite and muscovite has been interpreted as one of simultaneous growth (Pitcher and Read, 1963; Woodland, 1963) and as an indication of the formation of sillimanite and potash feldspar from muscovite (Mills, 1964; White, in prep.). Since potash feldspar never occurs in the pelitic schists, the second hypothesis can be rejected for this area. The author considers that the first interpretation readily explains the relationships in the pelitic schists, but points out that some sillimanite may have nucleated within or at the grain boundaries of the muscovite. It is also suggested that the Al and Si required for the formation of the sillimanite is derived from the dissolution of an earlier formed aluminosilicate and has been transported via the medium of an aqueous phase to suitable nucleation sites.

Plagioclase (oligoclase) is found as poorly twinned grains (0.08 to 0.3mm.) associated with quartz and is strongly fractured in specimens exhibiting  $S_2$  crenulations. Tourmaline has a pleochroism (E = colourless, O = golden brown) which is characteristic of the Adelaide Supergroup meta-sediments in this area (c.f. Kanantoo Group tourmalines). Most crystals contain an inner core of graphite inclusions and some are poorly zoned. It is commonly discordant to  $S_1$ , and  $S_2$  and therefore post dates these foliations. Graphite occurs as irregular sponge-like masses or "streamers" parallel to  $S_1$  or  $S_2$  and may constitute as much as 10 percent of a schist (e.g. 756).

### Garnet Schists.

The best outcrops of garnet schists are north-east of Trial Hill, but sporadic outcrops are also present in the southern part of the area. Many of the rocks have a gneissic habit, layers of quartz and feldspar alternating with biotite rich layers. In these rocks quartz augen are common. Others are finer grained and more schistose and may grade into the gneissose variant along strike. Crenulation cleavages  $S_2$  and  $S_3$  and crenulations  $B_2$  and  $B_3$  of varying wave length are conspicuous in many outcrops.

### Petrography.

Most garnet schists consist of quartz (40 to 65 p.c.), biotite 20 to 40 p.c.), plagioclase (10 p.c.), garnet (5 to 10 p.c.), sillimanite (0 to 10 p.c.) and the accessories graphite, tourmaline, pyrite and apatite. In the rare muscovite bearing garnet schists, muscovite may constitute 20 percent of the rock.

In thin section they commonly show complex textural relationships; many contain  $S_1$  and  $S_2$  or  $S_1$  and  $S_3$ , and in some  $S_2$  is folded about the  $B_3$  axis (Figs.28a and b). However,  $S_2$  is confined to the coarser grained variants. In these rocks the gneissosity is defined by alternating layers of sheaf-like biotite and coarse quartz-plagioclase mosaics parallel to the crenulation cleavage  $S_2$ . Within the quartz-plagioclase layers, curved trails of biotite flakes outlining  $S_1$  are present (Fig.28a), suggesting that the

FIG.28A.

Large thin section of garnet schist  
showing curved trails of  $S_1(?)$  between  
 $S_2$ . Location 953 268. Spec. No.A200-919.  
Length of specimen 3.8 inches (9 cms).

FIG.28B

Large thin section of garnet schist  
showing crenulated  $S_2$ . Section cut  
perpendicular to  $B_3$ . Location 954 267.  
Spec. No.A200-918. Length of specimen  
3.3 inches (8 cms).

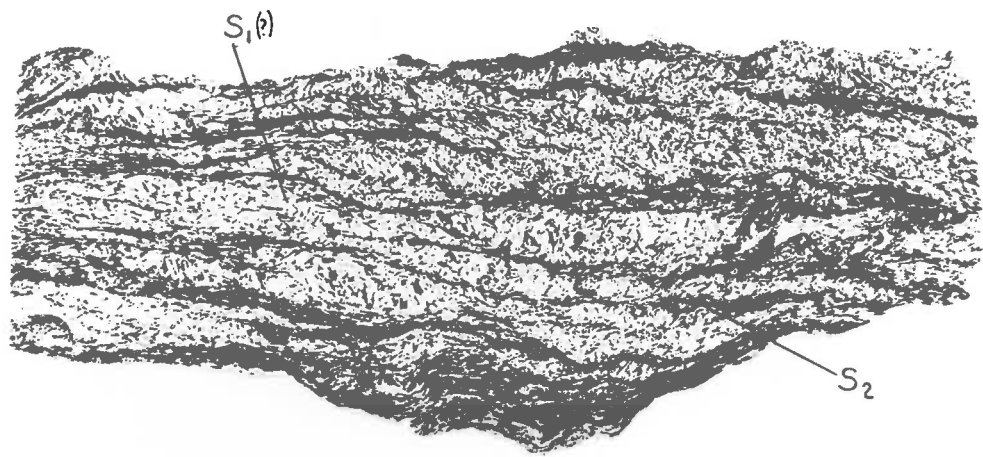


FIG. 28A.

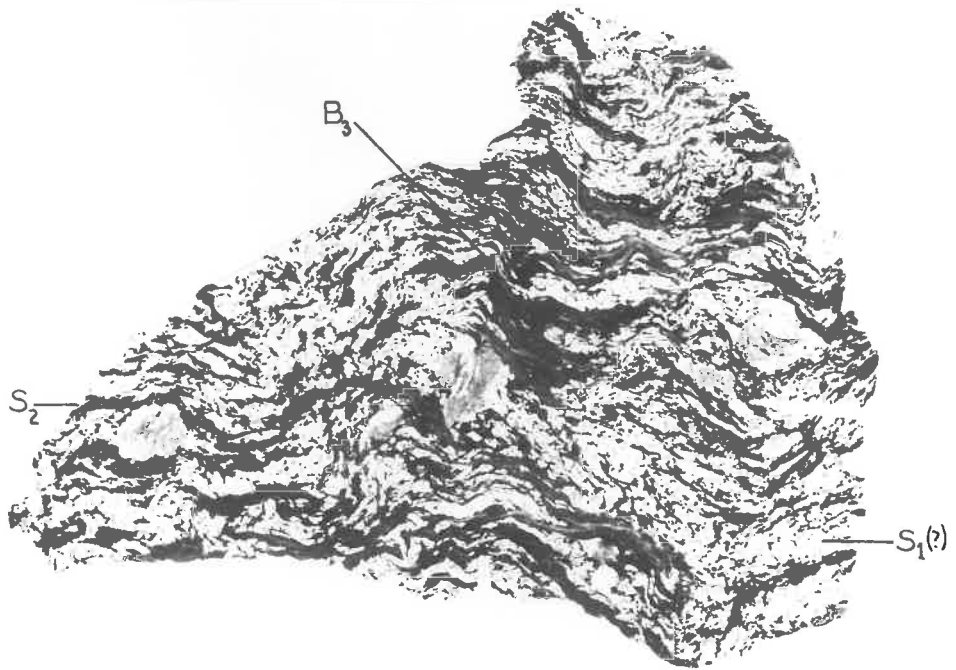


FIG. 28B.

banding has been formed by transposition of  $S_1$  by folding on  $S_2$  (see Talbot 1964). A notable increase in grain size occurs during the formation of this metamorphic layering (e.g. quartz 0.08 to 0.25mm. in the schistose variants to 0.3 to 1.0mm. in the gneissic varieties).

Garnet appears most commonly as sickle-shaped crystals (4.0 to 1.5mm.) containing sigmoidal, discontinuous trails of quartz and graphite (Fig.29a). This "snowball" or "pinwheel" structure is typical of metamorphic minerals growing during deformation (Spry, 1963 a). In this area the growth of the garnet has occurred during the  $B_1$  deformation as the  $S_1$  foliation is commonly continuous with the internal fabric ( $S_i$ ) of the garnet (see also Saxena, 1964). The sense of rotation shown by the inclusions is constant within the field of one thin section (c.f. Peacey, 1961). Some crystals exhibit post tectonic, idioblastic inclusion free rims. The lack of inclusions in the rim suggests that crystallization of the garnet proceeded at a much slower rate during the post  $B_1$  period (see Rast, 1965). During the formation of  $S_2$ , the garnets underwent rigid body rotation resulting in discordance between  $S_i$  and  $S_2$  (Fig.29b). In some specimens the garnets are discordant to  $S_1$  and have therefore grown post tectonic to the  $B_1$  deformation.

Plagioclase (An21 to 23) occurs as porphyroblastic, poorly twinned grains containing inclusions of biotite, quartz and tourmaline. Its grain size is larger in the gneissose variants

FIG.29A.

Sickle shaped garnet in Spec. No.  
A200-85. Foliation is  $S_1$ . Location  
957 247.

FIG.29B.

Large thin section of garnet schist  
showing orientation of sigmoidal in-  
clusions (outlined in ink) in garnets.  
Note the difference in orientation of  
the inclusions in individual garnets.  
Location 982 276. Spec. No.A200-251.  
Specimen natural size.



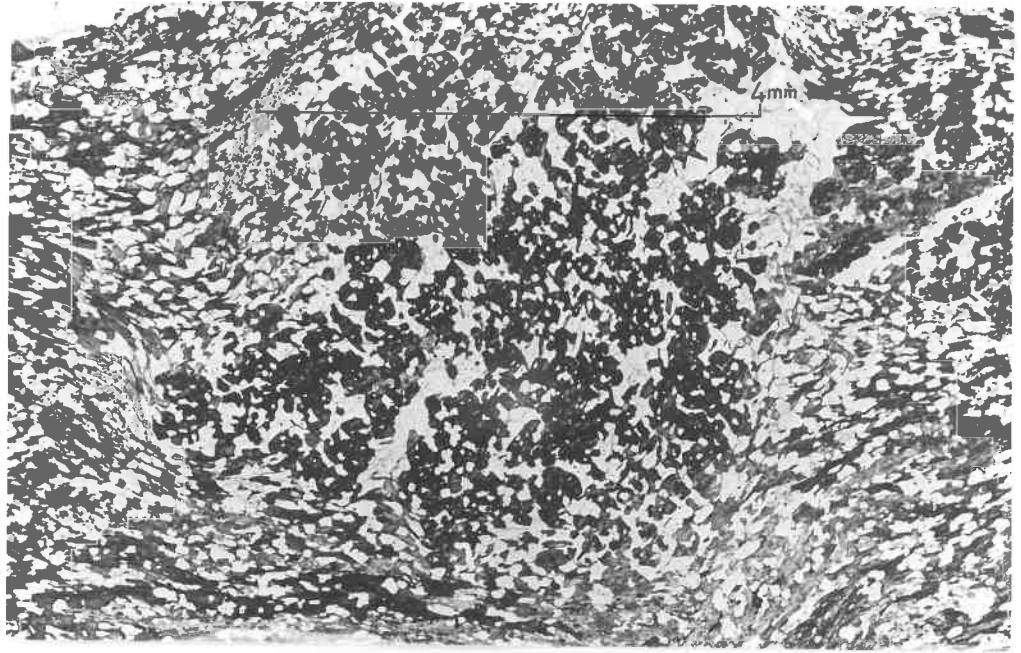


FIG. 29A.

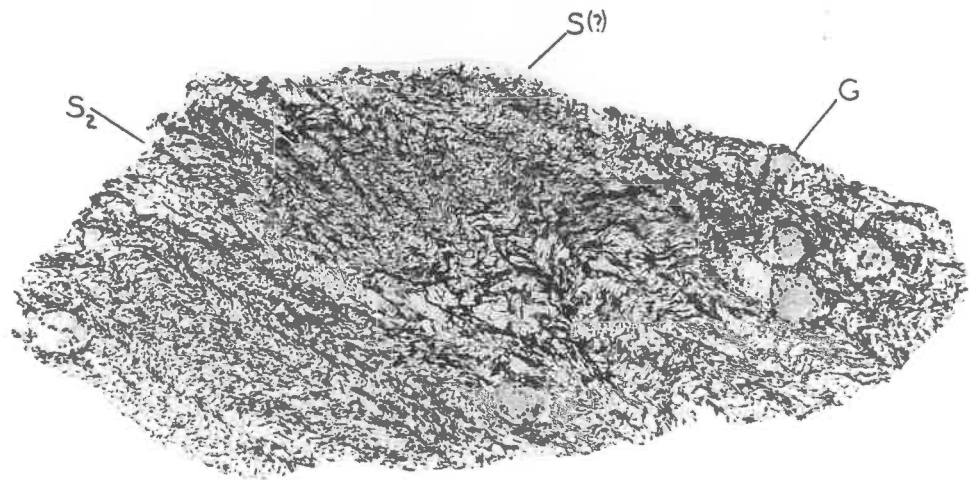


FIG. 29B.

FIG.30.

Photomicrograph of pelitic schist showing small prisms of sillimanite (arrow) in muscovite. The matrix consists of quartz and biotite. Location 957 144. Spec. No.A200-9. X 100.

FIG.31.

Typical outcrop of pebble bed. Pencil 6 inches (15 cms). Location 940 195.

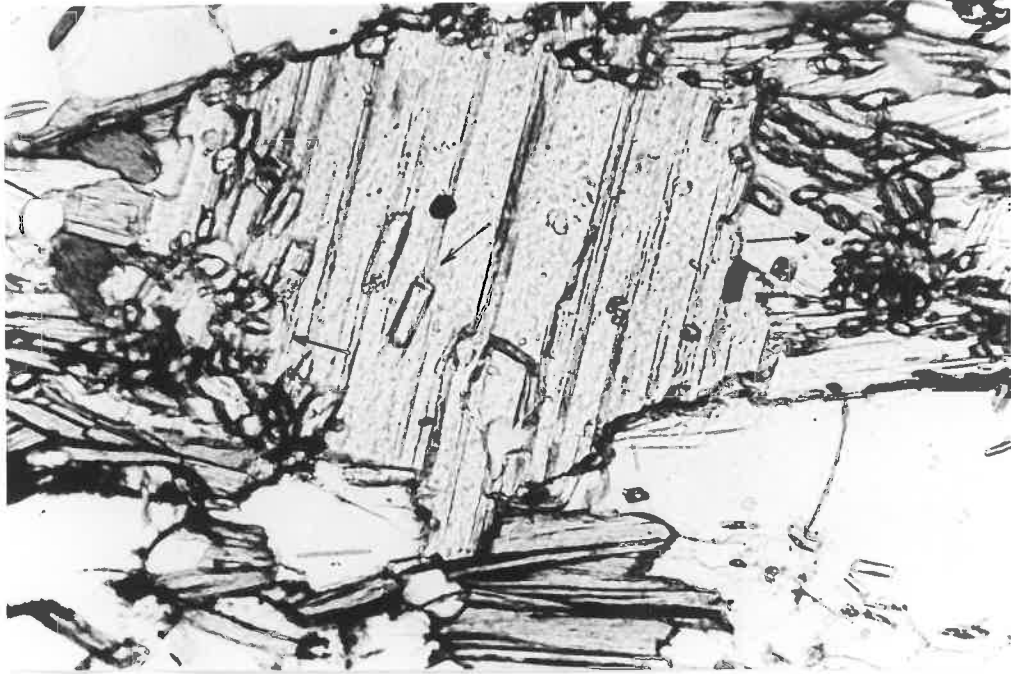


FIG 30.



FIG 31.

(e.g. 0.2 to 0.6mm. in 254 compared with 0.05 to 0.15mm. in 375). Biotite (X = very pale brown, Y = Z = chocolate brown to rust brown) is a major constituent of all schists. According to optical data ( $n_{\gamma} = 1.636$ ) it has an Fe/Fe+Mg ratio of 48 percent.<sup>1</sup> It delineates S<sub>1</sub> and S<sub>2</sub> and is commonly bent in the fold hinges of B<sub>3</sub> crenulations, indicating that crystallization has not accompanied this phase of folding in some cases.

Muscovite parallels S<sub>1</sub> and exhibits a colourless to pale green pleochroism. Deer et al.(1963) suggests that colour of pale green muscovites is due to Fe<sup>2+</sup>. Quartz is normally present as strain free mosaics between S<sub>1</sub> or S<sub>2</sub> foliae, but in rocks deformed by B<sub>3</sub> movements it shows a very strong undulose extinction and more rarely deformation lamellae. Staurolite appears as relic grains in the matrix of some schists. Sillimanite occurs as unoriented needles or small crystals in quartz, muscovite (Fig.30) or biotite. Some aggregates have been rotated into S-shaped whorls during the formation of S<sub>2</sub> and display the same sense of rotation as the micas between the S<sub>2</sub> planes. This suggests that the sillimanite has grown prior to the B<sub>2</sub> deformation and after the B<sub>1</sub> phase of folding.

#### QUARTZITES.

The quartzites of the Adelaide Supergroup form prominent

---

1. The curves given by Wones(1963) for the quartz-magnetite-fayalite buffer are applied here, as graphite is ubiquitous.

ridges in the central and southern parts of the area. They range from 1 to 20 feet in thickness and are massive or platy in outcrop. Bedding (S) defined by a compositional banding is present in many outcrops, but cross-bedding is rare. The quartzites are strongly jointed and in some a fracture cleavage ( $S_1$ ) is developed. A lineation ( $B_1$ ) defined by ribbing, feldspar spindles and smeared out muscovite is prominent in many outcrops. In hand specimen the quartzites have a glassy, saccharoidal appearance and show a variation in grain size from band to band. Mineralogically, the quartzites consist of quartz (95 to 99 p.c.) and minor microcline, plagioclase and muscovite. Tourmaline, biotite and zircon are accessories. The quartzites show predominantly equidimensional (mean diam. varies from 3.0mm. in 299 to 0.4mm. in 329) mosaics in sections perpendicular and parallel to  $B_1$ . Such a fabric is indicative of intense post kinematic (tectonic) recrystallization (Weiss et al., 1955). Undulose and domain extinction, deformation lamellae, and healed fractures which cross grain boundaries, are common features in the quartz. The grain boundaries are sutured and less commonly serrated. These textures indicate that the quartz has undergone plastic deformation (Carter et al., 1964).

Microcline and plagioclase occur as interstitial, irregular or subrounded grains in sections perpendicular to  $B_1$ , and are elongate in sections parallel to  $B_1$ . Muscovite is also elongate parallel to  $B_1$ . The accessories appear as inclusions trapped

within quartz.

### PEBBLE BEDS.

Two small pebble beds occur in the upper part of the Adelaide Supergroup sequence, 1 mile north of the Williamstown - Mt. Pleasant road. They generally form low sporadic outcrops. In hand specimen small (5.0cms. to 0.5cms. in diam.) subrounded to angular pebbles of quartz, feldspar, granite gneiss and albite(?) are unevenly distributed in a foliated biotite rich matrix (Fig.31). Many small biotite rich schlieren and schist pebbles are elongate parallel to the foliation  $S_1$ .

The matrix consists of small (0.16 to 0.8mm. in diam.) angular to sub-rounded fragments of quartz and minor turbid plagioclase set in a foliated aggregate of biotite (X = yellowish white, Y = Z = red brown), unstrained quartz (0.08 to 0.16mm. in diam.) and rare twinned plagioclase. Small clots of unoriented biotite also occur. Apatite, slightly rounded zircon and tourmaline (E = pale straw yellow; O = yellowish green) are accessories.

CHAPTER 7.CALC-SCHISTS AND CALC-SILICATEROCKS.

In the upper and lower parts of the Adelaide Supergroup sequence, calc-silicate rocks and calc-schists of variable thickness are intimately intercalated with pelitic schists. Calc-silicate bands 10 feet or more in thickness, weather out prominently and serve as useful marker horizons (Plate 1); the smaller calc-silicate bands commonly lens out along strike. In outcrop the calc-schists and calc-silicate rocks are intimately interlayered (Fig.32). Individual bands of calc-schist or calc-silicate rock show a fine lamination which is due to slight variations in mineralogical composition. In hand specimen the calc-schists are generally well foliated ( $S_1$ ) and commonly contain nodules of diopside or scapolite. Finer grained, more compact variants with weaker foliation are also present. On the bedding planes of some schists, deep green amphibole prisms exhibit a characteristic decussate texture. The calc-silicate rocks are generally finely banded, green to off-white rocks. The siliceous variants in the southern part of the area have a saccharoidal texture. Metamorphic segregations consisting of pale green diopside, greasy white scapolite, white potash feldspar and deep green amphibole occur in the noses of macroscopic  $B_3$  folds. Cleavage mullions and boudins parallel to  $B_1$  are common in some areas, and some outcrops show either  $B_1$ ,  $B_2$  or  $B_3$

FIG.32.

Typical outcrop of intercalated calc-silicate rock (prominent bands in the centre of the photo) and calc-schist. Location 950 237.

FIG.33.

Photomicrograph of calc-schist. Poikiloblasts of scapolite (S) and diopside (D) set in a foliated matrix (foliation is  $S_1$ ) of biotite and quartz. Location 947 251. Spec. No.A200-74A. X 40.





FIG 32.

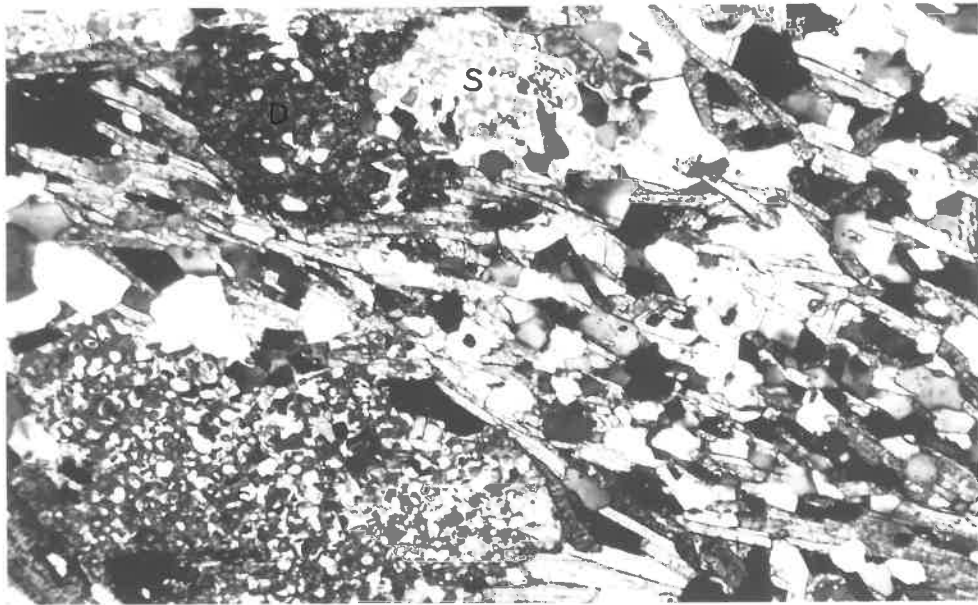


FIG 33

mesoscopic folds. A lineation defined by the intersection of  $S_1$  with the banding  $S$ , is conspicuous in many outcrops.

### Petrography.

The calc-schists and calc-silicate rocks show a wide range of textural and mineralogical variations. The range of mineralogical composition is illustrated in Table 15. The mineral assemblages that are commonly present, are listed below:

- (1) Diopside-actinolite-potash feldspar-biotite-scapolite(plagioclase).
- (2) Diopside-actinolite-potash feldspar-scapolite(plagioclase).
  - a. Diopside-potash feldspar-scapolite.
  - b. Actinolite-potash feldspar-scapolite.
  - c. Actinolite-potash feldspar-diopside.
  - d. Diopside-actinolite-plagioclase.
  - e. Actinolite-potash feldspar.
  - f. Actinolite-scapolite.
  - g. Diopside-scapolite.
  - h. Diopside-potash feldspar.
- (3) Diopside-biotite-potash feldspar-actinolite.
- (4) Diopside-biotite-scapolite(plagioclase)-actinolite.
  - a. Diopside-biotite-scapolite.
  - b. Actinolite-biotite-plagioclase.
  - c. Biotite-scapolite.
- (5) Diopside-scapolite-calcite.

Quartz is present in all assemblages and tourmaline, apatite, graphite and sphene are ubiquitous accessories. Such assemblages are typical of calcareous rocks metamorphosed to the upper almandine amphibolite facies (Turner and Verhoogen, 1960; Hietanen, 1963).

Since it is not possible to describe adequately all the

TABLE 15.

Estimated volume percentage of constituents in  
Calc-silicate rocks and Calc-schists.

<u>Rock Type</u>	<u>Calc-silicate rock</u>	<u>Calc-schist</u>	<u>Calc-schist</u>	<u>Calc-silicate rock</u>		<u>Siliceous calc-silicate rock</u>	<u>Calc-silicate rock</u>
<u>Layer</u>	(1)	(2)		(1)	(2)		
<u>Spec. No.</u>	865	865	258B	3A	3A	732	204
Actinolite	5	5	25	-	-	-	-
Diopside	15	15	-	25	10	20	25
Scapolite	15	25	-	60	45	15	25
Biotite	5	30	25	-	+	-	-
Quartz	55	20	30	15	45	60	40
Microcline	5	5	-	-	-	-	10
Plagioclase	-	-	20	-	-	-	-
Tourmaline	+	+	+	-	-	+	-
Graphite	+	+	+	-	-	-	-
Sphene	+	+	-	+	+	+	+
Apatite	-	-	-	+	+	+	+
Calcite	-	-	-	-	-	+	+
Zircon	-	-	-	-	-	-	+

TABLE 16.

Optical properties of minerals in the Calc-schists,  
Calc-silicate rocks and Metamorphic Segregations.

<u>Spec.No.</u>	<u>Rock Type</u>	<u>Amphiboles</u>		$n_{\alpha}$	<u>Composition (%)</u> Mg/Mg+Fe <sup>2+</sup> +Fe <sup>3+</sup> +Mn)
		2Vx	Z C		
339	Calc-silicate rock	79	14.5	1.624	24
74B	Calc-schist	84	15	1.628	31
74A	"	81	-	1.628	31
252	"	-	-	1.634	38
213A	Segregation	-	-	1.624	24

<u>Spec.No.</u>	<u>Rock Type</u>	<u>Pyroxenes</u>		
		2Vx	$n_{\beta}$	<u>Composition(%Fe<sup>2+</sup>)</u>
74B	Calc-schist	58	1.687	20
322B	Calc-silicate rock	54	1.680	10
213B	Segregation	58	-	-
1B	Calc-silicate rock	58	-	-
204	"	56.5	-	-
89	Segregation	55	1.685	16
213E	"	63-48 <sup>+</sup>	-	-

+Grains highly strained.

<u>Spec.No.</u>	<u>Rock Type</u>	<u>Scapolites</u>	
		$n_o$	<u>Composition</u> (%Meionite)
74A	Calc-schist	1.572	53
292	Calc-silicate rock	1.563	40.5
64	"	1.580	64
89	Segregation	1.574	55.5
127	Calc-silicate rock	1.566	45
74B	Calc-schist	1.570	50
398A	Calc-silicate rock	1.580	64
322B	"	1.575	57
213B	Segregation	1.565	43.5
260	Calc-silicate rock	1.570	50
204	"	"	"
302	"	1.579	62

textural and mineralogical variations in these rocks, descriptions of representative specimens will be given. A typical calc-schist (e.g. 74A) consists of a foliated aggregate of biotite, unstrained quartz and scapolite with poikiloblasts of scapolite, diopside and actinolite (Fig.33). The biotite foliation ( $S_1$ ) is bowed around the scapolite poikiloblasts, suggesting that they are pre-tectonic to  $S_1$  (Zwart, 1960). The scapolites have a composition ranging from  $Me_{50}$  to  $Me_{53}$  (Table 16). Rosettes of secondary epidote, clinzoisite and zoisite replace scapolite. Diopside (approx. 20 p.c.  $Fe^{2+}$ , Table 16) occurs as skeletal porphyroblasts athwart  $S_1$  and therefore post dates the  $B_1$  deformation. The pleochroism of the biotite is distinctive (X = straw brown, Y = Z = rust brown) and optical properties ( $n_\gamma = 1.629$ , 74A and B) suggest a composition near 40 percent  $Fe^{2+}/Fe^{2+}+Mg^{2+}$  (Wones, 1963).

Actinolite (X = very pale green, Y = pale green, Z = pale olive green,  $n_\alpha = 1.624$ ,  $2V_X = 81-84$ , Table 16) forms small euhedral porphyroblasts (0.5mm. in diam.), which cross-cut both the foliation  $S_1$  and the diopside porphyroblasts. Another variant of calc-schist (e.g. 252, 230) contains small idiomorphic crystals (0.05 to 0.5mm. in diam.) of actinolite ( $n_\alpha = 1.634 = 38$  p.c.  $Fe^{2+}/Fe^{2+}+Mg^{2+}+Fe^{3+}+Mn$ , Table 16) dispersed in a fine grained poorly foliated matrix of plagioclase, strain free quartz (0.01mm. in diam.) and biotite (pleochroism as above; Fig.34). In some of these schists the actinolite occurs as strained sheaf-like aggregates.

FIG. 34.

Photomicrograph of calc-schist showing post tectonic porphyroblasts of actinolite (A) cross cutting a foliated matrix (foliation is  $S_1$ ) of biotite, quartz and plagioclase. Location 960 270. Spec. No. A200-256B. X 100.

FIG. 35.

Photomicrograph showing polygonal aggregates of quartz at the grain boundaries of large strained quartz grains. Location 945 175. Spec. No. A200-208. X 126.

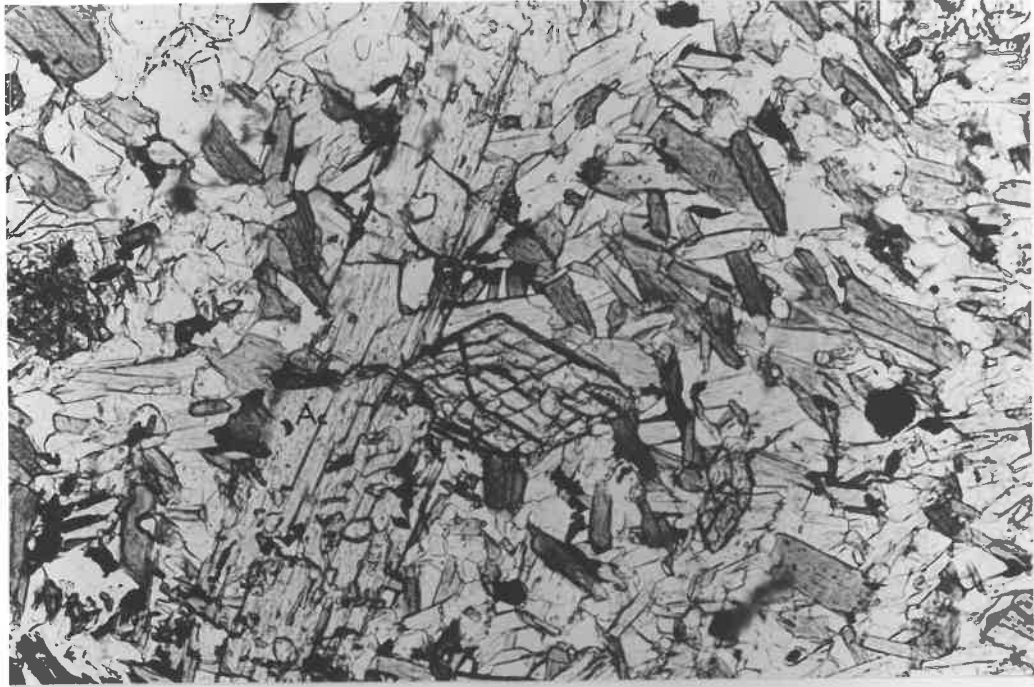


FIG.34.

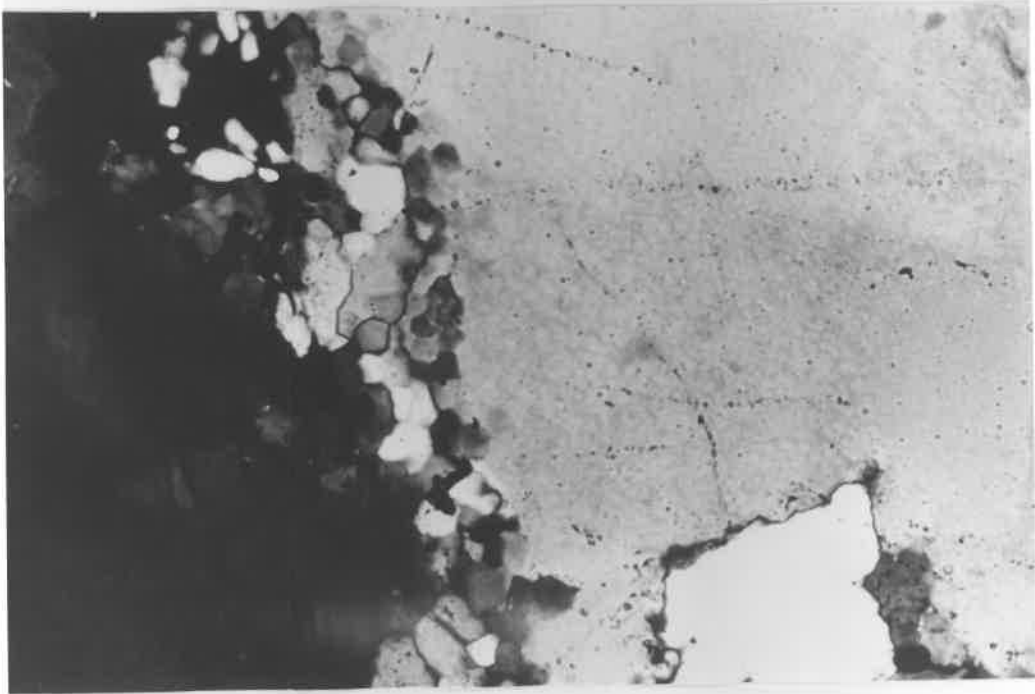


FIG.35.

Intercalated with the calc-schists are laminated (>3.0mm. thick) calc-silicate rocks. Commonly, the mineral assemblage in each band is similar, but the mineral proportions change from band to band (e.g. 3A, Table 15). Specimen 322B is characteristic of the calc-silicate rocks. It is composed of an unstrained<sup>1</sup> mosaic of scapolite and quartz in which are distributed aggregates or grains of diopside (0.15 to 0.6mm. in diam. 10 p.c. Fe<sup>2+</sup>, Table 16). Dewdrop shaped sphene, idiomorphic apatite and minor bent biotite are also present. Idiomorphic, post tectonic actinolites are more common in other calc-silicate rocks and are optically similar to the actinolites in the calc-schists (e.g. 339, Table 16).

The siliceous calc-silicates in the southern part of the area, consist of skeletal diopside (0 to 30 p.c.; 0.15 to 0.8mm. in diam.) or idiomorphic actinolite (0 to 10 p.c.) disseminated in a granoblastic matrix of quartz (40 to 85 p.c; 0.1 to 1.0mm. in diam.) and scapolite (or potash feldspar). They show more evidence of post-crystalline deformation than the calc-schists and calc-silicate rocks previously described. The quartz grain boundaries are commonly serrated and domain extinction is strongly developed. Some recrystallization has occurred at grain boundaries (Fig. 35). Deformation lamellae have been noted in some diopsides (e.g. 732). It is considered that these deformation features have occurred during the B<sub>3</sub>

---

1. Triple point relationships and straight boundaries are shown by quartz and scapolite.



phase of folding, as all specimens come from areas in which this phase has been most active.

Refractive index measurements ( $n_o$ ) of several scapolites from the calc-silicate rocks, reveals a range in composition (40.5 to 62 p.c. melionite Table 16) similar to that recorded in the Kanmantoo Group calc-silicate rocks (Table 11). The potash feldspar in the calc-silicate rocks is distinctly triclinic (Table 17; c.f. potash feldspars in Kanmantoo Group calc-silicate rocks) and generally lacks a perthitic texture. Zoning is rare. The tourmalines in the majority of calc-schists and calc-silicate rocks have the pleochroic scheme, E = colourless, O = golden brown, but in the siliceous variants E = pale blue and O = blue and blotchy green varieties have been noted. This suggests that the sediments for these rocks have been derived from different source areas.

The presence of actinolite in these rocks is noteworthy, as actinolite is normally replaced by hornblende at higher metamorphic grades (Shido, 1958). However, Layton (1963) has shown that members of the tremolite-actinolite series can exist in high grade rocks rich in silica (i.e. rocks with a high  $\text{SiO}_2/\text{Al}_2\text{O}_3$  ratio). The calc-silicate rocks and calc-schists of the Adelaide Supergroup contain quartz in abundance (Table 15), hence it would appear that these rocks were far too siliceous to allow the crystallization of hornblende.

The persistence of actinolite to this high grade is also thought to be due to the lack of calcite available to react

TABLE 17.

2Vx and Obliquity values of the Alkali Feldspars  
in the Calc-silicate rocks of the Adelaide  
Supergroup.

<u>Spec. No.</u>	<u>Rock Type</u>	<u>2Vx</u>	$\Delta$	<u>Comments</u>
213A	Segregation (80 rim 64 core)			Microcline twinning Untwinned
330	Calc-sili- cate rock	80	0.950	Microcline twinning
332	"	-	0.948	" "
127	"	-	0.874	" "
204	"	80	0.915	" "

with this amphibole to form diopside (equation 1).



This conclusion is supported by the occurrence of diopside not actinolite in these calc-silicate rocks containing free calcite.

#### Metamorphic segregations.

In the nose of  $B_3$  folds are pods of coarsely crystalline calc-silicate minerals which are believed to have been formed by metamorphic segregation. Primary diopside, scapolite, actinolite, microcline, quartz and sphene and secondary epidote, zoisite, actinolite, calcite and chlorite are the main constituents. There is a strong tendency for most minerals to have idioblastic outlines (Fig.36) rather than xenoblastic forms which are more common in the calc-silicate rocks. These different textures and the restriction of segregations to  $B_3$  folds, suggest that recrystallization of the calc-silicate rocks took place after the  $B_3$  folding.

The optical properties of the segregation minerals are similar to those in the calc-silicate rocks (Table 16). However, in a few specimens individual grains of potash feldspar show a variation in  $2V_x$ . For example, in specimen 213A, some grains consist of untwinned cores ( $2V_x=64$ ) surrounded by cross-hatched rims ( $2V_x=80$ ), others contain irregular, twinned zones (c.f. Mackenzie, 1954). Such variations in optical properties are due to variation in the structural state of the feldspars

FIG. 36.

Photomicrograph of calc-silicate metamorphic segregation showing idiomorphic crystals of scapolite (S) actinolite (A), diopside (D), and interstitial microcline (Mi). Location 941 172. Spec. No. A200-213E. X 100.



FIG. 36.

within single grains.

### Conclusions.

A study of the calc-silicate rocks and calc-schists of the Adelaide Supergroup has shown that a wide variety of mineral assemblages are present. The assemblages are typical of calcareous rocks metamorphosed under conditions of the upper almandine-amphibolite facies. The crystallization of these rocks appears to have commenced before deformation and continued after the final phase of folding. The presence of actinolite rather than hornblende is attributed mainly to the highly siliceous nature of calc-silicate rocks and calc-schists.

CHAPTER 8.METAMORPHISM.

The meta-sediments of the Adelaide Supergroup and the Kammantee Group in the Pewsey Vale area appear to have reached the same grade of metamorphism. Any differences between the assemblages in the two groups can be explained on lithological grounds. Therefore, a discussion of the metamorphism will include both groups of rocks.

Metamorphic zoning, facies and grade.Metamorphic Zoning.

In many high grade metamorphic terrains, a "sillimanite-potash feldspar isograd" (Guidetti, 1963) can be mapped which separates rocks of the sillimanite grade from the sillimanite-potash feldspar grade of metamorphism, (e.g. Heald, 1950; Chapman, 1952; Hayama, 1964). This isograd is defined by the reaction:



In the Kammantee Group rocks muscovite has undergone a partial or complete breakdown (as referred to above), in many pelitic schists, but is stable in most quartz-feldspathic schists and migmatites (Fig.37). Furthermore, unaltered muscovite can be found in the quartz-feldspathic schists, migmatites or pelitic schists adjacent to pelitic schists in which sillimanite-potash feldspar or sillimanite-muscovite-potash feldspar assemblages are apparently stable (Fig.37).

FIG. 37.

Location of samples examined in isograd study. Assemblages in these rocks are designated by the appropriate symbols. S, KF and M refer to sillimanite, potash feldspar and muscovite. All rocks contain quartz, plagioclase and biotite.



KANMANTOO GROUP.



 CALC-SILICATE ROCK.

 MIGMATITE.

 QUARTZO-FELDSPATHIC SCHISTS.

 TANUNDA CREEK GNEISS.

 ALBITISED MT KITCHENER GRANITE.  
ALBITITE.

ADELAIDE SUPERGROUP.



ASSEMBLAGES.

● S-KF  
○ S-M-KF } - PELITES.

⊖ S-M

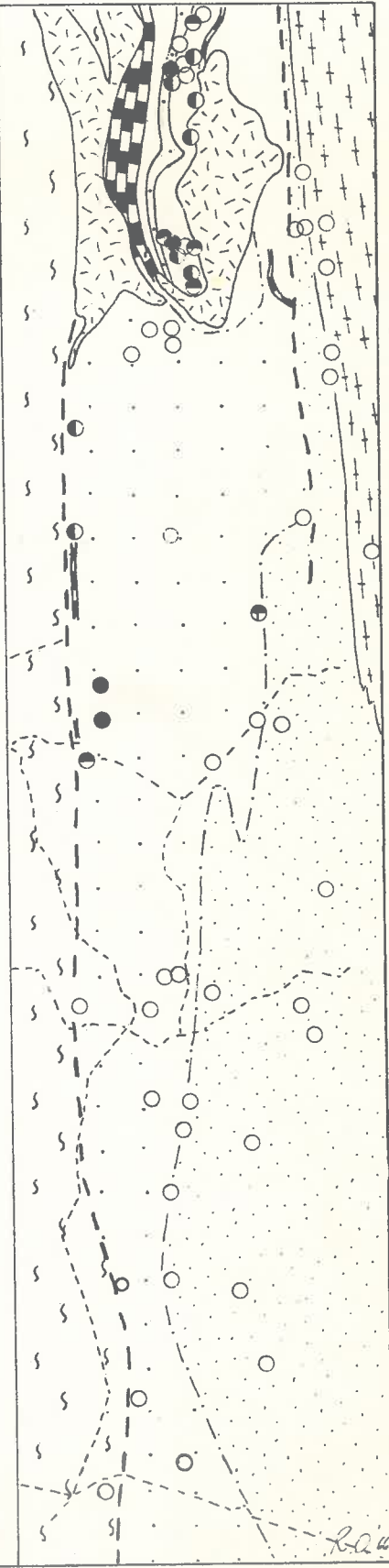
○ M

⊖ S-M

} - Q-F SCHISTS, MIGMATITE.



FIG. 37.



Generally, rocks with the pair sillimanite-potash feldspar are considered to be of higher metamorphic grade than those in which muscovite is stable. However, it is unlikely that rocks in the Pewsey Vale area with the pair sillimanite-potash feldspar represent a higher metamorphic grade (based on temperature), than those bearing muscovite. Unusually steep temperature gradients over short distances would be needed to produce the present intimate association of "higher" and "lower" grade assemblages (Fig.37). This conclusion is supported by the studies of Mr. D. Virgo (Geology Dept., University of Adelaide) who found a uniform Sr distribution coefficient ( $K_d = 0.94$ , Fig.38) in co-existing feldspars from 7 specimens<sup>1</sup> in the Pewsey Vale region. He concluded that these rocks had reached chemical equilibrium and that they had recrystallized at the same metamorphic temperatures. Hence, it appears that the sillimanite-muscovite and sillimanite-potash feldspar assemblages do not correspond to different "zones" in the usual sense. It is suggested that the intimate association of "higher" and "lower" grade assemblages is due to variations in water vapour pressure ( $P_{H_2O}$ ), as dehydration temperatures are lowered when  $P_{H_2O}$  is less than  $P_{Lead}$  (Yoder, 1955; Greenwood, 1961). Such variations in  $P_{H_2O}$  could be due to local original differences in the water content of the rocks over small distances.

---

1. These include 2 quartzo-feldspathic schists, 3 migmatites (both muscovite bearing) and 2 pelitic schists (sillimanite-potash feldspar bearing). See Appendix 1 for the composition of the feldspars.

The rocks in the Adelaide Supergroup are isofacial throughout the whole area and no metamorphic zones could therefore be delineated.

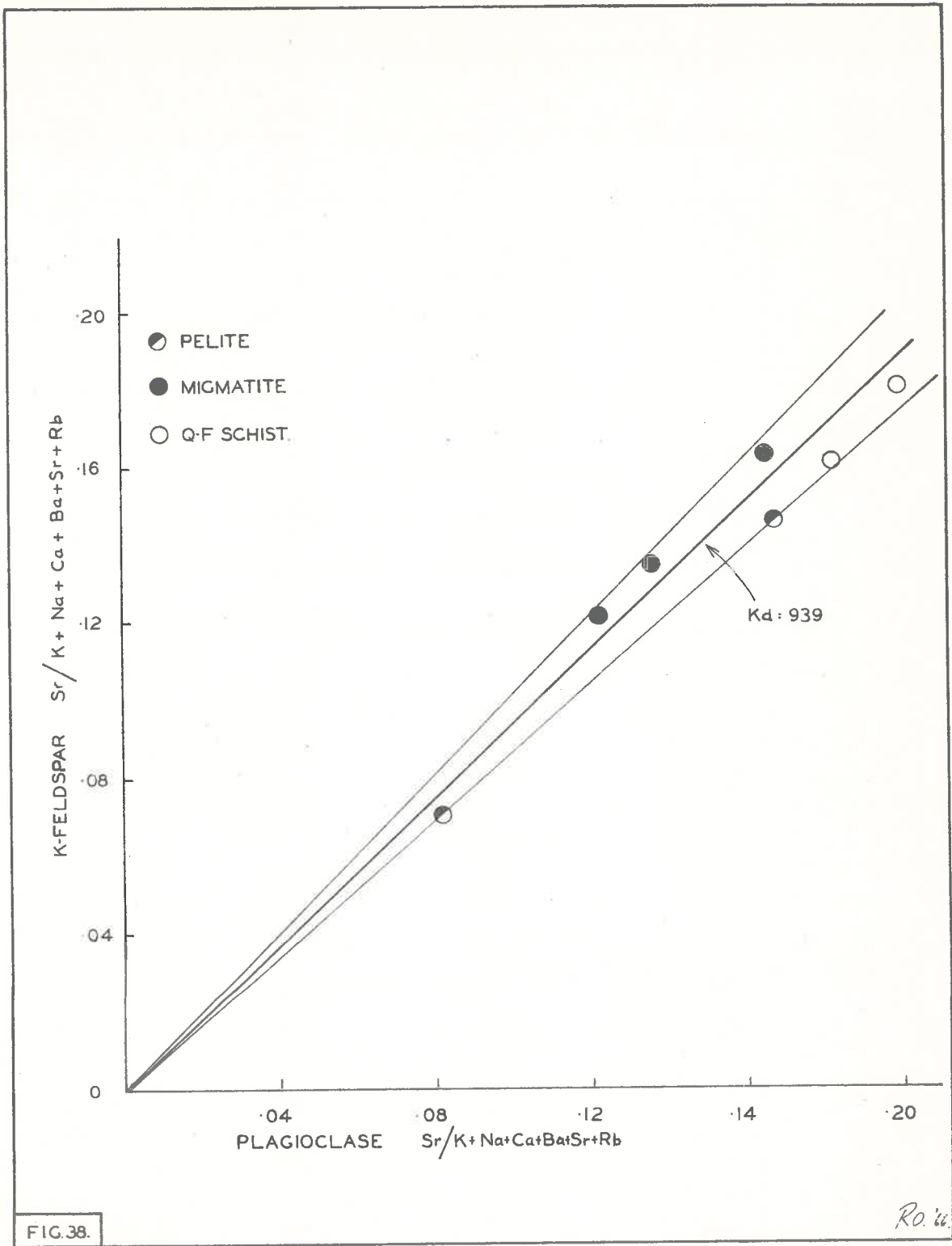
Metamorphic facies and grade.

The occurrence of the diagnostic assemblage hornblende-plagioclase (An<sub>35</sub> to An<sub>46</sub>) in the amphibolites (Chapter 9), and diopside in the calc-silicate rocks of both the Kanmantoo Group and Adelaide Supergroup, places the Pewsey Vale rocks in the almandine-amphibolite facies (Turner and Verhoogen, 1960); the absence of epidote restricts them to the upper part of this facies (Kretz, 1960). This is substantiated by the presence of the assemblages sillimanite-muscovite and sillimanite-potash feldspar in the pelitic schists of the Kanmantoo Group, and sillimanite-muscovite in the Adelaide Supergroup schists. The colour of hornblende in the meta-dolerites (Z = deep green) is also indicative of the sillimanite grade of metamorphism, since at lower grades a bluish-green or greenish-blue amphibole is normally present (Shidô, 1958; Miyashiro, 1958). The Sr distribution coefficient of 0.94 (see p. 68) between coexisting feldspars in the Kanmantoo Group rocks, is also similar to that of other upper amphibolite facies rocks (Virgo, Ph.D. thesis in prep., University of Adelaide).

Thus petrographic and chemical evidence clearly indicate that the meta-sediments in the Pewsey Vale area have reached the upper almandine-amphibolite facies of metamorphism.

FIG. 38.

Distribution of Sr-feldspar between  
K-feldspar and Plagioclase in rocks  
from the Pewsey Vale area.



Type of metamorphism.

After a survey of the petrography of many metamorphic terrains throughout the world, Miyashiro (1961) proposed a number of "metamorphic facies series", based on the pressure operating during metamorphism. He recognised five facies series, three standard types and two intermediate groups, which are listed below in order of increasing pressure.

1. Andalusite-sillimanite type.
2. Low pressure intermediate group.
3. Kyanite-sillimanite type.
4. High pressure intermediate group.
5. Jadeite-glaucophane type.

Facies series 2 and 3 contain staurolite.

In the meta-sediments of the Mt.Lofty Ranges the association andalusite-staurolite-sillimanite is ubiquitous (White,1956; Kleeman and Skinner,1959; Eggleton,1959; Offler,1960,1963; Fleming,1965) and in some areas cordierite (Sando,1957; Mills, 1964) and locally kyanite (Alderman,1942; Freytag,1957; Mills, 1963) have been reported.

The Kannantoo Group rocks of the Pewsey Vale area contain both andalusite (relic) and sillimanite, and in the adjacent Adelaide Supergroup meta-sediments, staurolite (relic) and sillimanite are present. It would appear then, that the rocks in the present area and in the remainder of the Mt.Lofty Ranges are an example of Miyashiro's low pressure-intermediate type of metamorphism. However, the occurrence of kyanite in certain

areas suggests that locally higher pressures operated.

Physical conditions during metamorphism.

In the last decade the stability fields of many rock forming minerals have been determined experimentally.<sup>1</sup> Although these investigations have provided information on the P-T conditions of formation of synthetic phases, they are still very limited in their application, because the systems dealt with in the laboratory are much simpler than those in most metamorphic rocks. Furthermore, in most experiments,  $P_{\text{Load}} = P_{\text{H}_2\text{O}}$ , a condition which may not be fulfilled during metamorphism (Miyashiro, 1961). Nevertheless, an approximate estimation of the pressures and temperatures of metamorphism can be obtained.

The experimental studies relevant to the assessment of the P-T conditions during the metamorphism of Pewsey Vale meta-sediments are the decomposition of muscovite in the presence of quartz<sup>2</sup>, the granite melting curve (Tuttle and Bowen, 1958; Luth et al., 1964), the alumino-silicate phase diagram<sup>2</sup> and the muscovite geothermometer.<sup>2</sup>

Breakdown of muscovite.

The maximum stability field of muscovite in the presence of quartz has been determined experimentally by Yoder and Eugster (1955), Segnit and Kennedy (1961) and Evans (1965). Miyashiro (1960) attempted to delineate the muscovite stability field using thermodynamic data. Evans (op.cit.) used the reaction

- 
1. For a complete list of references, see Albee (1965) and Winkler (1965).
  2. References are given in the following pages

rate technique (Fyfe, 1960) and found that muscovite decomposes at lower temperatures than those reported by other experimentalists.<sup>1</sup> His results are less at variance with geological evidence and are favoured here (curve(1), Fig. 39).

Since muscovite is a stable phase, the maximum metamorphic temperature permitted by the inter-section of curve(1) and the granite melting curve (curve(2), Fig. 39), is approximately 660°C. Allowing for the depressive effect of paragonite<sup>2</sup> on the decomposition temperature of muscovite, (Evans, 1965), temperatures are likely to have been lower.

#### Muscovite Geothermometer.

The muscovite-paragonite solvus was experimentally determined by Eugster and Yoder (1954a and b, 1955). Subsequently, Eugster (1956, written communication to Albee 1960, in Albee (1965)) measured the change with time of the basal spacing of a Ca free muscovite co-existing with paragonite. The apparent limit of basal spacings is approximately 9.943Å° at 600°C, 9.976Å° at 500°C, and 9.998Å° at 400°C. The basal spacings of two muscovites from rocks of the Adelaide Supergroup and two from the Kaminantoo Group are 9.981, 9.982, 9.992 and

- 
1. At 2 kilobars muscovite breaks down in the presence of quartz at 690°C in the synthetic experiments (Yoder and Eugster, 1955; Segnit and Kennedy, 1961) and at 600°C in the reaction rate method (Evans, 1965).
  2. The muscovites from these rocks contain small quantities of paragonite - see Appendix 2.



FIG.39.

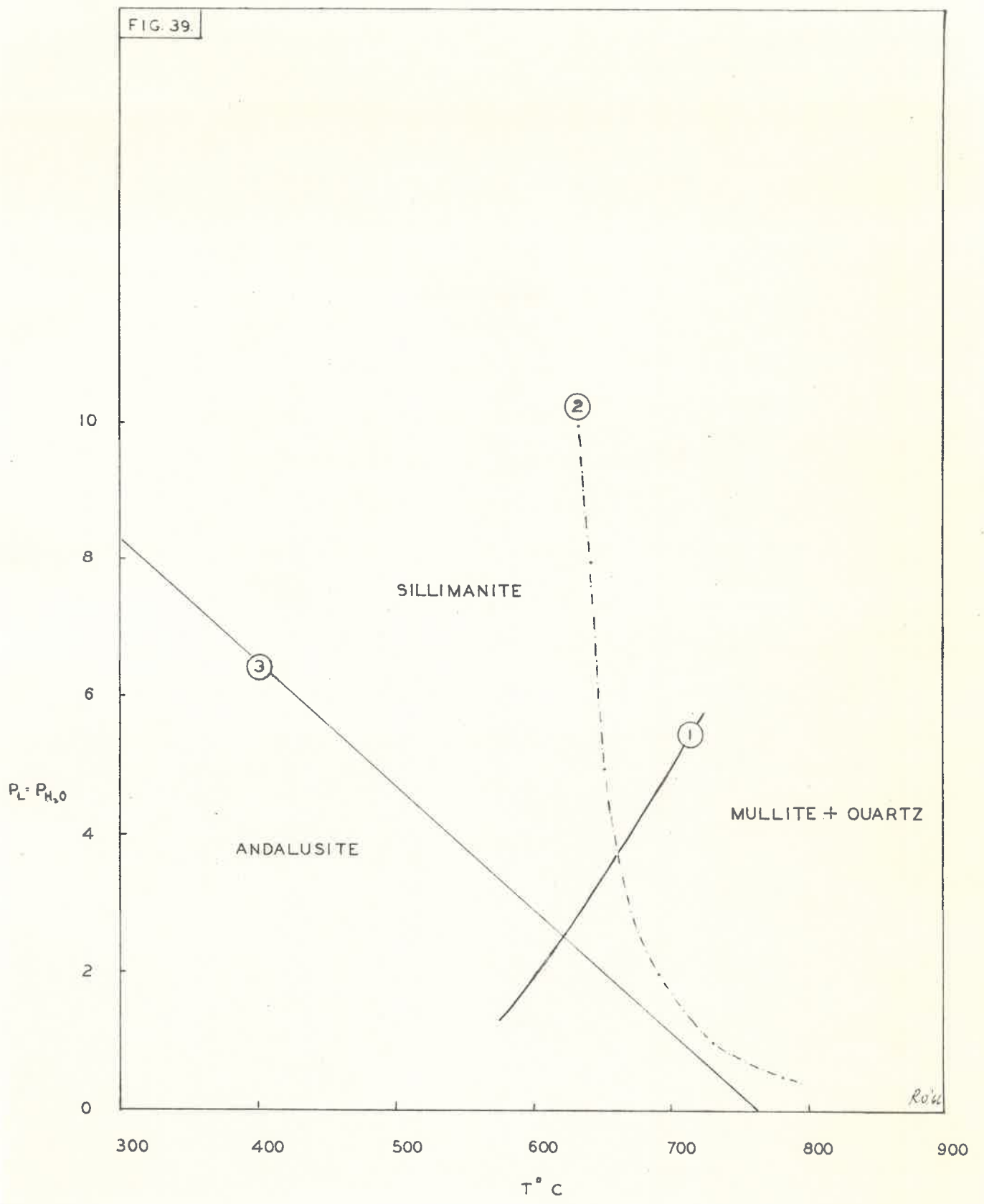
Stability relationships of muscovite,  
andalusite and sillimanite.

Curve 1: Stability curve for muscovite  
in the presence of quartz at  $P_{H_2O} =$   
 $P_{Load}$  (Evans, 1965).

Curve 2: Minimum melting curve for  
granites (Tuttle and Bowen, 1958;  
Luth et al., 1964).

Curve 3: Andalusite-sillimanite boundary  
proposed by Evans (1965).

FIG. 39.



9.936 respectively, indicating minimum<sup>1</sup> temperatures of 430° to 485°C.

The alumino-silicate relationship.

The stability fields of the alumino-silicate polymorphs have been studied experimentally by Clark et al.(1957), Clark(1961), Skinner et al.(1961), Khitarov et al.(1963), Bell(1963), Evans(1965) and Weill (in press).

There is considerable doubt that this experimental system can be applied to geological situations, particularly the stability relationships of kyanite (see Pitcher,1965; Rutland, 1965). The andalusite-sillimanite boundary proposed by Evans (1965) is probably the most reliable (it agrees closely with that of Weill (in press))and is plotted in Fig.39. When this curve is compared with curve(1),Fig.39, it is seen that a minimum pressure of 2.5 kilobars (approx. 30,000 feet) is necessary for the co-existence of sillimanite and muscovite. This is a reasonable estimate as the total thickness of the Adelaide Supergroup and Kanmantoo Group meta-sediments in the Mt.Lofty Ranges is approximately 55,000 feet (Mawson and Sprigg, 1950; Sprigg and Campana,1953).

The available experimental data therefore suggests temperatures in the vicinity of 460° to 650°C and pressures greater than 2.5 kilobars.

---

1. See Appendix 2 for discussion.

Oxide assemblages in the rocks of the Kanmantoo Group and their significance.

The sulfide and oxide mineral assemblages in rocks from different metamorphic terrains in Japan have been studied by Banno and Kanehira(1961) and Kanehira et al.(1964). Kanehira et al.(op.cit) found hematite only in rocks from the glaucophanitic terrains, but never in the andalusite-sillimanite type terrains. They therefore conclude that the metamorphic rocks from the andalusite-sillimanite type terrains are in a more reduced state than those in the glaucophanitic terrains.

Hematite, however, is a common constituent of the Kanmantoo Group rocks in the Pewsey Vale area and is present in most opaque assemblages (Table 18). Its occurrence in these rocks shows that it may be stable in low pressure-intermediate type terrains and not only in glaucophanitic terrains. Hematite has also been found in certain assemblages of kyanite bearing pelitic schists in Vermont (Albee, 1965) and Glen Cove (Chinner, 1960). These observations suggest that hematite may occur in metamorphic terrains covering a wide range of P-T conditions.

The variation in oxide assemblages of the Kanmantoo Group rocks is considered to be due to the presence or absence of graphite (Zen, 1963). It has been shown by Miyashiro(1964) and French and Eugster(1965) that magnetite is the stable iron oxide in the presence of graphite.

In the Kanmantoo Group rocks, graphite and hematite are never associated, but in some specimens magnetite and graphite have been observed.

TABLE 18.

Opaque assemblages in the metamorphic rocks  
of the Pewsey Vale area.

Spec.No.	Rock Type	Hematite <sup>1</sup>	Magnetite	Rutile
40	Quartzo-feldspathic schist	+	-	-
45	"	+	-	+
39B	"	+	-	+
56	"	+	-	-
866-7C	"	-	+	-
798	Tanunda Creek Gneiss	-	+	-
845A	"	+	+	-
796	"	-	+	-
A9-22	"	+	-	-
866A	"	-	+	-
879-1	"	-	+	-
824	Sillimanite schist	+	-	-
561	Migmatite	+	-	-
544	"	-	+	-

1. Hematite always contains exsolution bodies of ilmenite.

CHAPTER 9.INTRUSIVE ROCKS.Introduction.

A variety of intrusive rocks have been emplaced in the meta-sediments of the Adelaide Supergroup and Kanmantoo Group in the Pewsey Vale area. They include dolerites, pegmatites and minor granites and granodiorites; the pegmatites are generally localised in the Adelaide Supergroup rocks, and the dolerites in the rocks of the Kanmantoo Group. The following sections summarise the petrography of these intrusive rocks and the origin of the granites and granodiorites is discussed.

THE MT.KITCHENER INTRUSION.<sup>1</sup>

The Mt.Kitchener intrusion is a small elliptical body located within the rocks of the Kanmantoo Group (Plate 1). The intrusion has been extensively metasomatised and thus the granitic nature of the intrusion is for the most part no longer apparent. The albitites formed by this metasomatism are now strewn on the slopes of Mt.Kitchener as angular or tor-like outcrops (Fig.40). In the centre of this body partially unaltered parts of the intrusion are represented by fine grained biotite and hornblende

---

1. The term "intrusion" is used in place of a descriptive term such as "granodiorite" as the original nature is largely obscured by later alteration.

FIG.40.

Typical tor-like outcrop of the  
Mt. Kitchener Intrusion. Photo  
taken from location 984 266 looking  
east.

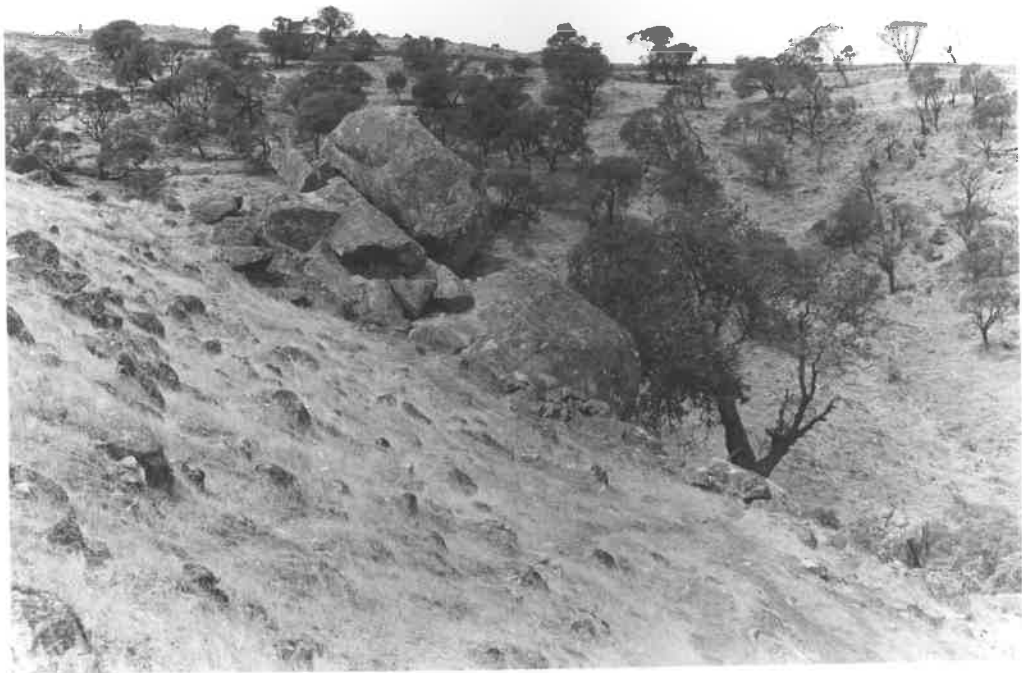
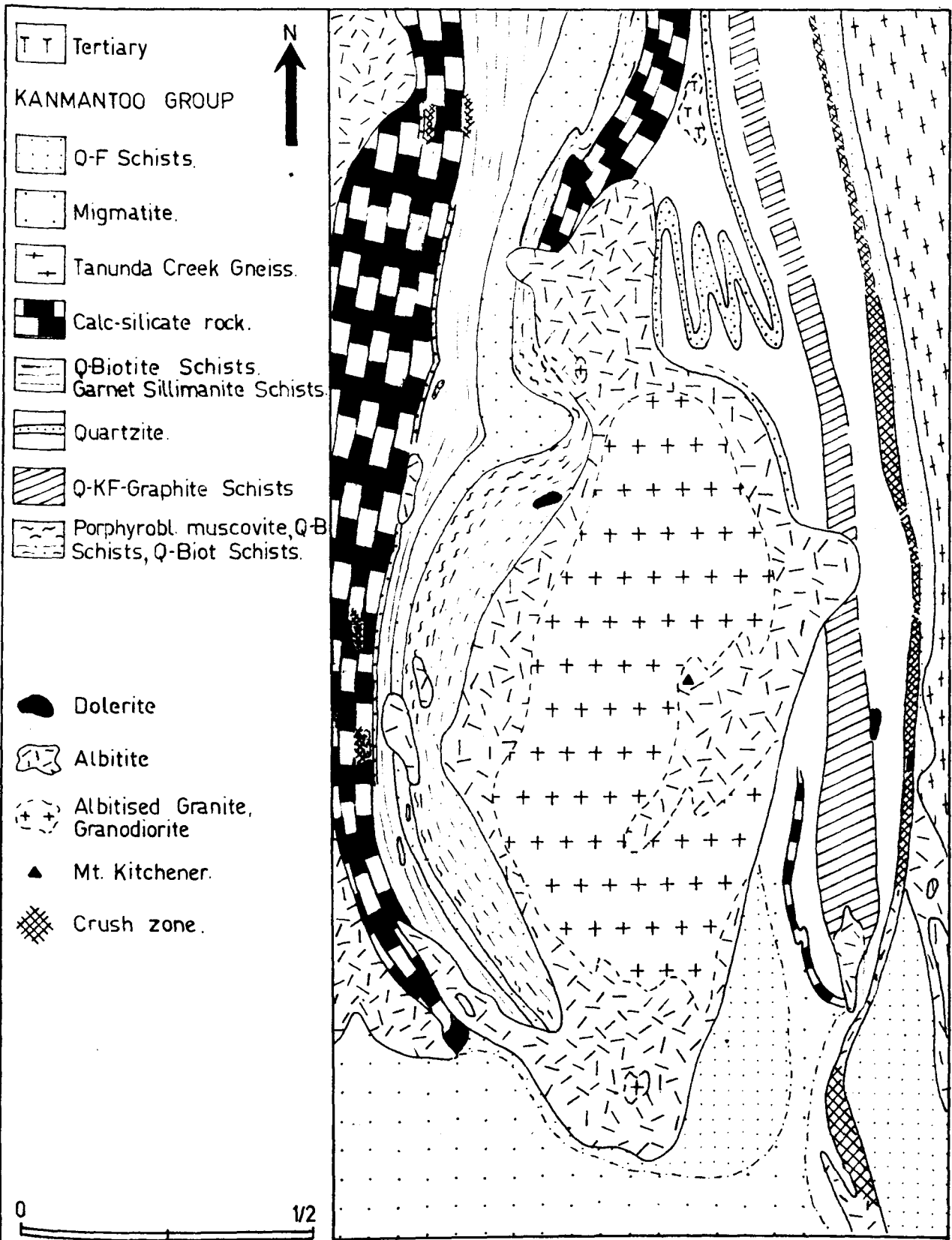


FIG. 40.



**FIG. 41.**

**Geology of the Mt. Kitchener area  
showing relationship of meta-sediments  
to the Mt. Kitchener Intrusion.**



T T Tertiary

KANMANTOO GROUP

Q-F Schists.

Migmatite.

Tanunda Creek Gneiss.

Calc-silicate rock.

Q-Biotite Schists.  
Garnet Sillimanite Schists.

Quartzite.

Q-KF-Graphite Schists

Porphyrobl. muscovite, Q-B  
Schists, Q-Biot Schists.

Dolerite

Albitite

Albitised Granite,  
Granodiorite

Mt. Kitchener.

Crush zone.

0 1/2  
MILES.

MT. KITCHENER INTRUSION.

FIG 41.

R046

albitites - the "Mt. Kitchener Granite" (Moulden, 1895; Hossfeld, 1925). These grade into actinolite or limonite-pitted albitites at the perimeter.

The unaltered rocks are fine grained granites and granodiorites in which biotite and hornblende show no preferred orientation. Xenoliths have not been observed in the intrusion. A few basic enclaves of dioritic composition occur within the granodiorites.

The meta-sediments surrounding the intrusion strike in conformity with the attitude of the igneous contact (Fig. 41). This feature suggests that granites and granodiorites have been forcefully injected into the meta-sediments (c.f. Leedal, 1952, p. 39). The lack of preferred orientation shown by hornblende and biotite indicates that the intrusives are post kinematic.

#### Petrography.

##### Unaltered rocks.

The unaltered intrusive rocks vary from micro-granites to micro-granodiorites (grain size 0.5mm. to 1.0mm.). The granites consist of microcline, plagioclase, biotite and quartz, with accessory amounts of muscovite, zircon, monazite, magnetite, sphene, pyrite and tourmaline. The granodiorites contain hornblende in addition to those constituents found in the granite. Modal analyses of representative rock types are given in Table 19.

Both rock types have a characteristic allotriomorphic texture in which clots of hornblende and/or biotite are

TABLE 19.

Modal analyses of two variants of the Mt. Kitchener Intrusion.

Spec. No.	143 <sup>1</sup>	25 <sup>1</sup>
Plagioclase	30.1	30.8
Microcline	26.6	12.8
Quartz	29.5	22.5
Biotite	12.0	18.2
Hornblende	-	8.4
Scapolite	(	(6.3
Epidote	(	(
Accessories	1.8	1.0
	<u>100.0</u>	<u>100.0</u>
	Adanellite	Granodiorite
	(Nockolds, 1954)	
Total No. Counts	4,236	4,883

1. Specimens kindly loaned by Dr. G. Chinner.  
The modal analyses were determined by the author.

randomly distributed amongst slightly larger quartz, microcline and hypidiomorphic plagioclase. The basic enclaves consist of fine grained equigranular (0.15mm.) mixtures of hornblende, biotite, plagioclase and quartz.

Plagioclase appears as delicate oscillatory or normally zoned crystals (core,  $An_{43-51}$ , rim,  $An_{4-6}$ ) with well developed albite-carlsbad and minor albite and pericline twinning. Deformed plagioclases exhibit glide (i.e. deformation) twinning (Vance, 1961; Vernon, 1965). Myrmekite is common at the contact between plagioclase and microcline. Scapolite, sericite, epidote and calcite are secondary alteration products. Microcline commonly exhibits a carlsbad twinning in addition to the normal "tartan" twins. Perthitic textures are rare. Quartz is "embayed" by microcline and plagioclase. In all grains undulose extinction and healed fractures are present. Biotite with an intense reddish-brown pleochroism (X = pale yellow brown, Y = Z = deep reddish brown,  $2Vx = 0-19$ ) is characteristic of both the granites and granodiorites. The biotite is commonly associated with hornblende and sphene, but may form symplectic intergrowths with quartz. Some biotites show deformation features such as kink banding and undulose extinction. Pale green chlorite replaces some of the biotite.

A subhedral, skeletal amphibole (X = pale olive green, Y = green, Z = deep green to bluish green,  $2Vx = 40 \pm 1$ ;  $Z^{\wedge}C = 20-22$ ) is a major component of the granodiorites. Lamellar twinning

is present in some grains. Zircon appears as doubly terminated, prismatic, colourless crystals (Fig.42). These are similar to the zircons figured by Mills, (1964) for the granodiorites in the Cambrai region.

### Albitites.

The granites and granodiorites have been progressively altered to biotite and hornblende albitites and finally to actinolite or limonite-pitted albitites.

In the earliest stages of alteration quartz and primary plagioclase are replaced by albite. The quartz is strongly embayed, and of the original plagioclase only cores of secondary scapolite, sericite and epidote remain. A patch work extinction appears in the albite crystals where the replacement of primary plagioclase is irregular. The composition of the albite ranges from An<sub>4</sub> to An<sub>11</sub>.

Biotite and hornblende commence to break down during the intermediate stages of alteration. The biotite alters to an aggregate of jarosite, limonite and rutile. Chlorite, muscovite and phlogopite(?) (X = colourless, Y = Z = golden brown) are minor breakdown products. Limonite and actinolite appear as the decomposition products of the primary amphibole, with epidote as a minor byproduct. Simultaneously microcline is largely replaced by albite.

Very few of the primary minerals remain during the final stages of albitization. Most of the microcline has been replaced and the few remaining relics are extremely turbid.

FIG.42.

Zircons separated from albitized granites  
and granodiorites. Note euhedral shape  
of zircons. Spec. Nos.A200-786 and 788.

Locations 979 271, 980 278.

Single crystals. X500 Aggregates X250.

FIG.43.

Strongly deformed albite crystal re-  
placed by polygonal twinned aggregates  
of albite. Location 979 271. Spec.  
No.A200-786. X 40.

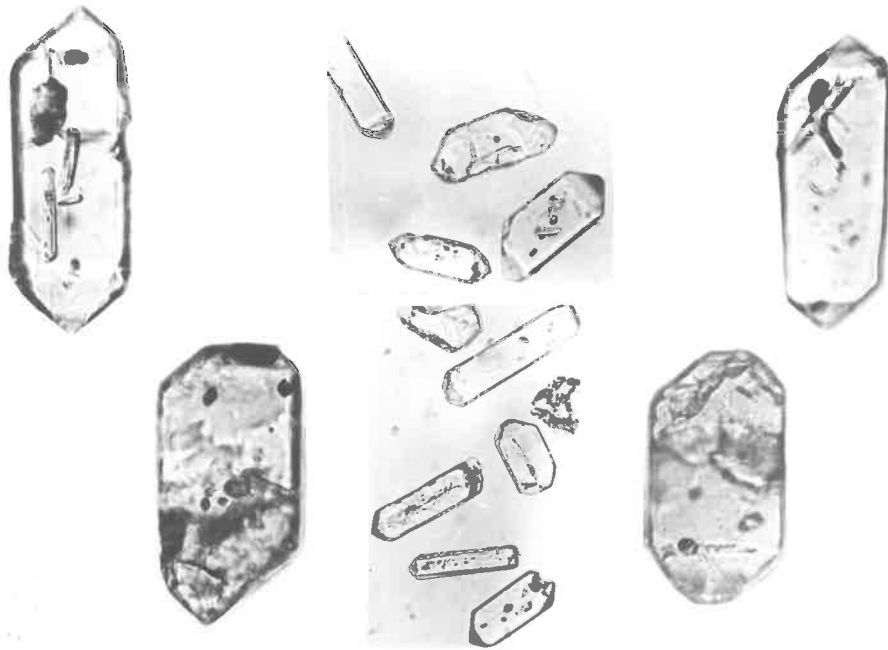


FIG. 42.

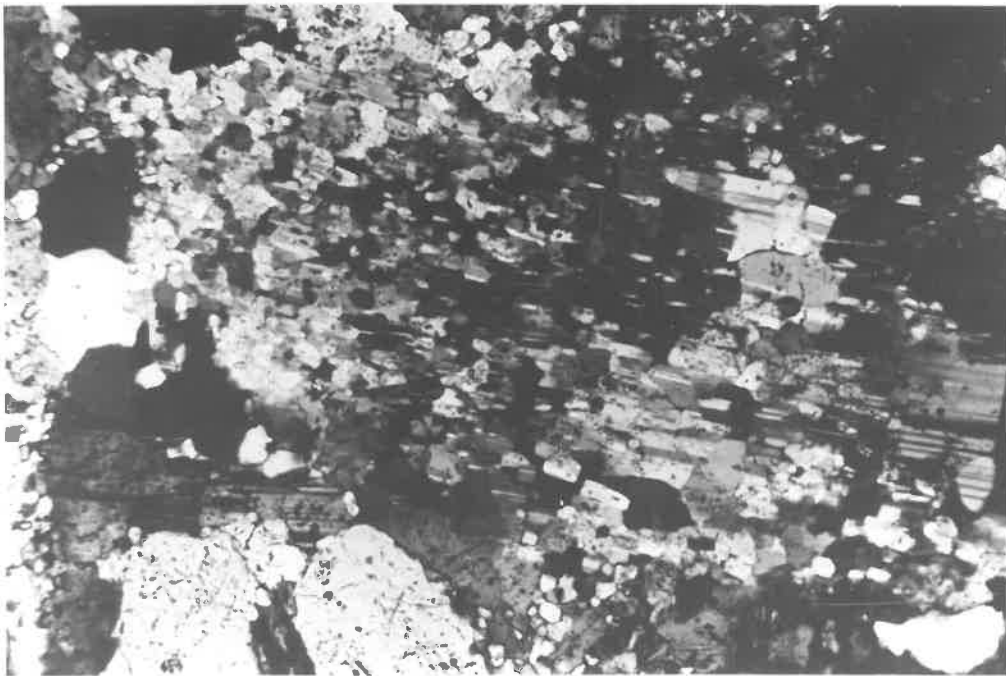


FIG. 43.



Biotite may be totally replaced by jarosite, limonite and rutile, or remain as bleached stringy corroded flakes. A few relic corroded quartz grains may be present. Sphene alters to leucoxene(?) along fractures in some instances. Apatite begins to show corrosion when all the remaining primary minerals have been replaced. Zircon is the only mineral to remain unchanged during albitization and retains its characteristic morphology in the completely altered rocks. Albite is the predominant mineral present.

A discussion of the chemical changes involved in this metasomation is given in Chapter 10.

Texturally, the albitites consist of a mixture of turbid interlocking grains (0.05 to 1.0mm.) of albite ( $An_4$ ) small quantities of limonite stained actinolite, strongly altered biotite, secondary jarosite, limonite, hematite and corroded quartz. In some albitites, strain free quartz aggregates are associated with strongly deformed albite. Many of the strained albitites are replaced by polygonal aggregates of fine grained albite (Fig.43). The characteristic texture produced by the polygonal aggregates replacing the large albitites, is called chessboard albite (Becke,1906). Chessboard albite can develop from either potassium feldspar or plagioclase by alkali exchange within their framework (Brown,1965) or by deformation (Starkey,1959; Talbot,1963). Its association with other deformation features in the Mt.Kitchener albitites suggests that it is a product of deformation.

### Origin of the Mt. Kitchener intrusion.

Previous authors have presented varying hypotheses to explain the origin of these rocks. Hossfeld(1925) considered that the Mt. Kitchener "granite" was intrusive while Whittle (1955) believed that the "granite" was formed "in place by metasomatic action on local Kanmantoo country rock by a process in which quartz of the sediments is replaced by feldspars". Chinner (1955) concluded that the close association of the "granite" with metasomatic rocks left the igneous origin open to question.

The author considers that the intrusion is of magmatic origin. The evidence in support of this conclusion is:

(1) The shape of the zircons.

Granites of magmatic origin "normally contain a majority of euhedral zircons" (Poldervaart, 1956), while granitised sediments exhibit zircons with rounded corners and edges or outgrowths (Poldervaart, 1950; Poldervaart and Eckelmann, 1955).

The zircons in the Mt. Kitchener granites and granodiorites are distinctly euhedral.

(2) The presence of oscillatory zoned plagioclases.

Oscillatory zoned plagioclases are commonly observed in igneous granodiorites and granites (e.g. Leedal, 1952; Phillips, 1956). The conditions required for this zoning, namely oscillation in temperature and pressure or fluctuation in water pressure (Turner and Verhoogen, 1960) would not be present in the environment under which granitic rocks of

metamorphic origin are produced.

(3) The warping of the meta-sediments adjacent to the intrusion.

The intrusive nature of the granites and granodiorites could be considered as further evidence for a magmatic origin. However, Smithson (1965) has suggested that granitic rocks, which were never magmatic, can intrude diapirically the super structure.

#### Regional Setting.

Granite and granodioritic bodies are extremely common in the high grade metamorphic zones on the eastern side of the Mt. Lofty Ranges. Many have been intruded during folding (White, et al., in press) or in the late stages of folding and in the dying stages of metamorphism (Mills, 1964). Others are post kinematic (White, 1956) and some have been forcefully injected into the meta-sediments (Mills, op.cit.).

It is considered that the intrusives in the Mt. Kitchener region belong to this same granite - granodiorite suite. This is suggested by their similar mode of emplacement, their presence in sillimanite grade meta-sediments and the similarity of their mineralogy to other granites and granodiorites in the Mt. Lofty Ranges.

They can be classified as "meso-zone" granites (Buddington, 1959).

#### Conclusions.

Granites and granodiorites of magmatic origin were injected

into the meta-sediments of the Kanmantoo Group subsequent to deformation. During this emplacement the meta-sediments adjacent to the intrusion were extensively warped. Later metasomatism altered these intrusives to albitites.

### PEGMATITES.

Granite pegmatites occur within the Kanmantoo Group and Adelaide Supergroup rocks of the Pewsey Vale area. They are believed to be members of the suite of pegmatites which generally occur in the higher grade meta-sediments on the eastern side of the Mt. Lofty Ranges. Normally they appear as sheet-like bodies parallel to foliation, but irregular bodies discordant to foliation are also present (Plate 1).

The wall rock foliation around many of the larger bodies is strongly warped and on a mesoscopic scale it is closely conforms to the irregularities in the pegmatites. These features suggest that the pegmatites have been forcefully emplaced (Chadwick, 1958). Small xenoliths have been observed in some pegmatites. No mineral zoning is apparent in any of the pegmatites in this area, although Eggleston (1959) reports zoning in some pegmatites in the Gumeracha region. Salmon pink, perthitic potash feldspar, white plagioclase, muscovite (often as books) tourmaline, quartz, minor pale green beryl and biotite are identifiable in hand specimen. Graphic or myrmekitic intergrowths of potash feldspar and quartz are a feature of some pegmatites, but the normal texture is one of a coarse intergrowth of plagioclase, muscovite

and quartz, with or without potash feldspar. Less common are fine grained "aplitic" pegmatites consisting of plagioclase, muscovite and quartz.

#### Petrography.

The grain size and mineral composition of the pegmatites is extremely variable. Table 20 illustrates the grain size and mineral variation in several representative specimens.

Plagioclase: In most specimens examined, primary plagioclase ( $An_5$ - $An_{23}$ , Table 21) and secondary albite are present. The primary plagioclase occurs as subhedral, turbid, twinned (Albite and Pericline twin laws most common) crystals intimately intergrown with quartz. In some specimens the plagioclase bears an unusual "sawtooth" relationship to the quartz (Fig.44), which according to Gates and Scheerer (1963) indicates that quartz has been introduced subsequent to the crystallization of plagioclase. The primary plagioclase commonly exhibits albitic rims when in contact with or enclosed by microcline perthite (e.g. 267A, 121A). Close examination of the contact between the albite rim and the potash feldspar reveals a zone devoid of shadow perthite, suggesting that the exsolved albite has migrated to the plagioclase. The plagioclase in the pegmatites near the Nairne Fault Zone are strongly deformed, as displaced twin lamellae, serrated grain boundaries and in some cases deformation banding (Siefert, 1965) are present.

TABLE 20.

Estimated volume percentage of constituents and variation  
of grain size in Pegmatites.

Spec.No.	441		267B		239A		256C	
	%	g.s.	%	g.s.	%	g.s.	%	g.s.
Plagioclase	45	1.0-2.6	20	0.5-3.0	75	1.0-9.0	60	10.0-12.0
Quartz	40	1.0-3.0	20	0.8-2.4	20	2.0-8.0	35	0.2-0.4
Muscovite	15	1.8-0.4	5	2.0-5.2	3	0.5-1.0	2	< 0.1
Microcline	-	-	55	10.0-15.5	2	0.4-0.8	3	0.2-0.5
Zircon	-	-	+	-	-	-	-	-
Pyrite	-	-	+	-	-	-	-	-
Biotite	-	-	-	-	+	-	-	-

g.s. = grain size in mm.

TABLE 21.

Composition of Plagioclases in  
the Pegmatites.

<u>Spec.No.</u>	<u>Optical</u> <u>Wt.%</u>	<u>X-ray</u> <sup>1</sup> <u>Wt.%</u>
615	5.0	7.5
239A	16.0	13.0
257	4.5	5.0
441	strained	23.0

---

1. See Appendix 3 for methods used in this determination.

FIG.44.

Photomicrograph of pegmatite showing "saw tooth" relationship of quartz to plagioclase. Location 000 225 - coordinates taken from 1" to 1 mile Cambrai Military Sheet. Spec. No.615. X 40.

FIG.45.

Photomicrograph of pegmatite showing quartz (Q) and muscovite (M) corroded by mosaics of fine grained albite (A). Location 965 259. Spec. No.A200-453. X 40.



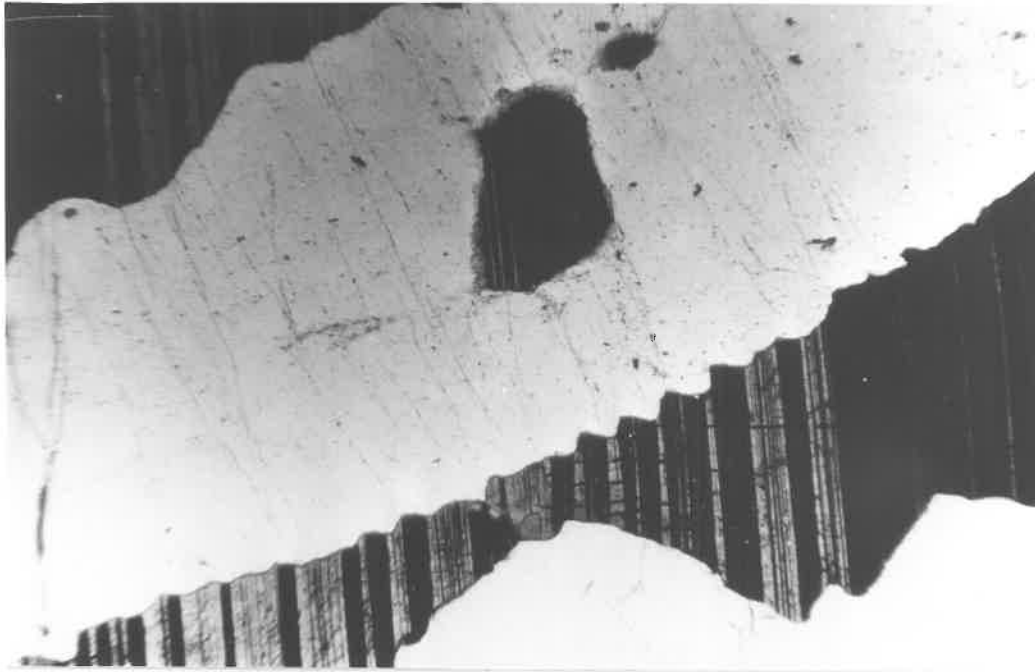


FIG.44.



FIG.45.

Secondary albite: Many pegmatites are partially or completely replaced by secondary albite. In the less altered pegmatites, the grain boundaries of the primary minerals are corroded by mosaics of fine grained albite (Fig.45). The primary minerals engulfed by the albite remain as embayed relics or as "dusty" inclusions. The strongly altered pegmatites consist predominantly of albite with minor ragged relics of muscovite, quartz and tourmaline. The albite shows abundant evidence of subsequent deformation, namely, microfaulted lamellae, glide twinning and domain extinction. The potash feldspar in the pegmatites is microcline ( $\Delta = 0.853$  to  $0.988$ ). In many specimens it appears as optically continuous relics within either primary or secondary albite, but in some pegmatites e.g. 267A, 121A and 636, large perthitic microcline megacrysts up to 1.5cm. in diameter are common. Shadow, string and vein perthites have been observed in these megacrysts. The vein perthite in many specimens appears to be the result of exsolution and migration of albite into fractures within the potash feldspar grains. Plagioclase and quartz inclusions are commonly present within or at the border of the megacrysts, the quartz appearing as irregular grains or as a graphic intergrowth.

Myrmekite is found within primary plagioclase, where the plagioclase is in contact with microcline perthite. An albite rim ( $An_4$ ) separates the myrmekite ( $An_{14}$ ) from the microcline perthite. The author considers that the myrmekite in the Pewsey Vale pegmatites has formed as an exsolution derivative from

alkali feldspar (Carman and Tuttle, 1963; Phillips, 1964) rather than by potash metasomatism (Francis, 1964) or deformation (Shelley, 1964) as there is neither evidence for potash metasomatism nor extreme deformation (apart from the deformation features shown by the pegmatites near the Nairne Fault Zone). Quartz exhibits strong undulose extinction and healed fractures. The healed fractures cross grain boundaries suggesting that fracturing and healing of the quartz is a post crystallization feature. Where quartz is enclosed by plagioclase or microcline perthite, it shows a typical anhedral or "embayed" grain shape.

Muscovite is normally a minor constituent, but may constitute 25 percent or more of some specimens (e.g. 441). It normally occurs as slightly pleochroic (very pale green) interstitial grains or as slightly plumose or symplectic intergrowths with quartz (e.g. 267A; c.f. Orville, 1960). In some specimens (e.g. 86) the muscovite appears as small oriented lathes either parallel, to  $\{010\}$ ,  $\{100\}$  and possibly  $\{110\}$  planes in primary plagioclase. Biotite (X = pale brown, Y = Z = deep brown) is relatively uncommon in the pegmatites and only appears in pegmatites containing abundant potash bearing minerals. Commonly the biotite is replaced by muscovite. Black tourmaline (core - E = very pale green, O = blue green, rims E = very pale brown, O = blotchy yellow brown) apatite, beryl, zircon and pyrite are accessories.

### Country rock alteration.

The country rock adjacent to or within the pegmatites shows various types of mineral transformations and metasomatic effects. The most common of these is the replacement of biotite by muscovite or sericitic mats (e.g. 254, 256A). Small nests of rutile occur within the muscovite and the surrounding foliae are heavily stained with limonite. Garnet is commonly replaced by a fine mat of sericite and chlorite, and plagioclase is sericitised.

The country rock underwent a further phase of alteration during the albitization of the pegmatites. The biotite in the schists reverted to chlorite and rutile, and the muscovite produced during the first stage of alteration was corroded by albite. Limonite - hematite biproducts formed during the alteration.

### Discussion.

The occurrence of muscovite in the contact zones around pegmatites is not uncommon. Recent experimental work by Hemley (1959) and Hemley and Jones (1964) has shown that muscovite can only be stable when  $a_{K^+}/a_{H^+}$  values are relatively high (see Hemley and Jones, op.cit., Fig.1, p.548). It is therefore suggested that during the emplacement and crystallization of the pegmatites in the Pewsey Vale area, potash rich fluids diffused into the country rock bringing about the formation of muscovite.

The subsequent formation of albite in the pegmatites and

in the wall rock suggests that fluids rich in soda (i.e. fluids with a very high  $a_{\text{Na}^+}/a_{\text{H}^+}$  value, see Hemley and Jones, 1964) were also introduced. The restriction of albite to a zone close to the pegmatites suggest that these fluids came via the same channelways as the pegmatites and have not been introduced externally.

The pegmatites appear to have been emplaced after the metamorphism, but before or during the faulting. This is suggested by the muscovitisation of the meta-sediments adjacent to the pegmatites and by the development of brittle deformation features in pegmatites next to the Nairne Fault Zone.

#### DOLERITES, META-DOLERITES AND AMPHIBOLITES.

In the northern part of the area, scattered pods and lenses of dolerite and amphibolite are associated with the meta-sediments of the Kammantoo Group (Plate 1). Most bodies are small, their diameters varying from 10 to 20 feet. Contact metamorphic affects are absent. In hand specimen the dolerites are fine grained, dark green to black rocks in which small phenocrysts (1 to 3mm.) are commonly discernable; some specimens contain bands of epidote. The amphibolites are dark green friable rocks showing a hornblende lineation and less common "augen" of hornblende and plagioclase.

#### Petrography.

Microscopically, these rocks show all stages of alteration from unaltered dolerites to completely recrystallized amphibolites. The amount of metamorphic recrystallization

varies within individual specimens. It is the purpose of this section to give a brief description of the unaltered and altered dolerites.

### Dolerites.

The unaltered dolerites have a characteristic subophitic to ophitic texture (Fig.46a) and consist of augite, labradorite with minor biotite, olivine, pigeonite, ilmenite and apatite. In some specimens phenocrysts of plagioclase are present.

Augite:  $2V_z$  and  $OA \wedge C$  measurements (Ruegg, 1964) on relatively unaltered, unstrained augites, indicate a compositional variation of  $Ca_{40-41}$ ,  $Mg_{43-51}$ ,  $Fe_{9-16}$  (Table 22).

Twinning on  $\{100\}$  is common and most crystals are completely or partly schillerised. Plagioclase lathes show normal and oscillatory zoning and are generally turbid. The plagioclase is near labradorite in composition (Table 23) but in specimens containing phenocrysts the ground mass plagioclase is andesine (e.g. 879-2, Table 23). Twinning is complex and variable with the Albite - Carlsbad law the most commonly observed twin law. Deformation or glide twins (Vance, 1961; Vernon, 1965) are also present (Fig.46b). The plagioclase lathes contain abundant inclusions of stubby pale green pyroxene, oriented iron ore needles (magnetite?) and apatite. Olivine is absent or rare in the dolerites of this area, but is more common in the dolerites emplaced in the Tanunda

FIG.46A.

Photomicrograph of dolerite showing  
characteristic ophitic texture.

Location 971 278. Spec. No.GAC 147.

X 40.

FIG.46B.

Photomicrograph of dolerite showing glide  
(deformation) twinning (arrow) in labra-  
dorite. Irregular aggregates of epidote  
(E) replace labradorite. Location 989 274.

Spec. No.A200-879-2. X 100.

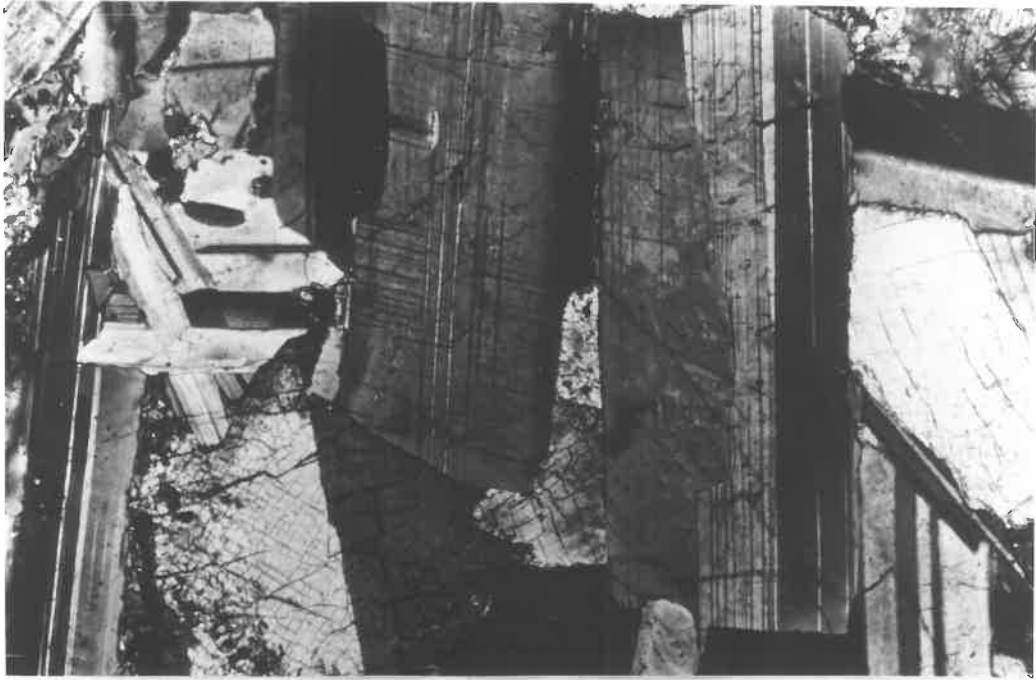


FIG. 46A.



FIG. 46B.



TABLE 22.

Optical Properties of Amphiboles, Pyroxenes and Scapolites  
in Meta-dolerites.

Amphiboles

<u>Rock Type</u>	<u>Spec.No.</u>	<u>2Vx</u>	<u>Z C</u>
Meta-dolerite	A200-795	68	16
"	A200-22	70	14.5
"	A200-849	70	15.5
"	A200-879(2)	71	
"	A200-790	80, 84, 76	(strained)
Amphibolite	A200-851	70	

Pyroxenes

<u>Rock Type</u>	<u>Spec.No.</u>	<u>2Vz</u>	<u>Z C</u>	<u>OA C</u>	<u>Composition</u>
Dolerite	GAC 147	50	40	15	Ca <sub>40</sub> Fe <sub>9</sub> Mg <sub>51</sub>
Meta-dolerite	A200-790	51	42.5	17	Ca <sub>41</sub> Fe <sub>16</sub> Mg <sub>43</sub>

Scapolites

<u>Rock Type</u>	<u>Spec.No.</u>	<u>n<sub>o</sub></u>	<u>% Melanite</u>
Amphibolite	A200-851	1.572	53
Meta-dolerite	A200-849	1.568	47.5
"	A200-790	1.563	40.5

TABLE 23.

Composition of Plagioclases in the Meta-dolerites.

Igneous Plagioclases.

<u>Rock Type</u>	<u>Spec. No.</u>	<u>%An core</u>	<u>%An rim</u>	<u>Twin Laws</u>
Meta-dolerite	A200-22	65-59		Albite Albite-Carlsbad
"	A200-790	80-70	59-55	Albite-Carlsbad Ala B Albite
"	A200-884	70-60	35-34	Albite, Albite- Carlsbad, Peri- cline
"	A200-879(2)	72-50 46-40 <sup>1</sup>	50-42	Albite-Carlsbad Albite
Dolerite	GAC-1472	76-68	56	Albite-Carlsbad Carlsbad Acline

Metamorphic Plagioclases.

Meta-dolerite	A200-795	46-39 (zoned)	39	Albite
		37-35 (unzoned)		Albite-Carlsbad
"	A200-849	41-39 (zoned)		Albite
"	A9-762	44-37 (zoned)	35	Albite Albite-Carlsbad
Amphibolite	A200-851	43-45 (unzoned)		Albite

1. Ground mass plagioclase.

2. Specimens kindly loaned to the author by Dr. G. Chinner.

Creek Gneiss (Chinner, 1955). It is generally replaced by a mixture of iddingsite and iron ore. Biotite (X = pale brown, Y = Z = yellowish brown) appears as small crystals replacing augite (e.g. 147).

#### Meta-dolerites and amphibolites.

The transformation of the dolerites to amphibolites has been arrested at various stages. In the least altered dolerites a pale green uralitic amphibole forms along the {110} cleavage planes and at the grain boundaries of the augite. Dusty magnetite and quartz are byproducts of this replacement. Other specimens show the development of hornblende, acid plagioclase and/or scapolite (Me<sub>40.5-47.5</sub>) at the contact between augite and labradorite (Fig. 47a). The scapolite and plagioclase also occur as "rivulets" across labradorite lathes (Fig. 47b). The labradorite loses its turbid appearance in the zones where the metamorphic minerals have formed. The hornblende at this stage varies in pleochroism (Z axial colour olive green, bluish green, pale bluish green in 790) and the metamorphic plagioclase is normally zoned (An<sub>39-41</sub>; 849). Epidote veins or aggregates form in the labradorite of some specimens (e.g. 795).

With further recrystallization, interlocking hornblende crystals replace the augite and in some cases the hornblende inherits the {100} twinning of the clinopyroxene. Iron ore originally present in the augite and labradorite as fine spicules, exsolves during recrystallization and coalesces to form irregular xenoblastic grains. Scapolite and acid plagioclase increase in

FIG.47A

Photomicrograph showing hornblende adjacent to and rimming augite in meta-dolerite. Metamorphic plagioclase ( $P_2$ ) occurs as irregular aggregates replacing labradorite ( $P_1$ ).

Location 993 255. Spec.No.A200-847 X 40.

FIG.47B.

Photomicrograph of meta-dolerite showing "rivulets" of scapolite (S) in labradorite ( $P_1$ ). Hornblende (H) surrounds labradorite. Location 989 279. Spec.No.A200-790 X 100.

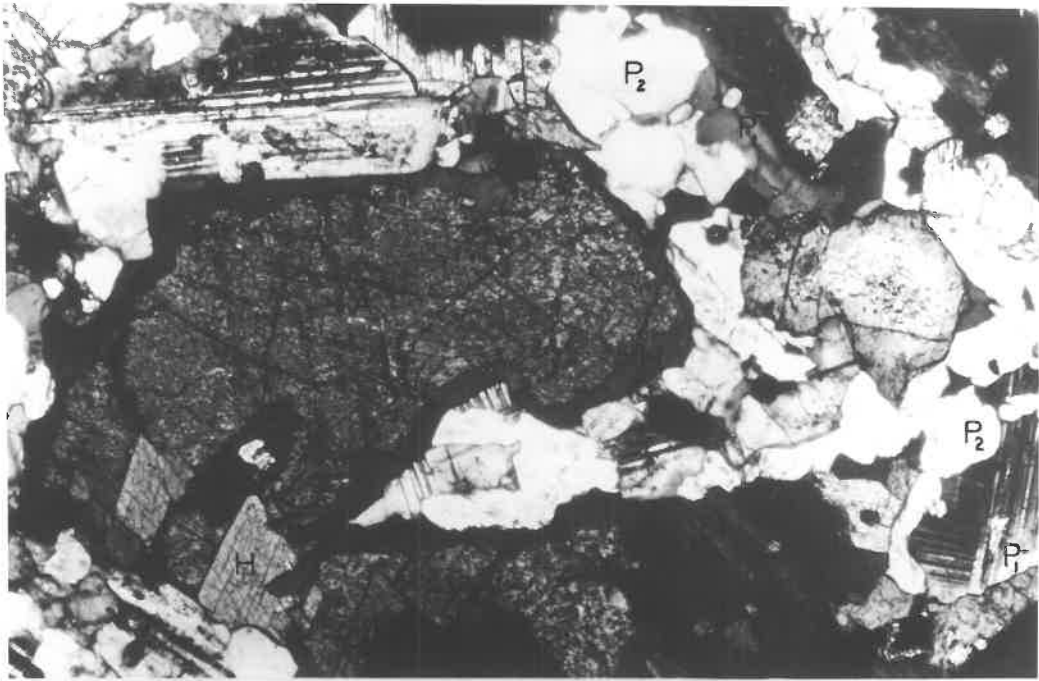


FIG. 47A.

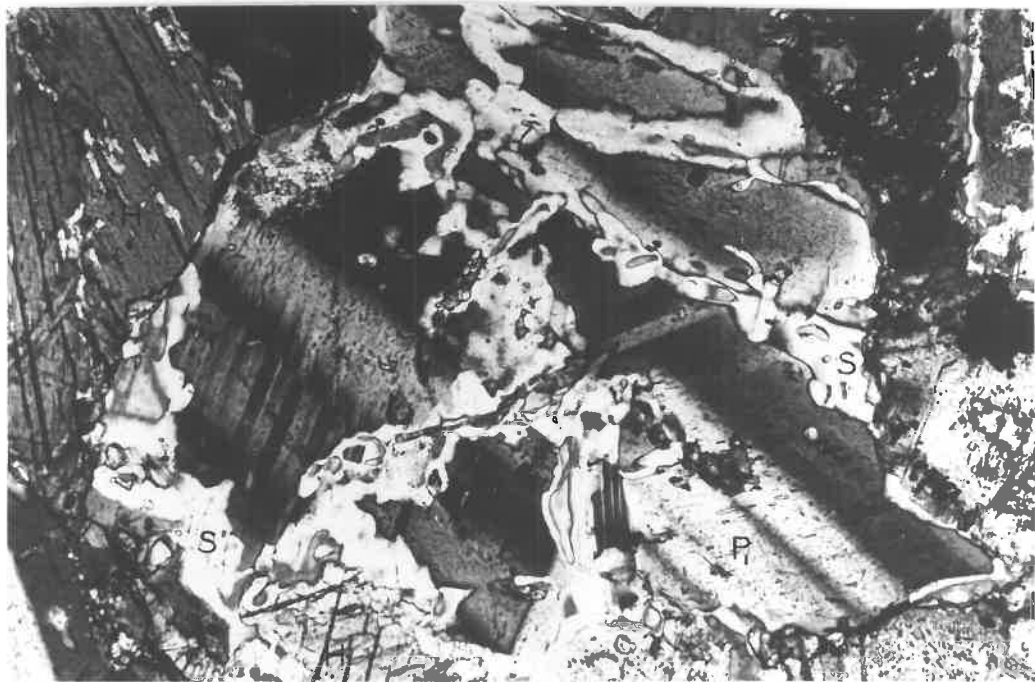


FIG. 47B.

size and are conspicuous as granoblastic mosaics (av.diam.0.08mm.) within the labradorite. Twinning in the metamorphic plagioclase is distinct and zoning is prominent. Epidote, clinozoisite and white mica occur as alteration products in some phenocrysts.

Complete recrystallization results in the total destruction of the ophitic texture and the formation of a granoblastic aggregate of hornblende (X = pale olive green, Y = olive green, Z = deep green;  $2Vx = 70, 851$ ), scapolite ( $Me_{53}, 851$ ), plagioclase ( $An_{45-48}, 851$ ) and minor quartz. Zoning is absent in the plagioclase and rare, highly saussiterised relics of the original labradorite may be present in some sections. The metamorphic plagioclase in the amphibolites is more anorthite rich than the secondary plagioclases in the less altered dolerites, indicating an increase in basicity with recrystallization (c.f. Walker et al., 1960). Sphene (as rims around ilmenite) and pyrite are accessories.

The Z axial colour (deep green) of the hornblendes and the composition of the plagioclase ( $An_{45-48}$ ) indicate that the amphibolites have reached the same grade of metamorphism as the surrounding rocks, namely, the sillimanite grade of metamorphism.

Factors affecting the recrystallization of the dolerites.

As yet, no reasons have been given for the different mineralogical and textural development shown by the meta-dolerites. A study of the literature, indicates that both water content (Poldervaart, 1953; Wilcox and Poldervaart, 1958; Buddington, 1963; Mills, 1964) and deformation (Sutton and Watson,

1951; Buddington, 1963) are important factors in the reconstitution of basic rocks.

In the present area, the stress field has been sufficient to control the orientation of the hornblende, but the preservation of labradorite phenocrysts up to the last stages of recrystallization, the minor development of glide twinning in plagioclase and undulose extinction in augite, indicate that deformation has only played a minor role in the transformation of the dolerites. What appears to be more important is the water content of the country rocks surrounding the intrusives. Dolerite plugs in "dry" rocks (quartzo-feldspathic schists, calc-silicates with no hydroxyl bearing minerals) often show only minor reconstitution. For example, specimen A200-22, a small fine grained doleritic sill in a quartzo-feldspathic schist, contains hornblende - quartz aggregates, minor white mica and epidote, fresh labradorite, and a general lack of reaction rim coronae. It is apparent here, that just sufficient water has been available to amphibolitise the augite, but too little to catalyse the breakdown of the labradorite. Those specimens which exhibit almost complete recrystallization, are associated with rocks containing abundant hydroxyl bearing minerals. Water, therefore appears to have been the main agent in the recrystallization of the dolerites.

#### Absence of garnet in the meta-dolerites.

The absence of garnet from the meta-dolerites of the Pewsey Vale area contrasts markedly with its common occurrence

in meta-dolerites from other metamorphic terrains (Wiseman, 1934; Wilcox and Poldervaart, 1958; Mason, 1962). The presence of garnet in amphibolites in the Dalradian and Glaucophanitic metamorphic terrains led Shido<sup>h</sup> (1958) to consider that high rock pressure favours its formation. An examination of the literature since Shido<sup>h</sup>'s original paper has shown that her conclusions concerning the paragenesis of garnet in amphibolites are basically correct. It seems that garnet will not form in rocks of this particular composition when the metamorphism is of the low pressure - intermediate or andalusite-sillimanite type. A study of the pelites of the Kamantoo Group (Chapter 5) indicates that the metamorphism is of the low pressure - intermediate type. This suggests that load pressures were too low to allow the crystallization of garnet.



CHAPTER 10.

ALBITITES AND ASSOCIATED ROCKS.

Albitites<sup>1</sup> occur commonly in the medium and high grade meta-sediments of the Mt. Lofty Ranges. In the central part of the ranges, at Gumeracha (Stillwell and Edwards, 1951) and Lobethal (Whittle, 1951), they are associated with talc ore bodies. The large talc ore bodies at Gumeracha are being operated at the present moment.

Albitites are prominent in the Pewsey Vale area and are particularly common north-west of Pewsey Vale Peak and west of Mt. Kitchener (Plate 1). Sporadic outcrops of talc and small talc ore bodies occur within many of the albitite zones.

Field occurrences of the Pewsey Vale Albitites.

The albitites are localised in fault zones at the perimeter of the Mt. Kitchener Intrusion (see Chapter 9) and within the meta-sediments. They form elongate bodies parallel to the regional foliation in the meta-sediments (Plate 1). The contact between the albitites and the country rock is generally sharp, but in some areas a transitional zone composed of country rock interleaved with albitite, is present. It is in these transitional zones that the mineralogical changes involved in the formation of albitites, is most clearly observed. The replacement of the country rock by the albitites does not distort the

---

1. In this study the term albitite is used to describe rocks rich in albite.

sedimentary or tectonic structures, suggesting that a volume-for volume replacement of the country rock has occurred (Agrell, 1939). The albitization of meta-sediments of different bulk composition results in albitites of varying mineralogy. For example, actinolite bearing albitites form from calcareous meta-sediments, and talc-albitites from pelitic schists and in some cases from calc-schists. Pyrite is a major constituent in albitites formed from both quartzo-feldspathic schists and semi-pelitic schists.<sup>1</sup> Minor pegmatitic and fine grained quartz-albitites also occur in the area, the fine grained variants forming from quartzo-feldspathic schists. Commonly, one or two generations of veins traverse the albitite bodies. They may consist of albite, albite-talc, albite-actinolite, albite-tourmaline and actinolite; small bleached zones occur in the albitite adjacent to the albite-tourmaline veins.

#### Petrography.

The pyrite bearing albitites consist of an equigranular, fine grained albite (0.05mm. in diam.; 85 to 90 p.c.) and interstitial xenoblastic pyrite (maximum 10 p.c.). The albite ( $An_{4-6}$ ) is generally cloudy and is twinned on the albite and albite-carlsbad laws. The pyrite is commonly replaced by earthy limonite aggregates or pisolitic aggregates of jarosite (O = yellow, E = pale cream to colourless). Minor corroded quartz and a relic layering defined by muscovite or bleached biotite occur in many specimens. Rutile, chlorite and zircon

---

1. It should be pointed out that pyrite commonly occurs in the other varieties of albitite, but in much smaller quantities.

are accessories.

Talc-albitites are normally fine grained rocks in which pale green crystals of talc are evenly distributed. Coarse grained pegmatitic and fine grained variants occur together at several localities. The talc (5 to 35 p.c.) in the fine grained rocks forms either radiating sheaf-like crystals (0.15 to 1.0mm.) or anhedral irregular grains; the talc is commonly iron stained and may contain rutile and relic biotite. The albite ( $An_{3.5}$  to  $An_7$ ; 65 to 95 p.c.) appears as twinned, interlocking lath-like crystals or anhedral grains, which enclose minor biotite and quartz. Rutile may constitute as much as 5 percent of some rocks (e.g. 379). In the pegmatitic variants albite (0.5. to 5.0mm.) generally exhibits strong domain extinction and serrated grain boundaries, indicating that a post crystallization phase of deformation has affected these rocks. Chessboard twinning is ubiquitous. Talc appears as sheaf-like crystals either interstitial to or along fractures in the albite. Pyrite and rutile are common accessories.

Actinolite bearing albitites are abundant in the zones of albitized calc-silicate rocks. In hand specimen fine and coarse grained variants may be present, as well as small veins of fibrous actinolite growing perpendicular to the vein-country rock border. Many fine grained rocks are massive, with clots or single crystals of actinolite dispersed in a matrix of saccharoidal albite; others show a lenticular

banding defined by alternating layers of actinolite and albite. In thin section the massive variants consist of a fine grained mosaic of albite 75 to 90 p.c.,  $Ang_{5-7}$ ) and idio-blastic pale green actinolite (X = colourless, Y = very pale green, Z = pale green) crystals. Minor talc, rutile and pyrite (replaced by jarosite) may also be present.

The banded varieties result from the replacement of layers of varying bulk composition in the calc-silicate rocks and calc-schists. For example, in 414 albite is concentrated in layers containing minor microcline and scapolite, and actinolite in bands with relic diopside. In other specimens albite accompanies actinolite in some bands and minor talc in others. The coarse grained variants consist of an interlocking aggregate of subhedral to anhedral, pale green crystals of actinolite (0.15 to 5.0mm.), strained albite ( $Ang_{8-10}$ ) with ubiquitous chessboard twinning, and minor bleached relic flakes of biotite and quartz.

#### Transitional rocks.

Transitional between the unaltered country rocks and the albitites are zones of partially albitized meta-sediments. The textures shown by these rocks vary with the lithology of the original rock. For example, in the calc-schists white spots of fine grained albite are abundant, but in the pelitic schists streaks and pods of albite are present between the mica foliae. In rocks such as the calc-silicate rocks and

the quartz rich semi-pelitic schists, cross-cutting veins of actinolite and albite are ubiquitous. The intensity of albitization of the rocks adjacent to the albite veins, varies with the lithology of the rock undergoing alteration. This is particularly clear in specimen 884, a cross-bedded meta-siltstone (Fig.48), where the zone of albitization is best developed in the less micaceous fore-set units. Microscopically the white spots (3.0 to 5.0mm. in diam.) in the partially albitized calc-schists consist of fine grained albite (0.05mm. or less in diam.), minor limonite stained actinolite (e.g.867B), bleached biotite, and rutile (Fig.49 c.f. Agrell,1939, Fig.6B).

In the partially albitized calc-silicate rocks veins of varying thickness and mineralogy are present. These veins change in mineralogy as they traverse bands of different mineralogy. For example, in 414 the veins consist of actinolite and minor pyrite where cutting diopside rich bands, and albite-epidote in scapolite rich bands (Figs.50a and b). The potash feldspar grains are more altered adjacent to the veins.

In many altered calc-silicate rocks veins are not present, and albitization appears to have preferentially taken place in potash feldspar or scapolite rich bands (e.g. 1A and 1B).

The transitional rocks between the pelitic schists and the albitites are of special interest concerning the genesis of talc. Specimens 380B, C, E and F are typical of the transitional rocks between a garnet schist and talc-albitite. In thin section the least altered garnet schist (380E) shows mosaics

FIG.48.

Large thin section of cross-bedded meta-siltstone showing small veins of albite. Note that the intensity of albitization is greatest in the mica poor horizons. Location 978 268. Spec. No.A200-884. Specimen natural size.

FIG.49.

Photomicrograph of partially albitized calc-schist showing "spots" of slight turbid albite and minor actinolite. Location 962 285. Spec. No.383. X 32.

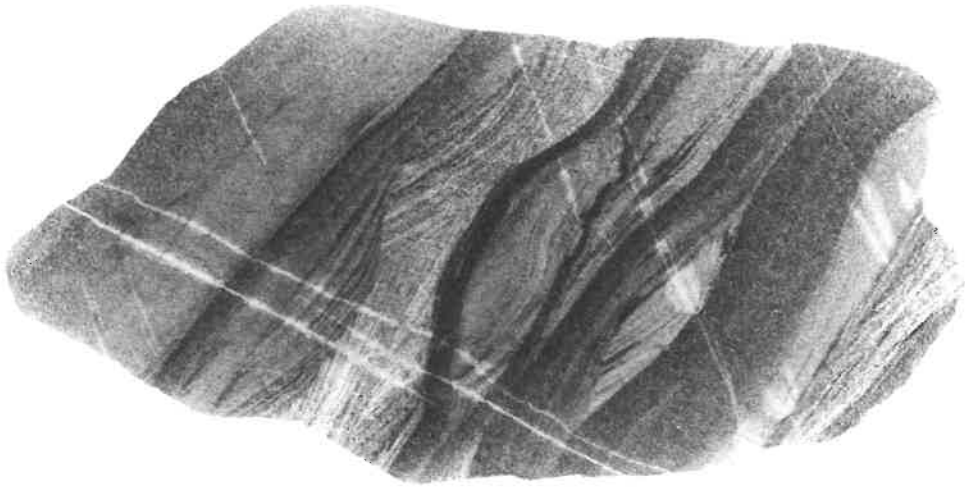


FIG.48.

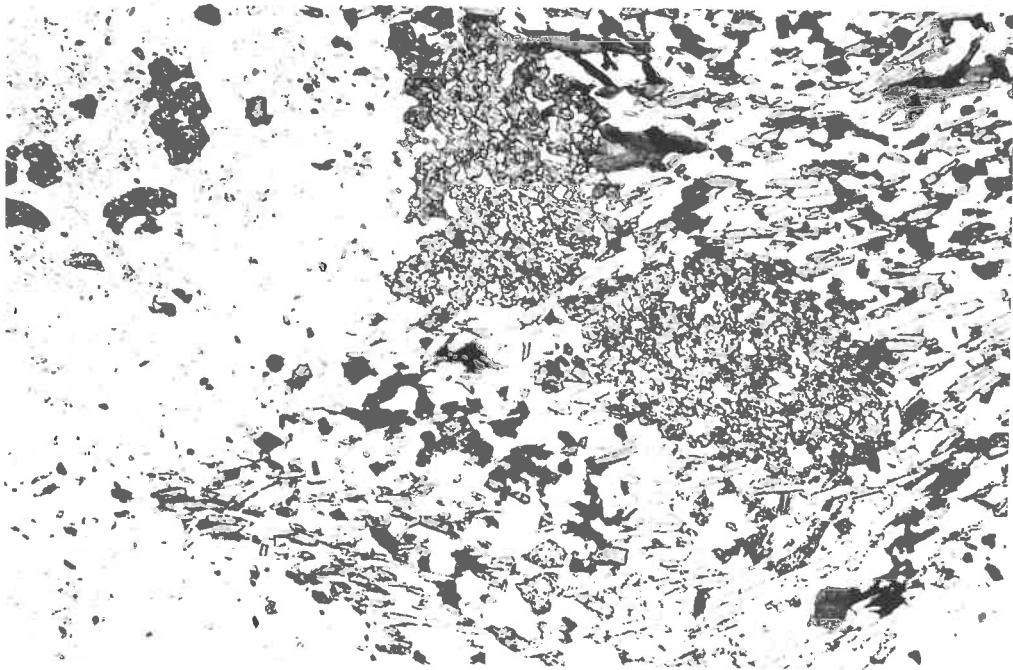


FIG.49.

FIG.50A.

Veins of actinolite (Ac) and pyrite,  
and epidote (E) and albite crosscutting  
diopside (D) -scapolite (S) band. Note  
that albite and epidote occur in the vein  
traversing the scapolite rich area.

Location 974 287. Spec. No.414. X 32.

FIG.50B.

Vein of actinolite (Ac), albite (A) and  
calcite (C) traversing diopside rich  
and scapolite rich bands. Location

974 287. Spec. No.414. X 32.



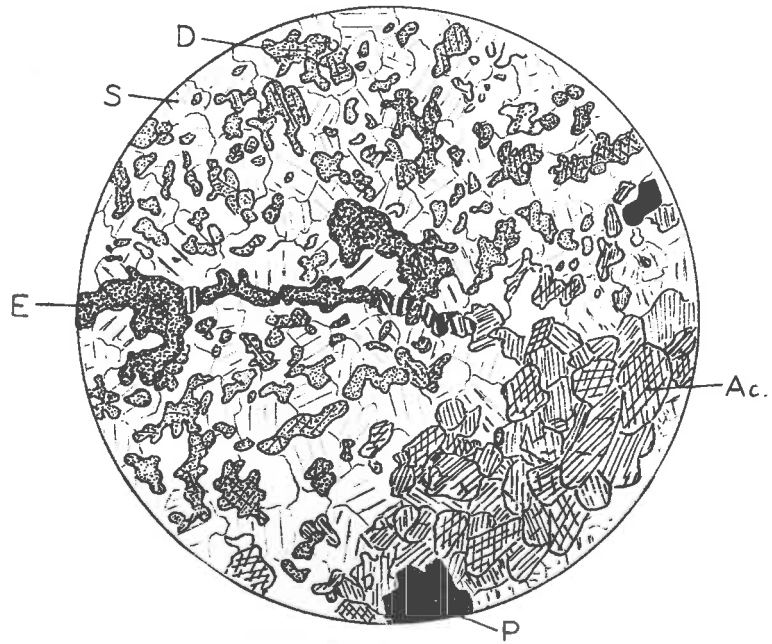


FIG. 50A.

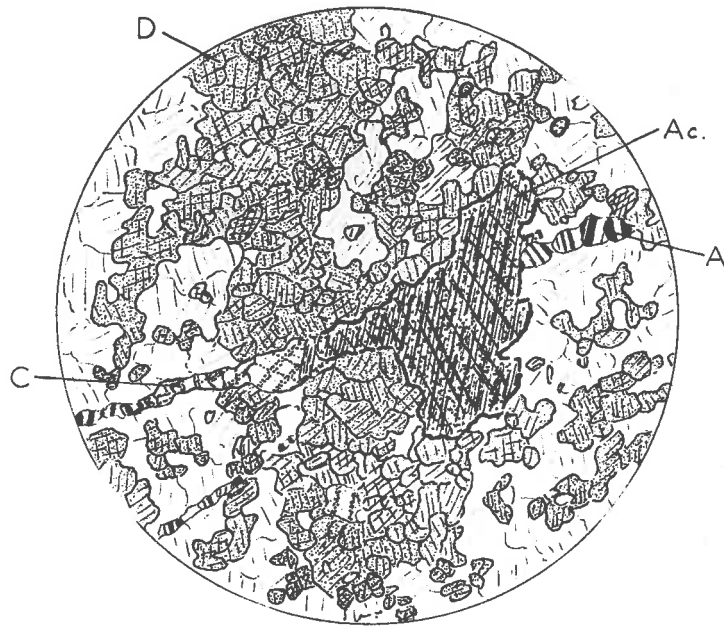


FIG. 50B.

of fine grained albite associated with corroded quartz and oligoclase between biotite foliae. Talc appears in the strongly albitized garnet schists (380F) at the borders of and within biotite (Fig.51b). Rutile forms concomitantly during this replacement. Oligoclase is replaced by a turbid mat of white mica, and garnet remains as relics within a chlorite-sericite aggregate. In the strongly albitized specimens (380B,380C) albite and talc are predominant, the talc appearing as elongate flakes containing relic biotite, or as sheaf-like interstitial crystals (Fig.51a). Quartz is no longer present and only minor relic garnet, apatite and tourmaline remain. Modal analyses of the transitional rocks, talc-albite and garnet schist are given in Table 24 and are represented in Fig.52.

#### Talc ore bodies.

Small talc ore bodies are developed in several localities in the Pewsey Vale area (Plate 1). They are generally elongate parallel to the regional foliation and are invariably surrounded by an aureole of albitite (often pyrite bearing), and then a zone of partially albitized schist. Within this outermost zone albite veins are commonly present. Minor inclusions of albitite and crystals of pyrite, rutile and albite occur sporadically in many talc ore bodies. Commonly structures present in the adjacent country rock are preserved in the talc ore bodies. In the Karawirra ore body (Olliver, 1964) cavernous structures were observed, suggesting that there has been a change in volume during the formation of this particular body. In hand specimen

FIG.51A.

Strongly albitized garnet schist showing predominantly albite (A) and minor talc (T), relict plagioclase (P), and garnet (G). Location 967 284. Spec. No.A200-380F. X 32.

FIG.51B

Photomicrograph showing talc (T) rimming biotite. Rutile (R) is associated with the talc. Location 967 284. Spec. No. A200-380F. X 80.

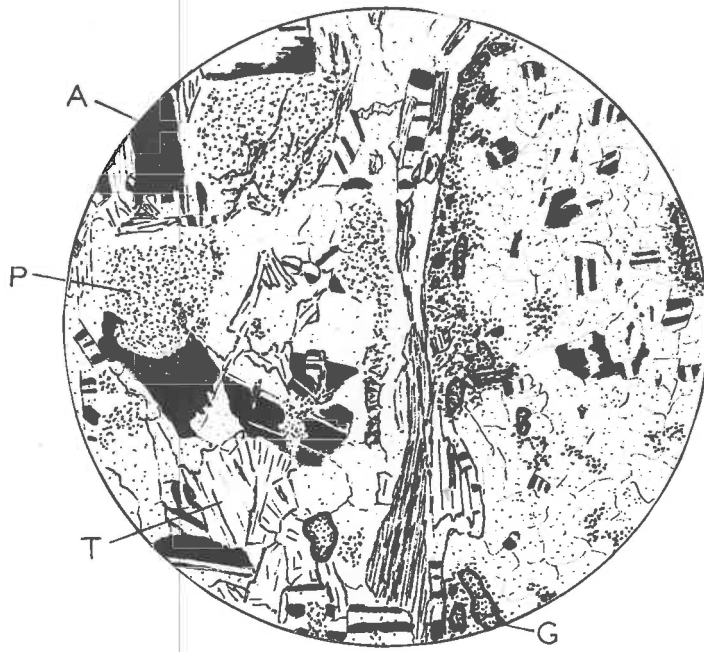


FIG. 5IA.

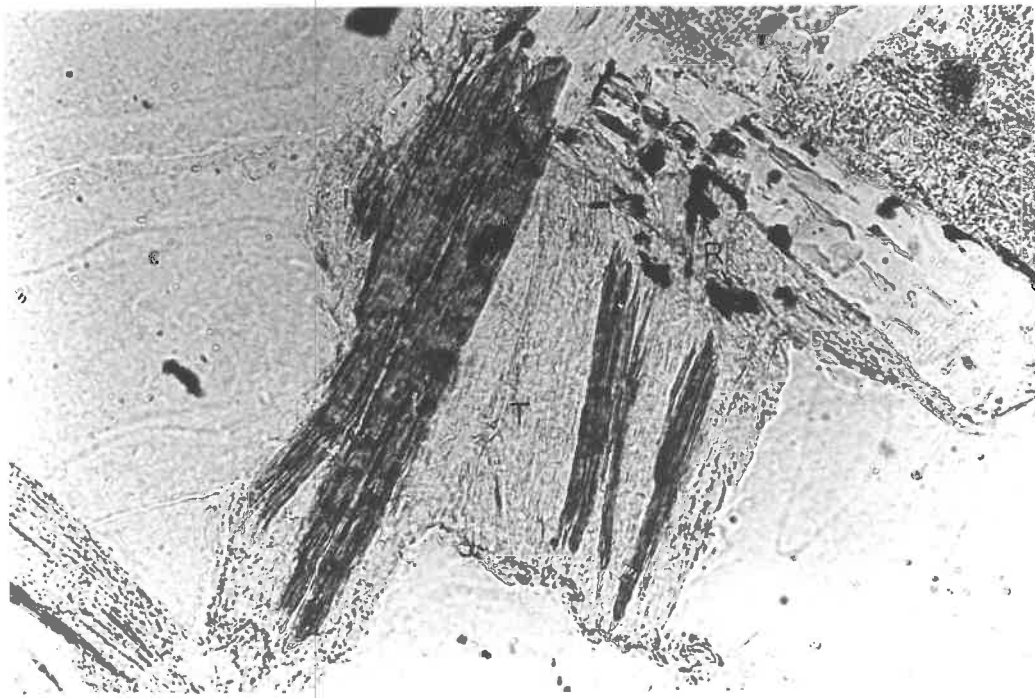


FIG. 5IB.

FIG.52.

Diagrammatic representation of the  
modal analyses in Table 24.

FIG. 52

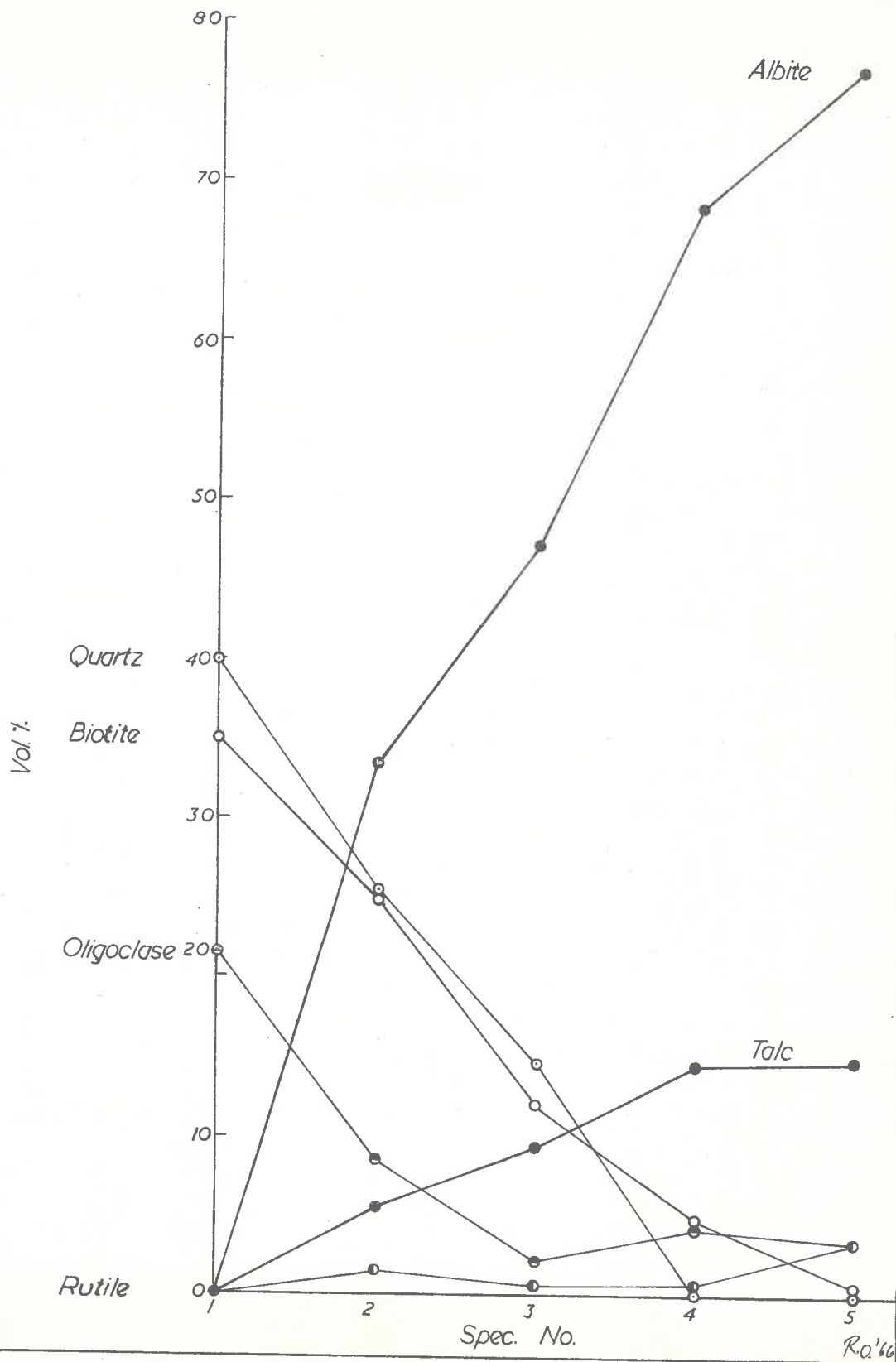


TABLE 24.

Modal analyses (vol.%) of Garnet Schist, Transitional Rocks and Talc-albite.

Spec.No.	Ab.	Talc.	Biot.	Rut.	Olig.	Garnet	Chl.	Qtz.	Apat.	Total No Counts
380D 1	-	-	35.0	-	21.8	2.8	0.3	39.9	0.2	3693
380E 2	33.6	5.2	24.0	1.8	8.7	0.2	1.0	25.5	-	3410
380F 3	47.1	9.6	12.2	0.7	2.2	11.1	-	14.8	0.5	3271
380B 4	68.3	14.5	4.9	0.9	4.5	2.6	4.0	-	0.3	4014
380C 5	77.3	14.9	0.8	3.4	3.5	-	0.1	-	-	3217

Calculated Na<sub>2</sub>O and Al<sub>2</sub>O<sub>3</sub> contents in specimens 380D and 380C

	380D	380C
Na <sub>2</sub> O <sup>1</sup>	1.7	7.2
Al <sub>2</sub> O <sub>3</sub>	11.6	15.0

1. Na<sub>2</sub>O and Al<sub>2</sub>O<sub>3</sub> have been calculated from the modal analyses given above. The composition of the oligoclase was assumed to be An<sub>20</sub> and the albite Ab<sub>100</sub>. The analysis of biotite 380D was used to calculate the proportion of Al<sub>2</sub>O<sub>3</sub> contributed by the biotite.

the talc is either white or pale green and has a fibrous or platy form. Limonite derived from the breakdown of pyrite commonly stains the talc.

### Discussion.

The features discussed in the previous sections, namely the preservation of tectonic and sedimentary structures in the albitites, the ubiquitous occurrence of crosscutting albite veins and the presence of the albitite in the fault zones, clearly indicate that these rocks are of replacement origin.

### Chemical and mineralogical changes involved in the albitization.

In order to explain the mineralogical changes it is necessary to postulate an introduction of soda (compare 1.7 p.c.  $\text{Na}_2\text{O}$  in 380D with 7.2 p.c.  $\text{Na}_2\text{O}$  in 380C, Table 24), sulfur (abundant pyrite), boron (tourmaline in some veins) and possibly water, (actinolite, epidote in some assemblages), and the removal of potash (potash bearing minerals absent from albitite assemblages). Petrographic evidence suggests that the Mg required for the formation of talc has been derived from the breakdown of biotite. Stillwell and Edwards (1951) considered that talc formed in the following way:



They also noted that talc formed from biotite moderately rich in Mg (analysis A, Table 25). During the present investigation it was found that biotites in some rocks (e.g. pelitic schists, calc-schists) altered to talc, and in others (e.g. quartzo-



feldspathic schists, Mt. Kitchener Intrusion) altered to chlorite and vermiculite (?). Two of the former biotites (368,380) and one of the latter (56) were analysed, but no significant differences in Mg/Total Fe ratios were noted (Table 25) although 56 (the biotite which altered to chlorite and vermiculite?) has the lowest Mg/Total Fe value. More chemical and experimental work<sup>1</sup> is needed to resolve this problem. The elements released from the breakdown of biotite to talc viz. Al<sup>III</sup>, Fe<sup>III</sup>, Fe<sup>II</sup>, K<sup>+</sup>, Ti<sup>IV</sup> either leave the system (e.g. K<sup>+</sup>) or react with other elements to form new minerals. For example, Ti<sup>IV</sup> forms rutile (or sphene if Ca is available) and Fe<sup>II</sup> reacts with introduced S to precipitate as pyrite, or when S is unavailable, forms limonite. The Al<sup>III</sup> combines with Na<sub>2</sub>O and SiO<sub>2</sub> (quartz) to form albite.

Apart from the replacement of scapolite and potash feldspar by albite, the main mineralogical transformation in the calc-silicate rocks appears to have been the replacement of diopside by actinolite (equation (2)):



The CO<sub>2</sub> required for this reaction may have been introduced, but it is more likely that it has been derived from the replacement of scapolite by epidote and albite. The calcite lens in the Nairne Fault Zone, north-west of Mt. Kitchener (Plate 1), may have formed as a result of the albitization of the Kanmantoo

---

1. The author suggests that a study of the reaction of biotites of different Mg/Total Fe values to varying  $a_{\text{Na}^+}/a_{\text{H}^+}$  (solutions of different Na<sup>+</sup> concentrations), temperature conditions might provide a solution to the talc genesis.

TABLE 25.

Partial Chemical Analyses<sup>1</sup> of Biotites.

<u>Spec. No.</u>	56	380D	368	A
SiO <sub>2</sub>	35.98	36.83	35.77	40.70
Al <sub>2</sub> O <sub>3</sub>	17.40	18.72	19.97	15.58
Total Fe	21.58	19.73	19.21	14.61
MgO	10.30	11.23	10.37	11.27
CaO	0.13	0.26	0.07	0.32
Na <sub>2</sub> O	0.15	0.40	0.25	1.03
K <sub>2</sub> O	10.19	8.17	7.68	6.22
TiO <sub>2</sub>	2.76	2.19	2.31	3.12
MnO	0.34	0.19	0.21	-
H <sub>2</sub> O over 100°C	-	-	-	5.84
H <sub>2</sub> O at 100°C	-	-	-	1.50
Mg/Fe	0.48	0.57	0.54	0.77

1. Analyses by D. Gray and P. Catford.  
 Na<sub>2</sub>O determined by Flame Photometer,  
 MgO by atomic absorption and the  
 remainder by X-ray spectrography.

56 Quartz-feldspathic schist.  
 368 Muscovite - biotite schist.  
 380D Garnet schist.  
 A Stillwell and Edwards (1951).



Group calc-silicate rocks to the north.

Source of Soda.

Having concluded that the albitites are of replacement origin and that soda is essentially the main constituent added to the rocks in the Pewsey Vale area, the question arises as to what is the source of the soda.

Albitites are commonly associated with both basic igneous rocks (Larsen, 1928; Agrell, 1939) and acid igneous rocks (Leedal, 1952; Joplin, 1956; Ayanov, 1964). The sodic rich solutions required for their formation are considered to be derived from these igneous rocks during the late stages of crystallization. There are however, albitites in some terrains which are in no way connected to magmatic bodies. Albitites of this kind occur within the low and high grade metamorphic rocks at Broken Hill, N.S.W. (Vernon, 1961). Vernon concluded however, that the sodic solutions necessary for their formation were derived from a magmatic source.

Albite-talc rocks are widespread in the central Mt. Lofty Ranges, extending from east of Lyndoch to Oakbank, a distance of 27 miles (Stillwell and Edwards 1951; Whittle, 1957). Quartz-albitites are found on the eastern side of the Mt. Lofty Ranges, but are considered to be older than the talc bearing albitites (Mills, 1964). There are no magmatic bodies in the Mt. Lofty Ranges visibly connected to the albitites, but at Encounter Bay (Browne, 1920; Bowes, 1954) and Cape Willoughby, Kangaroo Island (Tilley, 1919), albitites are associated with post kine-

matic granites.

In the Pewsey Vale area, post kinematic granodiorites and granites intrude the meta-sediments and are strongly albitized (Chapter 9). This suggests that albitite formation in the Pewsey Vale area may be related to these intrusions, but in view of the occurrence of albitites some distance from these rocks, this hypothesis must be rejected. It seems therefore that no satisfactory origin for the soda rich solutions can be given.

CHAPTER 11.STRUCTURE.FOLDING.

Three phases of deformation are recognised in the Adelaide Supergroup rocks and two in the rocks of the Kanmantoo Group. Each deformation is accompanied by the formation of both planar and linear elements (Table 26). In the following section the style of folds produced on a macroscopic and mesoscopic scale are discussed, and the geometry of linear and planar elements are interpreted. The symbols which have been assigned to the planar and linear elements associated with each deformation are illustrated in Table 26.

The techniques applied in this analysis are those outlined by Weiss and McIntyre (1957) and Turner and Weiss (1963). However, in many instances the phases of deformation are difficult to separate as the resulting structures are similar in style and differ only slightly in orientation (compare undifferentiated data with differentiated data Figs. 56 and 62). Only in outcrops where a direct overprinting relationship can be observed is the situation unequivocal. The structural geometry has been built up only from these outcrops.

Lithological layering S.

In many parts of the area, the lithological layering S is undoubtedly bedding, but in some localities (e.g. the

TABLE 26.

	ADELAIDE SUPERGROUP		KANMANTOO GROUP	
	S surface	Linear elements	S surface	Linear elements
First generation structures.	S = Lithological layering which in many cases is bedding.  S <sub>1</sub> = Foliation.	B <sub>1</sub> = Lination or axis of fold in S with S <sub>1</sub> as axial plane.	S = Lithological layering which in some cases is bedding.  S <sub>1</sub> = Foliation.	B <sub>1</sub> = Lination or axis of fold in S with S <sub>1</sub> as axial plane.
Second generation structures.	S <sub>2</sub> = First crenulation cleavage. Axial plane to B <sub>2</sub> folds or crenulations.	B <sub>2</sub> = Axis of fold or crenulation in S <sub>1</sub> with S <sub>2</sub> as axial plane.	A B S E N T	
Third generation structures.	S <sub>3</sub> = Second crenulation cleavage. Axial plane to B <sub>3</sub> folds or crenulations.	B <sub>3</sub> = Axis of fold or crenulation in S <sub>1</sub> or S <sub>2</sub> with S <sub>3</sub> as axial plane.	S <sub>3</sub> = Foliation	B <sub>3</sub> = Lination or axis of fold in S or S <sub>1</sub> with S <sub>3</sub> as axial plane.

migmatite zone) it appears to have been formed by transposition of bedding or by metamorphic differentiation.

### First deformation B<sub>1</sub>

#### Minor B<sub>1</sub> structures

S<sub>1</sub> is a foliation (parallel to the axial surface of B<sub>1</sub> folds) which is defined by the preferred orientation of platy minerals in the schists (quartz-feldspathic schists, calc-schists etc.) and more rarely by lenticular pods of light and dark minerals in the calc-silicate rocks of the Kanmantoo Group. In the quartzites and calc-silicate rocks of the Adelaide Supergroup S<sub>1</sub> is fracture cleavage which appears as closely spaced fractures; where oriented at moderate to high angles to S in some calc-silicate rocks, it is associated with cleavage and fold nullions (Wilson, 1953; Fig. 53). In outcrops of two distinct lithologies, S<sub>1</sub> is strongly refracted (see O'Driscoll, 1965 for the experimental production of this phenomenon).

#### Mesoscopic B<sub>1</sub> folds.

Small B<sub>1</sub> folds are comparatively rare in the Adelaide Supergroup rocks. This is believed to be a consequence of two factors :

- (1) Most of the Adelaide Supergroup rocks consist of homogeneous mica-schists in which bedding has been extensively transposed or destroyed.
- (2) In many areas S is equivalent to or at a slight angle to S<sub>1</sub>. Such conditions are unsuitable for the development of mesoscopic folds.

FIG.53.

Fold and cleavage nullions in small  
calc-silicate rock bands. Pencil  
6 inches (15 cms). Location 950 237.

FIG.54.

Asymmetric B, folds in calc-silicate  
rock-calc-schist sequence. Ruler  
(6 inches=15 cms) approximately parallels  
S1. Location 950 237.



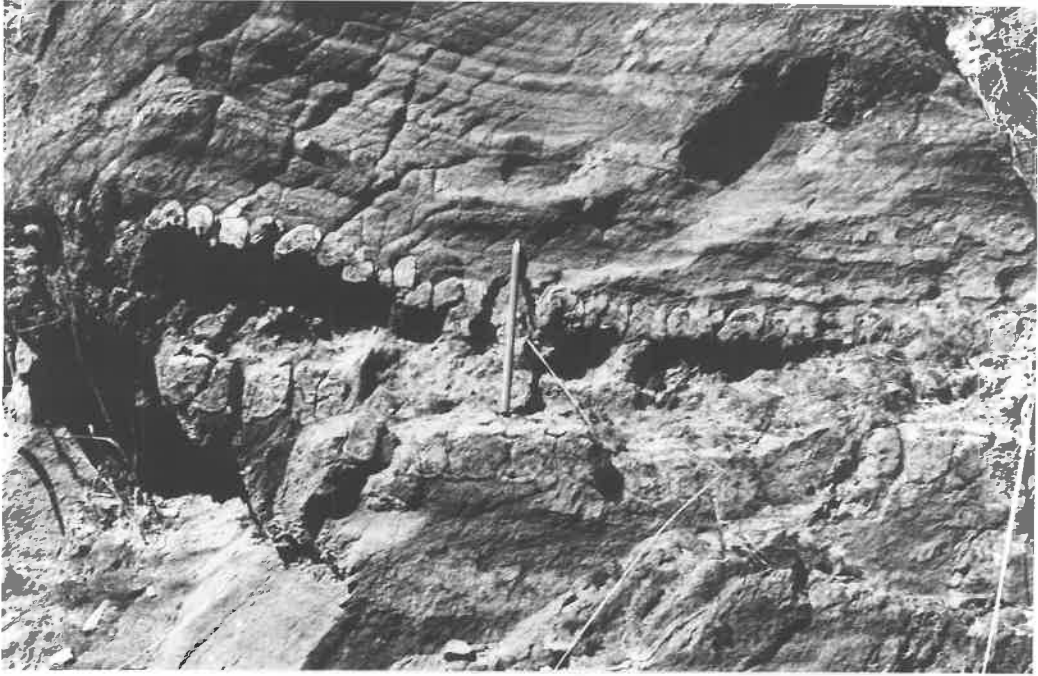


FIG. 53.



FIG. 54.

Most folds in the Adelaide Supergroup are asymmetric and may be open or tightly appressed. The foliation  $S_1$  is subparallel to the short limbs of the more appressed folds. In some rocks (e.g. the calc-silicate rocks) small scale faulting takes place along  $S_1$ ; in others, extensive thinning of the short limb or both limbs of some folds occurs in zones parallel to  $S_1$  (Fig. 54; c.f. Talbot, 1964). It is possible that this thinning has been brought about by a creep process involving movement on a granular scale (Hebbs, 1968). Quartz veins are also deformed during the  $B_1$  deformation and have been transposed into small open asymmetric folds whose axes are not coincident with the  $B_1$  axis in the surrounding schists, producing locally a triclinic fabric (c.f. Weiss, 1959a, p. 43); others form intrafolial folds within the mica schists.

By contrast  $B_1$  folds are common in the rocks of the Kannantoo Group. They are generally open, concentric (commonly disharmonic) folds with steep east or west dipping axial planes (Figs. 55A and B). Both asymmetric and symmetric types occur and some are recumbent. Many  $B_1$  folds are merely small scale rumples in bedding.

The differences in fold style in the two groups of rocks is attributed to differences in lithology, the Adelaide Supergroup rocks being predominantly less competent mica-schists and the Kannantoo Group rocks well bedded more competent quartz-feldspathic schists, calc-silicate rocks etc.

**FIG. 55A**

**Profile of asymmetric  $B_1$  fold.**

**Pencil (6 inches = 15 cms.)**

**dips steep east.**

**Location 980143.**

**FIG. 55B**

**Profiles of  $B_1$  folds.**

**Axial planes of c and e**

**dip east.**

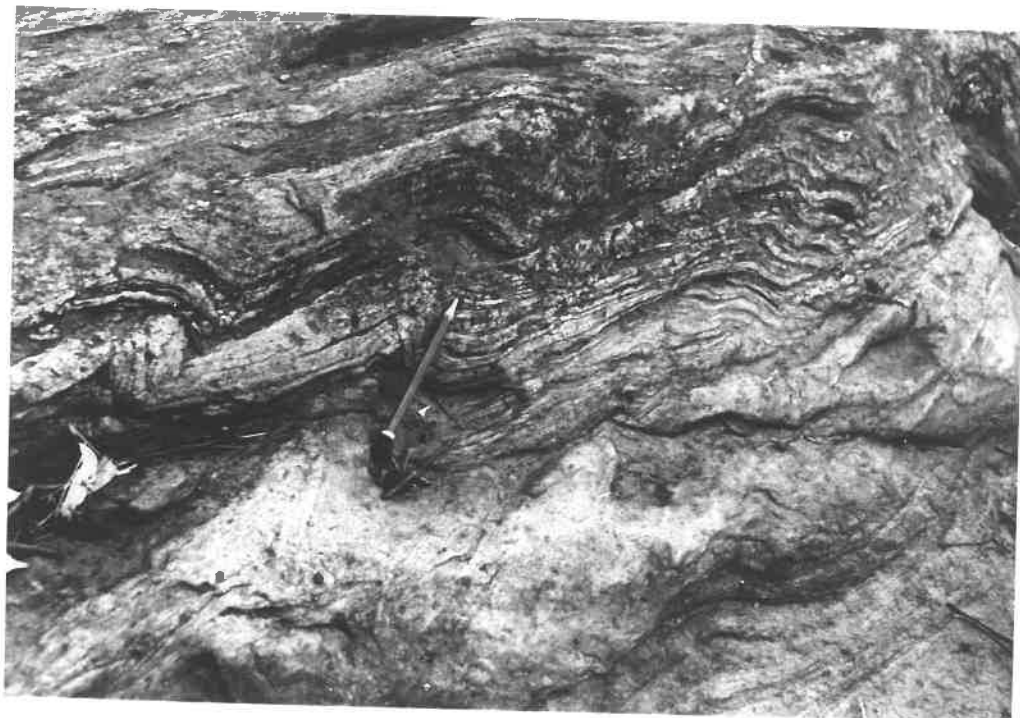


FIG. 55A.

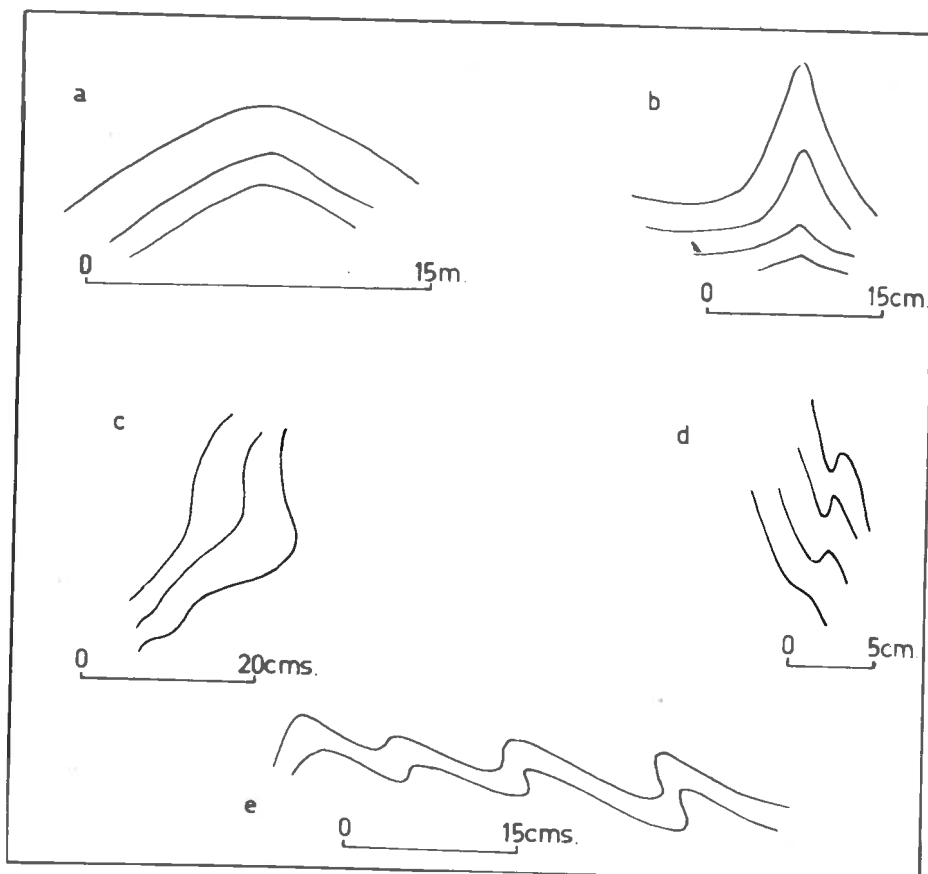


FIG. 55B.

A lineation parallel to  $B_1$  folds is well developed in both group of rocks. It is defined by :-

- (1) a mineral streaking - biotite, hornblende, sillimanite, feldspar.
- (2) cleavage or fold nullions in calc-silicate rocks and a ribbing in quartzites.
- (3) intersection of  $S$  and  $S_1$ .

The orientation of the linear and planar elements of the  $B_1$  deformation is illustrated in Fig.56. The majority of the  $B_1$  axes in the Adelaide Supergroup plunge  $10^\circ$  in a direction  $140^\circ$  (Fig.56a) but many are spread along two incomplete girdles; those in the Kannantoo Group rocks have a similar trend but are distributed along a more steeply dipping girdle (Fig.56d). The significance of these distributions will be discussed later.

The foliation  $S_1^I$  in the Adelaide Supergroup rocks fans about an axis  $\beta$  which plunges  $4^\circ$  in a direction  $143^\circ$  (Fig.56b). However, this fanning is in part due to the redistribution of  $S_1$  about the  $B_3$  axis, as the majority of the readings have been recorded in subarea I<sup>2</sup> where the  $B_3$  deformation is also evident (compare Fig.56c, a plot of  $S_1$  in subarea I with Fig.56b).

The majority of the  $S_1$  foliation planes in the Kannantoo

- 
1. Owing to the lack of outcrop and the fact that  $S_1$  has been strongly crenulated or transposed, only a small number of measurements could be made.
  2. See Fig.63 for the location of subareas in the Adelaide Supergroup rocks.

FIG.56.

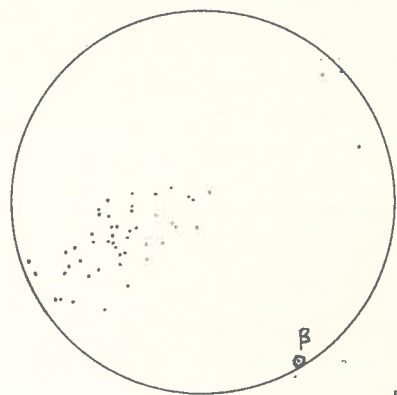
Collective diagrams of structural elements  
of the Pewsey Vale area.

- a Lineation  $B_1$ , 148 points. Contours  
1-2.5-5-7.5 % per 1% area. Adelaide Supergroup.
- b Foliation  $S_1$ , 50 points. Adelaide  
Supergroup.
- c Foliation  $S_1$  in subarea I. 32 points.
- d Foliation  $S_1$ , 32 points, lineation  
 $B_1$ , 75 points. Kanmantoo Group.
- e  $S_1$ ,  $B_1(X)$  and  $B_3(+)$  data for the  
Pewsey Vale Peak Synform.
- f Undifferentiated  $B_2$  and  $B_3$  axes, 250  
points. Contours 1-5-10% per 1% area.  
Adelaide Supergroup.
- g Undifferentiated  $S_2$  and  $S_3$ , 136 points.  
Contours 1-5-10% per 1% area. Adelaide  
Supergroup.
- h Foliation  $S_2$ , 26 points; lineation  $B_2$ ,  
106 points. Contours 1-5-10% per 1%  
area. Adelaide Supergroup.
- i Undifferentiated  $B_1$  and  $B_3$  axes, 223  
points. Kanmantoo Group.
- j Undifferentiated  $S_1$  and  $S_3$  planes, 101  
points. Kanmantoo Group.

FIG. 56



a



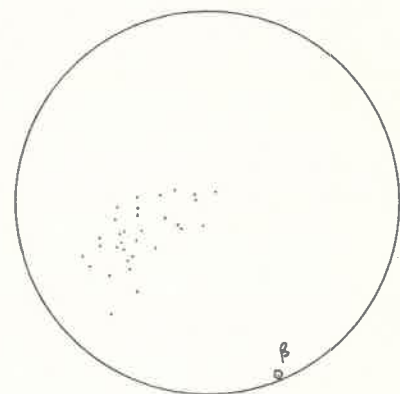
b



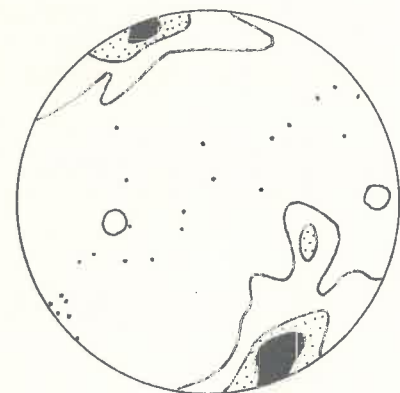
f



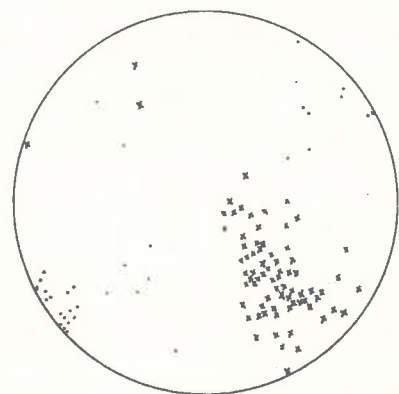
g



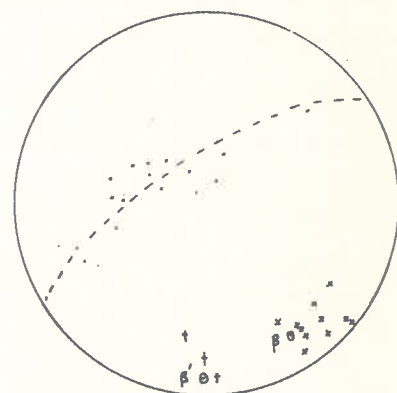
c



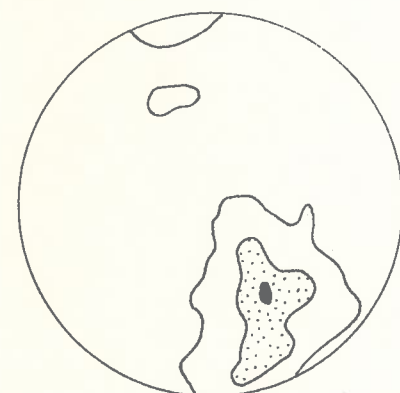
h



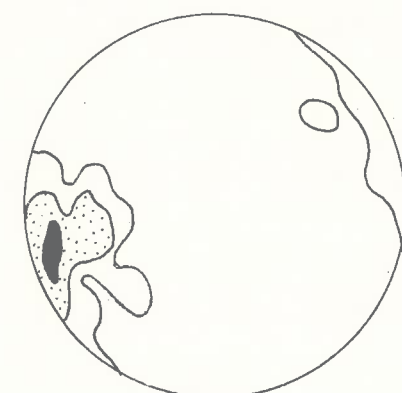
d



e



i



j

Group rocks, trend  $144^{\circ}$  and dip west or east  $30^{\circ}$  to vertical (Fig.56d).

### Major $B_1$ structures.

#### Adelaide Supergroup.

Most of the evidence of  $B_1$  structures have been obliterated by the  $B_3$  deformation, but there appears to be geometrical and field evidence for  $B_1$  folds in some areas. One such structure is an isolated synform centred around Pewsey Vale Peak (Plate 3). The statistical fold axis  $\beta$  in this small area, plunges  $20^{\circ}$  in a direction  $142^{\circ}$  and is approximately coincident with the  $B_1$  lineations (Fig.56e). However, there is a slight tendency for S to spread about a second girdle whose axis  $\beta'$  coincides with the axis of the third deformation  $B_3$ , suggesting some inhomogeneity in this small area.

In subarea A, no mappable units are present, but the geometry is consistent with that of the  $B_1$  deformation ( $\beta$  plunges  $0^{\circ}$  in a direction  $146^{\circ}$ ). A possible relic  $B_1$  isoclinal structure which has been refolded about  $B_3$  appears in subarea G.

#### Kanmantoo Group.

Owing to the lack of marker horizons in all but the northern part of the area, the style of the major  $B_1$  structures is difficult to determine. The form surfaces (Plate 3) show that the major structure in the area is a steeply plunging anticline. The geometry of subareas 3<sup>1</sup> and 5 (Fig.64

---

1. See Fig.64 for the location of subareas in the Kanmantoo Group rocks.



suggest that the anticline is a  $B_1$  structure, plunging  $44-60^\circ$  in a direction  $146^\circ$  to  $148^\circ$  and that the western limb is overturned.<sup>1</sup> In the southern part of the area, the  $B_1$  structures appear to have been obliterated by the  $B_3$  deformation.

### Second deformation $B_2$ .

$B_2$  structures have not been developed in the Kanmantoo Group rocks and are restricted in occurrence in the rocks of the Adelaide Supergroup.

### Minor $B_2$ structures.

#### Mesosopic $B_2$ folds.

Few mesoscopic  $B_2$  folds are developed in the area. Low amplitude symmetrical folds with vertical axial planes are present in the bimica schists and S shaped, concentric folds with near horizontal ( $10-15^\circ$  south) axial planes are found in the calc-silicate rocks. A crenulation<sup>2</sup> cleavage is parallel to the axial surface of these folds. A prominent lineation is defined by asymmetric or symmetric crenulations in  $S_1$ . No mineral orientation is developed parallel to  $B_2$ .

The orientation of  $B_2$  axes and  $S_2$  planes is shown in Fig.56h. Most  $B_2$  axes plunge  $10^\circ$  in a direction  $156^\circ$  and spread along a weakly defined girdle (c.f. spread of  $B_1$  lineations. Fig.56a). The  $S_2$  planes fan about an axis  $\beta$  plunging  $5^\circ$  in a direction  $146^\circ$ .

- 
1. Facings support this conclusion.
  2. The term crenulation cleavage formally defined by Rickard, (1961) is used here instead of strain slip cleavage.

### Major B<sub>2</sub> structures.

Major B<sub>2</sub> structures have not formed in the Adelaide Supergroup rocks. However, small broad rumples plunging 10° in a direction 146° are present in subarea F (Plate 3, Fig.63).

### Third deformation B<sub>3</sub>

#### Minor structures

#### Mesoscopic B<sub>3</sub> folds.

Small B<sub>3</sub> folds in the Adelaide Supergroup rocks have a typical low amplitude, open style (Fig.57; c.f. Best, 1963; Talbot, 1964). The axial surfaces of most B<sub>3</sub> folds is a crenulation cleavage, except in calc-silicate rock - calc-schist sequences where B<sub>3</sub> folds occur without S<sub>3</sub>. On the limbs of major B<sub>3</sub> folds, the mesoscopic folds are asymmetric, whereas on the hinges of major folds they are symmetric.

In areas where small B<sub>3</sub> folds deform foliation S<sub>1</sub> containing B<sub>1</sub> lineations, B<sub>1</sub> is distributed in a plane<sup>1</sup> (Fig.62e). This geometrical pattern is consistent with the B<sub>3</sub> folds being formed by displacement parallel to S<sub>3</sub> (Weiss, 1959b; Ramsay, 1960). Evidence for refolding of S<sub>2</sub> by B<sub>3</sub> movements has been observed in some localities, e.g. as in Fig.59 which shows the crinkling of S<sub>2</sub> about the B<sub>3</sub> axis in the hinge of the fold and a change in orientation of S<sub>2</sub> on the limbs.

---

1. N.B. These measurements were obtained from a B<sub>3</sub> fold which may not have been in situ.

FIG.57.

Oblique profile of B<sub>3</sub> fold in mica  
schists of the Adelaide Supergroup.  
Length of compass 3.5 inches (9cms).  
Location 929 210.

FIG.58.

Slightly disharmonic B<sub>3</sub> folding in a  
migmatite. Pencil 6 inches (15 cms)  
long. Location 982 192.



FIG. 57.

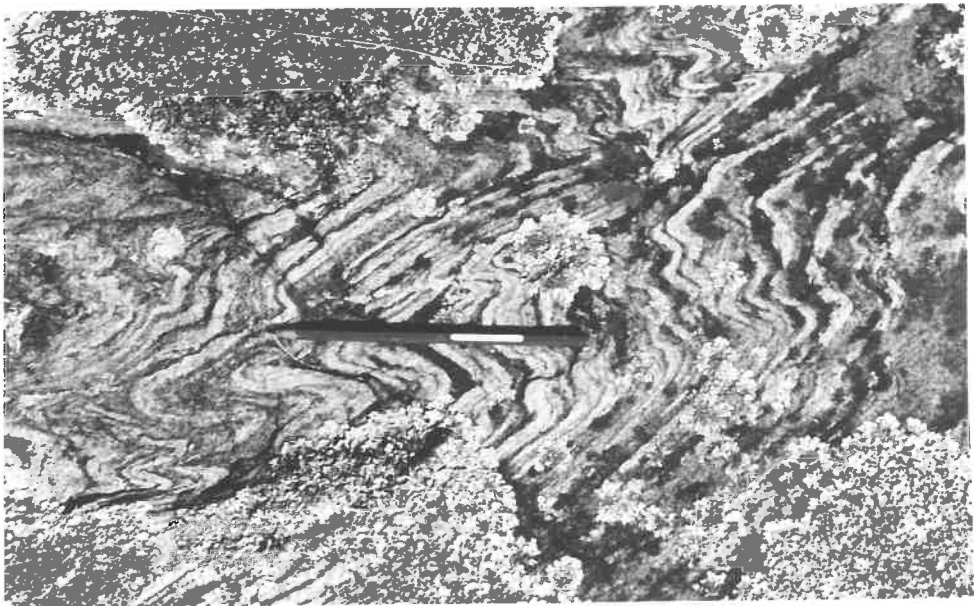


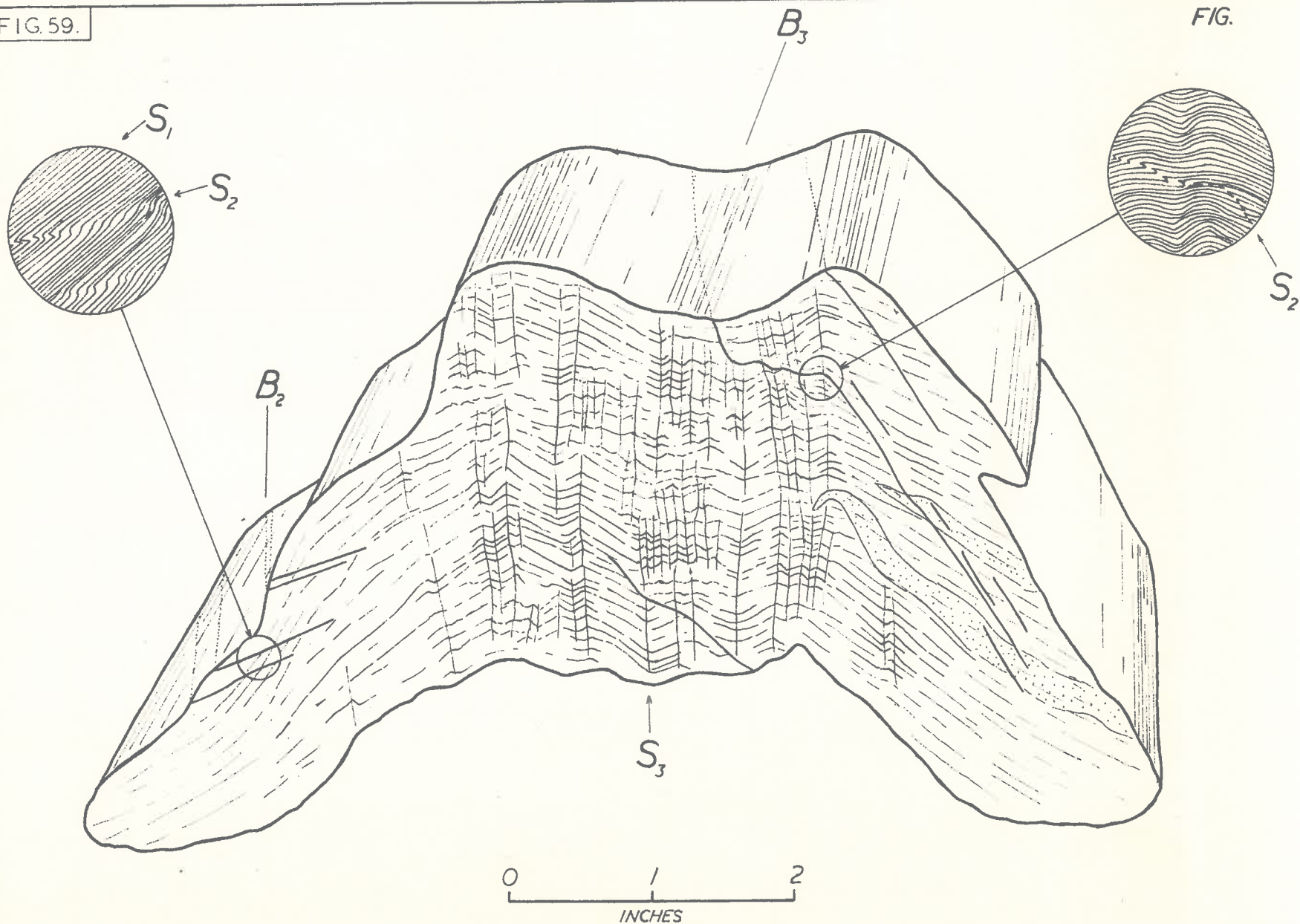
FIG. 58.

FIG.59.

Small  $B_3$  folding show refolding of  
 $S_1$  and  $S_2$  about the  $B_3$  axis.

FIG. 59.

FIG.



The style of  $B_3$  folds in the Kanmantoo Group rocks is markedly different to, and more varied than, the  $B_3$  folds in the rocks of the Adelaide Supergroup. Variation in fold style is greatest in the migmatite zone where concentric, similar and disharmonic variants (Figs. 58, 60, 61a and b) are present; all fold styles may occur within a small area. The axial planes of these folds may curve (Fig. 61a) or show a random orientation (but a common line of intersection) characteristic of polyclinal folds (Greenly, 1919). Ramsay (1958) noted a similar random orientation of axial planes in the migmatites of the Loch Monar area and attributed the distortion to movements resulting from plastic flow during migmatization.

A feature of the migmatites and some calc-silicate rocks is the presence of a new layering parallel to  $S_3$  which appears to have been formed by the transposition of original layering by folding. Relic hinges of these folds ( $B_3$ ) plunging at varying angles, occur between the new layering. In many localities microfaulting parallel to  $S_3$  has disrupted  $B_3$  folds and has resulted in discordant structures (Fig. 60).

$B_3$  lineations. In the Adelaide Supergroup rocks these include the hinges of small crenulations and lineations formed by the intersection of  $S_3$  with  $S_1$  or  $S_2$ . They are commonly associated with  $B_1$  and  $B_2$  lineations.  $B_3$  lineations in the Kanmantoo Group rocks are defined by a mineral orientation (biotite and more rarely muscovite), the intersection of  $S_3$  with  $S$  and rarely by the hinges of small crinkles.

FIG.60

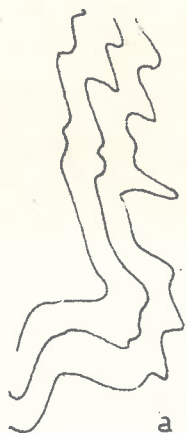
Profiles of  $B_3$  folds.

- a, f. Disharmonic folds in migmatites;  
quartz-feldspar vein cuts fold in f.
- b Open fold in quartzo-feldspathic schist.
- c, g. Discordant structures produced by movement parallel to  $S_3$ . c - calc-silicate rock, g - migmatite. Quartz-feldspar vein parallel to  $S_3$  in g.
- d Similar and concentric profiles in intercalated biotite schists and quartzo-feldspathic schists.
- e Similar folding in intercalated biotite schists and quartzo-feldspathic schists. Quartz-feldspar<sup>vein</sup> parallel to  $S_3$ .
- h Folded quartz-feldspar vein.



FIG. 60.

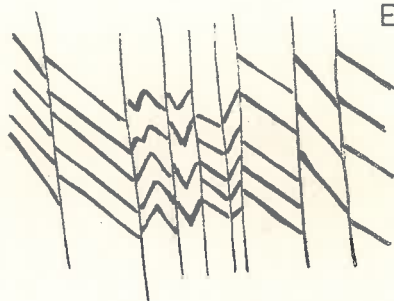
W



0 30cms.



0 15cms.



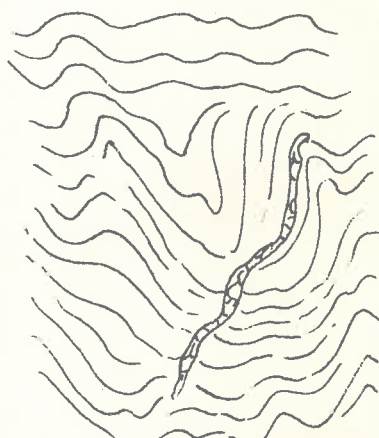
0 10cms



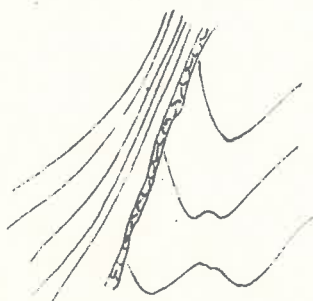
0 10cms.



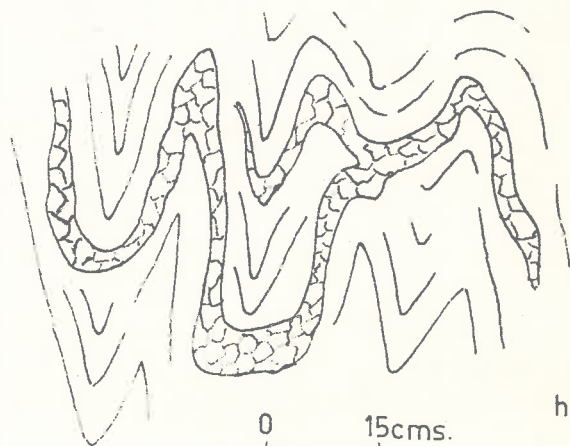
0 15cms



0 15cms.



0 15cms. g



0 15cms. h

R.O.

FIG. 61A

Large thin section of  $B_3$  fold showing curved trace of axial plane. Specimen natural size. Location 973 186.

FIG. 61B

Profile of  $B_3$  fold in quartzo-feldspathic schist. Location 986 240.



FIG. 6IA.

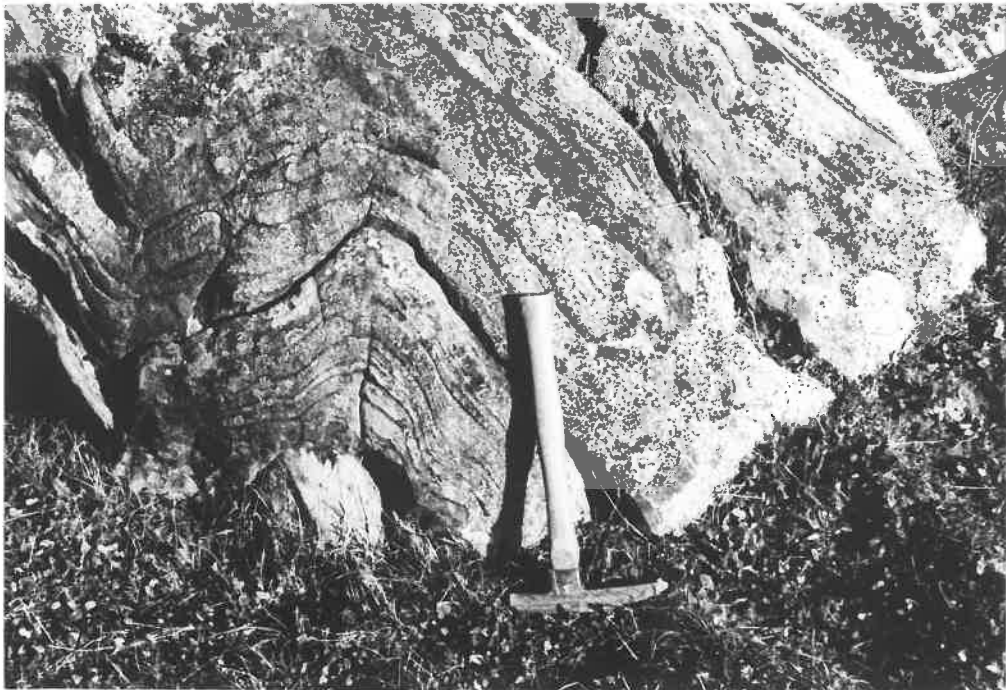


FIG. 6IB.

The foliation formed in the Adelaide Supergroup rocks during the third deformation is a crenulation cleavage, a cleavage represented by closely spaced planes which commonly form parallel to the long limbs of crenulations. In some areas  $S_3$  fans about the  $B_3$  axis; for example east of Tweedie Gully (subarea F)  $S_3$  varies in strike from  $174^\circ$  to  $192^\circ$  and dips  $75^\circ$  east to  $70^\circ$  west.

In the Kanmantoo Group rocks  $S_3$  is formed parallel to the axial planes of  $B_3$  folds in mica rich layers of the migmatites and as well defined banding in the calc-silicate rocks.

The distribution of the  $B_3$  axes and  $S_3$  planes is illustrated in Figs. 62a and b. The orientation of the linear and planar elements in both groups of rocks is essentially the same (e.g. the majority of  $S_3$  planes strike approximately  $348^\circ$  and dip east to  $60^\circ$  to vertical, and in the Kanmantoo Group rocks  $350^\circ$  and dip  $50^\circ$  east to vertical); the  $B_3$  axes in the Kanmantoo Group rocks however, generally plunge more steeply than the Adelaide Supergroup rocks.

#### Major $B_3$ structures.

##### Adelaide Supergroup.

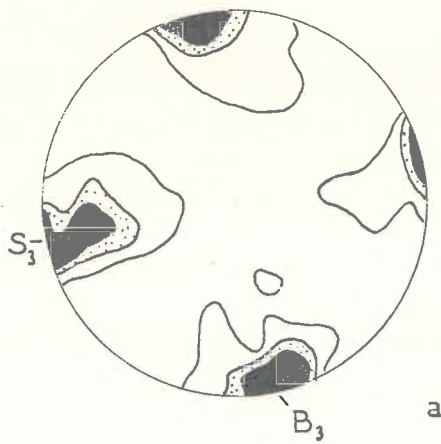
The major structures in the Adelaide Supergroup have been produced by the  $B_3$  deformation, and are represented by the Barossa Range Syncline (Campana, 1955) and Trial Hill Anticline (Plate 3). Generally, both structures have a broad, open style with limbs dipping shallow east or west (c.f. mesoscopic  $B_3$  folds). Steepening or reversal of dip

FIG. 62.

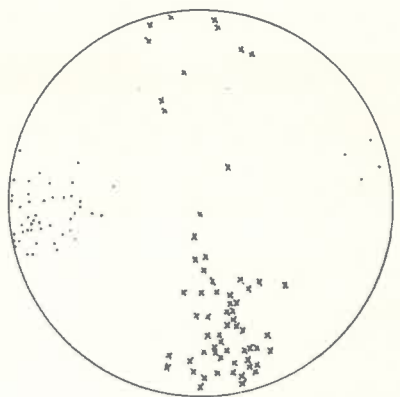
Collective diagrams of structural elements of the Pewsley Vale area.

- a Foliation  $S_3$ , 81 points. Lineation  $B_3$ , 139 points. Adelaide Supergroup. Contours 1-5-10% per 1% area.
- b Foliation  $S_3$ , 56 points. Lineation  $B_3$ , 68 points. Kanmantoo Group.
- c Lithological layering S. 368 points. Adelaide Supergroup.
- d Lithological layering S. 295 points. Kanmantoo Group.
- e Geometry of redistribution of  $B_1$  lineations by  $B_3$  folds (Adelaide Supergroup).
- f Geometry of  $B_1$  lineations in Adelaide Supergroup rocks (clashed great circles). Mean  $S_3$  plane from 62a (dotted great circle). "a" in diagram is the Kinematic "a" axis.

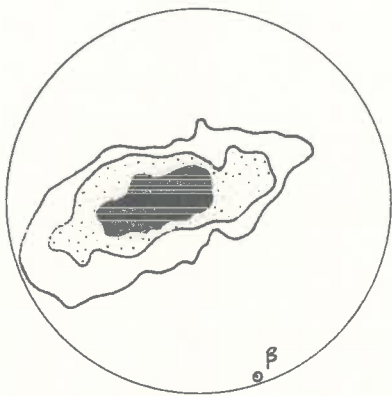
FIG. 62



a



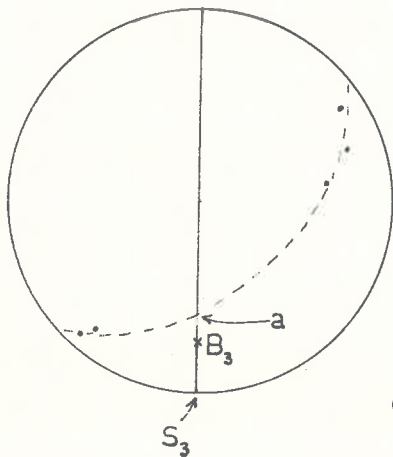
b



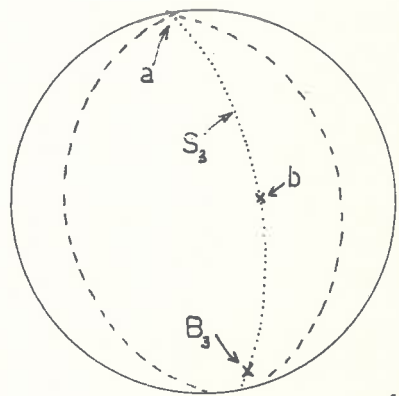
c



d



e



f

of the limbs (e.g. the east limb of the Barossa Range Syncline) occurs in some localities and in the southern part of the area, both limbs of the syncline dip east. Most subareas covering these structures are cylindrical about  $B_3$  (subareas C,D,G,I,H) but a slight departure from this axis is observable in subarea J. The geometry shows that both structures plunge at a low angle to the south, although in subarea C a north plunge is indicated. Locally, plunge reversals are common in the Barossa Range Syncline and have resulted in small basin and dome structures. Both structures show a characteristic of similar folding viz. thinning of the meta-sediments in the limbs and thickening in the hinges. However, small scale warping of the meta-sediments on the west limb of the Trial Hill Anticline about the  $B_3$  axis has resulted in an apparent thickening of this limb.

In the Kanmantoo Group rocks small, macroscopic, south plunging ( $13-20^\circ$ )  $B_3$  folds are located west and south-west of the keel of the Tanunda Creek Gneiss (Plate 3). They show sharp hinges and steeply dipping limbs (c.f. small  $B_3$  fold, Fig.61b) and their axial planes dip vertically or steeply east. A small synform in the north-west corner of the migmatite zone possibly represents a  $B_3$  structure. There are no macroscopic  $B_3$  folds elsewhere in the Kanmantoo Group rocks, but mesoscopic folds which show a considerable variation in plunge, are ubiquitous (Plate 3).

### Macroscopic Geometry.

The geometry of S is shown in Figs. 63 and 64. 10 subareas in the Adelaide Supergroup rocks and 6 in the Kanmantoo Group rocks have been delineated, each reasonably homogeneous with respect to a single axis. Collective diagrams of S for the whole area are given in Fig. 62c and d).

The collective diagrams of S are misleading as they convey an incorrect picture of the structure in both groups of rocks. For instance in the Adelaide Supergroup rocks, S appears to be mildly warped about an axis  $\beta$  plunging 5 in a direction  $160^\circ$  and in the Kanmantoo rocks S appears to be tightly folded about an axis  $\beta$  plunging  $25^\circ$  in a direction  $158^\circ$ . However the data from the subarea plots show that in the Kanmantoo Group rocks  $\beta$  is equivalent to  $B_1$  in subareas 3, 5 and 6 and  $B_3$  in 1 and 2<sup>1</sup>; in the rocks of the Adelaide Supergroup  $\beta = B_3$  in subareas B, C, D, E, G, H and I and in the other subareas  $\beta = B_2$  (F, J) or  $B_1$  (A).

### Discussion.

#### Origin of variation in $B_1$ axis orientations.

It has been shown that the  $B_1$  axes in the Adelaide Supergroup rocks are distributed along two girdles (Fig. 56a). The author considers that this variation is the result of the refolding of the  $B_1$  axes during the  $B_3$  deformation for the

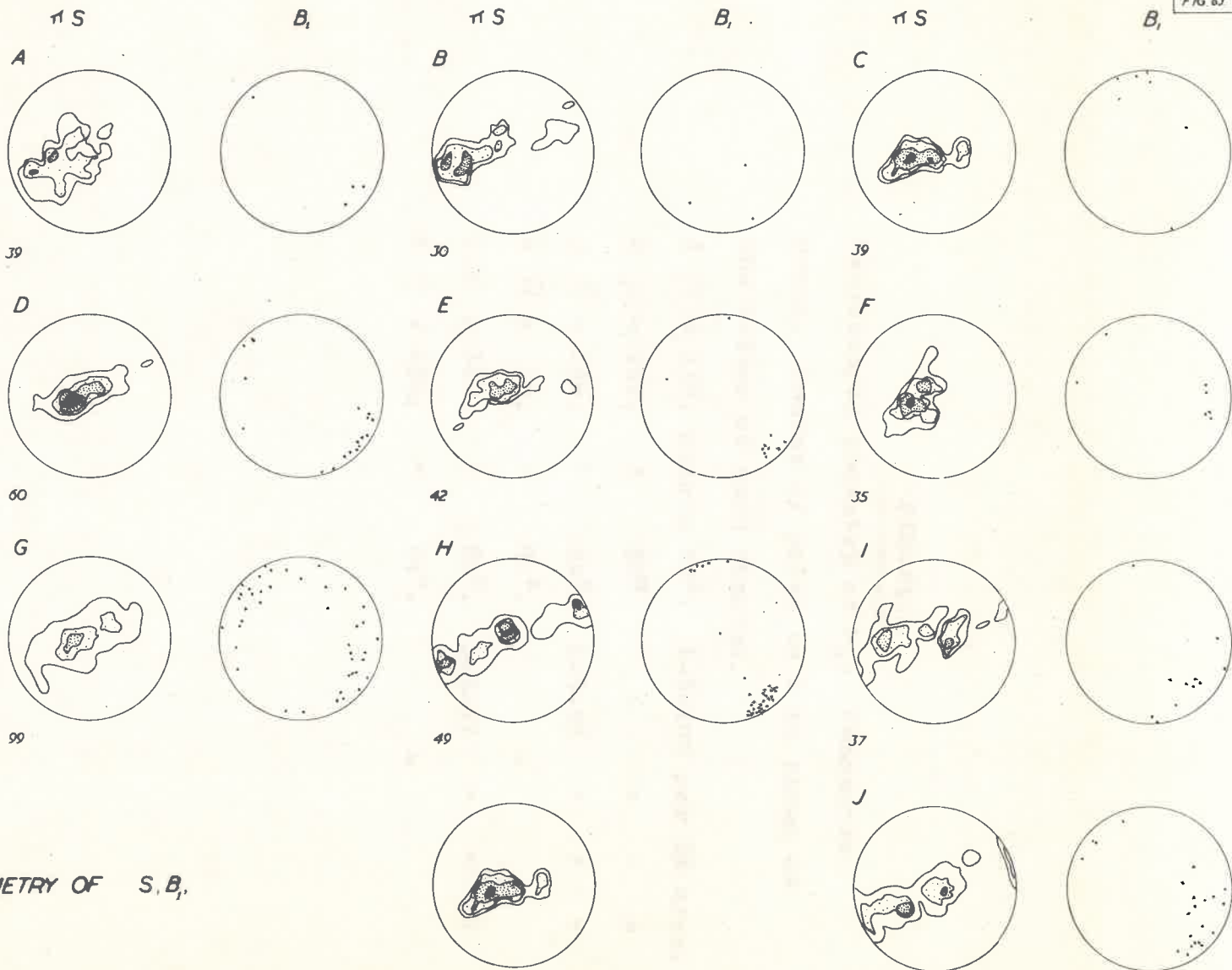
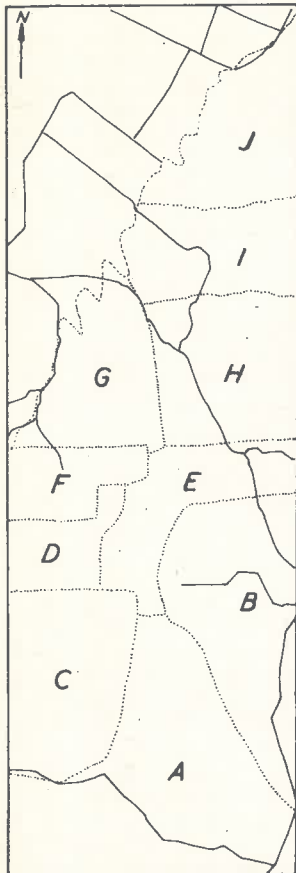
- 
1. The orientation in subarea 4 is not consistent with either  $B_1$  or  $B_3$ . It is possible that movement along the fault zone has disoriented the structures.



FIG. 63

Macroscopic geometry of S, Adelaide  
Supergroup.

A	$\beta = 146$ ,	plunge	0.
B	$\beta = 165$ ,	"	10.
C	$\beta = 350$ ,	"	6.
D	$\beta = 158$ ,	"	2.
E	$\beta = 161$ ,	"	10.
F	$\beta = 131$ ,	"	14.
G	$\beta = 158$ ,	"	16.
H	$\beta = 156$ ,	"	10.
I	$\beta = 172$	"	10.
J	$\beta = 154$	"	0.



MACROSCOPIC GEOMETRY OF S. B.

No of Poles to 11 S 39

Contours 1, 5, 10, ...%

FIG.64

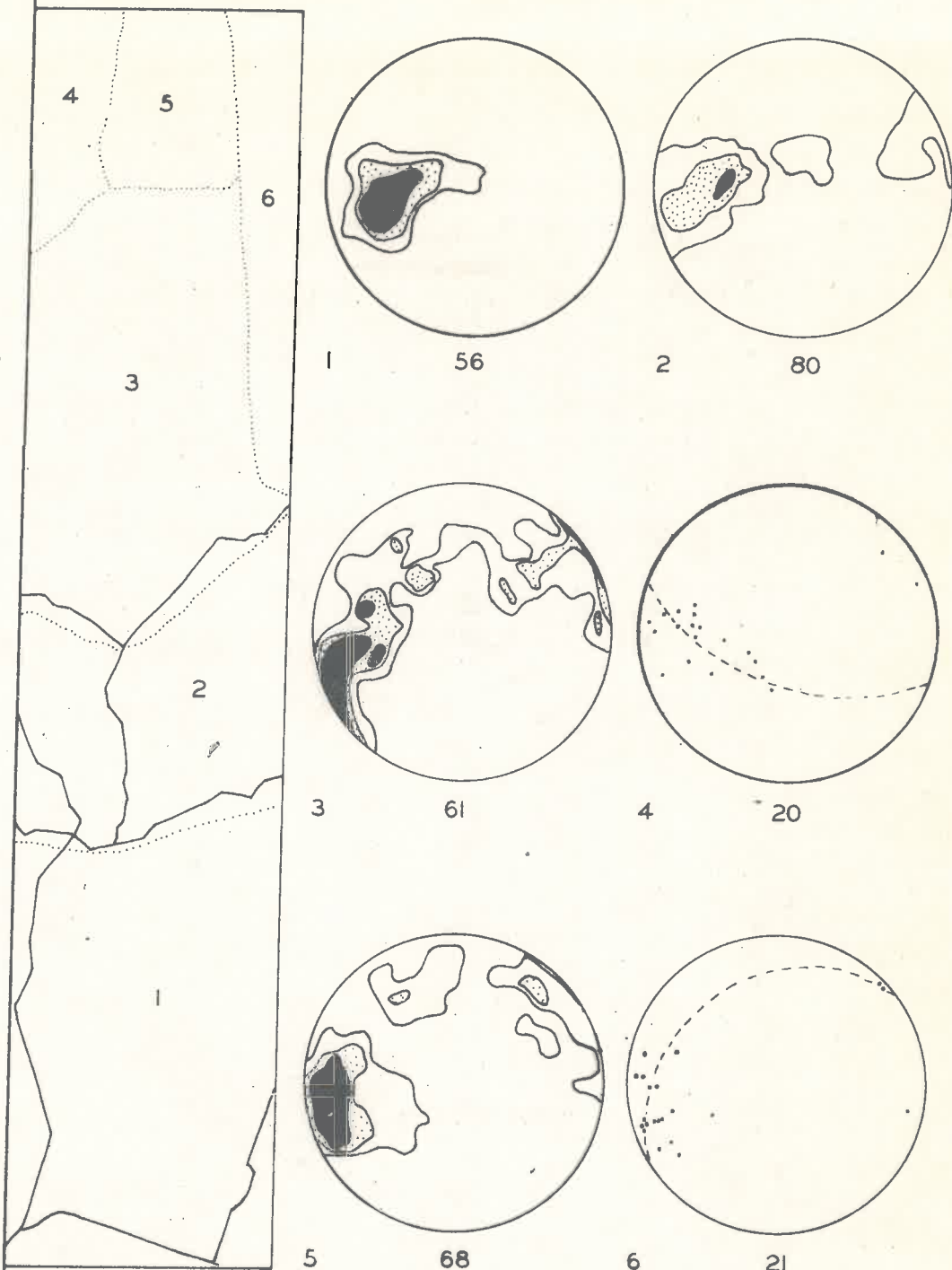
Macroscopic geometry of  $S_1$ . Kanmantoo

Group. Number of poles to S is given at  
the bottom of each diagram.

1	$\beta = 156$ ,	plunge $20^\circ$ .	1-5-10%	per 1%	area.
2	$\beta = 162$ ,	" $20^\circ$ .	"	"	" "
3	$\beta = 146$ ,	" $44^\circ$ .	1-3-5%	"	" "
4	$\beta = 16$ ,	" $30^\circ$ .	-		
5	$\beta = 148$ ,	" $60^\circ$ .	1-3-5%	"	" "
6	$\beta = 138$ ,	" $64^\circ$ .	-		

FIG. 64.

# MACROSCOPIC GEOMETRY OF S



0 2 MILES

0 4 KMS

following reasons :

- (1)  $B_1$  lineations are markedly different in orientation on the east and west limbs of the major  $B_3$  structures (Plate 3).
- (2) In individual small  $B_3$  folds,  $B_1$  is redistributed so that it lies in a single plane (Fig.62e).

According to Weiss (1959b) and Ramsay (1960) the intersection of the plane containing the refolded axes ( $B_1$ ) and the axial plane of the subsequent deformation ( $B_3$ ) is equivalent to the "a" kinematic axis. In the Adelaide Supergroup rocks this line plunges  $2^\circ$  in a direction  $350^\circ$  (Fig.62f).

The present distribution of the  $B_1$  axes in the Kaamantoo Group rocks may in part be due to affect of the  $B_3$  deformation as small  $B_3$  folds over print  $B_1$  folds in some localities, and to local strain inhomogeneities. Such inhomogeneities might be expected in migmatite terrains where rocks tend to deform by plastic flow (Ramsay, 1958)

#### Origin of variation in the $B_3$ axis orientation.

Most  $B_3$  axes in the Adelaide Supergroup rocks have shallow plunges north or south and a mean trend of  $347^\circ$  (Fig.62a). However, many are dispersed in a plane which strikes  $344^\circ$  and dips  $54^\circ$  east. It is most likely that this variation in the  $B_3$  orientation is due to :

- (1) The superposition of  $B_3$  folds on the earlier structures.
- (2) The fanning of the  $S_3$  planes (c.f. Weiss and McIntyre, 1957; Hobbs, 1965).

The explanations given for the  $B_3$  variation probably hold true for the Kanmantoo Group rocks. However, local strain inhomogeneities and the passive rotation<sup>of</sup> detached fold hinges (Voll, 1960) may also have been contributing factors. The latter mechanism is a major cause of the variation in fold axis orientation in the calc-silicate rocks.

## CHRONOLOGICAL ANALYSIS OF CRYSTALLIZATION AND DEFORMATION IN THE ADELAIDE SUPERGROUP AND KANMANTOO GROUP ROCKS.

### Introduction.

The relationship between deformation and crystallization in metamorphic rocks has been the subject of many papers in the last few years (Zwart, 1960, 1963; Chatterjee, 1961; Spry, 1963b and c; Johnson, 1962, 1963). Studies such as these have shown that their metamorphic history may be complex and that temperature fluctuations have occurred during metamorphism. Furthermore, these investigations have indicated that the metamorphic history may differ slightly from area to area in the one metamorphic terrain.

The purpose of this section is to summarise the essential data relating to crystallization and deformation in the Kanmantoo Group and Adelaide Supergroup rocks. The techniques used in this analysis are similar to those documented by Zwart, (1960) and Spry (1963b).

### Crystal Growth pre-tectonic to $B_1$ .

Evidence for crystallization before the first deformation

is scarce. One such example (A200-124A) contains poikiloblasts of potash feldspar which shows randomly oriented inclusions of biotite and quartz, both in sections parallel and perpendicular to  $B_1$ . In addition the inclusions within the poikiloblasts are smaller in grain size than the surrounding matrix and the foliation ( $S_1$ ) curves around the poikiloblasts. These observations suggest that the poikiloblasts grew prior to the first deformation.

Crystal growth syntectonic to  $B_1$ .

Crystal growth during this phase is indicated by the occurrence of rotated garnets, and by the growth of biotite and muscovite parallel to  $S_1$  and sillimanite to  $B_1$ . In the calc-silicate rocks of the Kanmantoo Group, hornblende prisms oriented parallel to  $B_1$  are present. Migmatisation commenced in this period resulting in the formation of quartz-feldspar veins parallel to the axial planes of  $B_1$  folds.

Crystal growth post tectonic to  $B_1$ .

A phase of static metamorphism followed the  $B_1$  deformation. In the Adelaide Supergroup rocks, this is an important period of crystallization as post tectonic, idioblastic crystals of actinolite, diopside, tourmaline, muscovite and sillimanite are abundant. Idioblastic,

inclusion free rims also grew around the "snowball" garnets (Fig.66). Static recrystallization has also been important in the Kanmantoo Group rocks. It appears to have continued over a considerable period of time as several stages of crystal growth can be recognised. Andalusite first crystallized in the pelitic rocks as skeletal, post tectonic porphyroblasts. A subsequent rise in temperature instigated the crystallization of sillimanite, and andalusite disappeared from most rocks. Later, muscovite and garnet grew, both engulfing and digesting the earlier formed matrix (Fig.65). In some rocks, a final phase of recrystallization took place, with the resultant formation of sillimanite and potash feldspar from muscovite.

#### Crystal growth syntectonic to B<sub>2</sub>.

Although the B<sub>2</sub> deformation is not recognised in the Kanmantoo Group rocks, it is recorded in many of the Adelaide Supergroup rocks. During this phase S<sub>1</sub> was transposed partially or completely into a new foliation (crenulation cleavage S<sub>2</sub>) and pre B<sub>2</sub> sillimanite and garnet underwent rigid body rotation. Presumably the micas oriented parallel to S<sub>2</sub>, underwent recrystallization during this phase.

#### Crystal growth post tectonic to B<sub>2</sub>.

During this phase extensive mimetic crystallization transformed the garnet and muscovite schists deformed by



FIG.65.

Photomicrograph of large muscovite porphyroblast engulfing biotite-quartz matrix. Note needles of sillimanite within porphyroblast. Location 980 266. Spec. No.A200-823A. X 100.

FIG.66.

Photomicrograph of garnet showing syntectonic core with S shaped inclusions and thin post tectonic rim Location 982 276. Spec. No.A200-251.

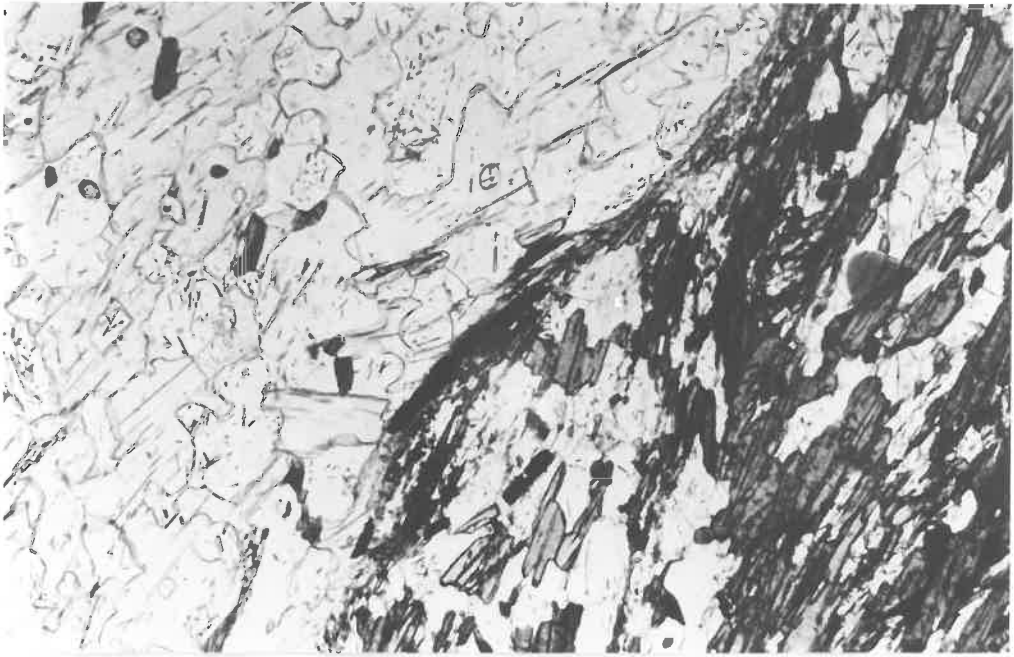


FIG. 65.

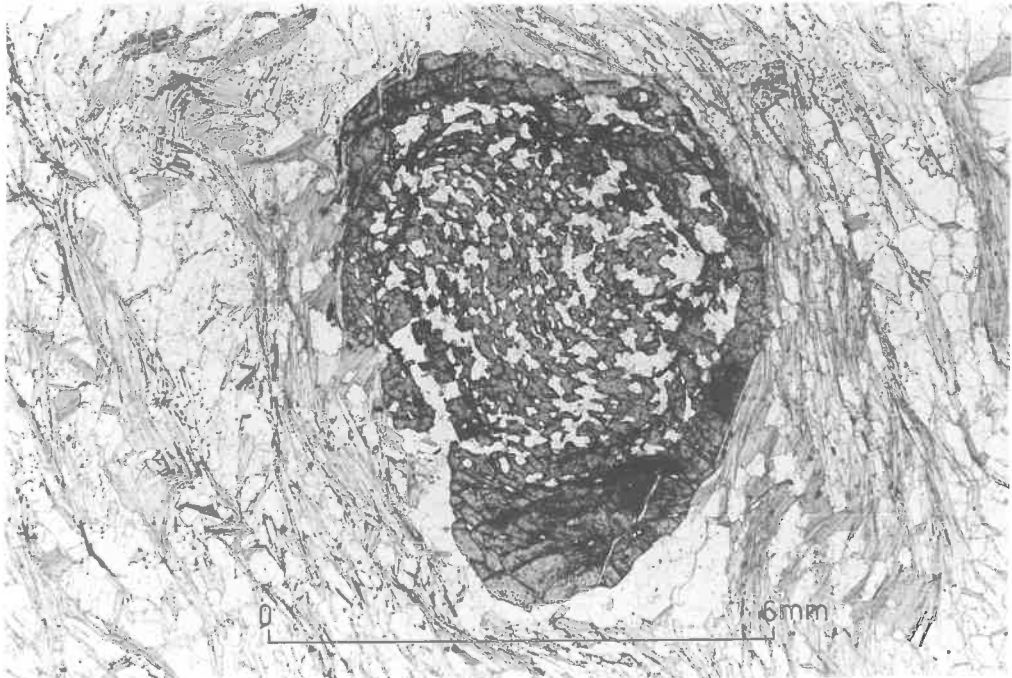


FIG. 66.

$B_2$  movements into gneisses (c.f. Post  $F_1$  phase in the Meine Rocks, Johnson, 1963, p.129). In the post mimetic stage, tourmaline and more rarely fibrolite crystallized within or athwart  $S_2$ .

Crystal growth syntectonic to  $B_3$ .

Crystallization continued during the final phase of folding, resulting in the growth of biotite and muscovite parallel to  $S_3$  or  $B_3$  in the quartzo-feldspathic schists of the Kannantoo Group. Post  $B_1$  muscovite porphyroblasts were crinkled during this phase. A second generation of quartz-feldspar veins formed parallel to  $S_3$  in the migmatites and veins formed during the first deformation were folded.

A second crenulation cleavage ( $S_3$ ) developed in the schists of the Adelaide Supergroup. Refolding of  $S_1$  and  $S_2$  and rigid body rotation of the "snowball" garnets took place.

Crystal growth post tectonic to  $B_3$ .

In the eastern part of the area, that is, in the Kannantoo Group rocks metamorphism remained at its peak. Diopside aggregates and biotite grew mimetically on  $B_3$  folds. Quartz-feldspar pods and veins discordant to  $S_1$ , and  $S_3$  or  $S_2$  <sup>in</sup> joint planes, developed in the migmatite zone. Veins formed or folded prior to this phase were recrystallized.

Post tectonic crystallization however, has not always followed the  $B_3$  deformation in the Adelaide Supergroup rocks, as mechanical deformation of crystals that grew in the earlier phases, is quite common. There are nevertheless, many specimens which are completely strain free and post kinematic growth of tourmaline has occurred in most rocks.

### Conclusion.

Crystallization in the metamorphic rocks of the Pewsey Vale area commenced before the first deformation. The main episodes of crystallization in the Kanmantoo Group rocks took place during and after the first and second deformations. In the Adelaide Supergroup rocks the main phase of crystallization commenced during the first deformation and continued until after the second deformation. During and subsequent to the third phase of folding the intensity of crystallization waned.

### PETROFABRICS.

#### Introduction.

The preferred orientation of quartz, scapolite<sup>1</sup> and biotite in rocks from the Adelaide Supergroup and Kanmantoo Group has been studied. The significance of the patterns is discussed and the diagrams are compared with those obtained by other authors from rocks elsewhere in the Mt. Lofty Ranges.

---

1 See Appendix 4 for scapolite petrofabrics.

## Quartz Petrofabrics.

### Adelaide Supergroup Quartzites.

The preferred orientation of the [0001] axes of quartz in 8 specimens<sup>1</sup> of quartzite is shown in Fig. 67. All sections examined were cut approximately perpendicular to  $B_1$  (where present) or to bedding  $S$ . Measurement of sections parallel to  $B_1$  in three specimens (114, 126-4, 721) indicated that the fabric was homogeneous. Where possible 200 or more grains were recorded from each specimen.<sup>2</sup> Planes of symmetry  $M_1, M_2$  and  $M_3$  were drawn on all diagrams.

The characteristics of the patterns may be summarised as follows:

- (1) All samples show partial or complete cross girdles. (OK1 girdles).
- (2) A partial peripheral girdle is developed in specimen A200-222.
- (3) The symmetry axis  $m_1 - m_2$  is never coincident with  $B_1$ .
- (4) The preferred orientation is independent of  $S$ .
- (5) If  $S$  is disregarded, most diagrams apart from A200-114 and A200-222 show near orthorhombic symmetry (c.f. with the monoclinic symmetry shown on a meso and macro scale).
- (6) The patterns obtained from non-lineated and lineated specimens are the same.

- 
1. For a general description of the Adelaide Supergroup quartzites see Chapter 8 and for descriptions of individual quartzites see Appendix 5.
  2. The extreme coarse grain size in 299 and 721 prevented the measurement of the required number of grains.

FIG.67.

Quartz data for the Adelaide Supergroup quartzites. Specimen numbers are placed at the top left hand corner and the number of  $[0001]$  axes of quartz measured at the top of each diagram.

Spec. Nos.A200-222, 289A, 326, 329, A126-4:  
1-2-3-4 p.c. per 1 p.c. area.

Spec. No.A200-721: 1-3-5-7 p.c. per  
1 p.c. area.

Spec. Nos.A200-299, 114: 1-2-3-5 p.c. per  
1 p.c. area.

Location co-ordinates are given in Appendix 4.

# QUARTZ PETROFABRIC DIAGRAMS.

A.S. QUARTZITES.

*m*.....symmetry plane

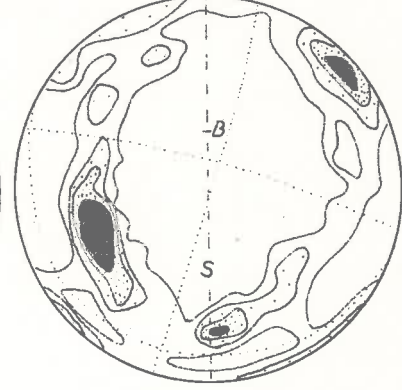
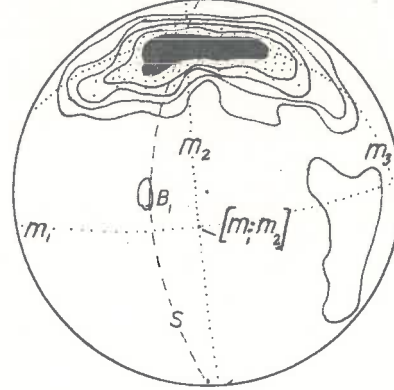
Q - Quartz

114

201Q

1264

2600



222

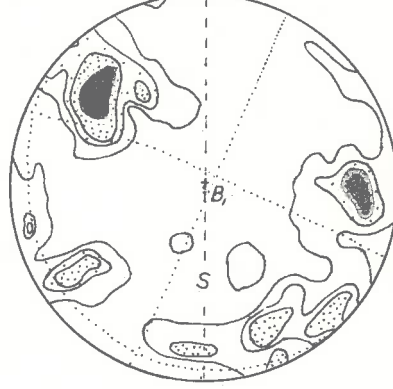
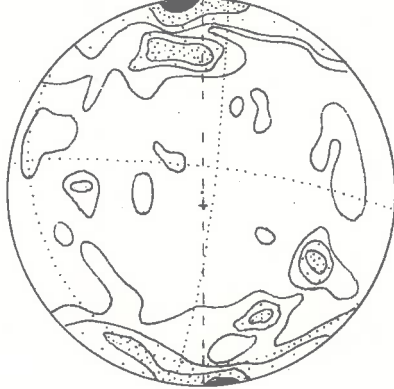
225Q

326

258Q

329

254Q



299

145Q

721

123Q

289

257Q

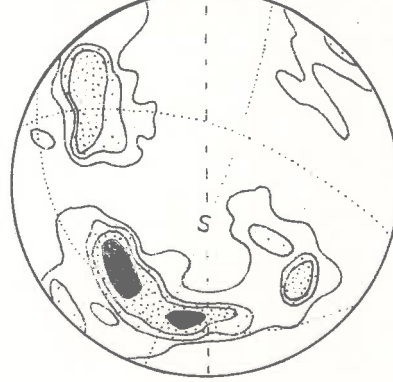
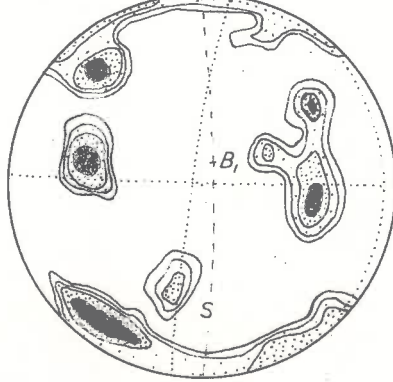


TABLE 27.

<u>Spec. No.</u>	$n_1 - n_2 \wedge B1$	$S \wedge n_2$
114	22°	22°
721	43°	29°
326	9°	23°
222	14°	10°
A126-4	11°	16°
299	14°	11°
329	43°	23°
289	-	22°



The preferred orientation shown by these specimens is similar to that obtained by Kleeman (1954) who studied the fabric of the Adelaide Supergroup quartzites from different regions in the Mt. Lofty Ranges. Talbot (1962) however, found no preferred orientation in quartzites of the Mt. Bera region. This lack of preferred orientation is possibly due to the fact that deformation has not been as penetrative in the Mt. Bera region as in other parts of the Mt. Lofty Ranges.

#### Axial Distribution Analysis (A.V.A.)

In order to study the quartz fabric in more detail and to determine the significance, if any, of the [OK1] girdles, A.V.A. (Ramsauer, 1941; Sander, 1950) diagrams were prepared from specimen Al26-4<sup>1</sup>. The procedure adopted for the analysis is similar to that outlined by Weiss (1954). Fig. 69 shows partial diagrams of the distribution of [0001] axes for four subareas and Figs. 70A and 71A are photographs of sections perpendicular and parallel to  $B_1$ . Figs. 69e, f, 70B and 71B are the orientation symbols and orientation diagrams for the two sections.

Examination of the subarea diagrams (Fig. 69) shows that although the fabric overall is quite homogeneous, the maxima in each subarea diagram are at different positions. The orientation diagrams indicate that the grains are not spatially related to S-planes, but occur in domains. Such a fabric has "direction homogeneity", (Ramsauer, 1941). Weiss (1954) obtained similar A.V.A. results from quartzites

FIG. 69

e Key to orientation symbols in Fig. 71B. 242[0001]axes.  
f " " " " " " 70B. 504 " .  
a b c d Partial diagrams for [0001] axes  
measured in section perpendicular to  $B_1$ .

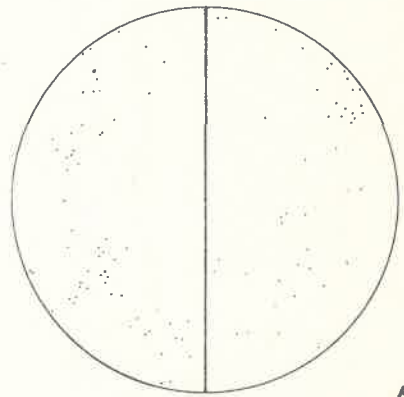
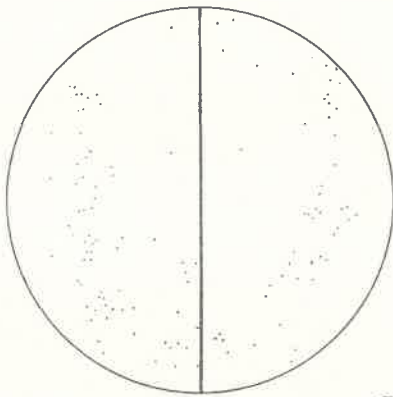
*Parallel to B*

*Perpendicular to B*



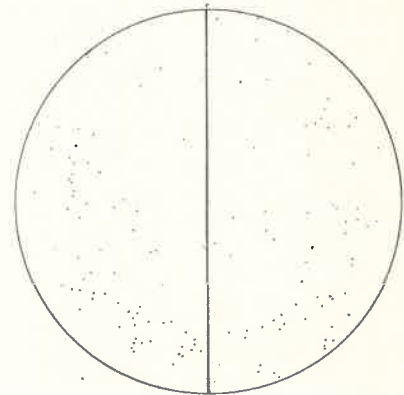
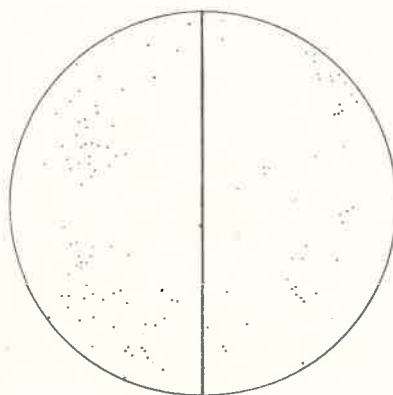
*e*  
*Partial diagrams.*

*f*



*a*

*b*



*c*

*d* R.O. '65.

**FIG. 70A**

**Photo micrograph of A126-4. X16**

**Section perpendicular to  $R_1$ .**

**FIG. 70B**

**A.V.A. trace of  $\Delta$  (Key in Fig. 69).**

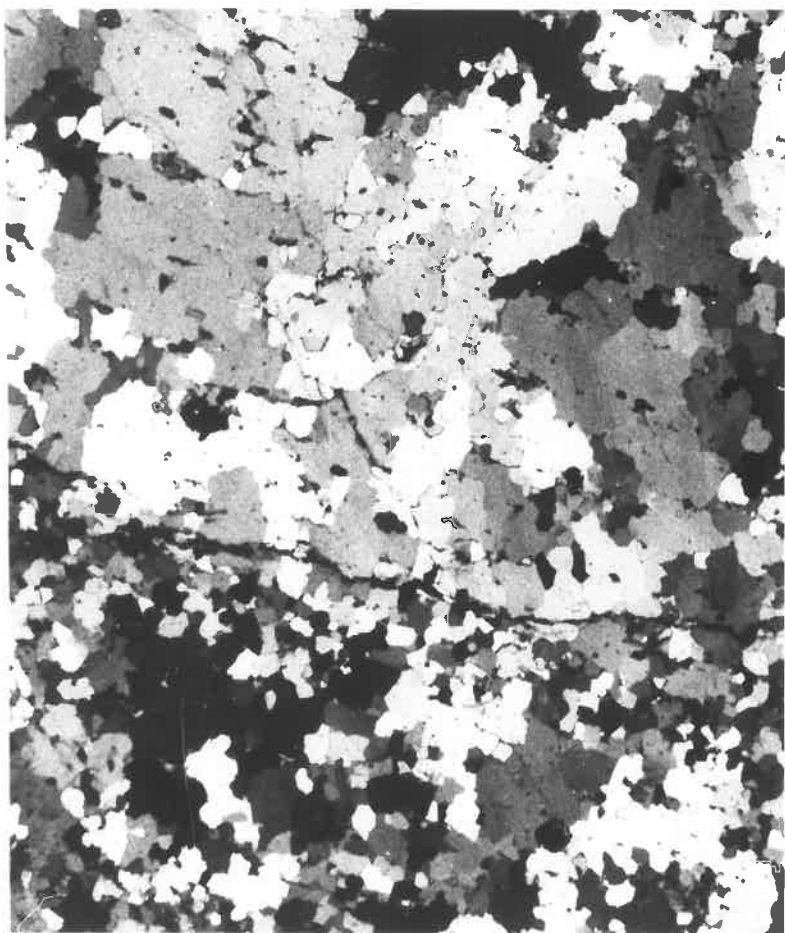


FIG.70A.

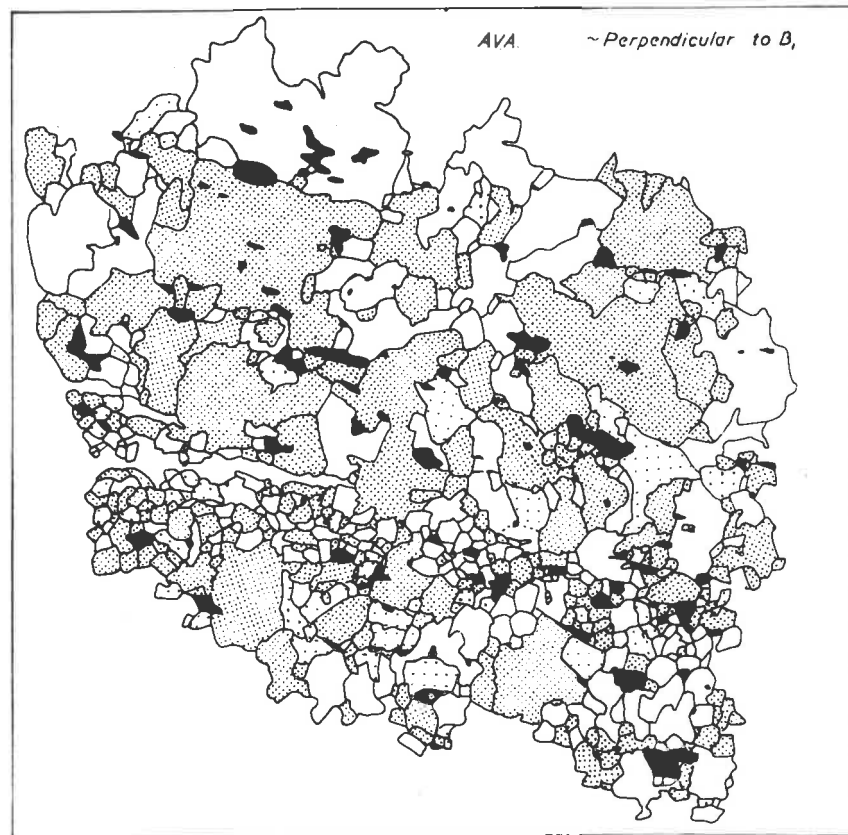


FIG.70B.

FIG.71A

Photomicrograph of A126-4. X22

Section parallel to B<sub>1</sub>.

FIG.71B

A.V.A. trace of A (Key fig.69)

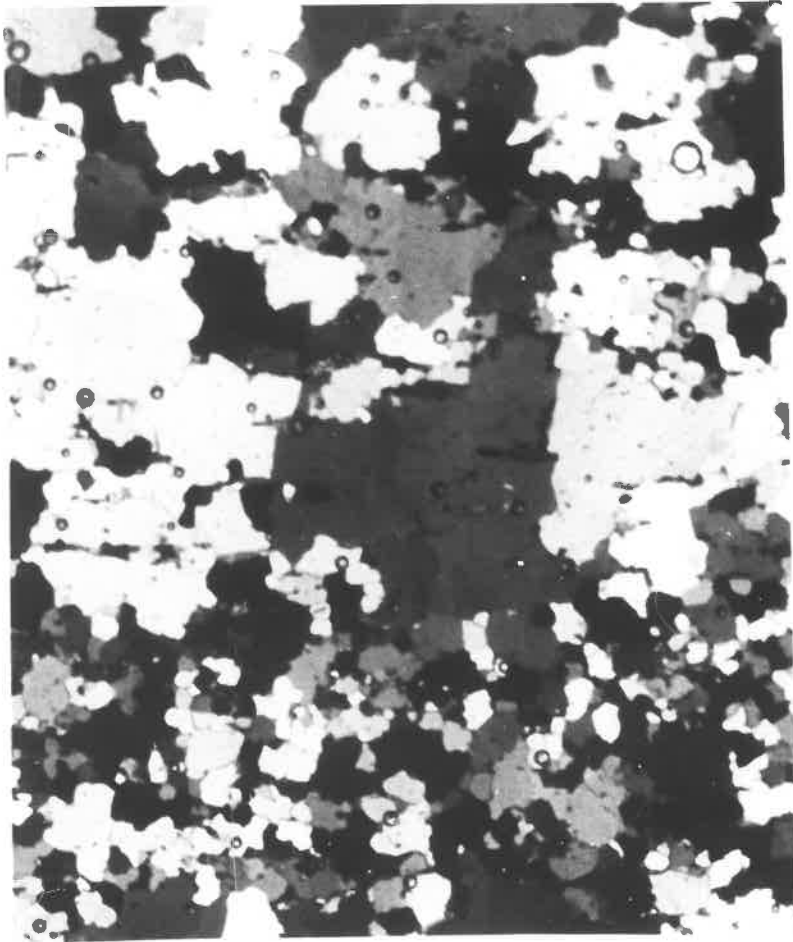


FIG.7IA

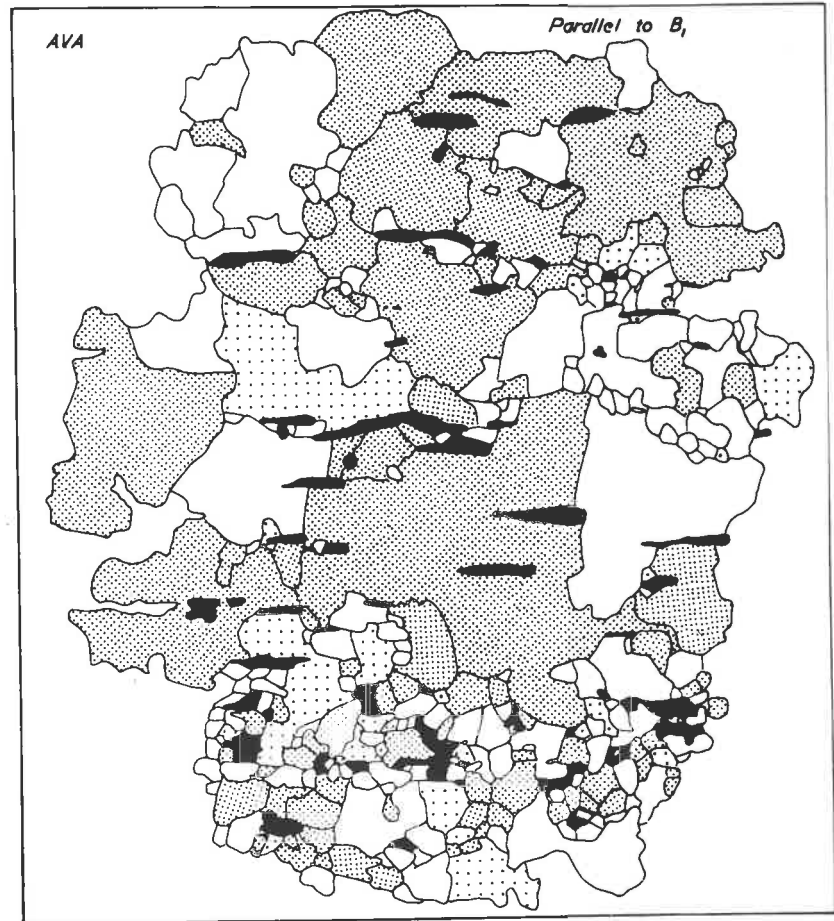


FIG.7IB

exhibiting cross-girdle patterns.

Homogeneity of the quartz fabrics for the whole area.

To test the degree of homogeneity in the quartz fabric throughout the whole area, the  $m_1 - m_2$ ,  $m_1 - m_3$ , and  $m_2 - m_3$  intersections and the main maxima from each diagram have been geographically re-oriented (Fig.68). It can be seen that the maxima and the symmetry plane intersections have no real homogeneity (c.f. Christie, 1963, p.402). The  $B_1$  axis and  $m_1 - m_2$  intersection of each specimen are plotted in Fig.68; this diagram shows that both axes are distributed along a girdle.

Discussion.

Three important features arise from this investigation. Firstly,  $B_1$  is not coincident with  $m_1 - m_2$  intersections. Secondly, the patterns obtained from the non-lined and lined specimens are the same, and thirdly, the quartz fabric elements are distributed approximately in the same great circle as  $B_1$  (Fig.68). The first two observations suggest to the author that the quartz fabric was imprinted after the macroscopic fabric had been formed and that the preferred orientation developed during a phase of penetrative movement by recrystallization in a stress medium (c.f. Christie 1963). The third feature suggests that the quartz fabric elements were rotated during the  $B_3$  deformation (see p.113 for the discussion on the distribution of  $B_1$  axes), but were not recrystallized during this phase.



GEOGRAPHICAL DISTRIBUTION OF SYMMETRY PLANES  $B_1$ ,  
 LINEATIONS AND MAXIMA FROM QUARTZ PETROFABRIC  
 DIAGRAMS.

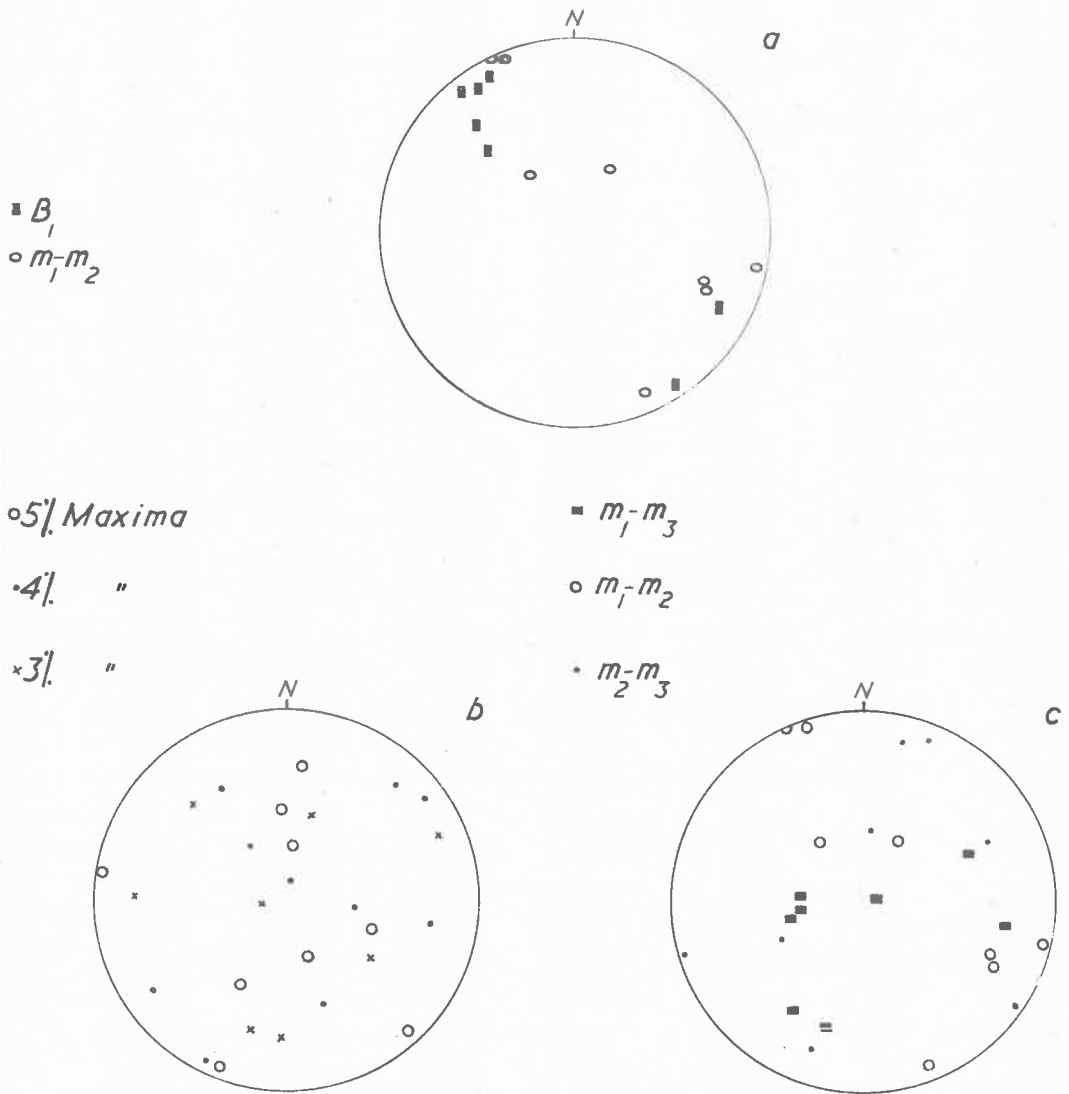


FIG. 68.

### Kanmantoo Group.

The  $[0001]$  orientation of quartz and  $[001]$  of biotite in several quartzo-feldspathic schists have been determined (Fig. 72).

#### Biotite.

The main features in the biotite diagrams are:

- (1) In most diagrams there is a single, strong maximum (A200-425, 29, 584); in others a partial (A200-27, 29) or complete girdle about the lineation ( $B_1$  in A200-422,  $B_3$  in A200-29).
- (2) The biotites may be oriented parallel to S (A200-584, 425),  $S_1$  (A200-422, 27) or  $S_3$  (A200-29).

The biotite fabrics thus give microscopic evidence of the formation of two deformational S planes ( $S_1$  and  $S_3$ ) and lineations  $B_1$  and  $B_3$ .

#### Quartz.

The features present in the quartz orientation diagrams are:

- (1) Some specimens show partial peripheral girdles (584<sup>1</sup>, 422, 27) and others cleft girdles 425, 29, 48; c.f. Adelaide Supergroup quartzites. The girdle axes are coincident with the lineation.
- (2) Some specimens show a strong preferred orientation (e.g. 584, 422).
- (3) All diagrams show monoclinic symmetry (if the preferred orientation of biotite is ignored).

---

1. A central maximum of quartz  $[1010]$  axes in 584 has also been recognised in X-ray texture goniometer patterns (Analysis kindly performed by Mr. P. Williams, Univ. Sydney).

FIG.72

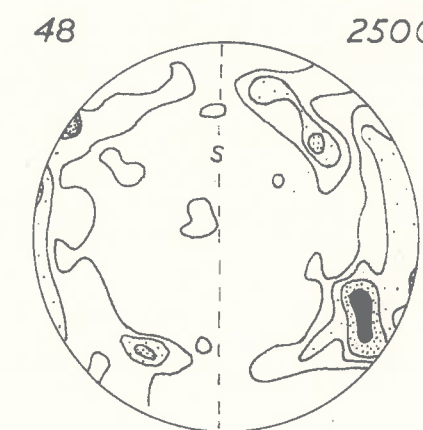
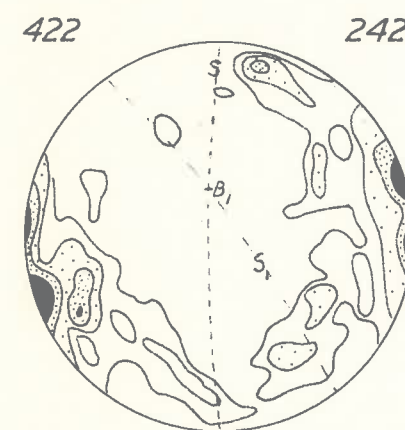
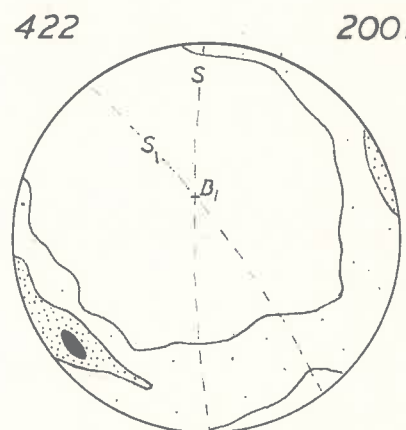
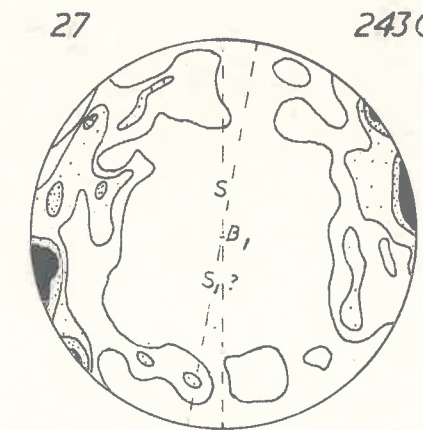
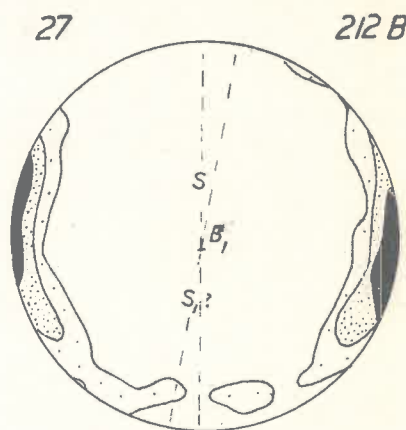
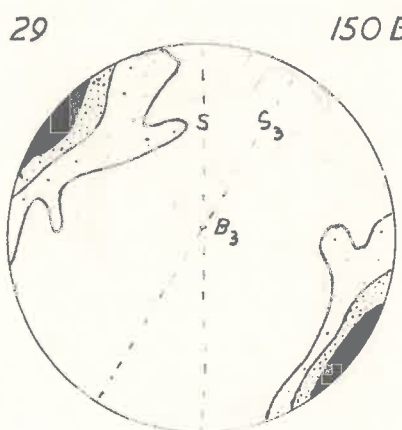
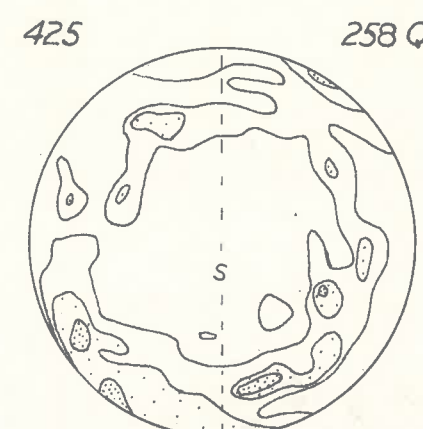
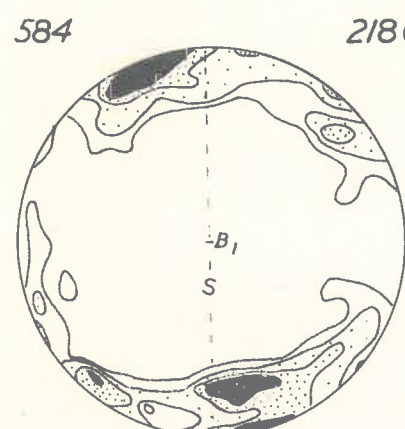
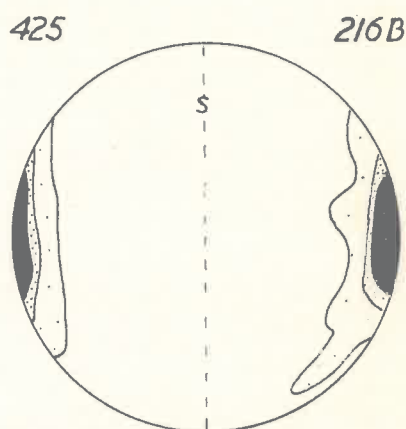
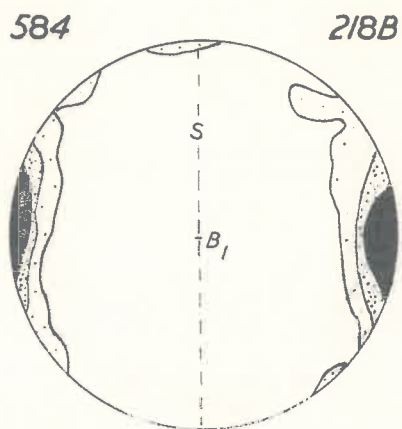
Quartz and biotite data for Kanmantoo Group rocks. The specimen numbers are given at the top left hand corner and the number of  $[0001]$  axes of quartz (Q) and  $[001]$  axes of biotite (B) at the top right hand corner.

A200-584	Location	997	237
" 425	"	977	258
" 29	"	984	178
" 27	"	978	184
" 422	"	976	260
" 48	"	977	174

PETROFABRIC DIAGRAMS

BIOTITE

QUARTZ



CONTOURS 1,5,9, per 1/area

CONTOURS 1,2,3,4, per 1/area

Discussion.

Quartz petrofabric studies by Kleeman (1954) and Mills (1964) and Hobbs and Talbot (in press) have shown that there is no significant orientation in the Kambantoo Group rocks in the eastern Mt. Lofty Ranges. However, Chinner (1955) has obtained diagrams from the Tanunda Creek Gneiss and the quartzites north of Mt. Kitchener which are similar to those of specimens A200-584 and 422 (i.e. they show partial peripheral girdles and a strong preferred orientation).

The possible reasons for the development of a strong quartz fabric in the Pawsey Vale region and the adjacent Tanunda Hills (Chinner, op.cit.) are :

- (1) The rocks contain less impurities (e.g. mica, feldspar) which might inhibit quartz orientation (Weiss, 1959a)
- (2) This region has been subjected to stronger penetrative movements.

The first explanation is less likely as the rocks examined by Mills (op.cit.) and Kleeman (op.cit.) are mineralogically similar to those in the Pawsey Vale region. Evidence for the second explanation is suggested by the megascopic and microscopic features in the specimens showing the strongest preferred orientation viz. a lineation defined by elongate augen of quartz and feldspar or a quartz ribbing in hand specimen, and elongate quartz parallel to the foliation in sections perpendicular to the lineation in thin section.

The rocks appear on this evidence to have been intensely deformed (i.e. the movements consisted mainly of axial flow of the rock mass parallel to the lineation -Weiss et al, 1955).

### FAULTING.

Two major north-south trending faults occur within the Pewsey Vale area, one separating the Adelaide Supergroup rocks from those of the Kanmantoo Group, the other dissecting the rocks on the eastern side of Mt. Kitchener (Plate 3). The former is the northward extension of the Nairne Fault (Sprigg and Campana, 1951) and the latter is considered by Thomson (pers. comm.) to be the Bremer Fault (White, 1956). A third smaller fault occurs on the western side of Mt. Kitchener. Lineaments (approximately east-west) on the aerial photographs suggest that there are other small faults in the area.

#### The Nairne Fault.

The contact of the Nairne Fault is never exposed, but in some areas the position of the fault can be located to within 50 to 100 feet. Breccia has been observed at only one locality (965254). Brecciated albitite cemented with specular hematite has been noted at location 974264, but this is some distance from the fault zone.

A wide variety of rock types are developed within or adjacent to the fault zone in the northern part of the area; these include pyrite bearing albitites, coarse talc and quartz albitites, "syenites", calcite and tremolite rock, dolerite and a small talc body. Within this talc

body there are numerous fragments of siderite-talc rock, calcite-talc rock and albitite.

In thin section the albitites are mineralogically similar to those outcropping elsewhere in the area (Chapter 10) but are commonly more highly deformed. Albite shows kink bands, fractures and displaced twin lamellae, and quartz strong domain extinction and ubiquitous healed fractures. Small unstrained mosaics of quartz, albite and, more rarely, chlorite "heal" fractures in the deformed albite in some specimens. However, not all albitites in the fault zone are deformed, suggesting that faulting ceased prior to the last phase of albitization.

#### Faults in the Kammantoo Group Rocks.

On the eastern and western sides of Mt. Kitchener, sporadic outcrops of coarse calc-silicate rock often with angular fragments of quartzite, delineate the faults in the Kammantoo Group rocks. These calc-silicate rocks have an essentially linear strike in areas of strong relief, suggesting that the attitude of the faults is approximately vertical. Albitites and less commonly small plugs of dolerite are associated with these rocks. The small fault on the western side of Mt. Kitchener can be traced for more than 1 mile before disappearing into albitite at location 974272. The fault on the eastern

side of Mt. Kitchener (The Bremer Fault) can be traced for a distance of 4 miles before meeting a large albitite body just north of the keel of the Tanunda Creek Gneiss. There is no field evidence for the existence of this fault further south. Mapping by Antmanis (pers. comm.) on the adjacent Cambrai Sheet and by the author, suggests that this fault represents the sheared off limb of the anticline in the Mt. Kitchener region and that it is a high angle thrust fault with the down-throw side to the west.

In this section the fault zone calc-silicate rocks show a wide variety of textures and are extremely variable in grain size. They contain minerals of the same grade as the adjacent calc-silicate rocks viz. diopside, actinolite, scapolite and sphene, suggesting that faulting took place either prior to or during metamorphism. Many of the rocks have been deformed by a subsequent phase of faulting resulting in the straining and replacement of large scapolite crystals by small zoned polygonal aggregates of scapolite, and the development of deformation lamellae in diopside (e.g. A200-842). Soda metasomatism appears to have occurred after this faulting as unstrained albite is ubiquitous in many specimens. However, in some specimens the albite is strained suggesting that a further, and probably final, phase of faulting took place.



Thus, the evidence in the rocks of the fault zones suggest that faulting occurred periodically over a considerable period of time and that metasomatism was active during these movements.

BIBLIOGRAPHY

## BIBLIOGRAPHY

- Agrell, B.A., 1939. The adinoles of Dinas Head, Cornwall.  
Mineralog.Mag. 25 : 305-337.
- Albee, A.L., 1965. Phase equilibria in three assemblages of  
Kyanite-zone pelitic schists, Lincoln Mountain  
Quadrangle, Central Vermont.  
J. Petrology 6 : 246-301.
- Alderman, A.R., 1942. Sillimanite, kyanite, and clay deposits  
near Williamstown, South Australia.  
Trans. R. Soc. S.Aust. 66 : 3-14.
- Ayanov, V.M., 1964. Petrographic and structural aspects of  
the North Caucasus Amphibole Asbestos in the Khatsavit  
Deposit.  
Int. Geol. Rev. 6 : 867-874.
- Banno, S. and Kanehira, K., 1961. Sulfide and oxide minerals  
in schists of the Sanbagawa and Central Abukuma  
Metamorphic Terranes.  
Jap. J. Geol. Geogr. 32 : 331-348.
- Becke, F., 1906. Zur Physiography der Gemengteile der  
Krystallinen Schiefer.  
Denkschr. Akad. Wiss., Wein, Math-nat.Kl. 25 : 97-152.
- Bell, P.M., 1963. Aluminum silicate system : Experimental  
determination of the triple point.  
Science, N.Y. 139 : 1055-1056.

Best, M.G., 1963. Petrology and structural analysis of metamorphic rocks in the southwestern Sierra Nevada Foothills, California.

Univ. Calif. Publs. geol. Sci. 42 : 111-158.

\_\_\_\_\_ and Weiss, L.E., 1964. Mineralogical relations in some pelitic hornfels from the Sierra Nevada, California.

Am. Miner. 49 : 1240-1266.

Bowes, D. R., 1954. The metamorphic and igneous history of Rosetta Head, South Australia.

Trans. R. Soc. S. Aust. 77 : 182-214.

Brown, W.L., 1965. Crystallographic aspects of feldspars in metamorphism.

Pitcher, W.S. and G.W. Flinn, Controls of Metamorphism.

Oliver and Boyd, Edinburg and London.

Browne, W.R., 1920. The igneous rocks of Encounter Bay, South Australia.

Trans. R. Soc. S. Aust. 44 : 1-57.

Buddington, R.F., 1959. Granite emplacement with special reference to North America.

Bull. geol. Soc. Am. 70 : 671-747.

\_\_\_\_\_, 1963. Isograds and the role of H<sub>2</sub>O in metamorphic facies of orthogneisses of the Northwest Adirondack, New York.

Bull. geol. Soc. Am. 74 : 1155-1182.

\_\_\_\_\_ and Lindsley, D.H., 1964. Iron-titanium oxide minerals and synthetic equivalents.

J. Petrology. 5 : 310-357.

- Burgers, W.G., 1963. The art and science of growing crystals.  
in J.J. Gilman, Wiley.
- Burley, B.J., Freeman, E.B. and D.M. Shaw, 1961. Studies on  
Scapolite.  
Can. Mineralogist. 6 : 670-679.
- Campana, B., 1953. Geol. Atlas of S. Australia, Gawler Sheet;  
Geological Survey S. Aust.  
\_\_\_\_\_, 1955. The geology of the Gawler Military Sheet.  
Rep. Invest. geol. Surv. S. Aust. 4.
- \_\_\_\_\_, and Horwitz, R., 1955. The Kannantoo Group of  
South Australia considered as a transgressive sequence.  
Aust. J. Sci. 18 : 128-129.
- Carman, J. H. and Tuttle, O.F., 1963. Experimental study  
bearing on the origin of myrmekite.  
Abstr. geol. Soc. Am. 29.
- Carter, N.L., Christie, J.M. and D.T. Griggs, 1964. Experimental  
deformation and recrystallization of quartz.  
J. Geol. 72 : 687-733.
- Chadwick, R.A., 1958. Mechanisms of pegmatite emplacement.  
Bull. geol. Soc. Am. 69 : 803-836.
- Chapman, C.A., 1952. Structure and petrology of the surface  
quadrangle, New Hampshire.  
Bull. geol. Soc. Am. 63 : 381-425.
- Chatterjee, N.D., 1961. The alpine metamorphism in the Simplon-  
Area, Switzerland and Italy.  
Geol. Rdsch. 51 : 1-72.

- Cheng, Y.C., 1944. The migmatite area around Bettyhill, Sutherland.  
Q. Jl geol. Soc. Lond. 99 : 107-154.
- Chinner, G.A., 1955. The granite gneisses of the Barossa Ranges.  
Unpubl. M.Sc. Thesis, University of Adelaide.
- \_\_\_\_\_, 1960. Pelitic gneisses with varying ferrous/ferric ratios from Glen Cova, Angus, Scotland.  
J. Petrology 1 : 178-217.
- \_\_\_\_\_, 1961. The origin of sillimanite in Glen Cova, Angus.  
J. Petrology 2 : 312-323.
- Christie, J.M., 1963. The Meise thrust zone in the Assynt region, Northwest Scotland.  
Univ. Calif. Publ. geol. Sci. 40 : 345-440
- Clark, S.P. Jr., 1961. A redetermination of equilibrium relations between kyanite and sillimanite.  
Am. J. Sci. 259 : 641-650.
- \_\_\_\_\_, Robertson, E.C. and A.F. Birch, 1957.  
Experimental determination of kyanite-sillimanite equilibrium relations at high temperatures and pressure  
Am. J. Sci. 255 : 94-100.
- Clarke, E deC., 1938. Middle and West Australia.  
Regionale Geol. d. Erde. Band 1. Abs. 7.

Collins, C.B., Russell, R.D. and R.M. Farquhar, 1953.

The maximum age of the elements and the age of the earth's crust.

Can. J. Phys. 31 : 402-418.

Compston, W., Crawford, A.R. and V.M. Bofinger (in press).

A radiometric estimate of the duration of sedimentation in the Adelaide Geosyncline, South Australia.

J. geol. Soc. Aust. (?).

Daily, B., 1956. The Cambrian in South Australia. XX Congreso Geol. Internacional, Mexico, 1956.

El sistema Cámbrico en Paleogeografía y el problema de su base. 2 : 91-147.

\_\_\_\_\_, 1963. The fossiliferous Cambrian Succession on Fleurieu Peninsula, South Australia.

Rec. S.Aust. Mus. 14 : 579-601.

Dalgarno, C.R., 1961. The geology of the Barossa Valley.

Unpubl. M.Sc. Thesis, University of Adelaide.

David, T.E., 1922. Occurrence of remains of small Crustacea in the Proterozoic (?) or Lower Cambrian (?) Rocks of Reynella, near Adelaide.

Trans. R. Soc. S.Aust. 46 : 6-8.

\_\_\_\_\_, 1932. Explanatory Notes to Accompany a New Geological Map of the Commonwealth of Australia. 177pp.

Arnold, London.

Deer, W.A., Howie, R.A. and Zussman, J. 1963. Rock forming minerals. In 5 volumes.

Longmans.

Dietrich, R.V., 1962. K-feldspar structural states as petrogenetic indicators.

Norsk geol. Tidsskr. 42 : 394-414.

Eggleton, R.A., 1959.

The geology of some pegmatites near Gumeracha, South Australia.

Unpubl. Honours Thesis, University of Adelaide.

Emmons, R.C., 1959. (Reprinted from 1943). The Universal Stage.

Mem. geol. Soc. Am. 3 : 1-205.

Engel, A.E.J. and Engel, Celeste, G., 1958. Progressive metamorphism and granitisation of the major paragneiss northwest Adirondack Mts., N.Y., Pt.1.

Bull. geol. Soc. Am. 69 : 1369-1414.

Ernst, W.G., 1962. Synthesis, Stability Relations, and occurrence of Riebeckite and Riebeckite-Arfvedsonite solid solutions.

J. Geol. 70 : 689-736.

\_\_\_\_\_, 1963. Polymorphism in alkali amphiboles.

Am. Miner. 48 : 241-260.

\_\_\_\_\_, 1965. Synthesis and stability relations of ferrotremolite.

Am. J. Sci. 264 : 37-65.

Eskola, P., 1932. On the principles of Metamorphic Differentiation.

Bull. Commn geol. Finl. No.97 : 68-77.



Eskola, P., 1933. The term « Metamorphic Differentiation »  
first proposed by Stillwell.

Bull. Comm. geol. Finl. No.103 : 45-46.

Eugster, H.P., 1956. Muscovite-paragonite join and its use  
as a geological thermometer.

Bull. geol. Soc. Am. 67 : 1693 (Abstract).

\_\_\_\_\_, and Yoder, H.S., Jr., 1954a. Paragonite.

Yb. Carnegie Instn Wash. 53 : 111-114

\_\_\_\_\_, and Yoder, H.S., Jr., 1954b. Stability and  
occurrence of paragonite.

Bull. geol. Soc. Am. 65 : 1248-1249 (Abstract).

\_\_\_\_\_, and Yoder, H.S., Jr., 1955. Micas.

Yb. Carnegie Instn Wash. 54 : 124-129.

Evans, B.W., 1965. Application of a reaction-rate method of  
the breakdown equilibria of muscovite and muscovite  
plus quartz.

Am. J. Sci. 263 : 647-667.

Everden, J.F. and Richards, J.R., 1962. Potassium-argon ages  
in eastern Australia.

J. geol. Soc. Aust. 9 : 1-49.

Kanehira, K., Banno, S. and K. Nishida, 1964. Sulfide and Oxide  
minerals in some metamorphic terranes in Japan.

Jan. J. Geol. Geogr. 35 : 175-192.

Fleming, P.T., 1965. The geology of an area east of Angaston,  
South Australia.

Unpubl. Honours Thesis, University of Adelaide.

- Forbes, B.G., 1957. Stratigraphic succession east of Grey Spur, South Australia.  
Trans. R. Soc. S.Aust. 80 : 59-66.
- Francis, G.H., 1956. Facies boundaries in pelites at the middle grades of regional metamorphism.  
Geol. Mag. 93 : 353-368.
- \_\_\_\_\_, 1964. Further petrological studies in Glen Urquhart, Inverness-shire.  
Bull. Br. Mus. nat. Hist. C. Mineralogy 1 : 163-199.
- French, B.M., and Eugster, H.P., 1965. Experimental control of oxygen fugacities by graphite-gas equilibria.  
J. geophys. Res. 70 : 1529-1539.
- Freytag, I.B., 1957. The Victoria Creek Marble, with observations on the geology of an area northeast of Williamstown, South Australia.  
Unpubl. Honours Thesis, University of Adelaide.
- Fyfe, W.S., 1960. Hydrothermal synthesis and determination of equilibrium between minerals in the subsolidus region.  
J. Geol. 68 : 553-566.
- Gaskin, A.J., and Sampson, H.R., 1951. Ceramic and refractory clays of South Australia.  
Bull. geol. Surv. S.Aust. 28 : 1-91.
- Gates, R.M., 1953. Petrogenic significance of Perthite.  
Mem. geol. Soc. Am. 52 : 55-69.
- \_\_\_\_\_, and Scheerer, P.E., 1963. The petrology of the Nonewaug granite, Connecticut.  
Am. Miner. 48 : 1040-1069.

- Gee, R.D., 1963. Structure and Petrology of the Raglan Range.  
Geol. Surv. Bull. Tasn. 47 : 6-40.
- George, R., 1963. Geology of the Talisker Mine Area.  
Unpubl. Honours Thesis, University of Adelaide.
- Gilbert, C.M., 1964. Synthesis and stability relations of  
the hornblende, ferropargasite.  
Abstr. geol. Soc. Am. 72-73.
- Gindy, A.M., 1953. The plutonic history of the district  
around Travenagh Bay, Co. Donegal.  
Q. Jl geol. Soc. Lond. 108 : 377-411.
- Goldsmith, J.R. and Laves, F., 1954. The microcline - sanadine  
stability relations.  
Geochim. cosmochim Acta 5 : 1-19.
- Greenhalgh, D. and Jeffery, P.M., 1959. A contribution to  
the Precambrian Chronology of Australia.  
Geochim. cosmochim Acta 16 : 39-57.
- Greenly, E., 1919. The geology of Anglesey.  
Mem. Geol. Surv. U.K. (formerly Great Britain) : 1-980.
- Greenwood, H.J., 1961. The system  $\text{NaAlSi}_3\text{O}_8 - \text{H}_2\text{O} - \text{Argon}$ :  
Total pressure and water pressure in metamorphism.  
J. geophys. Res. 66 : 3923-3946.
- Grootensart, T.B. and Holland, H.D., 1956. Sodium and  
potassium content of muscovites from Peerless pegmatite,  
Black Hills, S.D.  
Bull. geol. Soc. Am. 66 : 1569.

- Guidotti, C.V., 1963. Metamorphism of the pelitic schists  
in the Byrant Pond Quadrangle, Maine.  
Am. Miner. 48 : 772-791.
- \_\_\_\_\_, and Evans, B.W., 1964. Petrochemical study of  
pelitic schists across the sillimanite+K.feldspar  
isograd in Western Maine.  
Abstr. geol. Soc. Am. 79-80.
- Guitard, G., Raguin, E. and G. Sabatier, 1960. La symetrie  
des feldspaths potassique dans les gneiss et les  
granites des Pyrenees orientales.  
Bull. Soc. fr. Miner. Cristallogr. 83 : 43-56.
- Harker, R.I., 1962. The older ortho-gneisses of Carn  
Chuinneag and Inchbae.  
J. Petrology 3 : 215-237.
- Harne, M., 1962. An example of Anatexis.  
Bull. Comm. geol. Finl. 34 : 113-125.
- Harry, W.T., 1952. The migmatites and felspar-porphyroblast  
rock of Glen Dessarry, Inverness-shire.  
Q. Jl. geol. Soc. Lond. 107 : 137-158.
- \_\_\_\_\_, 1954. The composite granite gneiss of Western  
Ardgour, Argyll.  
Q. Jl. geol. Soc. Lond. 109 : 285-300.
- Hayama, Y., 1964. Progressive metamorphism of pelitic and  
psammitic rocks in the Komagane District, Nagano  
Pref., Central Japan.  
J. Fac. Sci. Tokyo Univ. (Sec II) 15 : 321-369.

- Heald, M.T., 1950. Structure and petrology of the Lovewell Mountain Quadrangle, New Hampshire.  
Bull. geol. Soc. Am. 61 : 43-89.
- Heier, K.S., 1957. Phase relations of potash feldspar in metamorphism.  
J. Geol. 65 : 468-479.
- \_\_\_\_\_, 1960. Petrology and geochemistry of high-grade metamorphic and igneous rocks on Langy<sup>ø</sup>, Northern Norway  
Norg. geol. Unders. No. 207.
- Henley, J.J., 1959. Some mineralogical equilibria in the system  $K_2O - Al_2O_3 - SiO_2 - H_2O$ .  
Am. J. Sci. 257 : 241-270.
- \_\_\_\_\_, and Jones, W.R., 1964. Chemical aspects of hydrothermal alteration with emphasis on hydrogen metasomatism.  
Econ. Geol. 59 : 538-569.
- Hess, H.H., 1949. Chemical composition and optical properties of common clinopyroxenes. Part 1.  
Am. Miner. 34 : 621-642.
- Hietanen, A., 1963. Metamorphism of the Belt Series in the Elk Series in the Elk River - Clarkia Area, Idaho.  
Prof. Pap. U.S. geol. Surv. 344-c.
- Hobbs, B.E. 1965. Structural analysis of the rocks between the Wyangala Batholith and the Copperhanna thrust, New South Wales.  
J. geol. Soc. Aust. 12 : 1-24.

- Hobbs, B.E., and Talbot J.L., (in press). The analysis of strain in Deformed Rocks.  
J. Geol. in press.
- Horwitz, R.C., Thompson, B.P. and B.P. Webb, 1959. The Precambrian-Cambrian boundary in the eastern Mt. Lofty Ranges region, South Australia.  
Trans. R. Soc. S. Aust. 92 : 205-218.
- Hosfield, P.S., 1925. The Tanunda Creek Granite and its field relations.  
Trans. R. Soc. S. Aust. 49 : 191-197.
- \_\_\_\_\_, 1935. The geology of part of the North Mt. Lofty Ranges.  
Trans. R. Soc. S. Aust. 59 : 16-67.
- Howchin, W., 1906. The geology of the Mt. Lofty Ranges. Part 2.  
Trans. R. Soc. S. Aust. 30 : 227-262.
- \_\_\_\_\_, 1926. The geology of the Barossa Ranges and neighbourhood in relation to the geological axis of the country.  
Trans. R. Soc. S. Aust. 50 : 1-16.
- \_\_\_\_\_, 1929. The geology of South Australia.  
Gillingham. Adelaide.
- Johnson, M.R.W., 1962. Relations of movement and metamorphism in the Dalradians of Banffshire.  
Trans. Edinb. geol. Soc. 19 : 29-64.
- \_\_\_\_\_, 1963. Some time relations of movement and metamorphism in the Scottish Highlands.  
Geologia Minb. 49e : 121-142.

- Jones, K.A., 1959. The significance of Schmitteffekt in petrofabric diagrams.  
Am. J. Sci. 257 : 55-62.
- Joplin, G.A., 1956. On the association of albitites and sodalites with potash granites in the Precambrian and older Palaeozoic of Australia.  
J. R. Soc. N.S.W. 90 (2) : 80-86.
- Keyser, F.De, 1965. The Barnard Metamorphics and their relation to the Barron River Metamorphics and the Hodgkinson Formation, North Queensland.  
J. geol. Soc. Aust. 12 : 91-103.
- Khitarov, N.I., Pugin, V.A., Chao, P., and A.B. Slutskii., 1963. Relation between andalusite, kyanite, and sillimanite at moderate temperatures and pressures.  
Geochemistry, Wash. (English translation of Geokhimiya) 3 : 235-245.
- Kleeman, A.W., 1954. A reconnaissance of the structural petrology of the Mt. Lofty Ranges.  
Unpubl. Ph.D. Thesis, University of Adelaide.
- \_\_\_\_\_, 1965. The origin of granitic Magmas.  
J. geol. Soc. Aust. 12 : 35-52.
- \_\_\_\_\_, and Skinner, B.J. 1959. The Kanmantoo Group in Strathalbyn-Harrogate Region, South Australia.  
Trans. R. Soc. S. Aust. 82 : 61-71.
- Kretz, R., 1960. The distribution of certain elements among coexisting calcic pyroxenes, calcic amphiboles and biotites in skarns.  
Geochim. cosmochim. Acta 20 : 161-191.

- Layton, W., 1963. Amphibole paragenesis in the Birrimian Series of the Winneba District of Ghana.  
J. geol. Soc. Aust. 10 : 261-272.
- Larsen, E.S., 1928. A hydrothermal origin of corundum and albitite bodies.  
Econ. Geol. 23 : 398-433.
- Lambert, R.S.T.J., 1959. The mineralogy and metamorphism of the Moine schists of the Meran and Knoydart districts of Inverness-shire.  
Trans. R. Soc. Edinb. 63 : 553-588.
- Leedal, G.P., 1952. The Cluanie igneous intrusions, Inverness-shire and Ross-shire.  
Q. Jl. geol. Soc. Lond. 103 : 35-63.
- Luth, W.C., Jahns, R.H., and O.F. Tuttle, 1964. The granite system at pressures of 4 to 10 kilobars.  
J. geophys. Res. 69 : 759-773.
- MacKenzie, W.S., 1954. The orthoclase-microcline inversion.  
Mineralog. Mag. 30 : 354-366.
- Mackie, J.B., 1947. Petrofabric analyses of two quartz-mica-piedmontite schists from northwest Otago.  
Trans. R. Soc. N.Z. 76 : 362-365.
- Madigan, C.T., 1925. The geology of the Fleurieu Peninsula, Pt.1 : The coast from Sellick Hill to Victor Harbour.  
Trans. R. Soc. S.Aust. 49 : 198-212.
- Mason, B., 1962. Metamorphism in the Southern Alps of New Zealand.  
Bull. Am. Mus. nat. Hist. 123 : 211-248.



- Mawson, D., 1948. Sturtian Tillite of Mount Jacob and Mount Warren Hastings, North Flinders Ranges.  
Trans. R. Soc. S.Aust. 72 : 244-251.
- \_\_\_\_\_, and Sprigg, R.C., 1950. Subdivision of the Adelaide System.  
Aust. J. Sci. 13 : 69-72.
- Mehnert, K.R., 1953. Petrographie und Abfolge der Granitisation im Schwarzwald.  
Neues Jb. Miner. Mh. 85 : 59-140.
- \_\_\_\_\_, 1957. Petrographie und Abfolge der Granitisation im Schwarzwald II.  
Neues Jb. Miner. Mh. 90 : 39-90.
- \_\_\_\_\_, 1962. Petrographie und Abfolge der Granitisation im Schwarzwald III.  
Neues Jb. Miner. Mh. 98 : 208-249.
- Mills, K.J., 1963. The geology of the Mt. Crawford Granite Gneiss and adjacent metasediments.  
Trans. R. Soc. S.Aust. 87 : 167-183.
- \_\_\_\_\_, 1964. The structural petrology of an area east of Springton, S.A.  
Unpubl. Ph.D. Thesis, University of Adelaide.
- Misch, P., 1964. Stable association wollastonite-anorthite and other calc-silicate assemblages in amphibolite facies crystalline schists of Nangar Parbat, Northern Himalayas.  
Beitr. Miner. Petrogr. 10 : 315-356.

- Miyashiro, A., 1958. Regional metamorphism of the Gosaisyo-Takanuki district in the central Abukuma Plateau.  
J. Fac. Sci. Tokyo Univ. Sec. II, 11 : 219-272.
- \_\_\_\_\_, 1960. Thermodynamics of reactions of rock-forming minerals with silica.  
Pt. IV. Decomposition reactions of muscovite.  
Jap. J. Geol. Geogr. 31 : 113-120.
- \_\_\_\_\_, 1961. Evolution of metamorphic belts.  
J. Petrology 2 : 277-311.
- \_\_\_\_\_, 1964. Oxidation and reduction in the Earth's crust with special reference to the role of graphite.  
Geochim. cosmochim. Acta 28 : 717-729.
- Moulden, J.C., 1958. Petrographic observations upon some South Australian rocks.  
Trans. R. Soc. S.Aust. 19 : 70-78.
- Munro, M., 1963. Errors in the measurement of 2V with the Universal Stage.  
Am. Miner. 48 : 308-323.
- Nicol, A.W. and Roy, R., 1963. Studies on the system muscovite-paragonite.  
Abstr. Geol. Surv. Am. p.122.
- Nockolds, S.R., 1954. Average chemical compositions of some igneous rocks.  
Bull. geol. Soc. Am. 65 : 1007-1032.
- O'Driscoll, E.S., 1965. Rheid morphology project.  
Report No.10 Aust.Min.Ind. Res.Assoc., Melbourne.  
Unpublished.

- Offler, R., 1960. The structure, petrology and stratigraphy of the Strathalbyn Anticline, South Australia.  
Unpubl. Honours Thesis, University of Adelaide.
- \_\_\_\_\_, 1963. Structural geology of the Strathalbyn Anticline, South Australia.  
Trans. R. Soc. S.Aust. 87 : 199-208.
- Olliver, J.G., 1964. Karawirra ore body - Lyndoch talc deposits.  
Unpublished Report, Department of Mines, S.Aust.
- Orville, P.M., 1960. Petrology of several pegmatites in the Keystone district, Black Hills, South Dakota.  
Bull. geol. Soc. Am. 71 : 1467-1490.
- Peacey, J.S. 1961. Rolled garnets from Morar, Inverness-shire  
Geol. Mag. 28 : 77-80.
- Pettijohn, F.J., 1957. Sedimentary rocks.  
2nd ed. Harper, New York.
- Phillips, W.J., 1956. The Criffell-Dalbeattie granodiorite complex.  
Q. Jl. geol. Soc. Lond. 112 : 221-239.
- Phillips, E.R., 1964. Myrmekite and albite in some granites of the New England Batholith, New South Wales.  
J. geol. Soc. Aust. 11 : 49-60.
- Pitcher, W.S., 1965. The aluminium silicate polymorphs. In Controls of Metamorphism. Editors Pitcher, W.S. and G.W. Flinn.  
Oliver and Boyd, Edinburgh, London.

Pitcher, W.S. and Read, H.H., 1963. Contact Metamorphism in relation to manner of emplacement of the granites of Donegal, Ireland.

J. Geol. 71 : 261-296.

Poldervaart, A., 1950. Statistical studies of zircon as a criterion in granitization.

Nature 165 : 574-575.

\_\_\_\_\_, 1953. Metamorphism of basaltic rocks. A review.

Bull. geol. Soc. Am. 64 : 259-274.

\_\_\_\_\_, 1956. Zircons in rocks. II Igneous rocks.

Am. J. Sci. 254 : 521-554.

\_\_\_\_\_, and Ecklemann, E.D., 1955. Growth phenomena in zircon of autochthonous granites.

Bull. geol. Surv. Am. 66 : 947-948.

Radoslovich, E.W., 1963. The cell dimensions and symmetry of layer-lattice silicates. V Composition limits.

Am. Miner. 48 : 348-367.

Ranberg, H., 1952. The origin of metamorphic and metasomatic rocks.

Chicago, Univ. Press.

\_\_\_\_\_, 1956. Pegmatites in West Greenland.

Bull. geol. Soc. Am. 67 : 185-214.

\_\_\_\_\_, 1962. Intergranular precipitation of albite by unmixing of alkali feldspar.

Neues Jb. Miner. Ms. 98 : 14-34.

- Ramsauer, H., 1941. Achsenverteilungsanalysen an  
Quartztektoniten. Bibliotheks aus dem Inst.  
Miner. Inbruck. Nr.304 : 3-26.
- Ramsay, J.G., 1958. Superimposed folding at Loch Monar,  
Inverness-shire and Ross-shire.  
Q. Jl geol. Soc. Lond. 113 : 271-308.
- \_\_\_\_\_, 1960. The deformation of early linear structures  
in areas of repeated folding.  
J. Geol. 68 : 75-93.
- \_\_\_\_\_, 1963. Structure and metamorphism of the Moine  
and Lewisian rocks of the northwest Caledonides.  
Ed. Johnson, ~~M.R.~~W. and F.H. Stewart.  
The British Caledonides. Edinburgh.
- Rast, N., 1965. Nucleation and growth of metamorphic minerals.  
In Controls of Metamorphism.  
Ed. Pitcher, W.S. and G.W. Flinn.  
Oliver and Boyd. Edinburgh and London.
- Read, H.H., 1931. The geology of central Sutherland.  
Mem. geol. surv. U.K. (formerly Scotland), p.88-164.
- Reitan, P.H., 1960. The Genetic Significance of Two Kinds  
of Basified Zones near small Pegmatite Veins.  
Int. Geol. Cong. 17 : 102-107.
- Rickard, M.J., 1961. A note on cleavages in crenulated rocks.  
Geol. Mag. 98 : 326-332.

- Ruegg, N.R., 1964. Use of the angle  $Al^{\wedge}C$  in optical determination of the composition of augite.  
An. Miner. 49 : 599-606.
- Rutland, R.W.R., 1965. Tectonic overpressures. In Controls of Metamorphism.  
Ed. Pitcher, W.S. and G.W. Flinn.  
Oliver and Boyd. Edinburgh and London.
- Sander, B., 1950. Einführung in die Gefugekunde der Geologischen Körper.  
Vienna and Innsbruck : Springer-Verlag.
- \_\_\_\_\_, Kastler, D. and J. Ladurner, 1954. Zur Korrektur des Schnitteffektes in Gefugediagrammen heterometrischer Körner.  
Sber. ost. Akad. Wiss. Math.-nat. Kl. Abt. 1 163 ; 401-424.
- Sando, M. 1957. The granitic and metamorphic rocks of the Reedy Creek area, Mannum, South Australia.  
Unpubl. M.Sc. Thesis, University of Adelaide.
- Saxena, M.N., 1964. The Continuity of Si and Se surfaces in garnets : An Observation.  
Geol. Mag. 101 : 502-503.
- Sederholm, J.J., 1923. On migmatites and associated Precambrian rocks of southeast Finland. Pt. I. The Pellingö Region.  
Bull. Comm. geol. Finl. 58 : 75-95.

Segnit, E.R. and Kennedy, G.C., 1961. Reactions and melting relations in the system muscovite-quartz at high pressures.

Am. J. Sci. 259 : 280-287.

Shaw, D.M., 1960. The geochemistry of scapolite. Part 1. Previous work and general mineralogy.

J. Petrology 1 : 218-260.

\_\_\_\_\_, Moxham, R.L., Filby R.H. and W.W. Lapkowsky, 1963.

The petrology and geochemistry of some Grenville Skarns. Part. II. Geochemistry.

Can. Mineralogist 7 : 578-616.

\_\_\_\_\_, Schwarcz, M.P. and M.F. Sheppard, 1965. The petrology of two zoned scapolite skarns.

Can. J. Earth Sci. 2 : 577-595.

Shelley, D., 1964. On myrmekite.

Am. Miner. 49 : 41-52.

Shidô, Fumiko, 1958. Plutonic and metamorphic rocks of the Nakoso and Iriteno Districts in the Central Abukuma Plateau.

J. Fac. Sci. Tokyo Univ. (Sec. II), 11 : 131-217.

Siefert, K.E., 1965. Deformation bands in albite.

Am. Miner. 50 : 1469-1472.

Skinner, B.J., 1956. Physical properties of end-members of the garnet group.

Am. Miner. 41 : 428-436.

- Skinner, B.J., Clark, S.P.Jr. and D.E. Appleman, 1961. Molar volumes and thermal expansions of andalusite, kyanite and sillimanite.  
Am. J. Sci. 259 : 451-468.
- Smith, J.V., 1956. The powder patterns and lattice parameters of plagioclase feldspars. I. The soda rich plagioclases.  
Mineralog. Mag. 31 : 47-68.
- \_\_\_\_\_, and Gay 1958. Powder patterns and lattice parameters of plagioclase.  
Mineralog. Mag. 31 : 744-762.
- \_\_\_\_\_, and Yoder, H.S., 1956. Experimental and theoretical studies of the mica polymorphs.  
Mineralog. Mag. 31 : 209-235.
- Smithson, S.E., 1962. Symmetry relations in alkali feldspars of some amphibolite facies rocks from the southern Norwegian Precambrian.  
Norsk geol. Tidsskr. 42 : 586-599.
- \_\_\_\_\_, 1965. The nature of the 'Granitic' layer of the crust in the southern Norwegian Precambrian.  
Norsk geol. Tidsskr. 45 : 113-133.
- Specht, R.L., Brownell, P.F. and P.M. Hewett, 1961. Plant Ecology of part of the Mt. Lofty Ranges South Australia 2. The distribution of Eucalyptus elacophora.  
Trans. R. Soc. S. Aust. 85 : 155-176.



Sprigg, R.C., 1952. Sedimentation in the Adelaide Geosyncline and the formation of the continental terrace. Sir Douglas Mawson Anniversary Volume, Ed. by M.F. Glaessner and E.A.R. Rudd, University of Adelaide, 153-159.

\_\_\_\_\_ and Campana, B., 1953. The age and facies of the Kamsantoo Group, Eastern Mt. Lofty Ranges and Kangaroo Island, S.A.

Aust. J. Sci. 16 : 12-14.

\_\_\_\_\_ and Wilson, B., 1954. Geological Atlas of South Australia, sheet Echunga.

Geol. Surv. S.Aust.

\_\_\_\_\_, Whittle, A.W.G. and B. Campana, 1961.

Geological Atlas of S.Austr., sheet Adelaide,

Geol. Surv. S.Aust.

Spry, A.H., 1963a. The origin and significance of snowball structure in garnet.

J. Petrology 4 : 211-222.

\_\_\_\_\_, 1963b. Precambrian rocks of Tasmania, Part V. Petrology and structure of the Frenchman's Cap Area.

Pap. Proc. R. Soc. Tasm. 97 : 105-127.

\_\_\_\_\_, 1963c. The chronological analysis of crystallization and deformation of some Tasmanian Precambrian Rocks.

J. Geol. Soc. Aust. 10 : 193-208.

Starkey, J., 1959. Chess-board albite from New Brunswick,  
Canada.

Geol. Mag. 96 : 141-145.

Stillwell, F.L., 1922. The rocks in the immediate neighbour-  
hood of the Broken Hill Lode and their bearing on its  
origin.

Mem. geol. Surv. N.S.W. No.8 : 354-396.

\_\_\_\_\_ and Edwards, A.B., 1951. Petrology of the  
Gumeracha Talc Deposit. In Talc Deposits in South  
Australia.

Bull. geol. Surv. S.Aust. 26 : 31-49.

Sutton, J. and Watson, J., 1951. Varying trends in the meta-  
morphism of deherites.

Geol. Mag. 88 : 25-35.

Talbot, J.L., 1963. Retrograde metamorphism of the Houghton  
Complex, South Australia.

Trans. R. Soc. S.Aust., 87 : 185-196.

\_\_\_\_\_, 1964. The structural geometry of rocks of the  
Torrens Group near Adelaide, South Australia.

J. geol. Soc. Aust. 11 : 33-48.

Thomson, B.P. and Horwitz, R.C., 1961. Cambrian-Precambrian  
Unconformity in Sellick Hill-Normanville Area of  
South Australia.

Aust. J. Sci. 24 : 40-41.

\_\_\_\_\_ and Horwitz, R.C., 1962. Geological Atlas of  
South Australia, sheet Barker.

Geol. Surv. S.Aust.

- Tilley, C.E., 1919. The petrology of the granitic mass of Cape Willoughby, Kangaroo Island, Part 1.  
Trans. R. Soc. S.Aust. 43 : 316-341.
- Troger, W.E., 1959, (reprinted). Optische Bestimmung der gesteinsbildenden.  
Minerale. Teil 1. Stuttgart.
- Turner, F.J. and Weiss, L.E., 1963. Structural analysis of metamorphic tectonites.  
New York : McGraw Hill.
- \_\_\_\_\_ and Verhoogen, J., 1960. Igneous and metamorphic petrology 2d ed. McGraw-Hill. New York.
- Tuttle, O.F. and Bowen, N.L. 1958. Origin of granite in the light of experimental studies in the system  $\text{NaAlSi}_3\text{O}_8 - \text{KAlSi}_3\text{O}_8 - \text{H}_2\text{O}$ .  
Mem. geol. Soc. Am. 74 : 1-153.
- Urban, K., 1934. Gefügeanalytische Untersuchungen an skapolithführenden Gesteinen aus den Tessiner Alpen.  
Neues Jb. Miner. Mh. 68A : 1-18.
- Vallance, T.G., 1960. Notes on metamorphic and plutonic rocks and their biotites from the Wantabadgery Adelong-Tumbarumba district N.S.W.  
Proc. Linn. Soc. N.S.W. 85 : 94-104.
- Vance, J.A., 1961. Polysynthetic twinning in plagioclase.  
Am. Miner. 46 : 1097 - 1119

- Vernon, R.H., 1961. Banded albite-rich rocks of the Broken Hill district, N.S.W.  
Mineragr. Invest. tech. Pap. C.S.I.R.O.Aust. 3 : 1-59.
- \_\_\_\_\_, 1965. Plagioclase twins in some mafic gneisses from Broken Hill, Australia.  
Mineralog. Mag. 35 : 488-507.
- Virgo, D., in prep. Some elemental distributions between coexisting feldspars in metamorphic rocks.  
Ph.D. Thesis in prep., University of Adelaide.
- Vogel, T.A., 1964a. Use of the Nakamura Plate in Universal stage orientations.  
Am. Miner. 49 : 406-408.
- \_\_\_\_\_, 1964b. Optical-crystallographic scatter in plagioclase.  
Am. Miner. 49 : 614-633.
- Voll, G., 1960. New work in petrefabrics.  
Lucol. Manchr. geol. J. 2 : 503-567.
- Walker, K.R., Joplin, G.A., Levering, J.F. and R.Green, 1960. Metamorphic and metasomatic convergence of basic igneous rocks and lime-magnesia sediments of the Precambrian of Northwestern Queensland.  
J. geol. Soc. Aust. 6 : 149-177.
- Webb, B.P., 1958. The Geology of South Australia.  
M.F. Glaessner and L.W.Parkin (editors).
- Wegmann, C.E., 1935. Zur Deutung der Migmatite.  
Geol. Rdsch. 26 : 307-350.

Weill, D.F., (in press).

Stability relations in the  $Al_2O_3-SiO_2$  system  
calculated from solubilities in the  $Al_2O_3-SiO_2-$   
 $Na_3AlF_6$  system.

Geochim. cosmochim. Acta.

Weiss, L.E., 1954. A study of tectonic style.

Structural investigation of a marble-quartzite  
complex in southern California.

Univ. Calif. Publ. geol.Sci. 30 : 1-102.

\_\_\_\_\_, 1959a. Structural analysis of the basement  
system at Turoka, Kenya.

Overseas Geol. Miner. Resour. 7 : 3-35, 123-153.

\_\_\_\_\_, 1959b. Geometry of superposed folding.

Bull. geol. Soc. Am. 70 : 91-106.

\_\_\_\_\_ and McIntyre, D.B., 1957. Structural geometry  
of Dalradian rocks at Loch Leven, Scottish Highlands.

J. Geol. 65 : 575-602.

\_\_\_\_\_, McIntyre, D.B. and W. Kursten, 1955. Contrasted  
styles of folding in the rocks of Ord Ban.

Geol. Mag. 92 : 21-36.

White, A.J.R., 1956. The granite gneisses and associated  
metamorphic rocks of Palmer, South Australia.

Unpubl. Ph.D. Thesis, University of London.

\_\_\_\_\_, 1959. Scapolite-bearing marbles and calc-  
silicate rocks from Tungkillo and Milendella, South  
Australia.

Geol. Mag. 96 : 285-306.

White, A.J.R., (in prep.) Genesis of migmatites from the  
Palmer Region of South Australia.

\_\_\_\_\_, Compston, W. and A.W. Kleeman, (in press).  
The Palmer Granite. A study of a granite within a  
regional metamorphic environment.

J. Petrology (?)

Whittle, A.W.G., 1957. The geology of the eastern portion  
of the hundred of Onkaparinga.

Unpubl. M.Sc. Thesis, University of Adelaide.

\_\_\_\_\_ in Campana, B., 1955. The geology of the  
Gawler Military Sheet.

Rep. Invest. geol. Surv. S.Aust. 4

\_\_\_\_\_ and others, 1951. Talc deposits in South  
Australia.

Bull. geol. Surv. S.Aust. 26 : 135.

Wilcox, R.E. and Poldervaart, A., 1958. Metadolerite dike  
swarm in the Bakersville-Roan Mountain area, North  
Carolina.

Bull. geol. Soc. Am. 69 : 1323-1368.

Wilson, G., 1953. Mullion and rodding structures in the  
Moine Series of Scotland.

Proc. Geol. Assoc. 64 : 118-151.

Wilson, A.F., 1959. Notes on the fabric of some charnockitic  
rocks from central Australia.

J. Proc. R. Soc. West.Aust. (formerly J.R.Soc.West.Aust)  
42 : 56-64.

- Winkler, M.G.F., 1965. Petrogenesis of metamorphic rocks.  
Springer - Verlag. Berlin - Heidelberg - New York.
- Wiseman, J.D.H., 1934. The central and southwest Highland  
epidiorites : a study in progressive metamorphism.  
Q. Jl. geol. Soc. Lond. 90 : 354-417.
- Woodland, B.G., 1963. A petrographic study of thermally  
metamorphosed pelitic rocks in the Burke Area,  
Northeastern Vermont.  
Am. J. Sci. 261 : 354-375.
- Woolnough, W.G., 1904. Petrographical notes on some South  
Australian quartzites, sandstones and related rocks.  
Trans. R. Soc. S. Aust. 28 : 193-211.
- \_\_\_\_\_, 1908. Notes on the geology of the Mt. Lofty  
Ranges, chiefly the portion east of the Onkaparinga.  
Trans. R. Soc. S. Aust. 32 : 121-137.
- Wones, D.R., 1963. Physical properties of synthetic biotites  
on the join phlogopite-annite.  
Am. Miner. 48 : 1300-1321.
- \_\_\_\_\_ and Eugster, H.P. 1965. Stability of biotite :  
experiment, theory and application.  
Am. Miner. 50 : 1223-1272.
- Wyllie, P.J., 1959. Discrepancies between optic axial  
angles of olivines measured over different bisectrices.  
Am. Miner. 44 : 49-64.

- Yoder, H.S., 1955. The role of water in metamorphism.  
in "The Crust of the Earth".  
Spec. Pap. geol. Soc. Am. 62 : 569-627.
- Yoder, H.S., Jr., and Eugster, H.P., 1955. Synthetic and  
natural muscovites.  
Geochim. cosmochim. Acta 8 : 225-280.
- Zen, E-an, 1963. Components, phases and criteria of  
chemical equilibrium in rocks.  
Am. J. Sci. 261 : 929-942.
- \_\_\_\_\_ and Albee, A.L., 1964. Coexistent muscovite and  
paragonite in pelitic schists.  
Am. Miner. 49 : 904-925.
- Zwart, H.J., 1960. Relations between folding and metamorphism  
in the Central Pyrenees, and their chronological  
succession.  
Geologie Minb. 39e : 163-180.
- \_\_\_\_\_, 1963. Metamorphic History of the Central Pyrenees  
Part II, Valle De Aran, Sheet 4.  
Leid. geol. Meded. 28 : 321-376.



**APPENDICES**

APPENDIX 1.Chemical analyses<sup>1</sup> of co-existing feldspars.Plagioclases.

Chemical analyses (K<sub>2</sub>O, Na<sub>2</sub>O, CaO in weight percent: Ba, Sr, Rb in p.p.m.)

Sample number	K <sub>2</sub> O	Na <sub>2</sub> O	CaO	Ba	Sr	Rb
A200/423	0.22	7.59	2.47	138	315	-
A200/871A	0.34	9.39	2.89	221	431	-
A200/561	0.30	9.48	2.27	191	501	-
A200/670B	0.26	9.21	3.01	200	624	-
A200/27	0.32	6.93	1.86	221	421	-
A200/124A	0.19	6.06	5.69	163	440	-
A200/887A	0.46	9.51	2.13	165	254	7.4

Calculated theoretical feldspar components (weight percent).

Sample number	Or	Ab	An	BaF	SrF	RbF	Total
A200/423	1.3000	64.2251	12.2539	0.0376	0.1171	-	77.9337
A200/871A	2.0093	79.4563	14.3376	0.0604	0.1602	-	96.0238
A200/561	1.7611	80.2179	11.2617	0.0522	0.1863	-	93.4792
A200/670B	1.5365	77.9332	14.9329	0.0600	0.2320	-	94.6946
A200/27	1.8911	58.6403	9.2276	0.0604	0.1565	-	69.9759
A200/124A	0.7683	51.2785	28.2287	0.0446	0.1635	-	80.4835
A200/887A	2.7185	80.4717	10.5820	0.0450	0.0944	.0028	93.9144

Calculated theoretical feldspar components (molecular percent).

Corrected for 100 percent feldspar

Sample number	Or	Ab	An	BaF	SrF	RbF
A200/423	1.5882	83.2791	14.9767	0.0340	0.1222	-
A200/871A	1.9917	83.6078	14.2203	0.0445	0.1357	-
A200/561	1.8222	88.1330	11.6623	0.0401	0.1648	-
A200/670B	1.5450	83.1869	15.0238	0.0448	0.1993	-
A200/27	2.5713	84.9329	12.5529	0.0609	0.1819	-
A200/124A	0.9747	65.0603	33.7585	0.0394	0.1671	-
A200/887A	2.7504	86.4207	10.7114	0.0339	0.0815	.0024

1. Chemical analyses by D. Virgo (Geology Dept., University of Adelaide).

K-feldspars.

Chemical analyses ( $K_2O$ ,  $Na_2O$ ,  $CaO$  in weight percent: Ba, Sr, Rb in p.p.m.)

Sample number	$K_2O$	$Na_2O$	$CaO$	Ba	Sr	Rb
A200/423	14.48	1.13	0.12	4760	376	321
A200/871A	15.75	0.90	0.05	8095	440	252
A200/561	15.02	1.14	0.07	7697	524	287
A200/670B	15.05	0.87	0.05	11108	569	237
A200/27	15.05	1.12	0.10	10417	520	247
A200/124A	13.84	1.47	0.08	8705	454	199
A200/887A	15.09	0.98	0.05	3703	224	211

Calculated theoretical feldspar components (weight percent).

Sample number	Or	Ab	An	BaF	SrF	RbF	Total
A200/423	85.5724	9.5618	0.6102	1.3012	0.1398	0.1219	97.3073
A200/871A	93.0778	7.6156	0.2381	1.6662	0.1636	0.0957	102.8570
A200/561	88.7637	9.6465	0.3572	2.1041	0.1948	0.1090	101.1753
A200/670B	88.9410	7.3448	0.2481	3.0289	0.2115	0.0903	99.8647
A200/27	88.9410	9.4772	0.4961	2.8477	0.1843	0.0938	102.0492
A200/124A	81.7607	12.4050	0.3721	2.6531	0.1689	0.0756	97.4353
A200/887A	86.1774	8.3180	0.2481	1.0123	0.0833	0.0802	98.9191

Calculated theoretical feldspar components (molecular percent.)

Corrected for 100 percent feldspar.

Sample number	Or	Ab	An	BaF	SrF	RbF
A200/423	87.7483	10.4073	0.6259	0.9896	0.1224	0.1070
A200/871A	90.4931	7.8588	0.2317	1.2013	0.1359	0.0798
A200/561	87.7286	10.1197	0.3532	1.5422	0.1645	0.0924
A200/670B	89.3935	7.8354	0.2496	2.2578	0.1816	0.0778
A200/27	87.3230	9.8763	0.4873	2.0734	0.1621	0.0789
A200/124A	83.8784	13.5078	0.3818	2.0186	0.1479	0.0665
A200/887A	89.9459	8.9049	0.2502	0.7572	0.0716	0.0693

Sample numberRock type

A200/423	Migmatite
A200/871A	"
A200/561	"
A200/670B	Quartz-feldspathic schist
A200/27	" "
A200/124A	Pelitic Schist
A200/887A	" "

APPENDIX 2.Muscovite geothermometry and comparison of muscovite compositions determined by X-ray Diffractometry and Wet Chemical Analysis.

The muscovite - paragonite solvus was first tentatively published by Eugster and Yoder (1955) and applied later as a geothermometer by Grootemaart and Holland (1956), Engel and Engel (1958), Lambert (1959) and Mason (1962). Although Grootemaart and Holland (op.cit.) successfully applied this geothermometer to zoned pegmatites, Lambert (op.cit.) obtained unsatisfactory results from mica schists. Both Engel and Engel, (op.cit.) and Mason (op.cit.) regarded their results with caution and pointed out that as plagioclase coexisted with muscovite in their rocks, the temperatures obtained were minimal.

The muscovite - paragonite system was again examined by Nichol and Roy (1963) at temperatures greater than 400°C and pressures above 1 Kilobar. The important features arising from this work were that at temperatures less than 625°C:-

- (1) The lattice parameters of muscovite were virtually unchanged despite solid solution of as much as 20 percent paragonite.
- (2) Only a small percentage of Na<sup>+</sup> was replaced by K<sup>+</sup> in paragonite.
- (3) No experimental evidence could be found for a marked temperature (or pressure) dependence of the crystalline solubility as claimed by Eugster and Yoder.

However, Radoslevich (1963) in his examination of the muscovite structure expected Na to be tolerated in the muscovite lattice with increasing temperature.

Finally, Zen and Albee (1964) in their study of the lattice parameters and chemical composition of naturally occurring muscovites and paragonites, predicted an asymmetrical solvus, instead of the symmetrical one proposed by Eugster and Yoder (op.cit.). Hence, in almost a decade most aspects of muscovite - paragonite relationships have been examined.

Four muscovites have been chemically analysed for  $\text{Na}_2\text{O}$  and  $\text{K}_2\text{O}$  to obtain possible temperatures of crystallization from the muscovite - paragonite solvus. Their compositions have also been determined by X-ray diffractometry.

#### Experimental Work.

One metamorphic segregation, two igneous pegmatites and one mica schist were crushed and pure muscovite obtained by hand picking, heavy liquids and magnetic separation.

##### (a) Chemical Analysis.

$\text{K}_2\text{O}$  and  $\text{Na}_2\text{O}$  have been determined with an Eel Flame photometer and the results, calculated in terms of mol percent muscovite, are given in Table 1.

##### (b) Diffractometer Measurements.

The (006) and (0010) planes of muscovite were measured using silicon (111) and  $(220\alpha_1)$  reflections as internal standards. Scanning speed and slit width were chosen such that the measurements showed good reproducibility ( $\pm 0.003$ ). The appropriate  $2\theta$  region was scanned six times and  $d_{002}$  calculated (Table 1). The composition of the muscovites

were determined by using the recent  $d_{002}$  values of synthetic muscovite and paragonite quoted by Zen and Albee (op.cit.), assuming  $d_{002}$  changes linearly with composition (Table 1).

### Discussion.

The mol percent paragonite in muscovite determined from X-ray analysis is lower than that obtained from chemical analysis (Table 1). The "synthetic" curve should therefore not be used for naturally occurring muscovites. If lattice parameters are to be employed as a method for determination of composition, then it is necessary to use a curve constructed from natural muscovites, such as that figured by Zen and Albee, (op.cit.p.917). This regression curve is plotted in Fig.1 as a dashed line and is compared with the synthetic curve (full line). On the same diagram in terms of mol percent paragonite, are plotted 17 more analyses (16 partial analyses, 1 full analysis) of muscovites for which the X-ray parameters are known (Table 1). The spread shown by these points is discouraging and it is possible that other elements within the lattice such as  $Fe^{2+}$ ,  $Fe^{3+}$ ,  $Mg^{2+}$  etc. may have a definite affect upon lattice parameters. Thus the "natural" curve will only provide an approximate muscovite composition.

The temperatures obtained from the geothermometer for the four specimens are contradictory. For example, similar temperatures of crystallization should be recorded by the metamorphic segregation (A200-17) and the mica schist (A200-87A) as both

have formed at the same grade of metamorphism. However, 87A contains more paragonite than 17 and therefore appears to have formed at higher temperatures. In 87A abundant muscovite is associated with minor amounts of biotite and plagioclase, and in 17, plagioclase and potash feldspar are present in greater quantities than muscovite. Thus it appears that in 17, the higher number and proportion of coexisting  $\text{Na}^+$  bearing phases, has limited the amount of  $\text{Na}^+$  available to go into the muscovite lattice.

## APPENDIX 2.

TABLE 1.

Spec.No.	Rock Type	d(002)	Composition Mol%		muscovite Temp. <sup>1</sup>
			X-ray	Chem.	
441	Pegmatite	9.994	88	90.9	420°
17	Segregation	9.992	87.5	92.3	400°
239A	Pegmatite	9.982	85.5	90.7	420°
15	Quartz-feldspathic schist	9.986	86	-	
368	Bimica schist	9.982	85		
87A	" "	9.981	85	86.0	510°
P. Slade <sup>2</sup> samples (pers.comm.)	Granite	9.987	86.5	93.7	
"	"	9.996	89	92.3	
"	"	9.986	86	94.0	
"	"	9.998	89	92.0	
"	"	9.996	89	94.8	
"	"	10.001	90	93.3	
"	"	10.003	90	96.2	
Radoslevich(1960) (pers.comm.)	"	10.049	> 100	94.2	
"	"	9.646	2.5	15.1	
"	"	9.908	67	4.9	
Skinner(1959)	Andal-Kyn.schist	9.940	75	85.0	
	Plag.-KF "	9.954	79	92.0	
Barker (1965)	Ab pegmatite	9.980	85	81.0	

1. Temperature determined from muscovite geothermometer using chemical data.
2. Geology Dept., University of Adelaide.

## REFERENCES.

- Barker, D.S., 1965.  
Alkalic rocks at Litchfield, Maine.  
J. Petrology 6 : 1-27
- Radoslevich, E.W., 1960.  
The structure of muscovite  $KAl_2(Si_3Al)O_{10}(OH)_2$ .  
Acta Cryst. 13 919
- Skinner, B.J., 1958.  
The Geology and metamorphism of the Nairne Pyritic  
Formation, a sedimentary sulfide deposit in South  
Australia.  
Econ. Geol. 5 : 546-562.



Regression curve between  $(002)_{2M}$  spacings and compositions of analysed muscovites and paragonites.

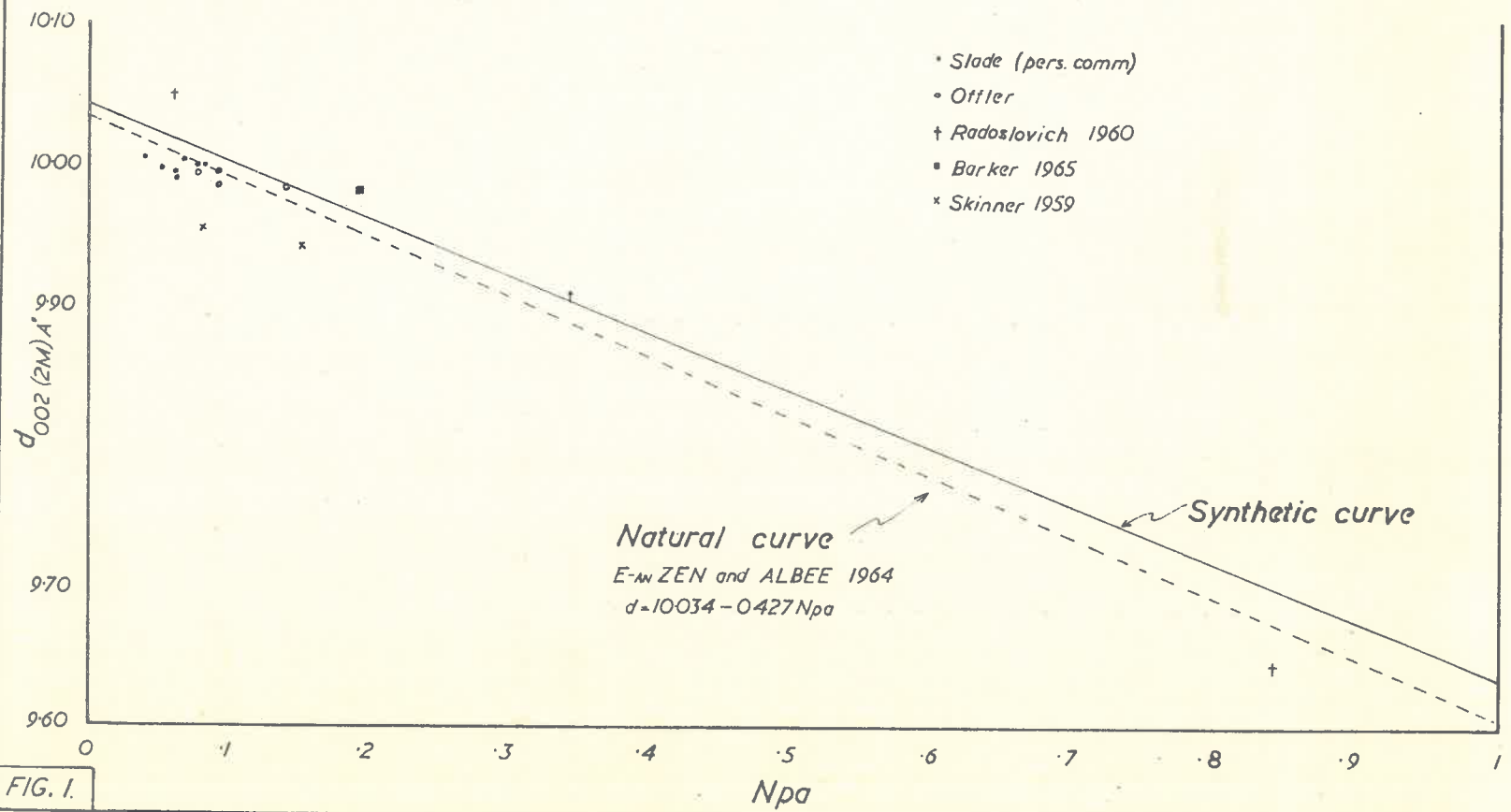


FIG. 1.

R. J. 65

APPENDIX 3.Comparison of plagioclase compositions determined  
by optical, X-ray and chemical techniques.Introduction.

The composition of several plagioclases from metamorphic rocks, albitites and igneous pegmatites have been determined by X-ray and Universal Stage techniques, using the X-ray curves of Smith (1956) and the migration curves of Emmons (1959) and Vogel (1964). Seven of these plagioclases have been analysed wet chemically and X-ray spectrographically by Mr. D. Virgo (Geology Dept., University of Adelaide) and are listed in Table 2.

Experimental methods.

The regions  $2\theta(111)$ - $2\theta(1\bar{1}1)$  and  $2\theta(131)$ - $2\theta(1\bar{3}1)$  have been scanned six times. The slit width and scanning speed were adjusted so that the measurements showed good reproducibility. Tables 1 and 2 list the results of the optical and X-ray determinations.

Discussion.

It can be seen that the compositions of the plagioclases determined optically, are in closer agreement with the chemical compositions than those determined by X-ray techniques (Table 2). In addition the anorthite content of the plagioclases found by X-ray methods is higher than in the chemically analysed plagioclases.

In the determination of plagioclase compositions from X-ray parameters, it was assumed that the plagioclases were in a low temperature thermal state. If the X-ray parameters and chemical composition of the plagioclases are plotted on Smith's (op.cit.) curves, all points appear above the low temperature curves, thus explaining the discrepancy between the X-ray and chemically determined compositions. It would appear then, that the composition of plagioclases cannot be determined satisfactorily by X-ray means unless the structural state is known (c.f. Smith and Gay, 1958). The Universal Stage method appears to provide a more accurate determination of plagioclase compositions than the X-ray method. In this technique a knowledge of the structural state is not necessary for the determination of the composition of the plagioclase. It would appear therefore that the Universal Stage method is superior to the X-ray method.

APPENDIX 3.TABLE 1.X-ray Parameters of Plagioclases.

<u>Spec. No.</u>	1	2	3	4
192	0.480	1.5	1.100	1.5
615	0.535	8.5	1.190	6.5
432	0.500	4.0	1.101	1.5
239A	0.580	14.0	1.302	12.0
313A	0.503	4.5	1.160	5.0
257	0.507	5.0	1.140	3.5
441	0.670	25.0	1.483	21.0
124A	off graph	-	1.752	39.0
17	0.568	12.5	1.261	10.5
462	0.500	4.0	1.140	4.0
423	0.603	17.0	1.412	17.5
861	0.582	14.0	1.339	14.0
27	0.609	18.0	1.383	16.5
670B	0.614	18.5	1.414	18.0
871A	0.615	18.5	1.400	17.0

- 1  $2\theta(111) - 2\theta(1\bar{1}1)$
- 2  $\text{Wt. \%}_{\text{An}}$  from 1, Smith (1956).
- 3  $2\theta(131) - 2\theta(1\bar{3}1)$
- 4  $\text{Wt. \%}_{\text{An}}$  from 3, Smith (1956).

APPENDIX 3.TABLE 2.Plagioclase Compositions.

<u>Spec. No.</u>	<u>X-ray</u> <sup>1</sup> Wt. % An	<u>Optical</u> Wt. % An	<u>Chem.</u> Wt. % An	<u>Rock Type.</u>
192	1.5	0.5		Albitite
615	7.5	5.0		Ig. peg.
432	3.0	5.0		Albitite
239A	13.0	16.0		Ig. peg.
257	5.0	4.5		Ig. peg.
313A	4.0	5.0		Albitite
441+	29.0	-		Ig. peg.
124A	39.0	38.0	35.6	Politic schist
17	11.5	9.0		Segreg.
462	4.0	4.0		Albitite
423	17.0	15.0	16.0	Quartzo- feldspathic schist.
561	14.0	14.0	12.3	"
27	17.5	14.0	13.6	"
670B	18.0	14.5	16.0	"
871A	18.0	14.0	15.2	"
887A	14.0	13.0	11.6	Politic schist

1. Average wt. percent.  
+ Plagioclase strained.

APPENDIX 4.Scapolite Petrofabrics.

The orientation of scapolite in a  $B_1$  fold nullion (A200-322) and a  $B_3$  fold in calc-silicate rocks from the Adelaide Supergroup and Kanmantoo Group rocks has been studied (Figs.4 and 5). It can be seen that certain features are common to most diagrams viz. the development of cleft and peripheral girdles and irregular central maxima. The scapolite appears to show a weak or random orientation in all diagrams.

Few studies of the orientation of scapolite in deformed rocks have been reported in the literature. The only data known to the author are that presented by Urban (1934), White (1956) and Wilson (1959). Their studies showed that scapolite can be oriented in a girdle either perpendicular (Wilson, op.cit., Urban, op.cit.) or parallel to " $b$ "<sup>1</sup> (Urban, op.cit.; White, op.cit.) and that the main maxima corresponds to " $b$ ". White (op.cit.) suggests that the scapolite fabric is due to the growth of scapolite crystals along lines (e.g. bedding-cleavage intersection) or planes of least resistance. When there is no plane or lineation present scapolite forms a random orientation. He considers that the scapolite would have form rather than lattice orientation as a result of this mechanism.

---

1. lineation.

APPENDIX 4

FIG. 4.

Scapolite data for Spec. No. A200-322.

Location 950 237. Wave length of

mullion 1.5 inches (4 cms).

a 262 scapolite "c" axes.

b 290 " " "

c 253 " " "

d represents e rotated to position  
perpendicular to  $B_1$ .

e 210 scapolite "c" axes. Section  
parallel to  $B_1$ .

f 363 scapolite "c" axes. Section  
parallel to  $B_1$ .

SCAPOLITE DATA FOR SPEC. 322.

CONTOURS 123 per 1/area.

FOLD MULLION A.S. CALC-SILICATE.

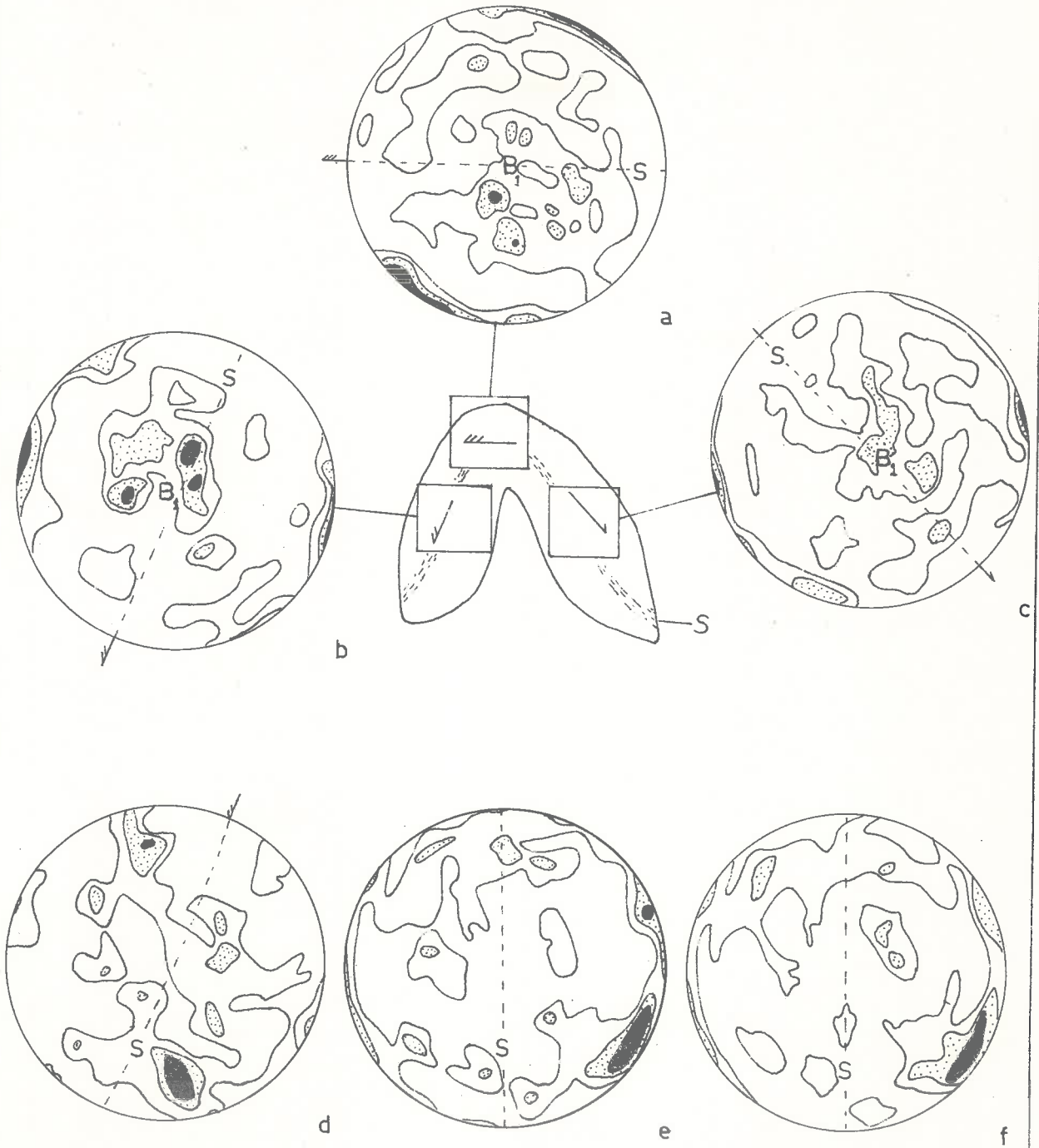


FIG. 4.

R.0'66



APPENDIX 4

FIG.5

Scapolite data for Spec. No.A200-411.

Location 975 289. Wave length of

fold 2 inches (5 cms).

a 161 scapolite "c" axes.

b 235 " " "

c 186 " " "

# SCAPOLITE FABRIC DATA FOR SPEC. 411.

CONTOURS 123 per  $1/\text{area}$

B<sub>3</sub> FOLD K.Gr. CALC-SILICATE

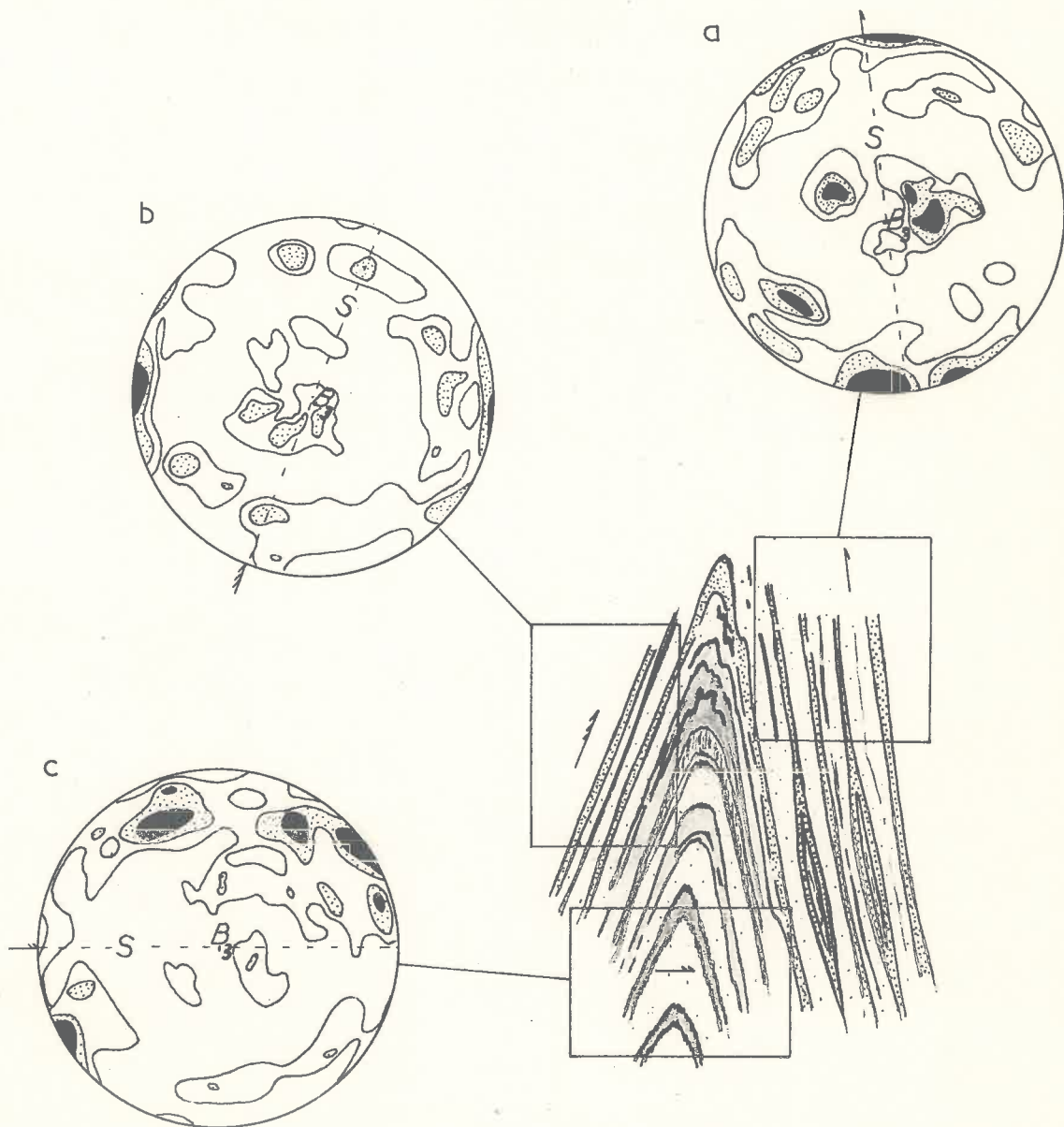


FIG. 5.

R.O.'65

The scapolites in specimens A200-322 and 411 have recrystallized post tectonically since all grains are strain free and show  $120^\circ$  triple point relationships. The essentially random orientation of these scapolites presumably is due to the lack of linear and planar elements in these rocks.

APPENDIX 4.Adelaide Supergroup.Quartz petrofabrics - bimica schists.

The [0001] axes of quartz were measured in four bimica schists (Figs. 2 and 3). Sections cut perpendicular to lineation or foliation were examined and in some specimens (A200-450, 368) two mutually perpendicular sections<sup>1</sup> were studied. A detailed investigation of the quartz orientation in the limbs and crest of a microfold (A200-368) was also made. The results can be summarized as follows :

- (1) All quartz diagrams show well developed cleft girdles and in some cases, partial small circle girdles.
- (2) The orientation of quartz is the same in mutually perpendicular sections (e.g. A200-450).
- (3) The preferred orientation of quartz is different in the limbs and crest of the microfold of specimen (A200-368).

Discussion.

The diagrams of specimens A200-450 and 368 from mutually perpendicular sections, on rotation cannot be correlated with one another. This indicates that the quartz has no preferred orientation. The diagrams obtained from 254 and 280 are

---

1. i.e. the second section was cut perpendicular to the first and to the foliation  $S_{11}$ .

APPENDIX 4

FIG.2.

Quartz data for Spec. No.A200-368.

Location 962 195. The number of

[0001] axes measured is placed at

the top of each diagram.

- a [0001] axes measured in section perpendicular to  $B_3$
- b " " " in second " " "
- c " " measured in hinge of microfold.
- d " " " " " " "
- e " " " in southern limb of microfold.
- f " " " " northern " " "
- g Section parallel to  $B_3$ .
- h Biotite diagram.

# FABRIC DATA FOR BIMICA SCHIST 368.

CONTOURS 1234 per 1% area

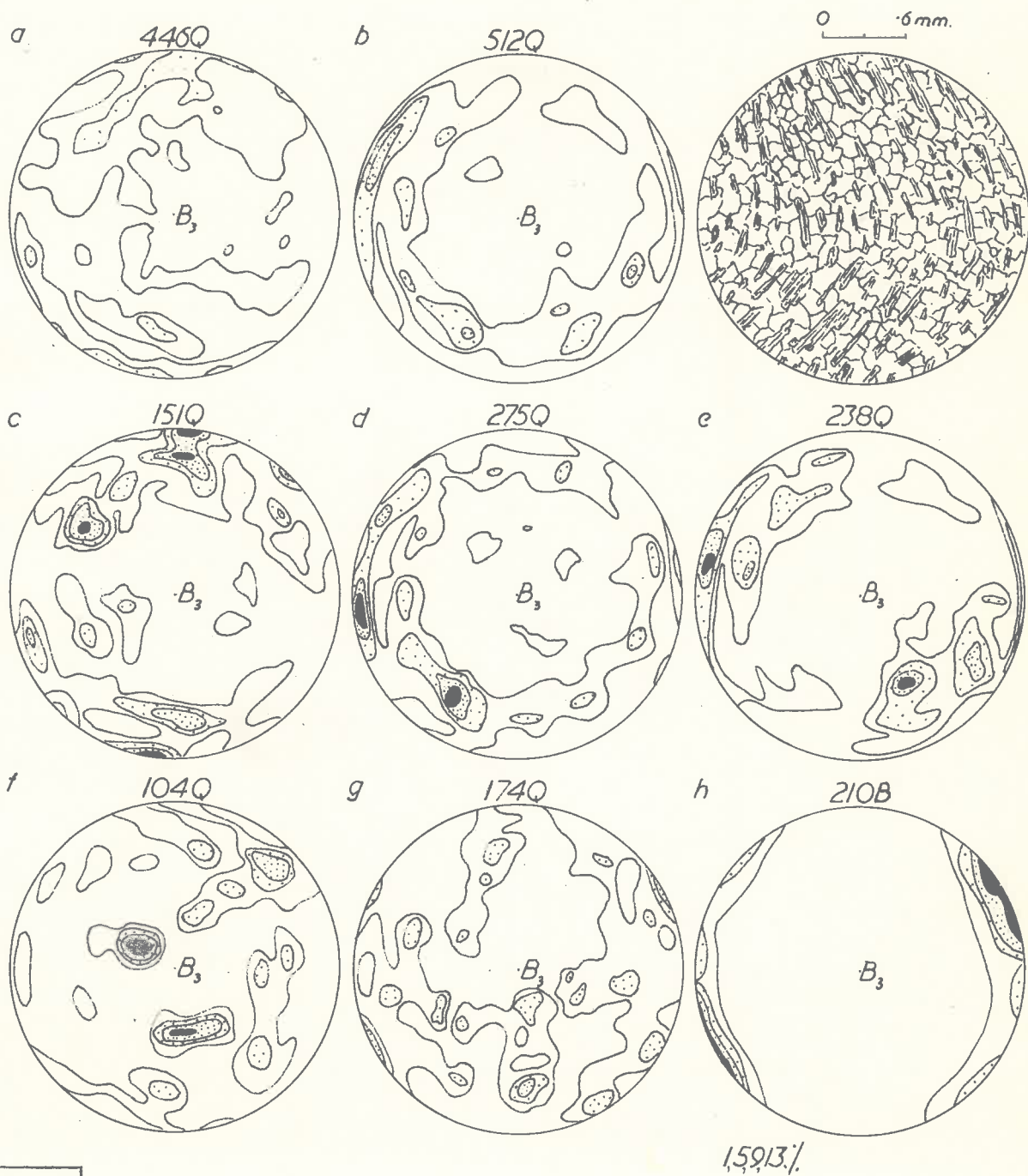


FIG. 2.

APPENDIX 4

FIG. 3

Quartz data for mica schists A200-254,  
280 and 450. Locations 952 273, 947 192,  
and 962 267. The number of [0001] axes  
measured is given at the top of each  
diagram.

254a First section perpendicular to  $S_2$

254b Biotite diagram.

254c Second section perpendicular to  $S_2$   
(same orientation as a).

280 Section slightly oblique to  $S_1$ .

450a Section perpendicular to  $S_1$ .

450b " " to 450a.

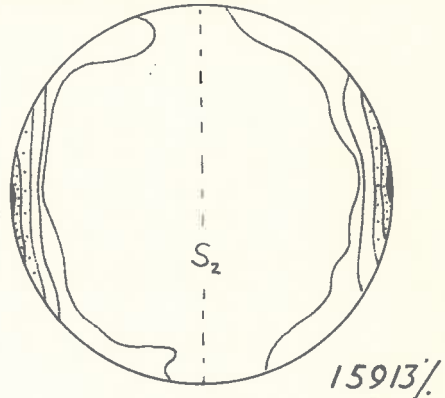
# FABRIC DATA FOR A.S. BIMICA SCHISTS.

CONTOURS 1234 per 1/area

254a 406Q



254b 200B



254c 225Q



280 241Q



450a 260Q



450b 150Q





are similar to those of 368 and 450, suggesting that quartz may also be unoriented in these rocks. It is considered that the "pseudo" preferred orientation exhibited in the diagrams is due to the "Schnitteffekt" (i.e. cut effect; see Sander et al., 1954; Jones, 1959). The possible reasons for the lack of preferred orientation are:

- (1) The original syntectonic fabric was destroyed by post tectonic recrystallization (c.f. Mackie, 1947).
- (2) Quartz remained as a passive component during folding, while the micas responded to deformation.

Probably both of these factors have contributed to the development of this essentially random orientation.

APPENDIX 5.Description of petrofabric specimens.Adelaide Supergroup.Quartzites.

A200-114. A strongly lineated ( $B_1$ ), weakly foliated medium grained quartzite. Lamination defined by elongate tracks of feldspar; quartz slightly elongate in sections parallel to  $B_1$ . Location 942234.

A200-326. A non foliated quartzite showing a strong lamination ( $B_1$ ) defined by elongate tracks of feldspar; quartz occurs as equidimensional interlocking grains. Location 939206

A200-222. A weakly foliated, medium grained quartzite. A faint lamination defined by ribbing is present; quartz occurs in equidimensional grains with interlocking boundaries. Location 928172.

A200-299. A non foliated coarse grained quartzite. A lamination defined by ribbing or muscovite is present; quartz occurs in large equidimensional grains with interlocking boundaries. Location 932199.

A200-289A. A faintly layered, non lineated coarse grained quartzite; quartz occurs as large equidimensional grains with interlocking boundaries enclosing small feldspar grains. Location 945194.

A200-329. A platy, fine grained quartzite showing a faint ribbing ( $B_1$ ); quartz occurs as equidimensional interlocking grains. Location 936209.

A200-721. A coarse grained, platy quartzite showing strongly elongate tracks of feldspar parallel to  $B_1$ ; quartz slightly elongate in sections parallel to  $B_1$ . Location 943231.

A126-4. A platy, faintly banded medium grained quartzite showing a faint lineation defined by elongate tracks of muscovite; quartz appears to be slightly elongate in sections parallel and perpendicular to  $B_1$ . Location 935163.

The grain size of quartz varies from 0.4 to 4.0mm. in 299, 721 and 289, and from 1.4 to 0.1 mm. in the remaining specimens.

#### Bimica Schists.

A200-450 is a fine grained biotite schist which contains small skeletal garnet porphyroblasts, quartz, biotite and minor plagioclase.  $S_1$  only is present.

A200-254 is a coarse garnet - quartz - plagioclase - biotite schist containing  $S_2$  with minor relic hinges of  $S_1$ (?).  $S_2$  is slightly buckled.

A200-268 is a crenulated fine grain<sup>ed</sup> bimica schist, with microfolds oriented parallel to  $B_3$ . Crenulation cleavage is not present.

#### Kanmantoo Group.

A200-422. A poorly foliated ( $S$ ) fine grained quartzo-feldspathic schist showing a lineation ( $B_1$ ) defined by a faint ridging. Location 976260.

A200-48. A slightly foliated (S) quartzo-feldspathic schist showing a small quartz-feldspar vein parallel to S. No lineation is present. Location 977174.

A200-425. A fine grained faintly banded (S) biotite poor quartzo-feldspathic schist. No lineation is present. Location 977258.

A200-584. A fine grained, non foliated, quartzo-feldspathic schist showing small porphyroblasts of feldspar. A well defined biotite lineation (B<sub>1</sub>) is present. Location 997237.

A200-29. A foliated (S?) quartzo-feldspathic schist (meta-greywacke variant) showing a well defined biotite lineation (B<sub>3</sub>). Location 984178.

A200-27. A fine grained, biotite poor, foliated (S) quartzo-feldspathic schist. A faint lineation defined by biotite is present. Location 978184.

Quartz occurs in all specimens interstitial to feldspar.

APPENDIX 6.Optical Axial Angle Measurements.

All measurements were carried out on a Leitz 5 axis Universal Stage mounted on a Leitz Dialux Pol microscope, using standard UM 2, 32 and UMK 32, 50 objectives and a hemisphere of R.I. = 1.544 combined with a central plate of R.I. = 1.52. After the mineral had been oriented correctly with the use of an Nakamura plate (Vogel, 1964) readings were taken, the number depending upon the amount of variation shown by the mineral. Both conoscopic and orthoscopic techniques have been used. Values of  $2H$  were converted to  $2V$  in a manner described by Emmons (1959). Errors were minimized as much as possible, by using low angles of tilt of the universal stage, diaphragms at correct settings, segments and central plates with similar R.I. etc. (see Wyllie, 1959; Munro, 1963). Most  $2V$  values given are believed to be reproducible to  $\pm 2^\circ$ .

Refractive Index Measurements.

The refractive indices have been determined by oil immersion using sodium light and are considered to be reproducible to  $\pm 0.001$ .

Determination of Scapolite Compositions.

The  $n_o$  values of scapolite have been measured in sodium light and their composition determined from the following

regression curve:

$$n_o = 1.5333 + 0.0007402 \text{ p.c. melonite.}$$

This curve has been constructed from the data of Shaw (1960, Tables 6<sup>1</sup> and 7). The author has found that results obtained from this curve are comparable with those determined from Shaw's mean refractive curve viz.

$$n_m = 1.5346 + 0.000507 \text{ p.c. melonite.}$$

The compositions of several scapolites were determined from the X-ray curve of Burley et al., (1961), but the results proved to be unsatisfactory.

- 
1. Numbers 11,12,17,18,19 have not been used in the calculation of this regression curve. Numbers 11,17 and 18 have unusual features of composition, and 12 and 19 are suspected of erroneous determinations or typography (Shaw,1960, p.253).